Cyclodextrin functionalized nanocellulose for biomedical applications

Bastien Michel

THÈSE

Pour obtenir le grade de

DOCTEUR DE L'UNIVERSITE GRENOBLE ALPES

Spécialité : **Matériaux, Mécanique, Génie civil, Electrochimie**

Arrêté ministériel : 25 mai 2016

Présentée par

Bastien MICHEL

Thèse dirigée par **Alain DUFRESNE,** Professeur, Université Grenoble Alpes
Et codirigée par **Julien BRAS,** Maitre de Conférences, Grenoble INP
et **Kristin SYVERUD**, Professeur, NTNU

Préparée au sein du **Laboratoire de Génie des Procédés Papetiers**
Dans **l'École Doctorale IMEP-2 – Ingénierie, Matériaux, Mécanique, Environnement, Energétique, Procédés, Production**

Fonctionnalisation de nanocellulose par des cyclodextrines pour des applications biomédicales

Cyclodextrin-functionalized nanocellulose for biomedical applications

Thèse soutenue publiquement le **03/12/2021**
Devant le jury composé de :

Dr. Bernard CATHALA
Directeur de Recherche, INRAE Centre Bretagne Normandie, Président
Dr. Carmen FREIRE
Chercheur, Universidade de Aveiro, Rapporteure
Pr. Sophie FOURMENTIN
Professeur des universités, Université de Dunkeque-Littoral, Rapporteure
Pr. Naceur BELGACEM
Professeur des universités, Grenoble INP, Examinateur
Pr. Alain DUFRESNE
Professeur des universités, Grenoble INP, Directeur de thèse
Pr. Kristin SYVERUD
Professeur, NTNU, Co-directrice de thèse, Invitée
Dr. Julien BRAS
Maitre de Conférences, Grenoble INP-UGA, Co-directeur de thèse, Invité
Dr. Ellinor B. HEGGSET
Chercheur, RISE PFI AS, Co-encadrante de thèse, Invitée

TABLE OF CONTENTS

ACKNOWLEDGEMENTS

Ce projet de thèse fut pour moi un réel accomplissement et m'a appris tant de choses. D'un point de vue scientifique avec la découverte de domaines si variés mais tous passionnant. D'un point de vue personnel avec un apprentissage de la résilience et la découverte de la confiance en soi. Mais surtout d'un point de vue humain, avec toutes les rencontres et mains tendues que j'ai eu l'opportunité de rencontrer lors de ces trois dernières années, et que je souhaite remercier ici.

First of all, I would like to thank the members of the jury, who gave me the honor of reviewing my work: Dr. Carmen Freire, Pr. Sophie Fourmentin, Pr. Naceur Belgacem and Dr. Bernard Cathala. Thank you all for your time and involvements. The fruitful discussion that we had during the defense helped me to present a better manuscript and will always be for me a nice memory in my career. I would also like to thank specially Pr. Sophie Fourmentin, for our first discussions in a summer school in Milan, when I knew almost nothing about cyclodextrins, which were of a great help, and for agreeing to respond to my invitation to a conference in Autrans.

I would like to express my deepest gratitude to my supervising team. This project was in collaboration with two laboratories in two different countries, which was a great experience for me. Kristin and Ellinor, thank you so much for your involvement, for the discussions, for the trust you had in me and for your kindness. It was not easy for both of you, especially since I was in France for most of the project… The cancelling of my stay in Norway is the deepest regret I have in this project, I would have really enjoyed working more with you in person. But I think that in the end, we managed well, and you have a lot of credit to take for that. I hope that we will meet each other again in the future, and wish you all the best for your future projects! Alain, tu n'étais pas initialement inclus dans ce projet, mais quand j'en avais besoin, tu as accepté de me venir en aide et tu m'as accompagné jusqu'à la fin, et pour cela je te suis profondément reconnaissant. Ton écoute, ta réactivité dès que j'en avais besoin et également (d'aucuns diraient surtout) nos pauses cigarettes furent autant de piliers sur lesquels j'ai pu compter, merci pour tout. Julien, tout a commencé avec toi, et je suis heureux que nous ayons pu finir ce projet ensemble. Les discussions scientifiques avec toi furent toujours intéressantes et ont systématiquement soulevé de nouvelles idées. Mais le plus important pour moi fut l'encadrement plus personnel que tu

m'as apporté depuis ton retour, à un moment où je me perdais (ce qui est un peu un euphémisme). Tu as su écouter mes doutes et me convaincre de leur accorder moins de crédits, tu m'as donné confiance en moi et dans mon travail, et pour ça je te remercie infiniment.

Je voudrais remercier Isabelle Desloges et Aurore Denneulin pour avoir accepté de faire partie de mon comité de suivi individuel. Ces réunions annuelles pendant lesquelles je vous présentais mes résultats ont systématiquement débouché sur des conversations utiles pour ce projet, et surtout vos encouragements m'ont toujours redonné de la motivation et de la confiance, merci à vous.

Je souhaiterais adresser des remerciements particuliers à Didier Chaussy et Evelyne Mauret, qui m'ont apporté une écoute et une aide précieuse lors de l'été 2020, avec un investissement et une bienveillance de tous les instants. Sans cela, je ne serais peut-être pas allé au bout de ce projet, merci à vous.

Je remercie Glyco@Alps pour avoir financé ce projet, et tout particulièrement Ferielle Podgorski, Emilie Gillon et Anne Imberty. Avoir eu l'opportunité de travailler avec vous fut un réel plaisir, et les conseils prodigués par Anne m'ont permis de découvrir tout un nouveau pan expérimental passionnant. Je suis fier que l'on ait pu concrétiser cette collaboration par une publication, merci à vous.

I would like to thank NTNU and RISE PFI for funding this project, and more specially the person that I worked with during my short stay in Trondheim: Ingebjørg Leirset, Johnny Kvakland Melbø, and Anne Marie Reitan.

Merci au personnel du LGP2 pour leur aide et leurs formations sur différentes technique expérimentales : Marie Christine-Brochier Salon, Bertine Khelifi, Stephane Dufreney, Karine Janel et Maxime Terrien. Merci à Raphael Passas pour les discussions et pour m'avoir fait confiance pour mener des TP, à Jérémy Viguier pour son incessante bonne humeur et bienveillance, merci aux services RH et informatiques du laboratoire qui m'ont sorti de galères plus d'une fois. Un merci particulier à Cécile Sillard: merci pour ton accompagnement pendant ces trois années, d'avoir partagé les galères de microbiologie, d'avoir supporté mon esprit des fois légèrement négatif et mon cynisme, d'avoir toujours eu

la porte ouverte pour écouter mes problèmes, d'avoir été un pilier sur lequel j'ai pu m'appuyer pour continuer ce projet. Merci pour tout.

J'ai eu la chance de pouvoir encadrer ou co-encadrer des stagiaires durant ce projet, qui ont contribué à la réalisation expérimentales mais également aux réflexions qui ont façonné mon raisonnement pendant ces 3 années. Ainsi, merci à Martha Groendhal, Marie Rinchet, Tugdual Haffner et Mathis Mignée. Je vous souhaite tout le meilleur pour vos expériences futures.

Merci aux anciens qui m'ont montré la voie quand je suis arrivé, surtout Hippolyte dont j 'ai plus ou moins pris la suite spirituelle, merci pour les conseils, les discussions, les courses à pieds et ton temps alors que celui-ci se faisait rare. Merci à Clémentine, la patronne, pour toutes nos discussions, pour ta bienveillance, ta gentillesse et pour m'avoir énormément aidé lors de ces (presque) 4 dernières années. Tu as été la meilleure des tutrices possible. Merci Hugo pour les randos, les discussions microbio et les pauses clopes. Merci Manon pour ta bienveillance et l'exemple que tu as su nous donner. Merci Andréa, Malek, et Lili pour avoir été de super partenaires de bureaux, le temps partagé avec vous fut des plus agréables. Merci aux (plus si) petits nouveaux Florian et Marlène pour leur implication, tendance à râler (dans laquelle je me retrouve) et acceptation de mon caractère, je vous souhaite tout le meilleur pour la suite, mais je n'ai pas trop de doutes. Merci à Lorelei, Eva (le futur des polysaccharides européens quand même) et Maxime, avec qui nous avons commencé le même jour et vécu ces 3 ans côte-à-côte. Nos discussions et échanges d'expériences sur nos travaux et nos galères m'ont énormément aidé et motivé, et je pense que nous nous sommes un peu tirés vers le haut, ce qui n'est quand même pas si mal, et pour ça encore merci. Merci à Etienne G. pour avoir été une source d'inspiration, un phare dans la brume de mon ignorance, une boussole sur la vaste étendue de la connaissance. Un merci particulier à Gabriel, pour avoir été un compagnon de galère privilégié. Quand je pense à toi, quelques mots me viennent en tête : camaraderie, humour, attentions, conversations, alcool et leadership, tout simplement. Merci pour tout, humainement t'es pas extra, mais t'as fait le job. En bref, merci à tous les thésards/thésardes et post-docs que j'ai eu la chance de rencontrer lors de ces 3 années relativement mouvementées pour tous, vous côtoyer a rendu cet exercice plus simple : Flavien, Amina, Fleur, Hippolyte, Manon, Estelle, Hugo, Gabriel,

Camille T., Camille D., Gioia, Gloria, Khaoula, Fanny, Juliette, Etienne G., Etienne M., Lili, Malek, Ahlem, Andrea, Lorelei, Eva, Maxime, Ge, Florian, Marlène, Laetitia, Joao, Enrique, Clémentine, Laurette, Emilien, Julia, Claire, Hélène, Arnaud, et également Paul et Antoine du Cermav.

Merci à mes parents et à ma sœur pour leur soutien et leurs encouragements, et pour me supporter depuis 27 ans, la tâche n'est pas si simple. Merci pour tout.

Merci aux copains, pour leur soutien et m'avoir permis de me sortir la tête de la thèse quand c'était nécessaire, merci d'être là. Merci aux amis d'un groupe certains, qui ont tous eu la délicatesse de soutenir après moi. Merci à Léo, qui m'a subi pendant deux ans, tu as eu du mérite. Merci à Alexia, j'espère que tu t'épanouiras dans ta thèse et te souhaite tout le meilleur.

Enfin, merci à Lise, qui a accompagné la dernière moitié de cette thèse et qui doit vivre au jour le jour avec mes doutes, mon anxiété et mon humour particulier. Tu as été un pilier pour moi lors de ces 18 derniers mois, et pour ça, tu as ma gratitude infinie. Maintenant, je n'ai qu'une hâte, c'est d'écrire notre prochain chapitre ensemble.

SCIENTIFIC CONTRIBUTIONS (2018-2021)

PUBLICATIONS IN SCIENTIFIC JOURNALS

1. B. Michel, J. Bras, A. Dufresne, E.B. Heggset, K. Syverud. *Production and Mechanical Characterisation of TEMPO-Oxidised Cellulose Nanofibrils/β-Cyclodextrin Films and Cryogel.* Published in *Molecules* (MDPI) in May 2020
2. B. Michel, A. Imberty, E.B. Heggset, K. Syverud, J. Bras, A. Dufresne. *Adsorption characterization of various modified β-cyclodextrins onto TEMPO-oxidized cellulose nanofibrils.* Published in *Sustainable Chemistry and Pharmacy* (Elsevier) in September 2021.
3. B. Michel, E.B. Heggset, K. Syverud, A. Dufresne, J. Bras, *Inclusion complex formation between sulfadiazine and various modified β-cyclodextrins*. Submitted to *Journal of Drug Delivery Science and Technology* (Elsevier) in March 2022.
4. B. Michel, E.B. Heggset, K. Syverud, A. Dufresne, J. Bras, *Drug release and antimicrobial properties of TEMPO-CNF/β-CDs/Sulfadiazine films and cryogels*. Submitted to *Carbohydrate Polymers* (Elsevier) in March 2022.

ORAL PRESENTATIONS

1. B. Michel, E.B. Heggset, A. Dufresne, K. Syverud, J. Bras, *Cyclodextrin functionalized nanocellulose for drug release application*, at American Chemical Society – National Meeting and expositions Spring 2021. Online event (2021)
2. B. Michel, J. Bras, A. Dufresne, E.B. Heggset, K. Syverud. *TEMPO-Oxidised Cellulose Nanofibrils/β-Cyclodextrin Films and Cryogels for biomedical applications*, at the 4th International EPNOE Junior Scientist Meeting. Online Event (2021)
3. B. Michel, E.B. Heggset, A. Dufresne, K. Syverud, J. Bras, *Cyclodextrin functionalized nanocellulose for drug delivery*, at the 6th ENPOE International Polysaccharides Conference. Aveiro, Portugal (2019)

POSTERS

1. B. Michel , E.B. Heggset, K. Syverud, J. Bras, *Cyclodextrin functionalized nanocellulose for tissue engineering applications* ,at the 4th International Summer School on Cyclodextrins. Milan, Italy (2019). Awarded Poster Special Prize by the Directors of the school.

2. B. Michel , E.B. Heggset, K. Syverud, J. Bras, *Cyclodextrin functionalized nanocellulose for tissue engineering applications,* at the Global Challenges Science Week. Grenoble, France (2019)

Two posters about the work of previous M2 intern have also been made and presented by the PhD candidate:

3. J. Solier, B. Michel, E. Cranston, J. Bras , *Furan/Maleimide Diels-Alder crosslinking of nanocellulose for biomedical applications,* at the 6th ENPOE International Polysaccharides Conference. Aveiro, Portugal (2019)
4. M. Patel, B. Michel, E. Cranston, J. Bras, *Improving nanocellulose cryogels through crosslinking for drug release applications in wet conditions*, at the 6th ENPOE International Polysaccharides Conference. Aveiro, Portugal (2019)

OTHER CONTRIBUTION

Part of the organization of Glyco@Club Days, Autrans, France (2019), a two-days summer-school

LIST OF ABBREVIATIONS

CHEMICALS AND MATERIALS

- **AGU**: Anhydroglucose unit
- **API** : Active principle ingredient
- **BNC** : Bacterial nanocellulose
- **CDs** : Cyclodextrins
- **cmCNFs** : Carboxymethylated CNFs
- **CM-β-CD** : Carboxymethylated β-Cyclodextrin
- **CNCs** : Cellulose nanocrystals
- **CNFs** : Cellulose nanofibrils
- **CNMs** : Cellulose nanomaterials
- **eCNFs** : Enzymatically pretreated CNF
- **EtOH** : Ethanol
- **HA** : Hyaluronic acid
- **HCl** : Hydrochloric acid
- **HP-β-CD** : 2-Hydroxypropyl β-Cyclodextrin
- **NaOH** : Sodium hydroxide
- **PEI** : Polyethyleimine
- **PhP** : Phenolphtalein
- **PLA** : Poly-lactic acid
- **Polyβ-CD** : polymerized β-Cyclodextrin
- **SD** : Sulfadiazine
- **SSD** : Silver Sulfadiazine
- **TEMPO** : 2,2,6,6-Tetramethylpiperidine-1-oxyl
- **toCNCs** : TEMPO-oxidized CNCs
- **toCNFs** : TEMPO-oxidized CNFs

CHARACTERIZATION TOOLS

- **AFM** : Atomic force microscopy
- **CrI** : Crystallinity index
- **DMA** : Dynamic mechanical analysis
- **DP** : Degree of polymerization
- **DS** : Degree of substitution
- **DSC** : Differential scanning calorimetry
- **FTIR** : Fourier transformed Infrared spectroscopy
- **ITC** : Isothermal Titration calorimetry
- **NMR** : Nuclear magnetic resonance
- **PSD** : Phase solubility diagram
- **QCM-d** : Quartz crystal microbalance with dissipation monitoring
- **SEM** : Scanning electron microscopy
- **TEM** : Transmission electron microscopy
- **TGA** : Thermo-gravimetric analysis
- **UV-vis** : UV-visible spectrophotometry

- **XRD** : X-ray diffraction
- **ZOI** : Zone of inhibition

OTHERS

- **CFU** : Colony-forming units
- **ECM** : Extracellular matrix
- **ESCs** : Embryonic stem cells
- **G-** : Gram negative
- **G+** : Gram positive
- **iPSCs** : Induced pluripotent stem cells

GENERAL INTRODUCTION

Biomaterials are materials exploited in contact with living tissues, organisms or microorganisms [1]. The development of biomaterials as we know them today originates in the late 40s, initiated by the development of scientific knowledge in both medicine and materials science. While the first biomaterials were originally developed for other applications and applied to medicine in an "off-the-shelf" solution, they have evolved to form a multidisciplinary field represented by a large community of researchers and industries developing solutions for a wide variety of applications such as drug delivery, wound dressing or soft/hard tissue engineering [2]. Depending on the application, various materials can be specifically engineered such as metals, ceramics, composites or polymers. Metallic biomaterials are used for load bearing applications due to their high fatigue strength. Ceramic biomaterials are used for bone-bonding surfaces in implants and articulating surfaces because of their hardness and wear resistance. Finally, polymeric materials are typically used in wound dressing applications for their flexibility and stability.

Polymeric materials, with a wide variety of physical properties, a high availability as well as tailoring possibilities in terms of size, shape, mechanical properties, hydrophobicity and chemical functionalization, are widely utilized as biomaterials. However, petroleum-derived polymers are still the most used nowadays, even if their use presents several issues. From a medical point-of-view, the potential release of plasticizer residues or by-products can lead to an adverse inflammatory response in the patient. Additionally, the petroleum resources are nonrenewable and it would be preferable, from an ecological point-of-view, to find more biobased alternatives. Synthetic biobased polymers, such as polylactic acid (PLA), have been regarded as an interesting alternative in healthcare area [3]. However, the most promising alternatives are natural biobased polymers, and biopolymers such as chitin, collagen or cellulose are therefore increasingly exploited as biomaterials [4]–[6].

Within this context, **an interesting candidate is cellulose nanofibrils** (CNFs). CNFs are nanoparticles with high aspect ratio formed by bundles of cellulose chains that consists of glucose subunits linked by β-1-4 glycosidic bonds, as illustrated by Figure 1.A. CNFs are produced from a cellulosic raw material, usually wood, and cellulose is the most abundant and renewable polymer available on earth. CNFs are produced by a combination of pre-treatments (which could be chemical, enzymatic or mechanical) and mechanical fibrillation

process. The different pre-treatment methods [7] allow a variety of surface chemistries, making CNF materials suitable for many applications, as illustrated in Figure 1.B. The recent industrialization of CNFs during the last decade confirms the numerous potential of such materials. In recent years, applications in wound healing [8], [9], drug delivery [10] and tissue engineering [11] have been investigated. In tissue engineering, the scaffold should stimulate cells to differentiate, proliferate and form tissue. The interplay between the matrix and cells must be driven by the action of signals, which can e.g. be a mechanical stimulation, a chemical compounds or a growth factor (usually a protein) [12]. The utilization of wood-based CNFs for tissue engineering applications is encouraged by recent studies that confirmed the safety of CNFs [13], [14], construction of cell-friendly porous structure [15] and control of mechanical properties [16], [17]. In drug delivery, the objective is to obtain a **sustained and controlled release of drugs** at the biological site, but also to increase the bioavailability of drugs. Different recent studies have shown that the use of CNFs is promising for extending the release time of various drugs [18]. However, improvements need to be implemented to achieve better control of the release and loading of such a device. Additionally, the design of structures in multiple forms, in "2D" such as membrane or in "3D" such as porous cryogels, needs to be analyzed in terms of efficiency and suitability for the wanted applications.

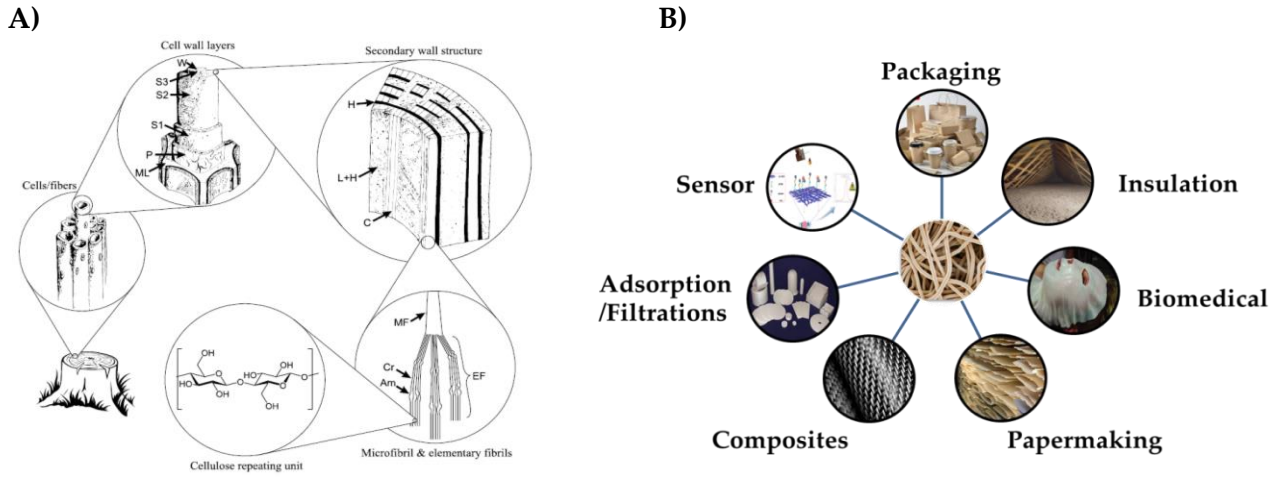

Figure 1 : A) Hierarchical structure of wood, extracted from [19]. B) Possible applications for cellulose nanofibrils.

One strategy to address these issues is the use of **cyclodextrins (CDs)**. Cyclodextrins are natural cyclic oligosaccharides consisting of glucose subunits linked by α-1-4 glycosidic

bonds, as shown in Figure 2.A. Because of their conformation, with a hydrophobic interior and a hydrophilic exterior, these macromolecules exhibit cage-like properties and can form an inclusion complex with hydrophobic compounds, as illustrated in Figure 2.B [20], [21]. These properties have led to use in various fields, such as cosmetics, food, environment and medicine [22]–[24]. Regarded as safe, they are widely used as an excipient in the pharmaceutical field [25], [26]. For such applications, β-CD, a cyclodextrin with 7 glucose sub-units, and its derivatives are the most commonly used [27], [28].

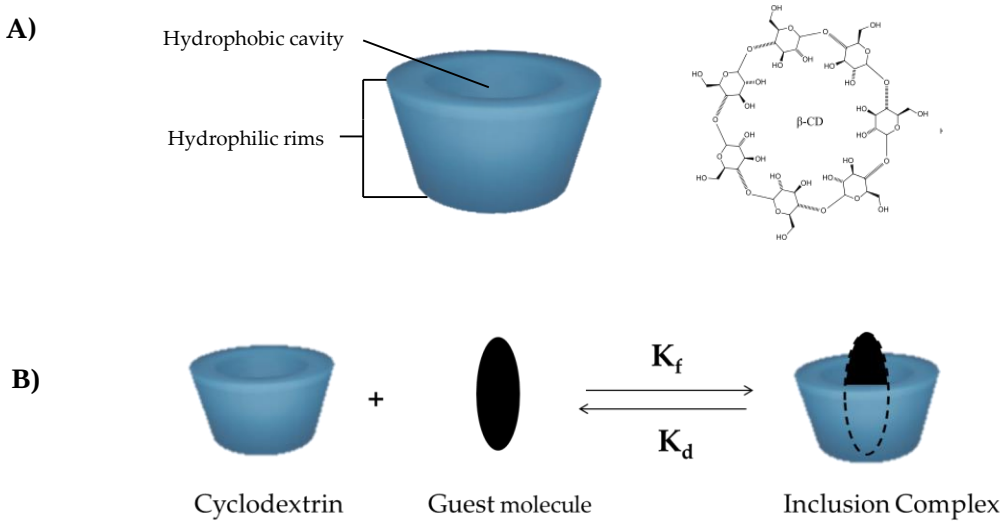

Figure 2 : Schematic representation of A) β-Cyclodextrin and B) formation of a 1:1 inclusion complex

The **association of CDs and CNFs** has not been extensively studied prior to this project, with only a dozen of publications on the topic. The difficulty of assessing the functionalization via adsorption or grafting of β-CDs onto CNFs has been pointed out as challenging due to the high chemical proximity of the two components and this was addressed as the main drawback to their utilization, although promising in theory. Additionally, other challenges involve finding solutions to improve the functionalization by β-CDs without using any cross-linker or harmful solvent. In that regard, the use of β-CD derivatives could be of interest. Indeed, β-CDs presenting carboxyl or hydroxypropyl groups could increase the potential interaction with CNFs. However, at the start of the project, this strategy has not been widely reported in literature.

The present Ph.D. research work entitled "Cyclodextrin-functionalized nanocellulose for biomedical applications" is a collaborative project between the Laboratoire Génie des Procédés Papetiers (LGP2) in Grenoble (France) and RISE PFI/NTNU in Trondheim (Norway). This work is supported by the French National Research Agency in the framework of the "Investissements d'avenir" program Glyco@Alps and NTNU Department of Chemical Engineering.

The main goals of this research work were to provide nanocellulose-based materials with improved properties due to the specific characteristics of β-CD and its derivatives. As such, the main objectives were:

- Prepare CNF/β-CD structures with controlled architecture as well as to identify the impact of β-CDs and different process parameters to obtain materials with suitable properties for biomedical applications.
- Find solutions to characterize the adsorption of various β-CDs onto CNFs.
- Assess the beneficial impact of β-CDs on the release and/or antimicrobial properties of the prepared structure with a low water-soluble model molecule.

To achieve these goals, an active collaboration was developed during the three years, with a stay in Trondheim in 2019 to perform experiments at the facilities of NTNU and RISE PFI, but also with local partners in Grenoble, which allowed the use of some specific characterization techniques (CERMAV).

This manuscript endeavors, in three chapters, to transcribe in a precise and detailed way the research approach carried out as well as the results obtained for the production, characterization and application of CNF/ β-CD materials.

In **Chapter I,** the literature review seeks to provide the reader with general information as well as detailed data from recent scientific publications. An overview of biomaterials, with its history, definition, fundamentals in microbiology and the different class of materials used are discussed. A focus on nanocelluloses, from production to applications, with a focus on biomedical applications is presented. Finally, cyclodextrins, its inclusion complex formation and characterization are described, with the presentation of past works combining β-CDs and CNFs.

Chapter II presents the results obtained for the design of CNF/β-CD nanostructured materials. In sub-chapter II-1, various TEMPO-oxidized CNFs (toCNFs) suspensions are produced at different charge rate, and further used in the production of films and cryogels. The impact of several parameters on physico-chemical properties of the produced structures are described, allowing to obtain indirect proof of functionalization. In sub-chapter II-2, the different methods implemented to characterize the adsorption of various β-CDs onto toCNFs are presented, with the identification of the optimized β-CDs. In sub-chapter II-3, the final design and the impact of the βCDs derivatives over the mechanical properties of the produced structure will be discussed.

Chapter III focuses on the biomedical application of the produced nanostructure. In sub-chapter III-1, the inclusion complex formation between the various β-CDs and a low-water soluble active principle ingredient chosen as a model molecule is characterized. Finally, sub-chapter III-2 presents the results obtained in release and the antimicrobial study highlights the beneficial impact of β-CDs in CNFs materials for biomedical applications.

The organization of these chapters is graphically represented in Figure 3. Most of the sub-chapters are structured as scientific publications.

This Ph.D. work provides the scientific community with interesting materials for biomedical applications, as well as interesting new results on the adsorption characterization for CNFs using Isothermal Titration Calorimetry. Additionally, CNF/β-CD materials could also be beneficial for other applications, such as filtration or depollution.

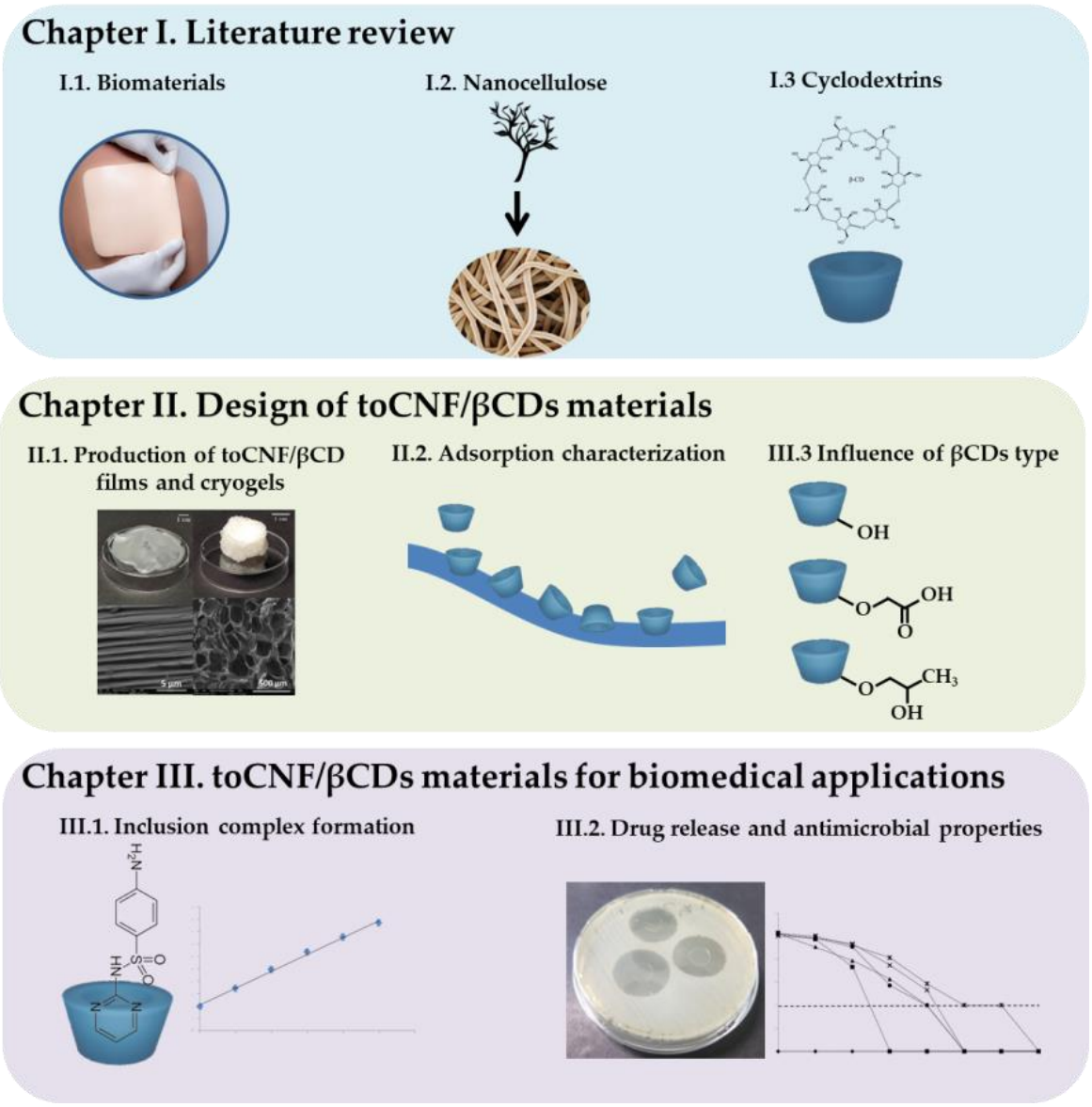

Figure 3 : Graphical representation of the PhD manuscript content

REFERENCES

[1] M. Vert *et al.*, 'Terminology for biorelated polymers and applications (IUPAC Recommendations 2012)', *Pure and Applied Chemistry*, vol. 84, no. 2, pp. 377–410, Jan. 2012, doi: 10.1351/PAC-REC-10-12-04.

[2] B. D. Ratner, 'Biomaterials: Been There, Done That, and Evolving into the Future', *Annu. Rev. Biomed. Eng.*, vol. 21, no. 1, pp. 171–191, Jun. 2019, doi: 10.1146/annurev-bioeng-062117-120940.

[3] V. DeStefano, S. Khan, and A. Tabada, 'Applications of PLA in modern medicine', *Engineered Regeneration*, vol. 1, pp. 76–87, 2020, doi: 10.1016/j.engreg.2020.08.002.

[4] F. Copes, N. Pien, S. Van Vlierberghe, F. Boccafoschi, and D. Mantovani, 'Collagen-Based Tissue Engineering Strategies for Vascular Medicine', *Front. Bioeng. Biotechnol.*, vol. 7, p. 166, Jul. 2019, doi: 10.3389/fbioe.2019.00166.

[5] H. Gao *et al.*, 'Construction of cellulose nanofibers/quaternized chitin/organic rectorite composites and their application as wound dressing materials', *Biomater. Sci.*, vol. 7, no. 6, pp. 2571–2581, 2019, doi: 10.1039/C9BM00288J.

[6] R. J. Hickey and A. E. Pelling, 'Cellulose Biomaterials for Tissue Engineering', *Front. Bioeng. Biotechnol.*, vol. 7, p. 45, Mar. 2019, doi: 10.3389/fbioe.2019.00045.

[7] F. Rol, M. N. Belgacem, A. Gandini, and J. Bras, 'Recent advances in surface-modified cellulose nanofibrils', *Progress in Polymer Science*, Sep. 2018, doi: 10.1016/j.progpolymsci.2018.09.002.

[8] A. Rees *et al.*, '3D Bioprinting of Carboxymethylated-Periodate Oxidized Nanocellulose Constructs for Wound Dressing Applications', *BioMed Research International*, vol. 2015, pp. 1–7, 2015, doi: 10.1155/2015/925757.

[9] T. Hakkarainen *et al.*, 'Nanofibrillar cellulose wound dressing in skin graft donor site treatment', *Journal of Controlled Release*, vol. 244, pp. 292–301, Dec. 2016, doi: 10.1016/j.jconrel.2016.07.053.

[10] R. Kolakovic, L. Peltonen, A. Laukkanen, J. Hirvonen, and T. Laaksonen, 'Nanofibrillar cellulose films for controlled drug delivery', *European Journal of Pharmaceutics and Biopharmaceutics*, vol. 82, no. 2, pp. 308–315, Oct. 2012, doi: 10.1016/j.ejpb.2012.06.011.

[11] E. Campodoni *et al.*, 'Polymeric 3D scaffolds for tissue regeneration: Evaluation of biopolymer nanocomposite reinforced with cellulose nanofibrils', *Materials Science and Engineering: C*, vol. 94, pp. 867–878, Jan. 2019, doi: 10.1016/j.msec.2018.10.026.

[12] D. Howard, L. D. Buttery, K. M. Shakesheff, and S. J. Roberts, 'Tissue engineering: strategies, stem cells and scaffolds', *Journal of Anatomy*, vol. 213, no. 1, pp. 66–72, Jul. 2008, doi: 10.1111/j.1469-7580.2008.00878.x.

[13] A. Rashad, K. Mustafa, E. B. Heggset, and K. Syverud, 'Cytocompatibility of Wood-Derived Cellulose Nanofibril Hydrogels with Different Surface Chemistry', *Biomacromolecules*, vol. 18, no. 4, pp. 1238–1248, Apr. 2017, doi: 10.1021/acs.biomac.6b01911.

[14] L. Alexandrescu, K. Syverud, A. Gatti, and G. Chinga-Carrasco, 'Cytotoxicity tests of cellulose nanofibril-based structures', *Cellulose*, vol. 20, no. 4, pp. 1765–1775, Aug. 2013, doi: 10.1007/s10570-013-9948-9.

[15] K. J. De France, T. Hoare, and E. D. Cranston, 'Review of Hydrogels and Aerogels Containing Nanocellulose', *Chemistry of Materials*, vol. 29, no. 11, pp. 4609–4631, Jun. 2017, doi: 10.1021/acs.chemmater.7b00531.

[16] K. Syverud, H. Kirsebom, S. Hajizadeh, and G. Chinga-Carrasco, 'Cross-linking cellulose nanofibrils for potential elastic cryo-structured gels', *Nanoscale Research Letters*, vol. 6, no. 1, p. 626, 2011, doi: 10.1186/1556-276X-6-626.

[17] K. Syverud, S. R. Pettersen, K. Draget, and G. Chinga-Carrasco, 'Controlling the elastic modulus of cellulose nanofibril hydrogels—scaffolds with potential in tissue engineering', *Cellulose*, vol. 22, no. 1, pp. 473–481, 2015, doi: 10.1007/s10570-014-0470-5.

[18] N. Lin and A. Dufresne, 'Nanocellulose in biomedicine: Current status and future prospect', *European Polymer Journal*, vol. 59, pp. 302–325, Oct. 2014, doi: 10.1016/j.eurpolymj.2014.07.025.

[19] O. Nechyporchuk, M. N. Belgacem, and J. Bras, 'Production of cellulose nanofibrils: A review of recent advances', *Industrial Crops and Products*, vol. 93, pp. 2–25, Dec. 2016, doi: 10.1016/j.indcrop.2016.02.016.

[20] S. V. Kurkov and T. Loftsson, 'Cyclodextrins', *International Journal of Pharmaceutics*, vol. 453, no. 1, pp. 167–180, Aug. 2013, doi: 10.1016/j.ijpharm.2012.06.055.

[21] J. Szejtli, 'Introduction and General Overview of Cyclodextrin Chemistry', *Chem. Rev.*, vol. 98, no. 5, pp. 1743–1754, Jul. 1998, doi: 10.1021/cr970022c.

[22] E. M. M. Del Valle, 'Cyclodextrins and their uses: a review', *Process Biochemistry*, vol. 39, no. 9, pp. 1033–1046, May 2004, doi: 10.1016/S0032-9592(03)00258-9.

[23] G. Crini, S. Fourmentin, M. Fourmentin, and N. Morin-Crini, 'Principales applications des complexes d'inclusion cyclodextrine/substrat', p. 21, 2019.

[24] N. Morin-Crini, P. Winterton, S. Fourmentin, L. D. Wilson, É. Fenyvesi, and G. Crini, 'Water-insoluble β-cyclodextrin–epichlorohydrin polymers for removal of pollutants from aqueous solutions by sorption processes using batch studies: A review of inclusion mechanisms', *Progress in Polymer Science*, vol. 78, pp. 1–23, Mar. 2018, doi: 10.1016/j.progpolymsci.2017.07.004.

[25] F. J. Otero-Espinar, J. J. Torres-Labandeira, C. Alvarez-Lorenzo, and J. Blanco-Méndez, 'Cyclodextrins in drug delivery systems', *Journal of Drug Delivery Science and Technology*, vol. 20, no. 4, pp. 289–301, 2010, doi: 10.1016/S1773-2247(10)50046-7.

[26] S. S. Jambhekar and P. Breen, 'Cyclodextrins in pharmaceutical formulations I: structure and physicochemical properties, formation of complexes, and types of complex', *Drug Discovery Today*, vol. 21, no. 2, pp. 356–362, Feb. 2016, doi: 10.1016/j.drudis.2015.11.017.

[27] O. Cusola, N. Tabary, M. N. Belgacem, and J. Bras, 'Cyclodextrin functionalization of several cellulosic substrates for prolonged release of antibacterial agents', *Journal of Applied Polymer Science*, vol. 129, no. 2, pp. 604–613, Jul. 2013, doi: 10.1002/app.38748.

[28] T. Loftsson and M. E. Brewster, 'Pharmaceutical applications of cyclodextrins: basic science and product development: Pharmaceutical applications of cyclodextrins', *Journal of Pharmacy and Pharmacology*, vol. 62, no. 11, pp. 1607–1621, Nov. 2010, doi: 10.1111/j.2042-7158.2010.01030.x.

CHAPTER I. LITERATURE REVIEW

INTRODUCTION

The present chapter provides an overview of the global context of this PhD thesis, and is intended for both expert and non-expert readers. Therefore, general information on the subject will be presented, as well as detailed data from recent scientific literature. *Regular specific points in relation to this PhD project will be underlined and visible in italic and grey in the text.*

Section I seeks to provide an overview of the materials used in **biomedical applications**, called biomaterials. It consists of a first part providing a definition and history of different fields of biomedical studies, explanations of fundamentals in microbiology and active principal ingredients, and a second part presenting the history of biomaterials, i.e. materials specifically designed for biomedical applications, the different types of materials used with a focus on **biopolymers**, the family to which **cellulose** belongs.

Section II describes one type of cellulosic materials, **nanocelluloses** in all its forms, with particular attention given to **wood-based nanocelluloses**, at the heart of this project from production to characterization. The different processes used to elaborate these materials will be discussed and their applications presented. Finally, the history and current use of nanocellulose materials for biomedical applications will be presented in more details.

Section III presents **cyclodextrins**, the family of molecules used in this project to **functionalize nanocellulose**. First, the history, origin and production of these molecules will be described, as well as the various types of cyclodextrins available. A focus will then be made on **the inclusion complex formation**, properties and characterization. Lastly, studies using both cyclodextrins and nanocelluloses prior to this project will be thoroughly discussed.

Finally, the scientific challenges to overcome will be outlined in the conclusion of this literature review.

I. INTRODUCTION TO BIOMATERIALS ENGINEERING

The final objective of this project is the development of devices for medical applications, whether for drug release, wound healing or tissue engineering. A good knowledge of the field of biomaterials engineering is therefore necessary. Thus, the first section focuses on the definition of the different biomedical applications, defining the objectives, challenges and problems inherent to each one. The second section presents the basics of microbiology and the various Active Principal Ingredients. Finally, the third section is focusing on biomaterials, their origin, the different classes of materials used, and finish with a focus on biopolymers, to which cellulose belongs. This will give the reader an overview of the state of the art in the area of biomaterials in general.

I. 1. BIOMEDICAL APPLICATIONS

Biomedical engineering can be defined as the application of engineering Principals to medicine and biology for healthcare purposes [1]. Its objective is to advance healthcare treatment in many different fields, such as diagnosis, therapy, monitoring and prosthetics. This part will be focused on three particular sub-fields of biomedical engineering, namely (i) drug delivery, (ii) wound repair and (iii) tissue engineering, with the objective to define them and to give the main properties needed for a beneficial application.

I.1.1. DRUG DELIVERY

The conventional method for drug administration is the periodic administration of the drug to the patient, varying the concentration of drug in the body, limiting the therapeutic effect by alternating the concentrations in and out of the therapeutic window. This method displays major drawbacks, with the possibility to reach a toxic concentration of drug for the patient and the need to have precise time of administration. Another problem with the classical administration of drugs is the delivery of poorly water-soluble drugs. The field of drug delivery was developed to address these issues. Drug delivery is the method or process of administering a pharmaceutical compound to achieve a therapeutic effect [2]. Several methods, such as encapsulation, grafting/adsorption onto a substrate and complexation have been developed by researchers to obtain a controlled or sustained release of drugs. A sustained delivery describes a slow delivery in the range of the therapeutic

window, while a controlled delivery describes a constant delivery in the therapeutic range. Figure I.1 illustrates these different behaviors.

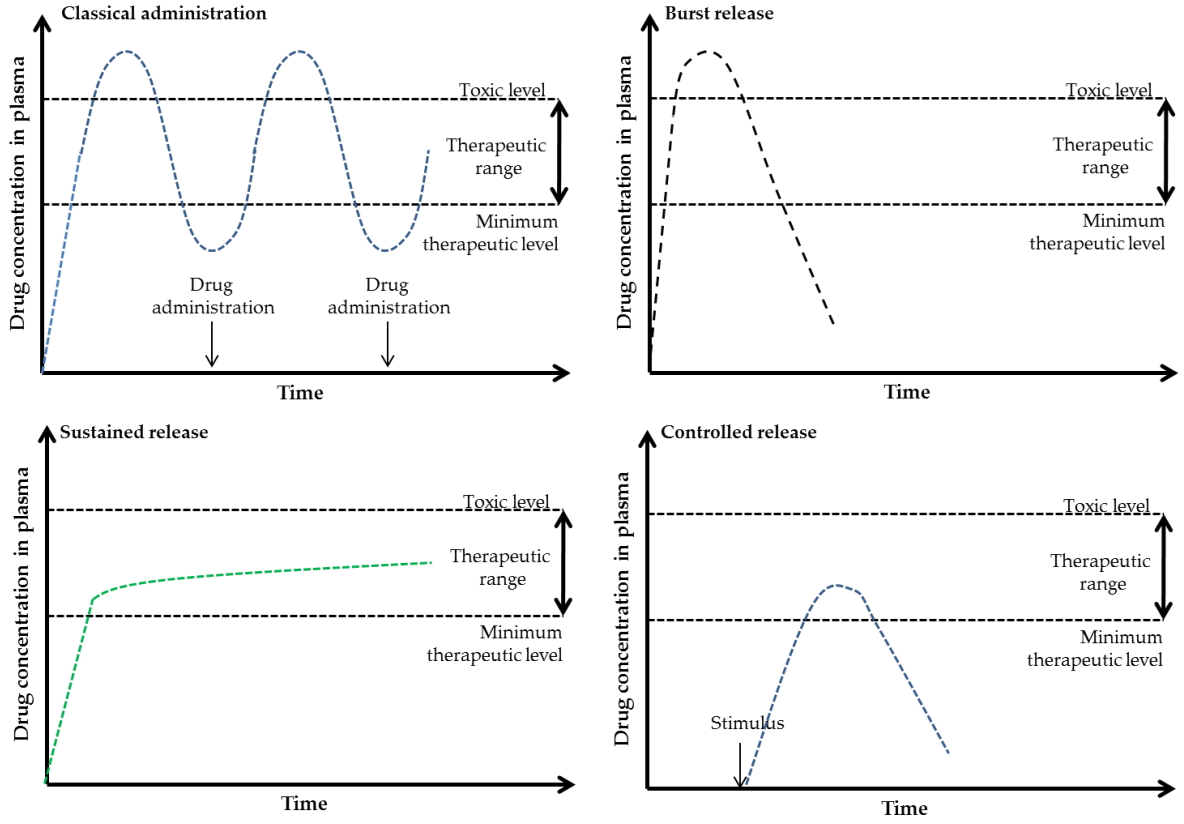

Figure I.1.: Different release profiles. From top to bottom and left to right: Classical administration, Burst release, Sustained release, Controlled release.

Another issue that needs to be addressed to design drug delivery systems is the burst effect, i.e. the immediate release of the majority of the Active Principal Ingredient (API).

The first drug delivery systems can be traced back to the 50's [3] , with the first formulations allowing a "sustained release" for 12h, opening the door for the first generation of controlled release systems. This first generation of delivery systems was mainly based on dissolution-controlled or diffusion-controlled systems, designed for oral or transdermal delivery [4]. The second generation of drug delivery systems was developed from the 70's, with the objective to obtain "smart delivery systems", which could react based on the environment and deliver the drug. For example, smart polymers, pH-sensitive and biodegradable proteins and nanoparticles were widely studied. However, one of the major issues with the second generation of drug delivery systems was the difficulty to overcome biological barriers, preventing the successful accumulation of therapeutic on the site of

interest and limiting its efficiency, leading to few successes in clinical trials [5]. Development of the third generation began in the 2010s, with the objective to design modulated delivery systems that can overcome these biological barriers.

The challenges occurring for drug delivery in the system we want to develop in the scope of this project would be a limited burst effect, a sustained release and the encapsulation of a poorly water-soluble drug.

I.1.2. WOUND DRESSING

The skin's primary function is to protect muscles, bones, ligaments and internal organs from the exterior environment. Cuts, burns or illness can affect the structure of the skin, creating a wound. Wounds are defined as disruption of tissue or cellular integrity due to either mechanical, physical or metabolism related injuries [6]. Depending on its severity, a wound will affect different depths of the skin, namely epidermidis, superficial dermis, deep dermis, and, in worst case, the underlying muscles. When a wound is occurring, the priority is to stop hemorrhage and to avoid microbial infection of the wound.

The process of wound healing consists of four steps [7]. First, the hemostasis process stops the leakage of blood, thanks to blood clotting and coagulation. At the same time, the inflammatory phase begins, controlling bleeding and preventing infection. During this phase, damaged cells, bacteria and other pathogens are removed from the site of infection. The white blood cells, nutrients, enzymes and growth factors needed at the site of infection to heal and repair cells are the main cause for the swelling, pain, heat and redness seen on a wound. At the end of this phase, when the wound is rebuilt with new tissue of extra-cellular matrix, the proliferative phase can begin. This phase consists of the building of new tissues and vascularization of the wound. Finally, the wound healing process ends with the maturation phase, when the cells no longer needed are removed and collagen is remodeled.

The process of wound healing is long and complex, and artificial wound dressings have been designed to optimize the recovery of the skin's primary function. Historically, the first wound healing methods can be traced back to the antiquity, with the use of plasters or oils [8], which were good to prevent infections, but made the bandages less adhesive to the wound. The introduction of antibiotics during 19th and 20th century was a major

breakthrough to prevent infection and reduce mortality. The "modern era" of wound dressing products began during the 20th century, with dressing composed of highly adsorbent materials that can deliver antibiotics or growth factor upon the site of wound. Demir et al [9] listed the characteristics needed to design an efficient wound dressing, summarized in Figure I.2 :

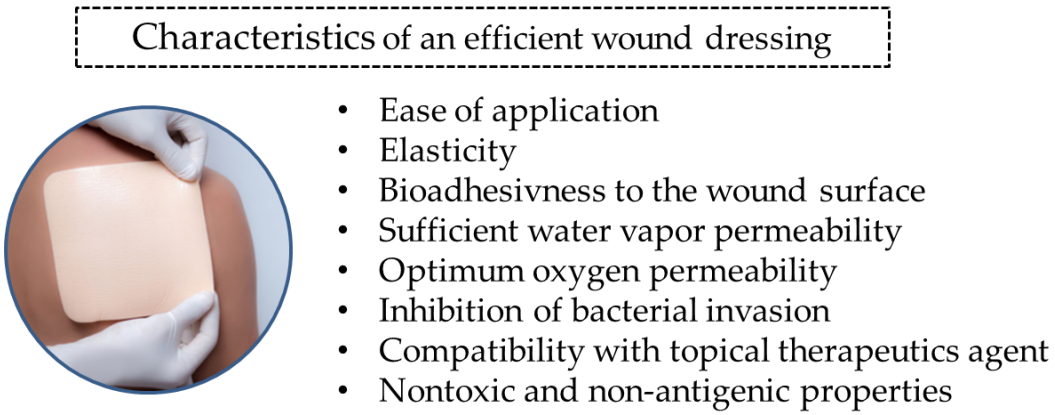

Figure I.2: Characteristics of an efficient wound dressing

For this project, the functionalization of nanocellulose with cyclodextrins aims to bring added value in terms of release of active ingredients and antimicrobial activities to films that already have other characteristics that make them relevant for the manufacture of wound dressing

I.1.3. Tissue Engineering

Tissue engineering aims to develop functional substitutes for damaged tissues [10]. The development of a biological substitute to maintain, restore, or improve tissue function implies to focus on three key aspects, schematized in Figure I.3: the production of a biocompatible scaffold with properties supporting cell growth and proliferation of the adequate cell type having also appropriate signals to induce cell differentiation and tissue formation.

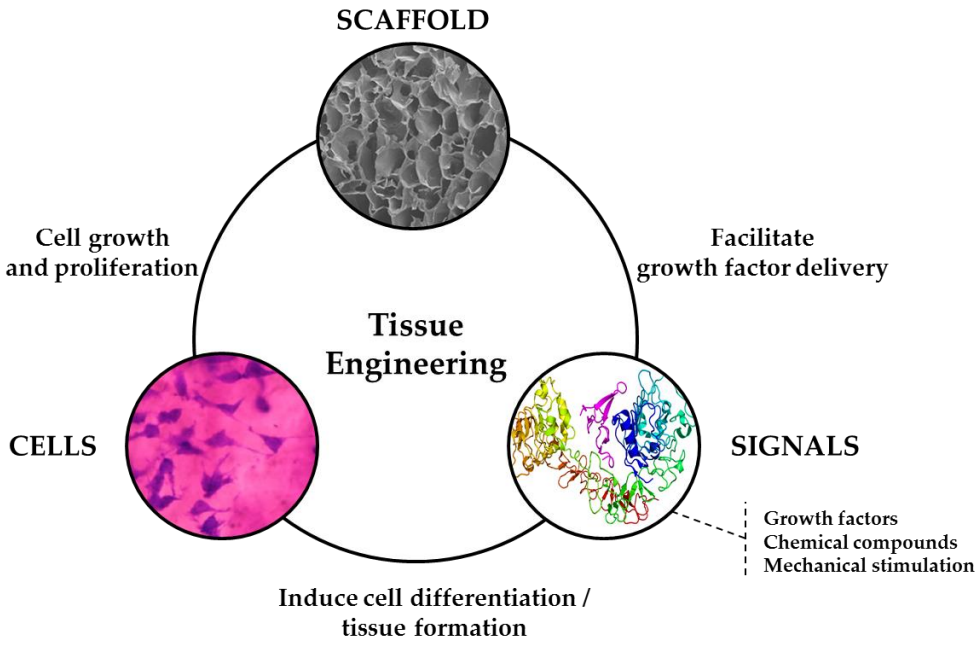

Figure I.3: Schematic representation of tissue engineering strategy

Two main approaches exist to create a tissue engineered construct. The first approach is to use the scaffold as a cell support *in vitro* by seeding cells that will produce the foundations of the tissue upon transplantation. The second approach is to load the scaffold with growth factor or chemical compounds upon implantation, so cells from the body are recruited to form the tissue throughout the scaffold matrix [11]. These two approaches are not exclusive and can be combined for better results.

The cells used to create a tissue engineered construct will depend on the final applications. The most common cell types used are stem cells. Stem cells are defined as any cell that has the ability to self-renew, differentiate and are immortal in vivo. There is a variety of potencies and differentiation potential depending on the type of stem cell. We usually differentiate three types of stem cells: Embryonic stem cells (ESCs), Induced pluripotent stem cells (iPSCs) and adult stem cells.

Scaffolds need to exhibit several features and should be carefully designed for each targeted tissue. They should possess the ability to mimic the form and function of the extracellular matrix (ECM) to promote good cell-material interaction (invasion, attachment, migration differentiation and proliferation), hence having mechanical properties that match the ECM, as well as topological properties and roughness. They should also present porosity (pore size, pore interconnectivity) sufficient for the transport of nutrients and cells, and allow the

vascularization of the scaffold [12]. To improve the properties of these materials for tissue engineering applications, the incorporation of growth factors into these structures can also be considered. Growth factors are molecules that promote growth, differentiation, and the formation of new cells, and are cell specific.

I.2. Microbiology and Active Principal Ingredients

One of the inherent challenges when using of biomaterials is the risk of infection by microorganism during the implantation. It is mandatory to have a look on microbiology to better understand the mechanisms involved.

Microbiology is the field of science dedicated to the study of microorganisms, living microscopic organisms. They represent most of the life on Earth and include bacteria, fungi, algae and protozoa. They are essential to the human life and the environment, e.g. participating in the carbon and nitrogen cycle. They are also widely present in the human microbiota, playing an important role in the digestion, but also on the human skin. However, some microorganisms are pathogeneous and therefore responsible for infectious diseases. In this part, we will focus mainly on bacteria, which are responsible for most of the infections.

Bacteria are unicellular prokaryotic microorganisms, which means that they possess one unique chromosome without nuclear membrane. Bacteria display a wide variety of shapes and sizes, but the majority of the bacterial species are either rod-shaped (*bacilli*) or spherical (*cocci*) [13]. Dimensions vary from 1 to 10 μm. *Cocci* bacteria can be organized in pairs (*diplococci*), group of four (*tetrads*), chains (*streptococci*), cubes (*sarcinae*) or cluster (*staphylococ*ci), while *Bacilli* are organized in pairs (*diplobacilli)* or in chains (*streptobacilli*). The shape of a bacteria is linked to the membrane structure and has an impact on the nutrient uptake, the adherence and the motility [14]. A distinction is usually made between two types of bacteria, classified according to the composition of their cell wall, by what is known as the Gram stain. The Gram stain is a protocol developed by Hans Christian Gram in 1884, allowing to differentiate bacteria by the chemical and physical properties of their cell wall. Gram positive (G+) bacteria have a cell wall composed of a single membrane covered with a peptidoglycan layer, while Gram negative (G-) bacteria have a cell wall composed of a thin peptidoglycan layer between two membranes, as displayed in Figure I.4.

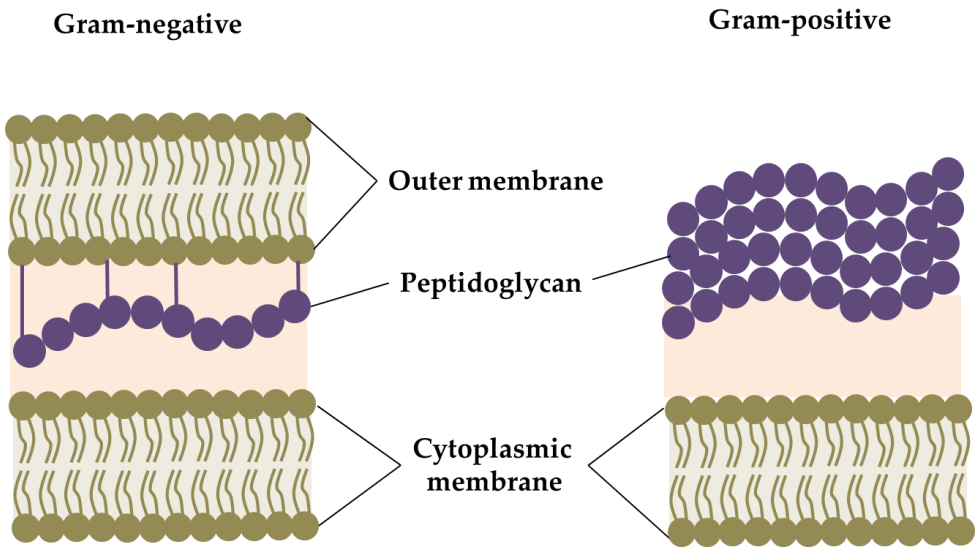

Figure I.4: Cell membrane schematic representation. Adapted from [15]

The difference in the composition of the cell wall structure has an impact on the susceptibility of bacteria to various API, depending on their mode of actions which will be highlighted later in the manuscript. These differences in composition, size and shape of the bacteria also lead to different mode of growth and potential toxicity. Microorganisms are classified into four different groups according to their potential infection risk. These groups are the following, as defined by the World Health Organization [16]:

- Group 1: Microorganisms which are unlikely to cause human or animal disease.

- Group 2: Pathogens that can cause human or animal disease but are unlikely to be a serious hazard to laboratory workers, the community, livestock or the environment. Laboratory exposures may cause serious infection, but effective treatment and preventive measures are available and the risk of spread of infection is limited.

- Group 3: Pathogens that usually cause serious human or animal disease but do not ordinarily spread from one infected individual to another. Effective treatment and preventive measures are available.

- Group 4: Pathogens that usually cause serious human or animal disease and that can be readily transmitted from one individual to another, directly or indirectly. Effective treatment and preventive measures are not usually available.

Mechanisms of bacterial pathogenicity are multiple, as displayed in Figure I.5.

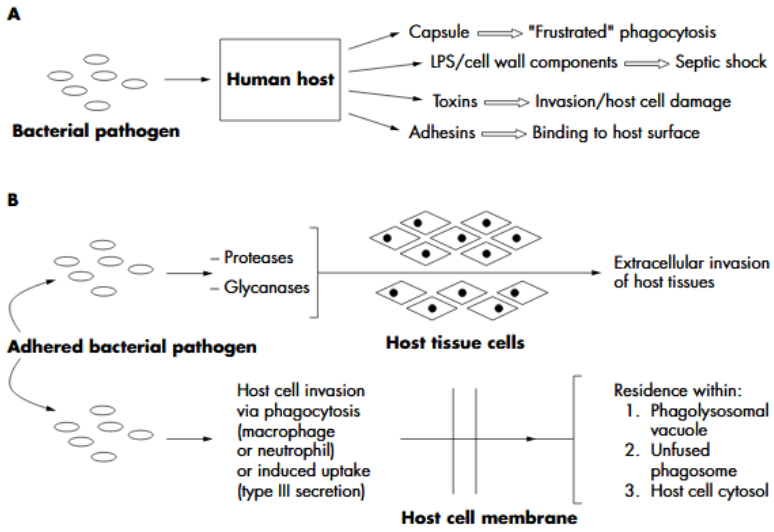

Figure I.5: Overview of bacterial mechanism for pathogenicity. Figure from [17]

In this study, we will use two strains of bacteria responsible for the majority of infections to characterize the antibacterial efficacy of our devices: a Gram-positive strain, S. aureus, and a Gram-negative strain, E. coli. Both strains are classified as class 2 micro-organisms.

In this study, we want to see if the different materials produced can have an antimicrobial activity. There are multiple microbiology protocols for determining the antimicrobial properties of materials. Of these, the one we used in this project is based on the Kirby Bauer test. This test is based on a disk diffusion method and was initially used to evaluate the sensitivity of a bacterial strain to a known antibiotic. In our case, we use this method to estimate the efficiency of our materials when our API is released and diffused on the agar. The steps are the following: i) Petri dishes containing nutrient agar of the suited nutrient broth are prepared. ii) Inoculum of the bacterial strain is prepared at 0.5 McFarland units. McFarland's are a measure of turbidity, which gives an equivalence of the concentration in colony-forming units (CFU) of the bacterial strains. iii) The inoculum is inoculated on the agar and circles of samples are placed on the agar. iv) Petri dishes are incubated for the suited amount of time at 37°C. v) After incubation, a bacterial mat is formed and, around the samples, 3 different results could be observed, schematized in Figure I.6.

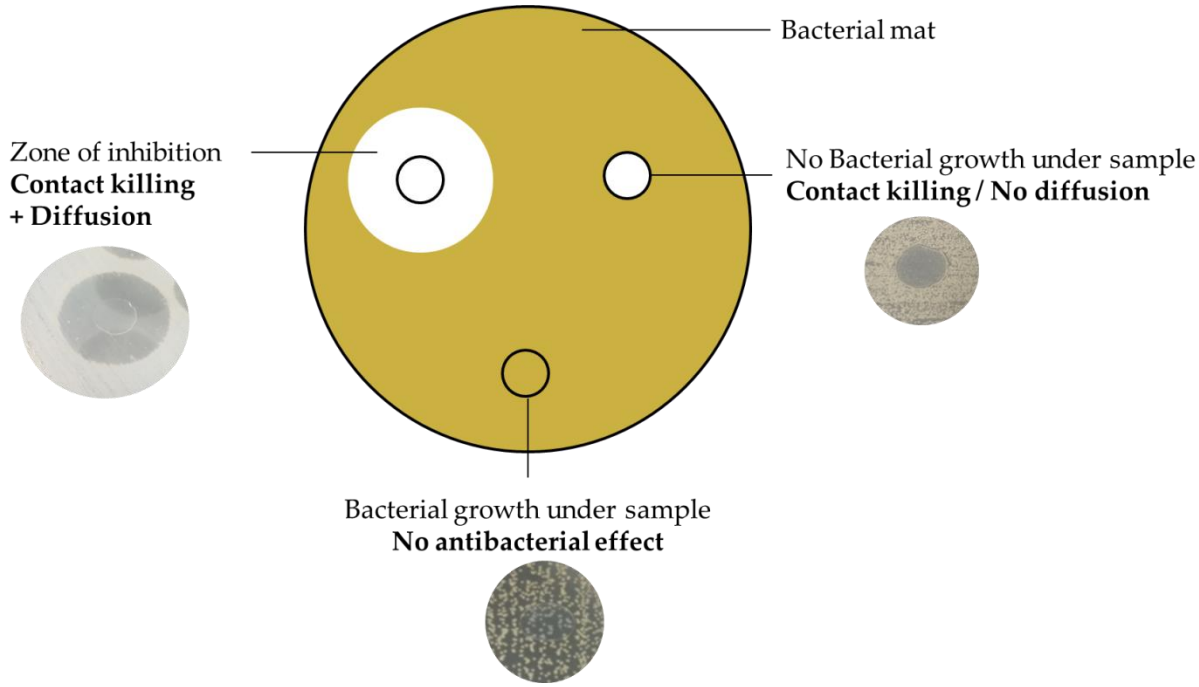

Figure I.6: Schematic representation of the disk diffusion method.

A zone of bacterial inhibition is observed if the bacterial growth was inhibited or if the bacteria were killed. The size of inhibition zone will depend on the diffusion properties of the API, its concentration and its efficiency against the bacterial strain tested.

Active Principal Ingredients

One of the most predominant strategies to improve biomedical devices is the use of Active Principal Ingredient (API) to prevent infections in the case of wound healing with chemical agents or to induce cell growth, proliferation and differentiation with growth factor in the case of tissue engineering

Chemical agents

The most used family of chemical agents to prevent infections is antibiotics. They are synthetic antimicrobial agents with specific effects against bacteria. Five different mechanisms are identified [18] :

- Inhibition of the cell wall synthesis
- Inhibition of the cell wall function
- Inhibition of protein biosynthesis
- Inhibition of nucleic acid synthesis

- Inhibition of other processes, such as folic acid metabolism.

Figure I.7 gives an overview of the different modes of action as well as some examples of antibiotics for each mode of action.

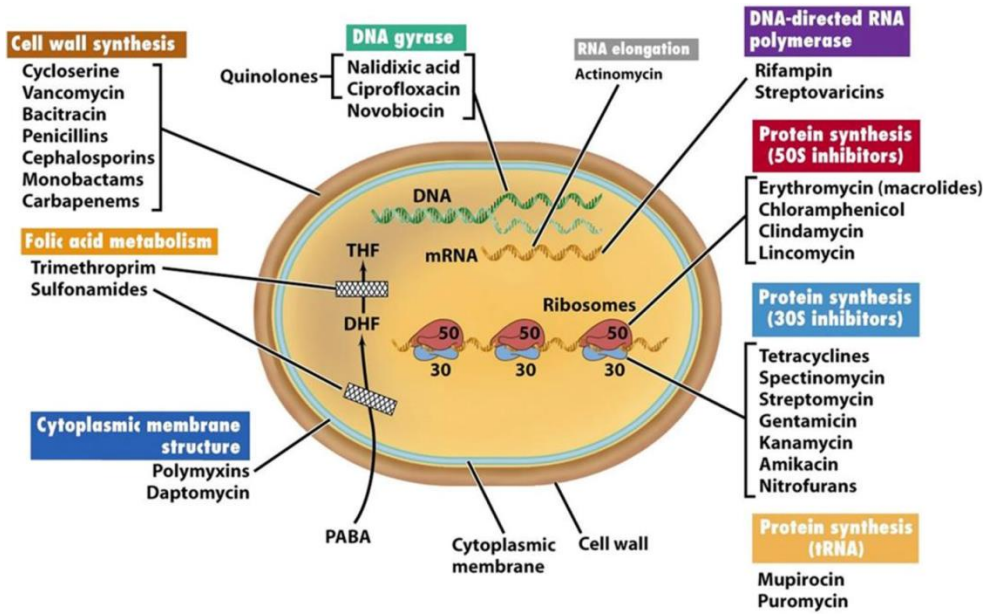

Figure I.7: Mode of actions of the principal families of antibiotics. Extracted from [19]

Each antibiotic has a different spectrum of activity, and can be bacteriostatic (i.e. it inhibits the proliferation of bacteria) or bactericide (i.e. it lyses bacteria). However, the use of antibiotics presents two major drawbacks. Firstly, they can present toxicity and side effect for the patient. And more importantly, bacteria can develop an antibio-resistance to the antibiotic, making them ineffective if used at too large scale. For this reason, research tend to find new antibiotic molecules in the nature, such as in honey or essential oils, that have been proven to display antimicrobial activity [20], [21].

Antibiotics remain the most widely used chemical compounds, but there is also reported evidence of antimicrobial effect from other compounds:

Metal ions, such as copper, silver and zinc ions present inherent antibacterial activities [22] and display a synergistic effect in the presence of some antibiotics [23]. However, there are some concerns about the bioremediation and the possible toxicity of these metals on humans and its environment [24]. Quaternary ammonium compounds display activity on the cell membrane stability [25]. By interacting with the cytoplasmic membrane, they initiate the

immediate leakage of intracellular constituent leading to the lyse of the bacteria. Some are currently used as a disinfectant, e.g. benzalkonium chloride is used as a cleaner and sanitizer [26]. Antimicrobial peptides are natural peptides produced by several organisms (animals, plants, bacteria, fungi) as a host-defense mechanism against pathogens. They display interesting antimicrobial properties, however, the synthesis of such molecules might be a hindrance to their use [27]. Finally, oxidizing agents, such as hydrogen peroxide or chlorine, are also used as disinfectants. The oxidation of the cell membrane leads to the lysis of the bacteria.

For this project, we chose to use as a model molecule sulfadiazine, a broad-spectrum sulfonamide antibiotic commonly used in the prevention of infections and, together with its silver derivative, in the treatment of burn wounds. The properties and uses of this molecule will be discussed in more detail in the following sections.

I.3. INTRODUCTION ON BIOMATERIALS

I.3.1. DEFINITION AND HISTORY

A biomaterial is a material exploited in contact with living tissues, organisms or microorganisms [28]. This term should not be confused with *biobased materials*, which are materials extracted from the biomass, such as biopolymers or biomacromolecules. Biomaterials must be biocompatible, meaning that they have the ability to be in contact with living systems without producing an adverse effect. Biomaterials are crucial tools for many biomedical applications, such as wound dressing, drug delivery, implants and tissue engineering [29]. This field of study is called biomedical engineering and is at the crossroads of multiple fields such as chemistry, medicine, material science and mechanical engineering to name a few.

Historically, the first biomaterial can be traced back to the late 40's [30], with the observation by Harold Ridley, a British ophthalmologist, who reported that poly(methyl) methacrylate shards in a pilot's eye healed without exterior intervention. This observation lead to the creation of the first implant lenses. At the beginning, biomaterials were used to replace deficient organisms and were content to be inert, and the field of research had to evolve in order to offer biomaterials that could provide new functions and could possibly be

responsive to external stimuli. Depending on the applications, a variety of materials can be specifically engineered to produce biomaterials, such as metals, ceramics, composites or polymers. Metallic biomaterials are used for load bearing applications due to their high fatigue strength. Ceramic biomaterials are used for bone bonding surfaces in implants and articulating surfaces due to their hardness and wear resistance. Polymeric materials are usually used in wound dressing applications for flexibility and stability. Some examples of different biomaterials and their applications are shown in Figure I.8.

The most important property of biomaterials is the biocompatibility, i.e. the ability of the material to perform within the host for a particular application. Other important factors are the mechanical properties, which need to match the properties of the implantation site, non-fouling properties, and biodegradability. All of these properties need to be controlled. Another important aspect in biomaterials is the bioreaction, i.e. the biological response to a material. These bioreactions can be cell spreading, protein adsorption, bacterial adhesion to name a few. These bioreactions are dependent of the properties of the materials such as the surface chemistry, porosity, mechanical properties, and swelling behavior.

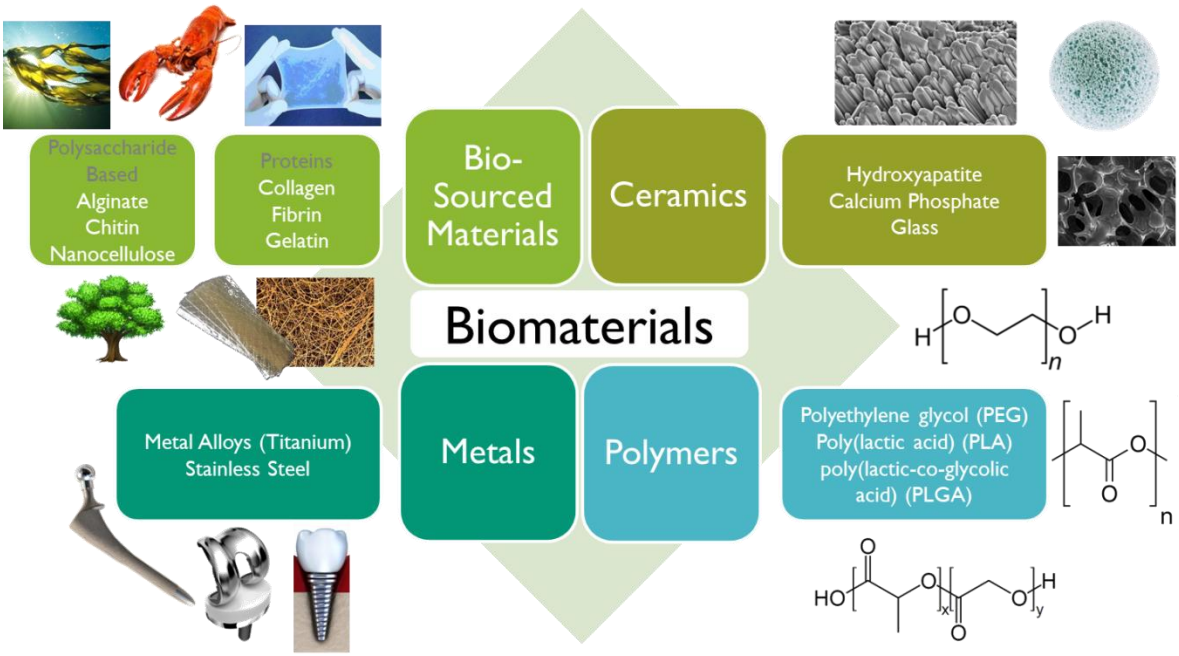

Figure I.8: Most commonly used biomaterials. Extracted from [31]

1.3.2. Different classes of biomaterials

Ceramics

Ceramics are interesting materials for biomedical applications, more specifically for orthopedics, dentistry and hard tissue engineering. Their good biocompatibility, moderate degradation and high mechanical strength lead to the ideal candidate for applications needing high mechanical resistance [32]. Bioceramics (ceramics used in biomedical applications) can be divided into three subclasses: bio-inert, bioactive and bioresorbable, with various properties and applications, as displayed in Table I.1.

Bioinert ceramics are mostly used in implants that must withstand important and regular mechanical pressure, for a long period, making them mainly used in orthopedics. Bioactive ceramics, with their ability to interact and form bonds with surrounding living tissues are used for reconstruction application. Finally, bioresorbable ceramics, such as hydroxyapathite, have found applications in the construct of scaffold materials.

Table I.1: Applications for the different Bioceramics

Bioceramics	Exemples	Advantages	Inconvenient	Applications	Ref
Bioinert	Zirconia, Alumina	-High hardness -Low friction -Wear and corrosion resistance - Physicochemical stability	-Weak in tension -No biodegradation	Implants for reconstructions (Knee, Hip, Shoulder, Elbow…)	[33]
Bioactive	Bioglass	-Induce the host response	Fragile	Spinal fusion	[34]
Bioresorbable	Hydroxyapathite	-Biodegradable	-Potential toxicity of the degradation products	Tooth, bone	[35]

Metals

Metallic materials are divided into two categories: pure metals and metallic alloys. These materials are widely used in orthopedic applications due to their high fatigue strength and mechanical strength, which allow them to withstand daily constraints. The most used

metallic materials are 316L stainless steel, cobalt chromium alloys (CoCrMo), and titanium-based alloys (Ti-6Al-4V) [36]. Some examples of the different metals used for different applications are displayed in Table I.2. The major drawback for the utilization of metallic materials is the potential release of metallic particles due to corrosion. These particles can be toxic and provoke infection reaction from the immune system [37].

Table I.2: Types of metals for various applications. Extracted from [38]

Division	Example of implants	Type of metal
Cardiovascular	Stent Artificial valve	316L SS; CoCrMo; Ti Ti6Al4V
Orthopedic	Bone fixation (plate, screw, pin) Artificial joints	316L SS ; Ti ; Ti6Al4V CoCrMo; Ti6Al4V ;Ti6Al7Nb
Dentistry	Ortodontic wire Filling	316L SS ; CoCrMo ; TiNi ;TiMo AgSn(Cu) amalgam, Au
Craniofacial	Plate and screw	316L SS; CoCrMo; Ti; Ti6Al4V
Otorhinology	Articial eardrum	316L SS

POLYMERS

With a variety of physical properties, an important availability and tailoring possibilities, polymers are widely studied for medical applications. Polymers can be tailored in terms of size (molecular weight), mechanical properties, hydrophobicity and chemical functionalization depending on the targeted applications. This versatility allows them to be widely utilized as biomaterials. We will differentiate the polymers into two classes: Synthetic polymers and natural polymers.

SYNTHETIC POLYMERS

The synthetic polymers can be divided into two sub-categories: Petroleum-derived polymers and biobased synthetic polymers.

Petroleum derived polymers can be used as biomaterials for numerous applications where their specific properties are particularly interesting. Among them, their attractive flexibility as well as the relatively low melting temperature (in comparison with metals and ceramics) allow for an easy melt processing, and the design of flexible structures, which have led to their use in the design of flexible vascular grafts for example. Table I.3 gives an overview of the main types of synthetic polymers used for biomedical applications and reviews their use as biomaterials:

Table I.3 : Types of petroleum-based polymer for various applications. Adapted from [39]

Petroleum-based polymers	Example of applications
Polyesters	Suture, drug delivery, scaffold
Polycarbonates	Membrane for oxygenator, hemodialyzer
Polytetrafluoroethylene	Vascular graft
Polyethylene	Artificial knee prostheses
Polyvinyl chloride	Extracorporeal devices
Silicone rubber	Artificial skin
Polymethyl methacrylates	Bone cement

However, the use of petroleum-based polymers presents several issues. First of all, the petroleum resources are finite, and from an ecological point of view, it would be better, if possible, to use more biobased materials. Additionally, the release of by-products, plasticizers or initiator induced by the degradation in physiological conditions can cause an inflammatory response. However, petroleum-based polymers are currently the most used type of polymers, but the use of bio-sourced polymers tends to increase with advances in research. In the case of synthetic biobased polymers, the raw material comes from biomass,

and, similarly to petrol-based polymers they undergo several processing routes to obtain the final synthetic polymer.

Among the synthetic biobased polymers, the polylactic acid (PLA) is currently the most used for medical applications. This homopolymer is synthetized from starch and is nowadays considered the first natural alternative to petroleum-based polymers. With its thermoplastic behavior, allowing to manufacture highly specific products with ease, its suitable mechanical properties, as well as biodegradability and low-cost, PLA is promising for applications in almost all of the healthcare areas [40]. Current limitations for its use are price, source and degradability/recyclability. Indeed, the price is still higher than for fossil based plastics. The first generation PLA uses food crop as raw materials, which can induce pollution via intensive agricultural practices, and it is not really compostable, nor recyclable with other plastics [41].

I.3.3. Focus on natural polymers

Biopolymers (also called natural polymers) are organic molecules synthetized by living organisms. They can be from diverse origins, such as animals (collagen, chitin / chitosan), plants (starch, cellulose), bacteria (bacterial cellulose), algae (alginate) or fungi (chitin / chitosan) [42]. These materials present some advantages in comparison to synthetic polymers due to their biodegradability, biocompatibility and renewability [43]. The most used biopolymers for wound healing or tissue engineering are collagen and polysaccharides such as chitosan, alginate, hyaluronic acid and cellulose. Since the use of cellulosic materials will be described thoroughly later in the text, this part will focus on the others.

Collagen

Collagen is one of the most important proteins in the extracellular matrix of mammalian cells. The main sources of collagen are bovine, porcine, poultry and marine (wild and farmed fish), with the bovine market representing 35% of the gross production in 2019 [44]. But, due to a rising demand for collagen and increasing concerns about the disease transfer from raw materials sources, marine sources are expected to grow in the following years. This material is of great interest for biomedical applications because of its intrinsic mechanical properties, which mimic what can be found in the biological system without modification. In addition, due to its weak antigenicity, good biocompatibility, good cell

adhesion that it promotes and its biodegradability, it is the most used biopolymer in tissue engineering [45]. Collagen has been used in wound healing applications [46], as well as tissue engineering scaffold [47], with promising results. Moreover, collagen can be used in formulations for 3D printing ink, opening the door to more structured scaffold with controlled porosity [48]. Figure I.9 presents some examples of studies using collagen as the primary biomaterial. However, its animal source and the competition with food industry could present an obstacle for its use.

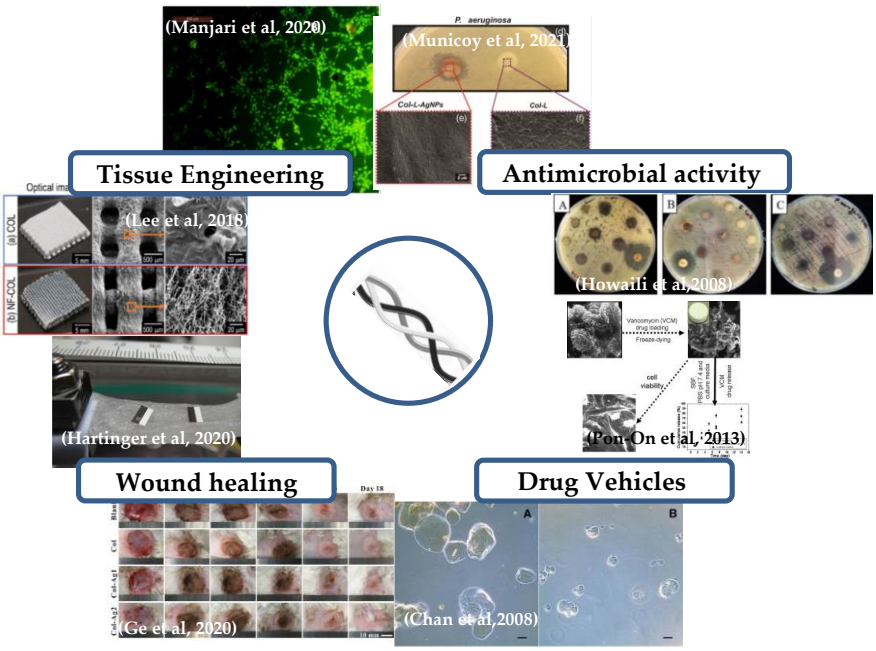

Figure I.9: use of collagen in biomedical applications : tissue engineering [48], [49] ; wound healing [50], [51] ; drug vehicles [52], [53] ; antimicrobial activity [54], [55]

POLYSACCHARIDES

Polysaccharides are, along with oligosaccharides, the most abundant group of biopolymers [56]. They consist of polymer chains of carbohydrates composed of monosaccharide units bound together by glycosidic linkages. Their function in nature could be either for energy storage, such as starch, which can be digested by both human and animals thanks to amylases (i.e. enzymes that can break alpha-linkages of starch), or structure, such as cellulose. Indeed, the structural components of plants are made primarily

of cellulose. It exists a wide variety of polysaccharides from different sources and with varying properties. Following, the most used polysaccharides for biomaterial applications are presented (see also Figure I.10).

Chitin and chitosan

Chitin is present in crustaceans, mollusks, insects and can be synthetized by some fungi. It is composed of β-(1-4)-N-acetyl-D-glucosamine units and is the second most abundant biopolymer on earth after cellulose. Chitosan is obtained from chitin via a partial deacetylation by acid or enzymatic hydrolysis [57]. Chitosan has been shown to accelerate the tissue regeneration and stimulate hemostasis [58]. Additionally, chitosan is the only cationic biopolymer. Thanks to its positively charged molecules, it can target the negatively charged cell wall of bacteria and display natural antibacterial effect [59]. It also displays good biocompatibility and biodegradability [60]. However, their low mechanical properties may be a drawback for their use in tissue engineering applications.

Alginate

Alginate is extracted from algae and is composed of β-D-mannuronic acid and α-L-guluronic acid linked by α-(1-4) glycosidic linkages. In a dressing, alginate provides a moist environment and absorbs the exudate, helps the hemostasis process and lowers the infection of the wound [61]. Alginate is used in pharmaceutical applications as a thickening, gel forming or stabilizing agent [62], for drug delivery or protein delivery [63]. Its gel-forming ability, biocompatibility, non-cytotoxicity and high absorption capacity have made alginate based-hydrogels widely used for wound healing applications.

Hyaluronic acid

Hyaluronic acid (HA) is a biopolymer naturally present in the skin, composed of D-glucuronic acid and N-acetyl-dD-glucosamine linked by alternating β-1,4 and β-1,3 glycosidic linkages. Hyaluronic acid is produced either by extraction from animal tissues (mainly rooster combs) or synthetized by the strain of bacteria *Streptococcus* [64]. The main features of HA are its structural characteristics, a random coiled structure in solution caused by a combination of internal hydrogen bonds, the chemical structure of the disaccharides and interactions with solvent [65]. This particularity has an impact on the viscoelastic properties of HA in solution. In addition, the natural presence of HA in the extracellular

matrix and its biocompatibility have made it interesting for a wide variety of applications in the medical field, such as tissue engineering, cancer treatments [66] or in cosmetics [67]. Figure I.10 presents the structure of chitin/chitosan, alginate and hyaluronic acid.

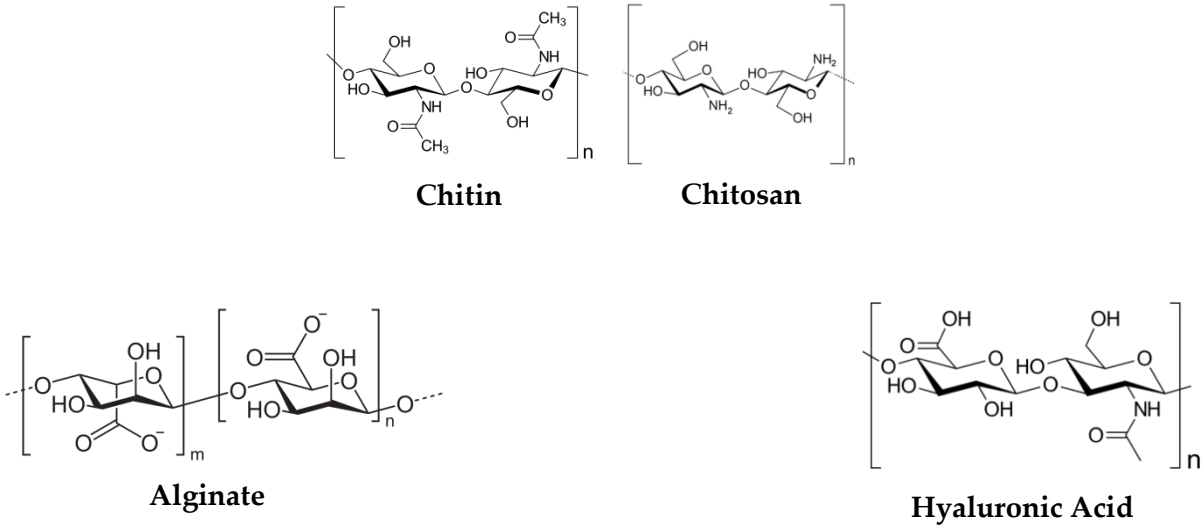

Figure I.10: Chitin/Chitosan, Alginate and Hyaluronic Acid

CELLULOSE DERIVATIVES

Since cellulose and nanocellulosic materials will be the focus of the next part, only cellulose derivatives used in medical applications will be discussed here. Amongst the variety of cellulose derivatives available, two have been mainly regarded as beneficial for medical applications: cellulose ether derivatives and cellulose ester derivatives [68]. Figure I.11 displays the different routes of conversion to obtain these cellulose derivatives and their respective chemical structures. Cellulose derivatives displays various properties such as an increased solubility, tunable viscosity and surface activity making them interesting for applications such as drug excipient, film formation and prolonged release [69].

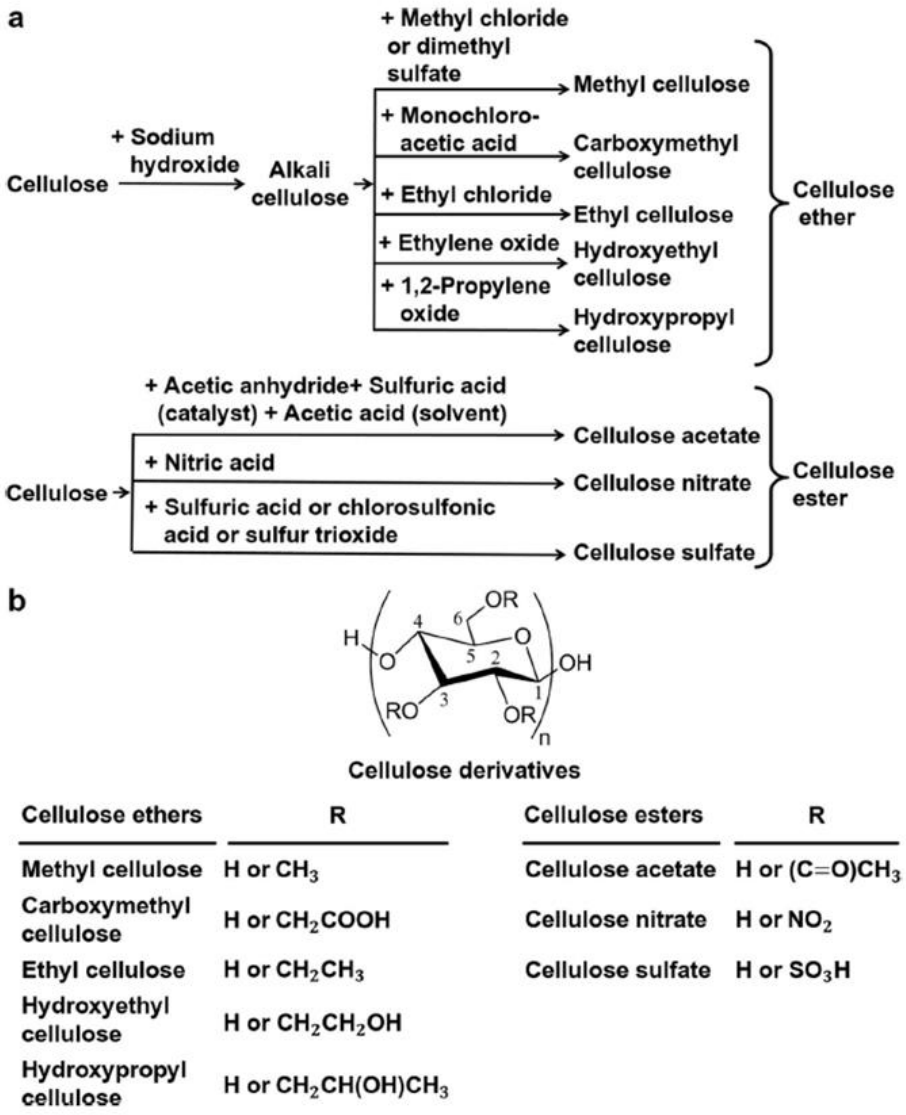

Cellulose ethers	R	Cellulose esters	R
Methyl cellulose	H or CH_3	Cellulose acetate	H or $(C{=}O)CH_3$
Carboxymethyl cellulose	H or CH_2COOH	Cellulose nitrate	H or NO_2
Ethyl cellulose	H or CH_2CH_3	Cellulose sulfate	H or SO_3H
Hydroxyethyl cellulose	H or CH_2CH_2OH		
Hydroxypropyl cellulose	H or $CH_2CH(OH)CH_3$		

Figure I.11: classification of cellulose derivatives A) chemical conversion procedure of cellulose to its derivatives. B) Chemical structure of cellulose derivatives. Extracted from [70]

This section has presented the different types of medical applications currently being studied, trying to explain their objectives, methods and constraints. A description of the fundamental principles of microbiology has been presented to facilitate the understanding for the readers when reading the main results of this thesis. Finally, the materials currently used for medical applications have been presented in order to better position our proposal in the current market. The following section will focus more specifically on our raw material, namely nanocellulosic materials.

II. NANOCELLULOSIC MATERIALS

Nanocelluloses, especially cellulose nanofibrils, are at the heart of this project. The aim of this chapter is to describe the three different types of nanocellulose that exist, their origins and production processes, in order to illustrate the variety of materials available. The different ways of material elaboration and the characteristics obtained will be presented. Finally, the different applications of these materials will be presented with a focus on the biomedical applications. The objective of this chapter is to elaborate on the choice and the relevance of the material used in the project.

II.1. DIFFERENT CLASSES OF NANOCELLULOSES

Cellulose is the most abundant biopolymer on earth. Produced by photosynthesis at a rate of 10^{11}-10^{12} tons/year [71], it is a renewable source of raw material for multiple applications. Cellulose is mainly found in the plant cell wall, where the cellulose chains are organized in elementary fibrils up to a full cellulose fiber as shown in Figure I.12, but can also be produced by bacteria or even by some marine animals such as tunicates [72].

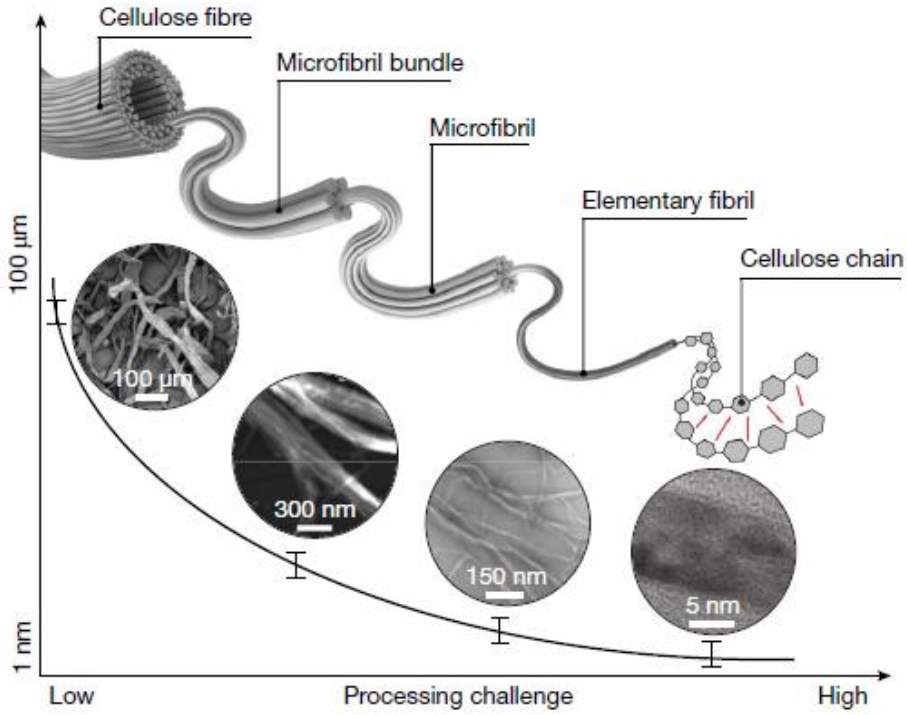

Figure I.12: Schematic description of the hierarchical structure of fibrillated cellulose. Extracted from [73]

II.1.1. CELLULOSE STRUCTURE AND PROPERTIES

Historically, cellulose was first isolated from several plants by Anselme Payen in 1838 [74], with a treatment based on nitric acid. Payen made the observation that the cell wall

structure of several plant materials was made of the same fibrous materials, which he named cellulose. However, the determination of the basic cellulose formula $C_6H_{10}O_5$ was first established in 1913 [75]. A succession of investigations during the 20th century led to the final characterization of the cellulose chain: a linear homopolymer of anhydro-D-glucopyranose units (AGU) linked by β(1-4) glycosidic linkages. These β(1-4) linkages alternately point in opposite directions, hence the repeating unit of the cellulose is composed of two AGU and is called cellobiose. Additionally, AGU are in chair conformation, with hydroxyl groups in equatorial positions, which favors the intra- and inter molecular interactions due to hydrogen bonding. The structure of cellobiose and of a cellulose chain is presented in Figure I.13.

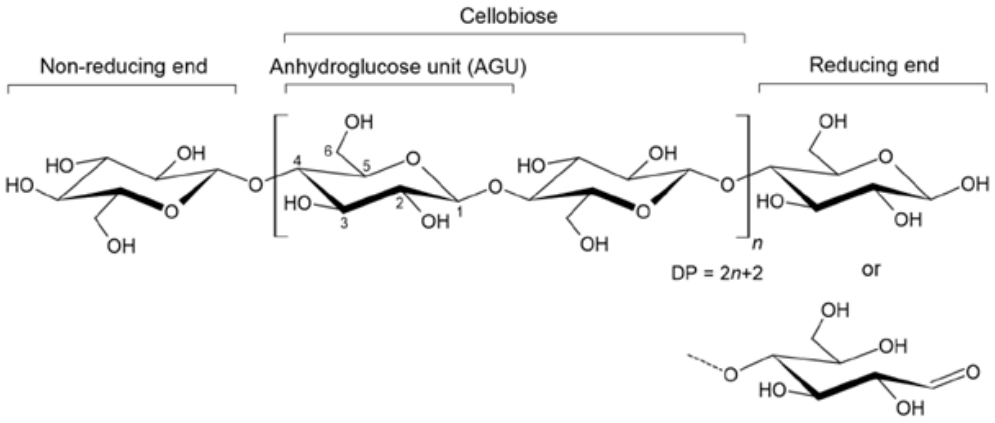

Figure I.13: Chemical structure of the cellulose chain, identifying the cellobiose unit, as well as the reducing and non-reducing end of the cellulose molecule.

The high number of free hydroxyls groups and possible hydrogen bonding are the reason for two important characteristics of cellulose chains: its crystallinity and its chemical reactivity.

CRYSTALLINITY

Cellulose chains can present several ordered crystalline arrangements, due to their high number of free hydroxyl groups and potential hydrogen bonding. This property is called polymorphism, and each arrangement is defined as an allomorph. In total, four different allomorphs were identified, known as cellulose I, II, III and IV [76]. The native and most abundant form of cellulose, is cellulose I. The other allomorphs can be obtained through various treatments, such as mercerization (i.e. treatment with a caustic solution) or

regeneration. The transformation of cellulose I into its different allomorphs is schematized in Figure I.14.

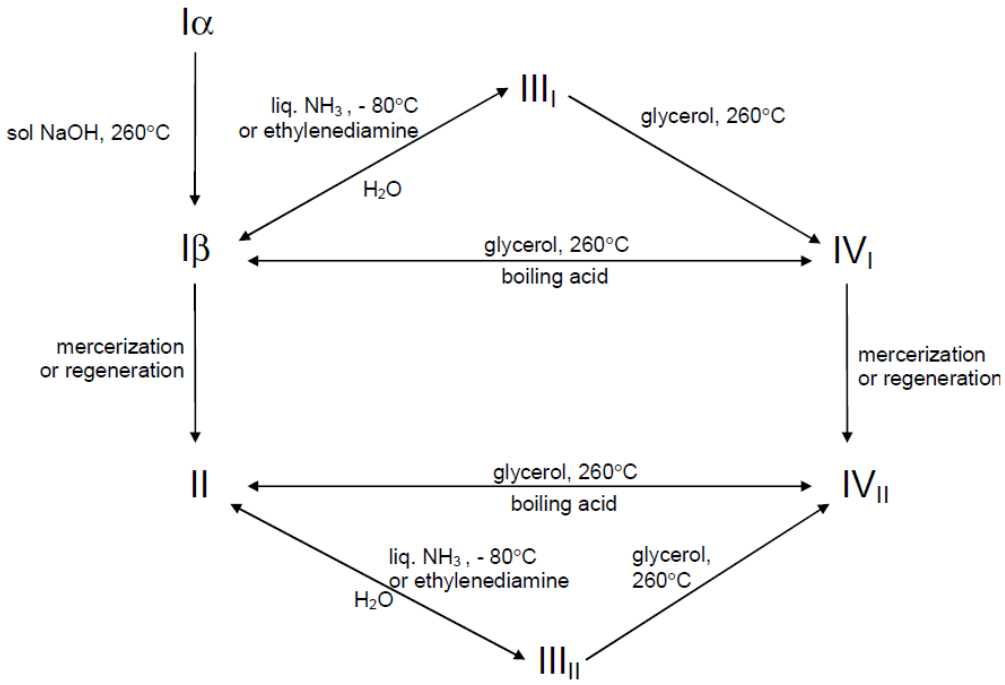

Figure I.14: relationship between the different cellulose allomorphs. Extracted from[76]

However, cellulose is also composed of amorphous domains, which have a great influence on most of the chemical and physical properties of cellulose materials. Both the crystalline and amorphous domains of cellulose impact the interactions of the fibers with water, enzymes or any reactive substance, as well as their physical and mechanical behavior. Crystallinity can vary among the sources and is thus an important point to consider.

Chemical reactivity

The presence of three hydroxyl groups in each AGU leads to a high chemical reactivity of cellulose. These hydroxyl groups can be substituted by esters, ethers, or other functional groups, making cellulose an interesting platform for functionalization. Additionally, these hydroxyl groups make cellulose hydrophilic, which is a key property.

Cellulose fibers are organized into fibrillary elements, with a width comprised between 10µm and 50µm, and a length of several µm. The dimensions can vary depending on the source of cellulose. The polymer chains are composed of crystalline ordered domains linked by amorphous regions, and the chains are aggregated and stabilized by hydrogen bonds.

These cellulose fibers are the raw materials when producing nanocellulosic materials. The first step is to isolate the cellulose fibers, which will be explained in the following part.

II.1.2. CELLULOSE IN WOOD AND ISOLATION OF CELLULOSE FIBERS

Vegetal biomass, such as plants, wood, cotton or hemp, is the typical raw material for cellulose. The amount of cellulose that can be extracted differ among the sources, reaching 90% for cotton and 40% for wood. However, wood represents almost 90% of the biomass produced each year, which makes it the main source of cellulose. Wood is composed of cellulose, hemicelluloses and lignin. In order to isolate (nano)cellulose, purified cellulose fibers must be obtained and separated from the other wood non-cellulosic components, i.e. hemicelluloses, lignin, pectin and extractibles. Hemicelluloses are the second most abundant polysaccharides in the vegetal biomass after cellulose. They are usually composed of hetero-polysaccharides. Their function in wood is to bind cellulose microfibrils together to form a strong network. Lignin is the third major component of wood. Lignin binds the different constituents together, specifically by covalently linkages with hemicelluloses, which is bound to cellulose by hydrogen bonds. In addition to these three major components, wood contains extractives. Extractives, such as the pectins, phenols or tannins, are used in different applications in various industries.

The isolation of cellulose fibers from wood is a complex multi-stage process in order to remove these different components. It is interesting to note, however, that the different compounds are also being studied with the aim of recovering the by-products of cellulose isolation, as e.g. bio-fuels for hemicelluloses [77] or composite materials for lignin [78]. The improvement of the processes implemented in the isolation of cellulose fibers and valorization of the other compounds is a driving force for the development of (nano)cellulosic materials from wood compared to bacterial cellulose, which is pure by nature but complicated to produce.

It is worth noting that cellulosic (nano)materials also can be isolated from tunicates, a marine animal [79].However, the rate of production, due to the lack of raw material, is a drawback to its generalization. Here, we focus on the production of wood-based nanocellulose.

Alkali/bleaching treatment

The first step when isolating cellulose fibers from wood is a cooking process to obtain isolated and purified cellulose fibers as well as the elimination of lignin. The paper industry has implemented these methods. One of the most well-known processes is the Kraft cooking, where a hot mixture of water, sodium hydroxide and sodium sulfide are used to break the bonds between lignin, hemicelluloses and cellulose. The cooking is followed by several bleaching treatments to eliminate the colored residual lignin. At the end of these two steps, cellulose fibers are obtained. The other most frequently used process is the sulfite pulping, which is based on the actions of the bisulfite anion HSO_3^- at a temperature ranging from 120°C to 170°C. It is worth noting that the crystallinity and mechanical properties of the purified cellulose fibers are impacted by the process [80].

II.1.3. Wood-based nanocellulose production

Two main types of nanocellulose can be produced from wood: cellulose nanocrystals (CNCs) and cellulose nanofibrils (CNFs). A recent report by Global Market Insights [81] estimated a nanocellulose market size of 146.7 million USD in 2019, with a predicted growth of 21.4% annually between 2020 and 2026. Among the biggest industrial actors in this field, we can name Nippon Paper Group, CelluForce, RISE, Sappi Limited, Borregaard ASA, FPInnovations, American Process, Kruger, Daicel Corporation, Melodea Ltd., J. Rettenmaiere & Sohne, Asahi Kasei Corporation, CelluComp Ltd, Oji Holdings Corporation, Stora Enso, and Holmen AB.

The general procedure to obtain CNC and CNF from cellulose pulp is schematized in Figure I.15.

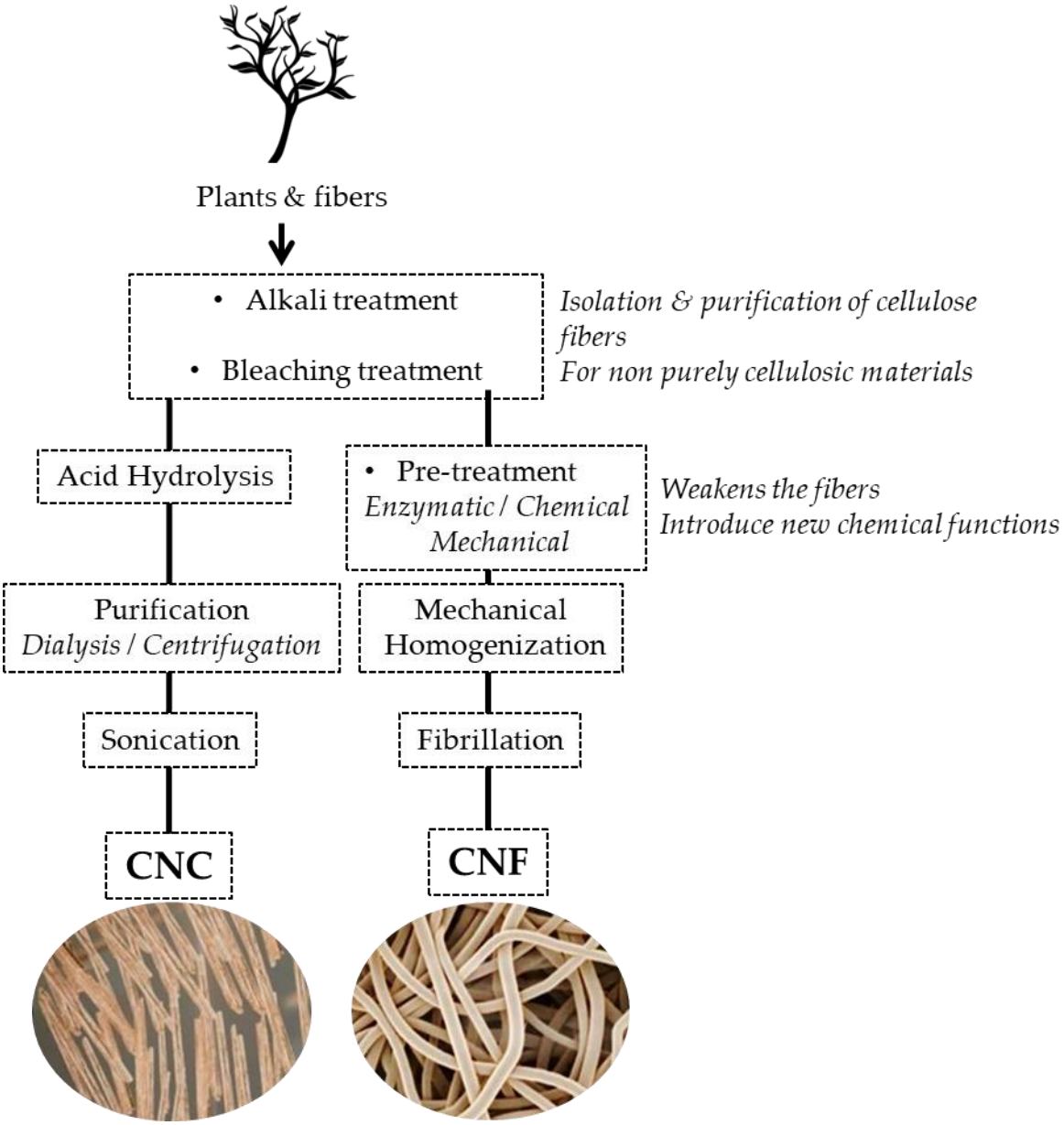

Figure I.15: General procedure to obtain nanocellulose. TEM images of CNCs adapted from [82] .

In this part, we will go into the details of CNF production, since it is the material used in this project.

CNCs

Cellulose nanocrystals (CNCs) are isolated from cellulose through different processes, such as acid hydrolysis, combined mechanical shearing, and enzymatic hydrolysis [83]. However, the main process to extract CNCs from cellulose fibers is based on acid hydrolysis [84]. The amorphous or disordered regions of cellulose are hydrolyzed and the crystalline regions, with a better resistance to acid attack, remain untouched and are released as rod-like nanoparticles of high crystallinity. The resulting suspension is washed by

successive centrifugations and dialyzed until free molecules are removed. Since the organization of crystalline and amorphous regions in the cellulose fibers differs among the sources, the final properties of CNCs depend on the source materials and on the process used for their extraction. The acid used to perform the hydrolysis can also have an impact on the surface chemistry of the CNC produced. Sulfuric acid introduces sulfate half-esters with negative charge while hydrochloric acid renders the crystals neutral.

CNCs are widely used in applications in such as composites as reinforcement due to their excellent mechanical properties or in hydrogels for medical applications. However, the lack of entanglement and low viscosity of CNC suspension might be a disadvantage for some applications, notably for sustained release, hence we choose to use CNFs in this research study.

CNFs

Production

CNFs are currently produced by a combination of chemical/enzymatic pre-treatments and mechanical treatments. Turbak et al [85] were the first to report CNF isolation by passing a cellulose suspension through a homogenizer. Nowadays, different mechanical treatments are performed [71], [86], the most common being using homogenizer [85], micro fluidizer [87] or a grinder [88]. A schematic representation of these three methods is given in Figure I.16.

- **Homogenizer**: Cellulose suspension, pumped at high pressure, passed through a small gap present in the homogenizer created by a valve and an impact ring. Valve is opened and closed rapidly and the fibers are submitted to high shear and impact forces. These forces provoke the nano fibrillation of cellulose fibers. Depending on the pretreatment, one pass is sometimes enough.
- **Micro fluidizer**: Cellulose suspension is injected using high pressure through a Z or Y shape chamber with a tiny channel diameter. Cellulose is then expulsed through an orifice with a width between 100 and 400 μm. High pressure and impacts on the channel create high shear force and fibrillate the pulp. Several passes are needed, and the chamber should be changed to improve fibrillation which can be a limit for the industrialization.

- **Grinder:** A cellulose slurry is passed through rotary and static stones. The distance between grinding stones is variable and is decreased with the number of passes. Indeed, with the number of passes, fiber size decreases and disks can be brought closer without clogging problems. Shear forces are created between the two disks and celluloses fibers are delaminated. Several passes are needed. Grinding can also be used as a pretreatment [89].

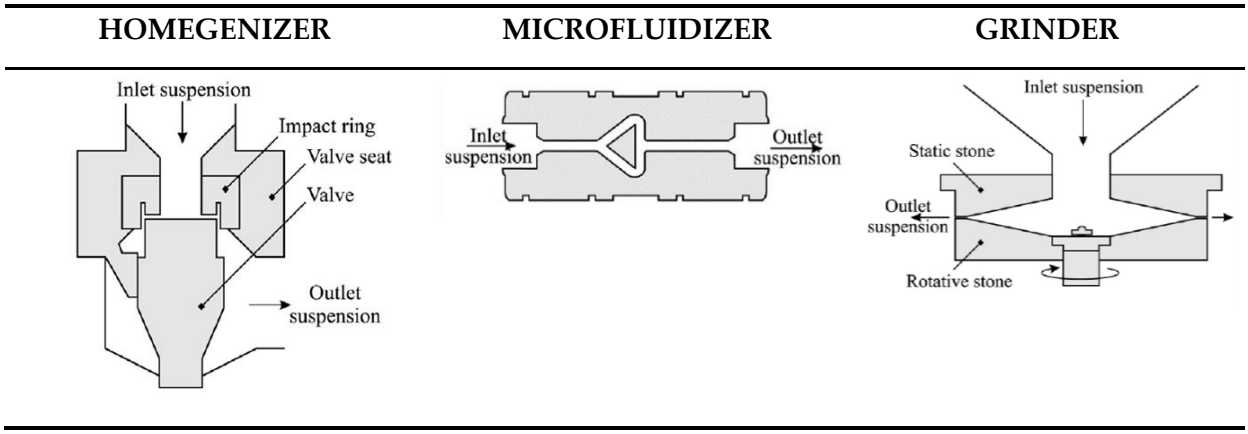

Figure I.16 : The most applied mechanical treatment for CNF productions. Adapted from [71]

These methods, while being efficient, involve huge energy consumptions. To reduce the environmental impact of such a process, pre-treatment methods have been put in place to weaken the fibers prior to mechanical treatment, thus reducing the energy required for fibrillation.

PRE-TREATMENTS

To minimize the energy consumption of the fibrillation process, different strategies have been proposed to reduce the cohesive strength and the stiffness of cellulose fibers prior to the mechanical treatments. The alternatives are a) limiting the hydrogen bonds between the fibers, b) introducing negative charge to the fibers, hence creating repulsive force or c) limiting the degree of polymerization (DP) of the individual fibers. It exists a wide variety of pre-treatment methods, thoroughly described in a review by Rol et al. [71]

ENZYMATIC PRE-TREATMENT

The enzymatic hydrolysis of cellulosic fibers was found to enhance further the mechanical treatment, therefore reducing the energy needed for the fibrillation [90]. Specific enzymes, cellulases, are mixed with the cellulose pulp, to perform the hydrolysis of cellulose

chains. The enzymatic hydrolysis of cellulose chains can be performed in three different ways or as a combination of those:

- The amorphous regions are randomly hydrolyzed by endoglucanases, thus creating new chain extremities, reducing and non-reducing-ends.
- The chain ends are progressively degraded by exoglucanases, releasing disaccharides (cellobiose) and tetrasaccharides (cellodextrin).
- Cellobiases degrade cellobiose and tetrasaccharides released by the action of exoglucanases

These mechanisms are illustrated in Figure I.17.

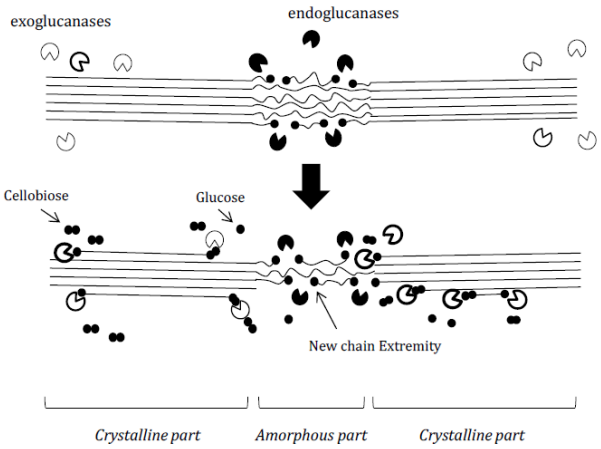

Figure I.17: Action modes of endoglucanases and exoglucanases for enzymatic pretreatment. Extracted from [91]

Enzymatic pre-treatment combined with mechanical treatment was first reported in 2007 in two different studies by Paäko et al. [92] and Henriksson et al. [90]. These studies proposed the combination of refining to increase the swelling of the fibers, thus increasing the accessibility of the enzymes, followed by a washing step, and a second refining before a homogenization process in a micro fluidizer. Both studies used similar procedure with the exception of the concentration in enzymes and the number of passes in the micro fluidizer.

TEMPO OXIDATION

The currently most used pre-treatment is TEMPO-mediated oxidation. This oxidation, by introducing (negatively charged) carboxylate groups at the surface of the

cellulose chains, induces charge repulsion by ionic interaction between the fibers, thus facilitates the fibrillation process during a mechanical treatment. This pretreatment is based on the selective oxidation of primary hydroxyl groups of sugars using sodium hypochlorite in the presence of catalytic amounts of (2,2,6,6-tetramethyl-piperidin-1-yl)oxyl, also known as TEMPO. The reaction is illustrated in Figure I.18.

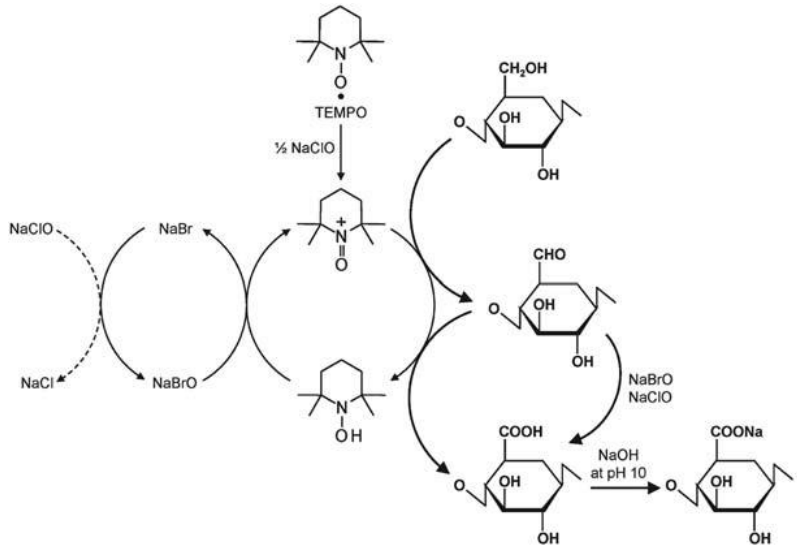

Figure I.18: Regioselective oxidation of c6 primary hydroxyls of cellulose to c6 carboxylate groups by TEMPO/NABr/NAClO oxidation in water at ph 10-11. Extracted from [93]

TEMPO-mediated oxidation of sugar molecules was first described by Davies and Flitsch in 1993 [94] and was adapted for cellulose later by Saito et al. [95]–[97]. An optimization of the process was proposed in 2011 by Isogai et al. [93], where the carboxylate content of the final suspension was shown to be dependent of the quantity of NaClO introduced, with a maximum charge content of 1.7 mmol/g reached. Another process has been developed using TEMPO/NaBr/$NaClO_2$ in neutral conditions [98] and this method has been shown to limit the depolymerisation occurring at pH 10. The use of this pretreatment allows for a reduction in the energy consumption when producing highly fibrillated CNFs. Such modified CNFs, with aldehydes (non-fully converted carboxyl groups) and carboxylic surface groups, in addition to hydroxyls groups, are interesting materials for functionalization and high added-value applications. In 2017, Tarrès et al. [99] compared the properties of enzymatically pretreated CNF (eCNF) and TEMPO-oxidized CNF (toCNF) with different enzymatic or sodium hypochlorite concentrations. Table I.4 reports the different properties of the two kinds of

CNF at the maximum concentrations of enzymes for eCNF and sodium hypochlorite for toCNF.

Table I.4: Characterization of toCNF and eCNF : carboxyl content (CC), diameter (d), transmittance (T), crystallinity index (CrI), degree of polymerization (DP), and morphological parameters (Aspect ratio, diameter, length). Adapted from [99]

CNF	CC [μeq/g]	d [nm]	T at 600 nm [%]	CrI [%]	DP	Length [nm]	Aspect ratio	Yield [%]
toCNF	1526 ± 103	7.7	83.4	52	197 ± 8	87	11.3	97.1
eCNF	42.1 ± 2.2	25.1	43.7	57	309 ± 18	567	22.6	38.9

TEMPO-pretreatments allow obtaining toCNFs with reduced size (diameter, length, aspect ratio, DP) in comparison with eCNFs. This reduced size allows reaching higher specific surface area. Also, the introduction of charge at the surface of CNFs allows for a tunable viscosity of suspensions by adjusting the pH, which can be of use in specific interactions.

Because of these particular properties, such as the carboxylic content and increased specific surface area, we have chosen to use TEMPO-oxidized CNFs for this PhD project.

II.1.4. Bacterial Nanocellulose

There is another nanocellulosic material available, which is not derived from wood and which presents interesting properties for high added-value applications: bacterial nanocellulose (BNC). BNC is produced by many bacteria sources [100], with the most common one being *Gluconacytobacter xylinus* [101]. Compared to plant cellulose, BNC is produced in a pure form, with no lignin, pectin or hemicellulose [102]. Its high crystallinity, controllable water content, degree of polymerization and membrane orientation [103], in addition to its purity (no possible contamination), make BNC a material of choice for high-added-value applications, as displayed by the numerous recent reviews covering its use in various fields of application [104]–[106]. However, its price and low production rate are drawbacks to its utilization and for the elaboration of new materials [107].

II.1.5. Nanocellulose characterization

Given the variety of sources, pretreatments and mechanical processes available to obtain nanocellulose materials, clear guidelines for the characterization was needed, for both researchers and industry to be able to identify the best processes and materials for each

application. In 2018, a review published by a vast conglomeration of renown scientists in the field was released, providing guidelines and methods for characterization of nanocellulose materials [108]. They identified five main topics crucial for the characterization of nanocellulose materials, represented in Figure I.19. This study emphasizes the importance of knowing the base materials. Indeed, with the great variety of raw materials, production processes and suppliers available, there are hundreds of different grades of cellulose nanomaterials (CNMs), which can differ in terms of proportion between micro- and nano-sized elements, concentrations and ability to be dispersed, impurities to name only a few. It is then mandatory to characterize thoroughly these materials prior to use, but also at each step of the process, since any modifications (mechanical, chemical) can have an impact on the CNM's morphology and properties. They also highlighted the importance of characterizing these materials in terms of health and safety, which will be crucial for the development of the use of such materials.

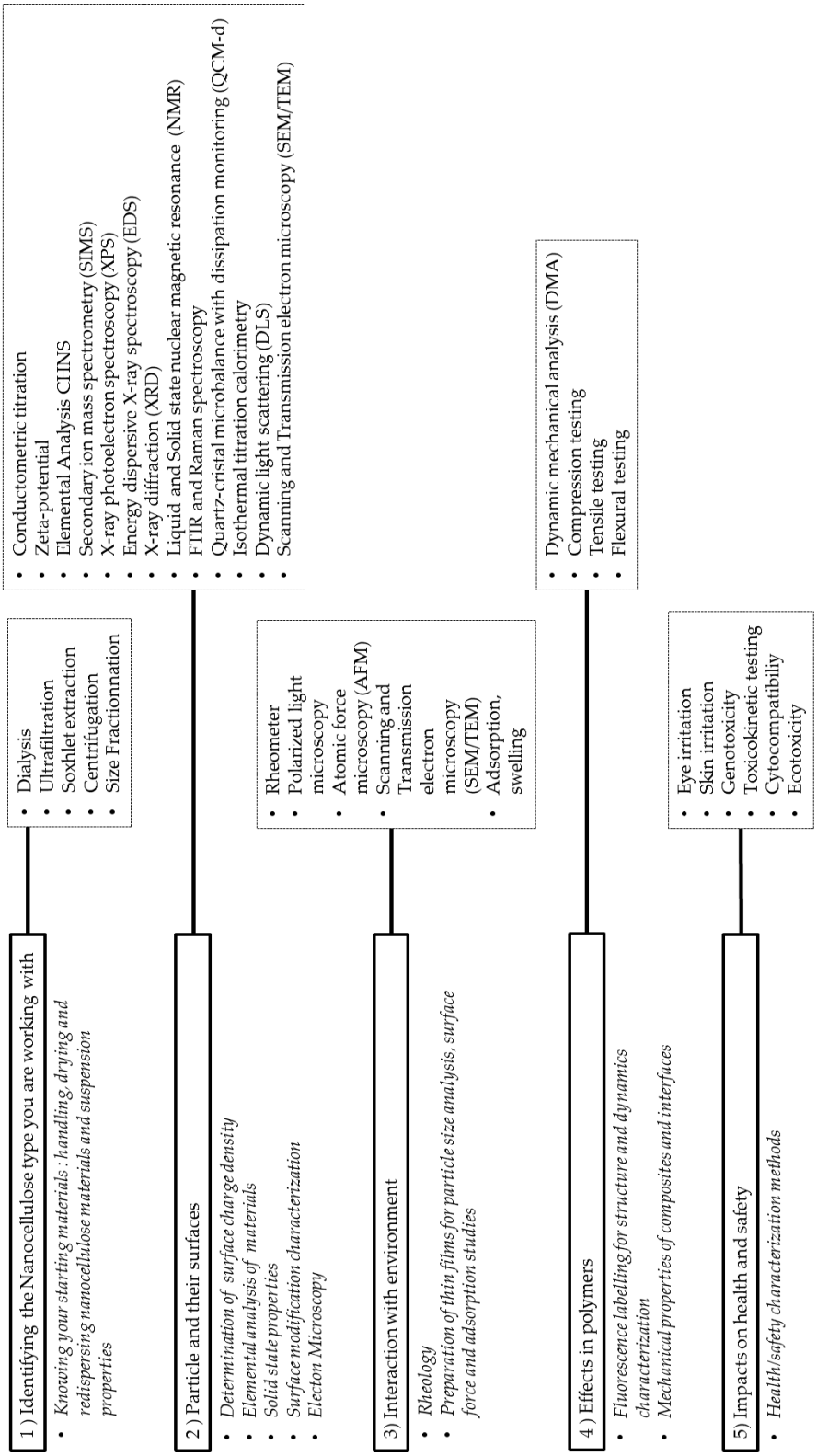

Figure I.19: Five topics for the characterization of nanocellulosic materials and associated characterization tools. Adapted from [108], [109]

Desmaisons et al [110] proposed a quality index, a multi-criteria method consisting of measuring the nanosized fraction, turbidity, Young's Modulus, porosity, transmittance, tear resistance, macro size and homogeneity of CNF suspensions. In this quality index, they assign a value for each measured property in relation to its behavior compared to the commonly measured values for these different characteristics and calculated a final score allowing a comparison between different suspensions, creating an interesting tool for benchmarking.

II.2. PROCESSING AND DIFFERENT APPLICATIONS

II.2.1. PROCESSING

Nanocellulose materials can be processed in many different ways, represented in Figure I.20, depending on the desired applications. Here, "2D-structures" is used for thin films, membranes or coatings, while "3D-strucutures" is used for hydrogels, cryogels and aerogels.

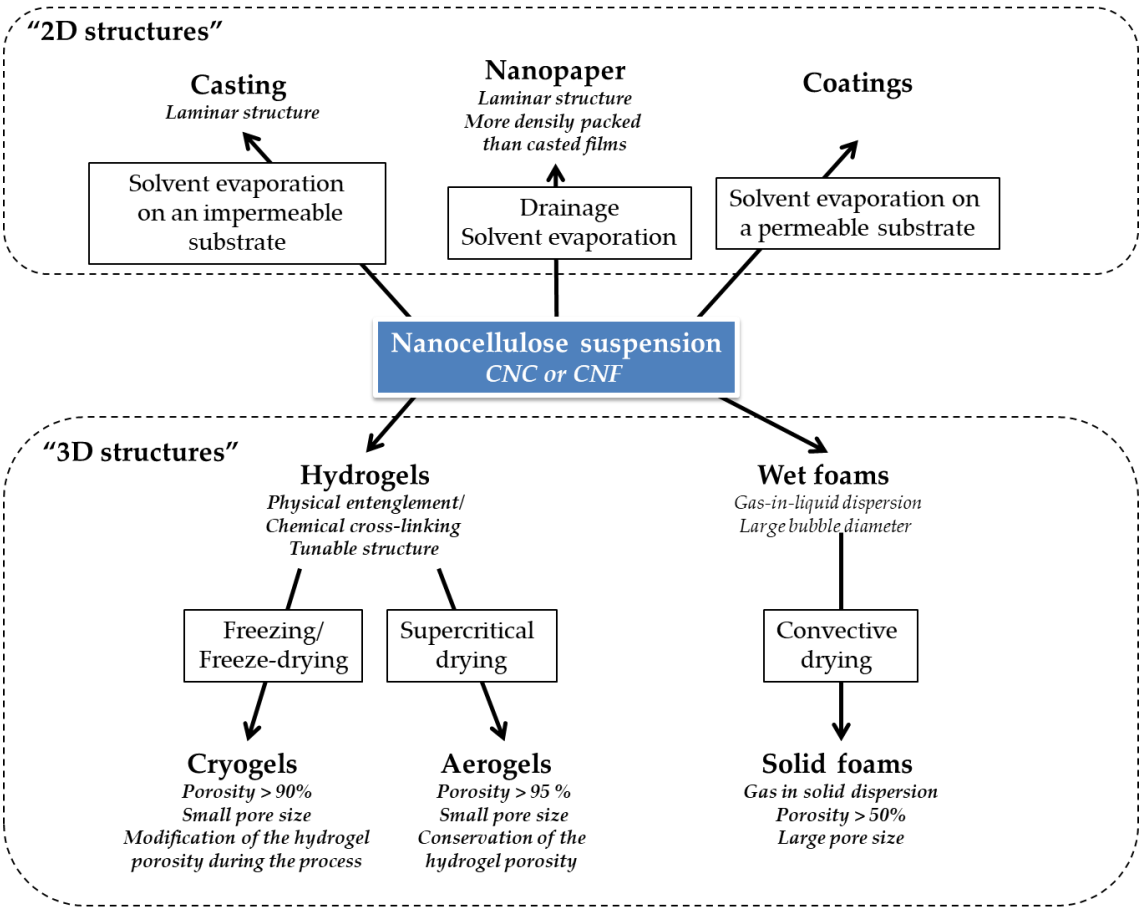

Figure I.20: Different processing routes

2D STRUCTURES

The use of nanocelluloses in the form of thin films or coatings is of great interest for many applications such as packaging and drug delivery. As schematized in Figure 20, there are multiple ways to obtain both 2D and 3D structures.

SOLVENT CASTING

The nanocellulose suspension is poured onto an impermeable substrate and the solvent is evaporated under controlled conditions. When using water as a solvent, strong hydrogen bonds occur between the fibers, making a dense film with interesting properties notably for barrier applications [111]. However, depending on the type of nanocellulose used, the drying kinetics is variable, with time of drying varying from few days to few weeks to obtain dry films. Notably, it takes longer time to dry a toCNF suspension compared to an enzymatic CNF for the same volume of suspension. The drying time can be a major drawback for further industrialization. Increasing the temperature can reduce the drying time but can also cause thermal degradations of the nanoparticles and a phenomen of hornification, resulting in lower porosity in the films. The drying process should be adapted based on the desired film properties.

NANOPAPERS

Nanopapers are prepared by filtration from a diluted aqueous nanocellulose suspension [112]. Nanopapers form more densely packed structures than solvent casted films and are quicker to obtain due to the filtration process. However, the filtration process can induce an orientation in the film that can be prejudicial for some applications. Nanocellulose nanopapers have been shown to have good mechanical properties with Young's moduli between 6 and 17.5 GPa and tensile strengths between 100 and 250MPa [113].

COATINGS

Coating is a method based on the deposition of a layer of nanocellulose on a solid substrate, in order to benefit from the physico-chemical properties of nanocellulose, such as its barrier properties, while maintaining the mechanical properties of the substrate. Different coating techniques are known e.g. spin-coating, dip coating and spray coating to name only a few. The spin-coating method is based on the application of a nanocellulose suspension onto a solid substrate. High speed agitation is used to form the nanocellulose film and to

remove water. This method makes it possible to obtain thin layers with very good reproducibility [114], even though it is not industrially feasible at the moment. The spray coating method consists of the deposition of suspension droplets on the surface of the substrate, followed by a flattening and solidification phase. This method makes it possible to obtain very homogeneous layers.

3D- STRUCTURES

There is an increasing interest for 3D-structured materials for varying applications such as scaffold for biomedical applications or insulation. Recent reviews by De France et al. [115] and Gupta et al. [116] described the various preparation processes and properties of 3D-CNF and CNC materials. These reviews emphasize the variability in the sources of the raw material with the lack of systematic studies to link the material properties to the final properties of the 3D construct. Different 3D-structures are known: foams, hydrogels, cryogels and aerogels. The different processing routes for these structures are schematized in Figure I.20. In 2017, Lavoine and Bergstrom [117] proposed the following distinction between nanocellulose-based foams and nanocellulose aerogels:

- Nanocellulose-based foams are multi-phase porous materials with a porosity larger than 50% in which gas is dispersed in liquid, solid or hydrogel, with a bubble diameter usually larger than 50 nm.
- Nanocellulose-based aerogels are mesoporous solid materials with porosity higher than 90% and with pore size between 2 nm and 50 nm.

According to these definitions, cryogels that present porosity higher than 90% and a pore size in the 2-50 nm range should be classified as aerogels. In 2019, Vareda et al. [118] proposed to call aerogel any material derived from gels that are with a moderate impact on the solid network and a high porosity, regardless of the drying approach. However, since the drying process has an impact on the pore morphology, we will keep the distinguished named for cryogels and aerogels in this review.

FOAMS

Foams usually describe porous materials made from porogen templating that displays pore sizes of ca. 200 µm [119]. Porogen templating is typically based on the generation of gas bubbles within an aqueous dispersion, followed by steps including

gelation, curing, solvent exchange and a convective drying. This process presents advantages such as being simple and relatively quick, however, there are some drawbacks as e.g. lack of control over the morphology of the pores, possible coalescence of the nanomaterials and a large pore size. Generally, the porosity in foams represents more than 50% of the total volume.

HYDROGELS

Hydrogels are three-dimensional networks of hydrophilic polymers which have an ability to swell in water and in biological fluids [120], [121] and to maintain their shape in gel form. Cellulose nanofibril based hydrogels differs from other hydrogels since cellulose is non-soluble and the cross linking is due to physical entanglement of fibrils combined with electrostatic stabilization [122], [123]. To strengthen the network, chemical cross-linking or ionic cross-linking may be considered. As an illustration, Basu et al. [124] prepared self-standing toCNF hydrogels by incorporating Ca^{2+} ions as a cross-linking agent, creating ionic interactions with carboxylate functions of toCNF. Aarstad et al. [125] proposed the preparation of Alginate/CNF hydrogels stabilized with CA^{2+} ions that displayed remarkable mechanical stability. The wet state of hydrogels can be very beneficial for medical applications, for example.

CRYOGELS

Cryogels are gel matrices formed by cross-linking at a temperature below zero and freeze-drying. Ice crystals formed during the freezing process act as pore forming agents [126]. The solidified solvent is then removed by freeze-drying, leaving a porous material where the pores are the direct replica of the crystals, as shown in Figure I.21.

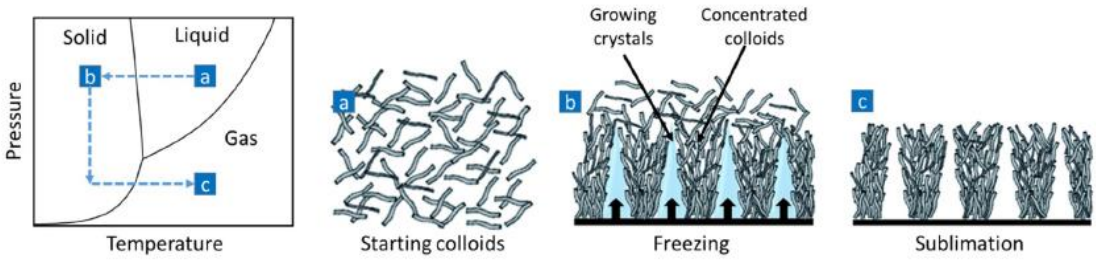

Figure I.21: Ice-templating process. Extracted from [116]

By controlling the growth of ice-crystals, 3D-strucuture with oriented porosity can be obtained [72]. It is worth noting that the crystallization and subsequent freeze-drying process modify the porosity shape of the initial hydrogel. Generally, porosity in cryogels represents more than 90% of the total volume, with small pore size. The advantage of this production method is that it is easy to implement due to the ease and accessibility of the freeze-drying process.

AEROGELS

Aerogels are obtained by supercritical drying of gel matrices. The use of supercritical drying leads to 3D porous structures with high porosity (>95%) and no modification of the gel-state porosity [127]. Confusion is sometimes made between cryogels and aerogels, the difference being the drying process. However, this definition is not globally used to this date and in some studies confusions are still made. This method is the most suitable one to obtain the initial structure of the hydrogel and gives the largest pore volume, and therefore potentially the largest specific surface areas. However, the supercritical drying process can be more complicated to implement than the freeze-drying process used to obtain cryogels.

The methods of shaping cellulosic materials are diverse and each of them has specific features that make it more or less suitable for a specific application. Particular attention must therefore be paid to the final application in order to choose the most appropriate shaping method.

II.2.2. APPLICATIONS

Nanocellulosic materials display very interesting physicochemical properties that make them suitable and promising for a wide variety of applications. Recent reviews [128]–[130] have been published which present the use of nanocellulosic materials in areas such as purification, filtration, packaging, structural reinforcement, sensors, energy storage, rheological modifiers and medical applications. Table I.5 summarizes some of the possible applications based on recent publications, with the exception of medical applications, that will be elaborated in the next section.

Table I.5: Technological applications of nanocellulosic materials. Adapted from [131]

Application	Specification	Examples	Ref
Adsorption/Filtration	Removal of pollutant from aqueous solutions	Toxic dye (Methylene blue)	[132]
		Heavy metal ions (Cu(II), Pb(II) and Cr (VI))	[133]
		Drugs (Ciprofloxacin, Diclofenac)	[134]
		Oil	[135]
	Air purification	Odor removal	[136]
	Immobilization	CNC/alginate for protein adsorption	[137]
	Haemodialisys membrane	Polypyrrole/CNF membranes	[138]
	Virus removal	CNF filter	[139]
Packaging	Food packaging	Paper sheets modified with CNC and chitosan	[140]
		CNC/PLA coatings	[141]
	Bioactive packaging	CNF and silver nanowires	[142]
Thermal applications	Insulator	Nanocellulose with graphene oxide	[143]
	Fire retardant	Nanocellulose with clay	[144]
		Nanocellulose with graphene oxide	[145]
		Nanocellulose with zirconium phosphate-reduced grapheneoxide	[146]
Energy	Batteries	Carbonation of toCNF for lithium-sulfur batteries	[147]
		toCNF hydrogels precipitated as conductive substrate	[148]
	Solar cells	CNF with graphene oxide	[149]
	Capacitor	CNC films with aluminium sheets	[150]
Structural reinforcement	Civil engineering	Nanocellulose in cement	[151]
	Paper making	CNF in paper	[152]
		CNF in recycled cardboard	[153]
	Composites	CNCs with natural fibres	[154]
		CNCs in wood panel	[155]
Sensors	Optical	CNF hydrogels with carbon dots	[156]
	Chemical	Detection of urea with modified CNC	[157]
	Electro-chemical	Electrochemical sensing of drug	[158]
	Piezoelectric	CNC Thin films	[159]
Rheology modifier	Oil recovery	CNC	[160]
	Food additives	CNF as viscosifier in mayonnaise	[161]
	Food additives	Avocado oil emulsions stabilized with CNF	[162]
	Cosmetics	Pickering emulsions	[163]

II.3. NANOCELLULOSIC MATERIALS FOR BIOMEDICAL APPLICATIONS

Among all the applications presented above, biomedical applications are among those for which the use of nanocellulosic materials is the most promising. The objective of this section is to review the different challenges inherent to their use in this context, as well as to present the history of their use for medical purposes.

II.3.1. FOCUS ON ADSORPTION

Of all the analysis methods available for nanocellulosic materials, the characterization of adsorption is of high relevance for this study. Understanding and measuring the interactions of cellulose nanomaterials with their environment is crucial to explain the self-organization of the materials, but also the co-organization with other possible compounds. It is even more important for applications such as drug release or pollutant removal, where the interactions between nanocelluloses and molecules of interest are key for a beneficial application. This part intends to give an overview of the different adsorption mechanisms and isotherms, as well as to describe two highly relevant methods for characterization, namely QCM-d and ITC.

ADSORPTION ONTO A SOLID INTERFACE

Adsorption is defined as the adhesion of atoms, ions or molecules (adsorbate) onto a surface (adsorbent) by attractive interactions. Adsorption between adsorbents and adsorbates can be classified into two categories depending on the interactions involved: Physisorption and chemisorption. Physisorption describes an adsorption directed by weak interactions (Van der Walls interactions, apolar interactions), which take place without modification of the molecules involved, do not generate strong enthalpy variations, and are reversible and easily resorbable [164]. Chemisorption describes adsorption driven by the formation of strong covalent or ionic bonds, which result in a high heat of reaction, can cause irreversible modification of the materials and is not easily reversible. Interactions in chemisorption are typically two-order of magnitude stronger than that of physisorbed species [165]. A solid surface presents sites where the adsorbate can be adsorbed. The amount of surface coverage θ is defined by Equation I.1:

$$\theta = \frac{number\ of\ sites\ occupied}{total\ number\ of\ sites} \quad \text{(Eq. I.1)}$$

The formation of the adsorbed layer is illustrated in Figure I.22.

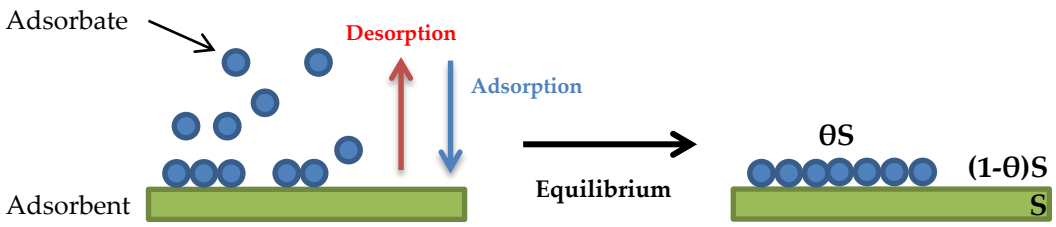

Figure I.22: Illustration of the adsorbed layer

Adsorbent and adsorbate are in a chemical equilibrium. For a liquid-solid interface, the variation of θ as a function of the activity of the adsorbed species is defined as the adsorption isotherm. Isotherms can be either experimentally measured or calculated. In 2019, Lombardo et al [166] published a review in which they described thoroughly the different isotherms pertinent for nanocellulosic materials. In this study we will focus only on one of them, the Langmuir isotherm.

The Langmuir isotherm is based on three assumptions: a) There is no multilayer adsorption b) The adsorbent and adsorbate present homogeneous surfaces with identical binding sites c) There are no interactions between adsorbed molecules. The Langmuir isotherm is usually expressed by Equation I.2 [167] :

$$q_e = \frac{Q_L K_L C_e}{1+(C_e \times K_L)} \quad \text{(Eq.I.2)}$$

Where q_e is the amount of adsorbed molecules normalized by the total amount of adsorbent, Q_L is the maximum adsorption capacity, C_e is the concentration of the adsorbate at the equilibrium and K_L is the Langmuir constant. This isotherm is only truly valid for the adsorption of an ideal gas onto homogenous surface. In the case of cellulose nanofibrils, we don't have homogeneous surface nor identical binding sites, with hydroxyl, carboxyl and aldehyde groups. However, this is still the model which is most used due to its simplicity, and it has been shown to fit reasonably well with experimental data [166].

EXPERIMENTAL METHODS

Multiple techniques have been developed to measure and to understand the adsorption phenomena. Among them, the two techniques that interested us during this project are Quartz Crystal Microbalance with dissipation monitoring (QCM-d) and Isothermal Titration Calorimetry (ITC).

The principle of QCM-d was first described by Rodahl et al. in 1995 [168]. The QCM-d technique makes it possible to follow the modification of the resonance frequency of a quartz crystal when a flux passes over its surface. If the molecules in the flow adsorb on the surface of the sensor, the resonance frequency of the crystal will be shifted and by using the Sauerbrey equation, the adsorbed mass can be calculated (Equation I.3):

$$\Delta m = -C\frac{\Delta f}{n} \quad \text{(Eq. I.3)}$$

Where C is a constant related to the density and thickness of the quartz crystal, Δf is the shift in frequency and n is the overtone number. The shift in dissipation gives an indication of the viscoelastic properties of the adsorbed layer. It is worth noting that the Sauerbrey model is only valid if the created film is rigid, uniform and that the mass adsorbed is small compared to the mass of the sensor. Other models, like Voigt's and Maxwell's [169] have also been developed for more viscoelastic films. Although this method seems to be quick and easy, it presents some difficulties. First of all, the preparation of the sensor is crucial to obtain usable data. Indeed, in the case of a study between two polymers, one coated on the sensor and the other in the flow passing on the surface, it is necessary that the surface of the sensor is perfectly covered by the polymer. Furthermore, this method does not allow the determination of the thermodynamic parameters of interactions. Nevertheless, it remains an efficient way to estimate the adsorption strength and the quantity of adsorbed molecules.

ITC is a method developed to determine the thermodynamic parameters during the interaction between two molecules. This method is based on the measurement of the heat released as a result of the interaction between the two molecules during a titration, as presented in Figure I.23. First developed for molecules in solution, this method has recently been used to measure interactions between a molecule in solution and suspensions, in particular nanocellulose suspensions [170]. Nevertheless, in the case of measuring adsorption on nanocellulose suspensions by ITC, some questions remain. Firstly, in the case of non-

specific interactions, such as hydrogen bonds, the heat of reaction is low, which makes the measurement more subjected to experimental noise. Furthermore, to be able to calculate association constants between the adsorbed molecule and nanocellulose, the number of sites present on nanocellulose must be known which in the case of non-specific interactions is difficult. Finally, the viscosity of the suspension can be a problem for the measurement of the heat of reaction and the homogenization during the measurement. Measuring the interaction between a molecule and a CNF suspension is therefore a major challenge.

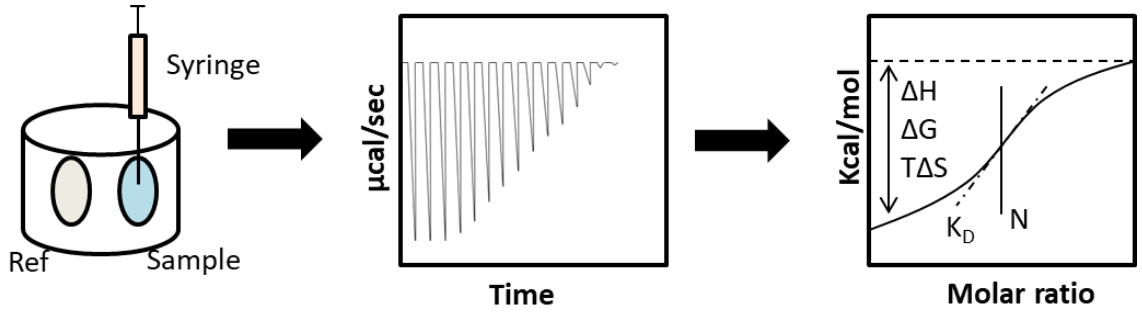

Figure I.23: Schematic representation of an ITC measurement

II.3.2. History of cellulosic nanomaterials for biomedical applications

Nanocellulose and its derivatives are used in drug delivery systems in two different ways [171]. Nanocellulose can be used as drug excipient, to help the vectorization of the drug, being used as thickener, binding agent, stabilizer, emulsifier, film former or surfactant. Nanocellulose is also used as drug delivery matrix in which a drug can be incorporated. All these uses of nanocellulose products mainly aim at obtaining a sustained release of the Active Principal Ingredient (API). The modification of the drug release by nanocelluloses can be obtained by various mechanisms, such as water retention, film formation and adhesion [172], all depending on the nature and the form of the nanocellulose used.

Bacterial nanocellulose

Bacterial nanocellulose displays a variety of properties that makes it perfectly suited for biomedical applications. It displays a near-perfect purity, good mechanical properties [173] and more importantly a water retention capacity and morphology similar to collagen, i.e. the extracellular matrix [174]. This last point makes BNC-based materials promising for cellular immobilization, adhesion and proliferation. Due to its near-perfect purity related to

its production by bacteria, bacterial nanocellulose was the first nanocellulosic material to be considered for wound healing products. The first example can be traced back to 1990, with the invention of Biofill [175], a wound dressing, developed from *Acetobacter* cellulose pellicle, used for the treatment of severe burns as temporary skin substitute. Other BNC-based materials were developed and commercialized afterwards, such as Xcell (Xylos co., USA) and Bioprocess (BioFill Produtos Biotecnologicos, Brazil) [176].Clinical trials have been performed, and these trials showed that BNC-based materials displayed good adhesion to the wound and were able to maintain a proper moist environment around the wound as well as a good absorbance of the wound exudate. In 2001, Klemm et al. [177] proposed a BNC-based artificial blood vessel for microsurgery that displayed high mechanical strength in wet state, high water retention value and a complete vitalization. BNC was also regarded as a potential tablet excipient for drug delivery applications, for paracetamol [104] or model protein albumin [178]. Finally, BNC is regarded as one of the most suited materials for tissue engineering applications [179], and BNC-based composite scaffolds were studied as an alternative for bone tissue scaffold, by mixing BNC with hydroxyapatite, displaying an enhanced cell attachment, proliferation and differentiation in comparison with unmodified BNC-scaffold [180]. BNC has been approved by the FDA as a component of other commercialized products, as shown in Table I.6. Nevertheless, despite its almost perfect suitability for biomedical applications, the price of the raw material, due to the cost of production, is a hindrance to the generalization of the use of BNC for biomedical applications.

Table I.6: Products based on BNC available on the market. Reproduced from [104]

Product	Type	Clinical indication/use	Company/Agency
Basyc	Vessel implant (tubes)	CABG (Coronary artery bypass surgery)	Jenpolymer materials Ltd. & Co.
BioFill	Wound care system	Burns	Robin goad
Bioprocess	Artificial skin	Burns	Biofill Produtos Biotecnologicos
Cellulon	Binder	Medical applications including non-woven structure	CP Kelco
Cellulon PX microfibrous cellulose	Suspending agent	Suspension of particles, encapsulated enzymes	CP Kelco
Celmat © MG & CelMat ® MG	Protective dressing/jackets	Protection for miners from potential burns	Government of Poland
Dermafill	Wound care dressing	Burns	Fibrocel
Gengiflex	Non-resorbable cellulose membrane	Periodontitis	Biofill Produtos Biotecnologicos
MTA protective tissue	Biocompatible implant	Injury and wound care	Xylos corporation
Securian	Tissue reinforcement matrix	Tendon repair	Xylos corporation

WOOD-BASED NANOCELLULOSE

The production of nanocelluloses from lignocellulosic biomass opened a new opportunity for the development of nanocellulose-based biomaterials. Its availability and low cost compared to bacterial cellulose, in addition to outstanding properties, have made these materials well-studied over the last two decades for applications such as wound dressing, drug delivery and tissue engineering. Figure I.24 displays the number of publications concerning the use of nanocelluloses for biomedical applications over the period 2008-2018.

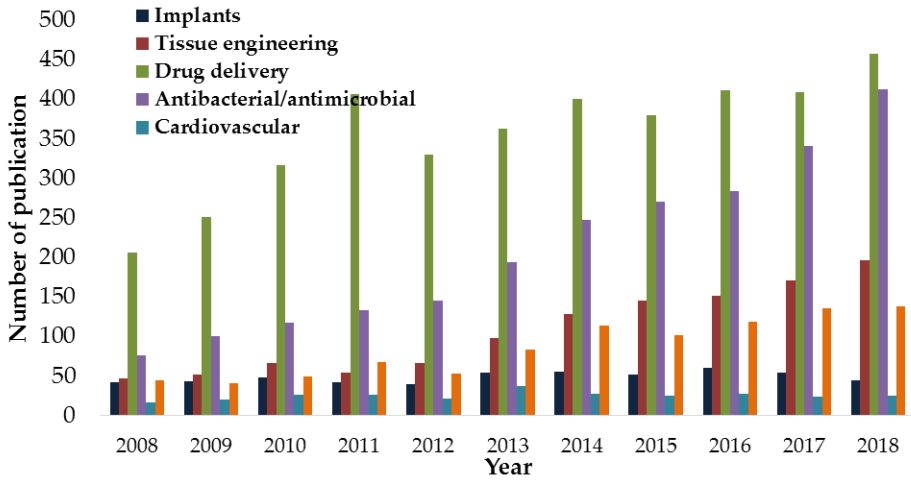

Figure I.24: Number of publications concerning nanocellulose for biomedical applications. Extracted from [15]

Both CNCs and CNFs display biocompatibility, biodegradability, renewability and moderate toxicity [181].

CNCs exhibit very high strength; elastic modulus, high surface area and unique liquid crystalline properties [182], and thus have received much attention as nanoparticle reinforcement. In 2011, Letchford et al [183] studied the potential use of CNCs as drug excipient and reported the binding of water soluble antibiotics to CNCs, as well as the potential of cationic CNCs to bind hydrophobic drugs.

Due to their interesting properties, and more specifically their possibility to form an entangled network and allow for the formation of hydrogels without chemical modifications, CNF-based materials have been considered for medical applications, with several reviews and chapters published in the recent years [181][184][185][186], [187]. The first study about the potential use of CNF based-materials for controlled drug delivery was published by Kolakovic et al [188] in 2012. They produced a film-like matrix loaded with poorly water-soluble drugs (Indomethacin, Itraconazole, Beclomethasone dipropionate) and reached an entrapment efficiency >90% and a sustained release over a 3 month period, assuming that the tight fiber network around the drugs sustained the release, making CNFs a promising material for this applications. In a later study, they focused on the interaction between drugs and CNFs by the means of permeation, incubation methods and isothermal titration calorimetry [189] to get a better understanding of the binding mechanism occurring. They found a pH dependence and identified electrostatic forces as the main mechanism. In 2014,

Lavoine et al. [190] obtained a controlled release of chlorhexidine digluconate with a coating of CNFs on paper. The nanoporous structure of the coatings allowed a sustained antibacterial activity by sustaining the release of the active Principal ingredient. Attempts have been made to covalently bind drugs to CNF-based material, to obtain longer-lasting effect. Durand et al. [191] explored the impact of thickness of ciprofloxacin-loaded CNF membrane on release and antimicrobial properties, and compared the results for adsorbed ciprofloxacin versus grafted ciprofloxacin via esterification with a thermal treatment under vacuum. They observed a more sustained release for thicker films and a prolonged antibacterial activity for ciprofloxacin-grafted films. These studies are indicating that pure CNF- based devices, due to the entanglement and natural retention properties of drugs, in addition to outstanding water retention properties, are promising devices for drug release application. CNF materials have been proved to have the ability to mimic the extra-cellular matrix due to this entanglement. In 2013, Alexandrescu et al. [192] assessed the toxicity of wood-based CNF- structures on fibroblast cells, and no cytotoxicity of neat CNF structures was measured. Recently, Rashad et al. [193]–[195] studied the inflammatory response and tissue reactions to wood-based modified CNF hydrogels (carboxymethylated and TEMPO-oxidized suspensions). They seeded mouse fibroblasts in both hydrogels, and no toxic effect was observed for any of the suspensions. The carboxymethylated hydrogels influenced the morphology of the cells and limited their spreading, while normal behavior where observed for the TEMPO-oxidized hydrogel. After implantation in rat, after 4 days, they observed that the production of inflammatory cytokines was lower in the case of scaffold compared to gelatin control. However, after 180 days, no degradation of the scaffold was observed, resulting in a foreign body reaction. This highlights one the major challenges for the application of nanocellulose-based materials for tissue engineering applications, i.e. the degradation of the scaffold in-vivo.

II.3.3. Recent works on the use nanocellulose materials for biomedical applications

The aim of this section is to give the reader an overview on various recent works to get a general idea of the current state in the field. The different publications have been organized in a table format in order to facilitate the search for information.

Some examples of recent studies using nanocellulosic materials for drug delivery/wound dressing/wound healing applications are displayed in Table I.7. CNCs are generally used in combination with other polymers, such as chitosan and alginate, as reinforcement in a matrix, either in the form of solid composites or hydrogels, while BNCs and CNFs, by forming intricate networks that can be self-standing, are generally used without other materials.

Some examples of recent studies on the use of nanocellulosic materials for tissue engineering applications are displayed in Table I.8. Nanocellulose materials for tissue engineering applications are rarely used without other materials, such as chitosan or alginate; to achieve more suitable mechanical properties of the scaffold. Another reason is also to provide scaffold degradation properties. Indeed, cellulose is either not degraded in vivo by the human organism or too slow. The potential toxicity of such materials is discussed in the following section.

Table I.7: Recent studies (2017-...) on the use of nanocellulose materials for drug release/wound dressing applications

NC	Form	A.P.I.	Application	Date	Ref
BNC	Matrix	Octenidine	Wound Dressing	2017	[196]
BNC	Composite	Diclofenac	Dermal/Oral	2017	[197]
BNC	Films	Crocin	Transdermal delivery	2019	[198]
BNC	Films	Diclofenac/ Hyaluronic acid	Oral/Transdermal delivery	2020	[199]
CNC	Matrix/Hydrogel	Ibuprofen		2018	[200]
CNC	Hydrogel with chitosan			2017	[201]
CNC	Hydrogel with Chitosan	Curcumin	Stomach release	2017	[202]
CNC	Composite with alginate	Ampicillin	In vitro delivery	2018	[203]
CNC	Emulsifier for pickering emulsion		Drug Delivery	2017	[204]
CNC	Hydrogel	Ceftriaxone	Drug delivery	2019	[205]
toCNC	Hydrogels	Clofazimine	Drug delivery	2019	[206]
CNC	Hydrogels	Paclitaxel	Controlled release	2020	[207]
CNC	Film	Honey	Wound dressing	2020	[208]
CNC	Hydrogels	Neomycin	Wound dressing/Healing	2020	[209]
toCNF	Matrix/Hydrogel	Tetracycline	Wound Healing	2018	[210]
toCNF	Hydrogel	BSA/Lysozyme/Fibrinogen	Wound Dressing	2018	[211]
CNF	Gel-membrane	Piroxicam	Transdermal	2019	[212]
CNF/toCNF	Films	Acetaminophen		2020	[213]
toCNF	Hydrogel with polydopamine	Tetracycline	Wound Healing	2018	[214]
toCNF	Composite cryogel with gelatin	5-Fluorouracil	Drug delivery	2019	[215]
cmCNF	Films	Ciprofloxacine	Drug delivery	2019	[216]
CNF	Hydrogels	Metoprolol/Nadolol (beta blockers)	Drug release	2020	[217]

Table I.8: recent studies (2017-...) on the use of nanocellulose materials for tissue engineering applications

NC	Form	Application	Date	Ref	Comments
CNF	Freeze-dried with quaternized chitin	Skin tissue	2019	[218]	Good biocompatibility, antibacterial properties, high mechanical strength
CNC	Freeze-dried with PVA	Skin tissue	2017	[219]	Good mechanical, thermal and swelling properties
toCNF	3D-printed with gelatin methacrylate	Skin tissue	2019	[220]	Tunable surface stiffness and Young's modulus
CNC	Solvent-castedwith chitosan, genlatin/calcium peroxide	Skin tissue	2019	[221]	Good biocompatibility, antibacterial properties, high mechanical strength
CNF	Electrospinned with PLA/PBS	Vascular tissue	2019	[222]	Good biocompatibility, Sustainable degradation
CNC	3D-printed hydrogels with alginate/gelatin	Bone tissue	2021	[223]	Good biocompatibility, mineralization of the scaffolds

II.3.3. TOXICITY OF NANOCELLULOSE

The development of the use of nanocelluloses for biomedical applications requires serious consideration of the toxicology of these materials. The first work on assessing the potential toxicity of nanocelluloses was conducted by Kovacs et al. [224]. They observed low toxicity potential and environmental risk of CNC materials via an ecotoxicological evaluation on several aquatic species. In their review published in 2014, Lin and Dufresne [185] listed studies evaluating the cytotoxicity of nanocellulosic materials, highlighting the low-toxicity and the lack of evidence of cytotoxicity, at the exception of modified CNF [192]. In 2020, Khalil et al. [225] have published a review on the use of nanocellulose for medical applications, including a summary of recent research on the toxicology of these materials. Notably, there has been no clear evidence for serious impact of cellulose-based materials at both cellular and genetic level as in vivo organ. However, one potential risk in the use of nanomaterials is the size of the nano elements, prone to cause pulmonary infections [226]. Additionally, the non-degradation of cellulose materials in the body could cause infection reactions, as reported by Rashad et al [195]. The main challenge identified is to find a way to degrade the scaffold in vivo. For external use, such as wound dressing, nanocellulosic

materials do not display any intrinsic toxicity and can therefore, according to the current knowledge, be used for these applications [226].

III .CYCLODEXTRINS, A NEW STRATEGY TO IMPROVE NANOCELLULOSE-BASED DEVICES

In order to improve the properties of cellulosic nanofibrils used in this project, we propose the complexation with cyclodextrins. Thus, the aim of this chapter is to present this family of molecules, its origins, its production and the different varieties available. A focus will be made on its properties, in particular that of being able to form an inclusion complex and on the different characterization methods available. Finally, previous studies combining nanocelluloses and cyclodextrins will be presented, in order to demonstrate the possibilities and challenges inherent to the project, and to identify its innovative character.

III.1. DEFINITION OF CYCLODEXTRINS

III.1.1. ORIGIN AND PRODUCTION

Cyclodextrins (CDs) are cyclic oligosaccharides composed of D-glucose units linked through α1-4 linkages. A Greek letter indicates the number of glucose units in the composition of the CD: α for 6 glucose units, β for 7 glucose units, γ for 8. Figure I.25 presents the chemical conformation for the three main types of CDs; α, β and γ.

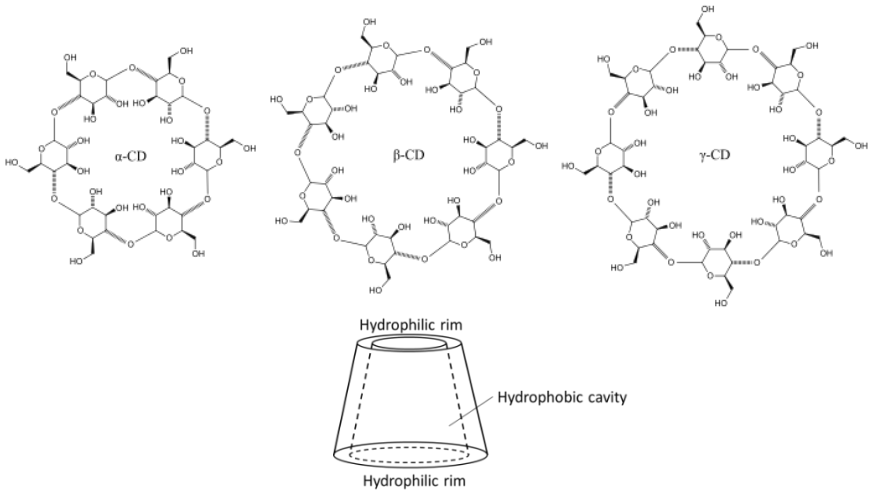

Figure I.25: Schematic representation of CDs

CDs are synthetic substances obtained via an enzymatic degradation of starch. In a review in 2014, Crini [227] retraces in details the history of cyclodextrins. Only the major advances will be developed in this manuscript. The first observation of cyclodextrins was made in 1891 by

Antoine de Villiers [228], who observed the formation of a crystalline substance after the digestion of starch by *Bacillus amylobacter*., and named these compound "cellulosine". In 1903, Schardinger isolated the bacterial strain *Bacillus macerans* responsible for CD production, and glucosyltransferase (CGTase), an enzyme that transforms starch into CDs. He named these compounds "Schardinger dextrins" [229]. This bacterial strain is still to this day the most used for the production of cyclodextrines. In the late 30's, Freudenberg et al. described the cyclic organization of CDs in detail, at this time only for α-CD and β-CD, composed of maltose units (2 glucose linked by α-1,4 bonds) and first evoked the lipophilic character of the central cavity, leading to their capacity to form inclusion complex with hydrophobic compounds [230]. In the 50's, γ-CD was discovered [231], and the first protocols for the industrial-production of cyclodextrines were proposed [232]. It was also during this period that the ability of cyclodextrin to form inclusion complexes with hydrophobic molecules was further studied, and the resulting stabilization, solubilization and protection properties of the guest molecules began to interest more and more industrial fields. However, due to erroneous toxicity studies, the use of cyclodextrins on an industrial scale really started in the 1980's [233]. To illustrate the interest in cyclodextrins from that time and onwards, the evolution of price and quantity of β-CDs produced annually can be evaluated. In 1980, the annual production of β-CD did not exceed a few tons/year at a price of a few hundred dollars per kg. In the early 2000s, production exceeded 10,000 tons/year at a price of a few dollars per kg [234]. Nowadays, native cyclodextrins and modified cyclodextrins are used in multiple industrial processes [235], [236]. Among the producers of cyclodextrins, we can mention Roquette and Wacker which are the most important in terms of annual tonnage, or Cyclolab for the production of modified cyclodextrins. The modified cyclodextrins and the various fields of applications will be described later in the manuscript.

III.1.2. PROPERTIES

The main physicochemical characteristics of the most commonly used native cyclodextrins are shown in Table I.9.

Table I.9: Physicochemical properties for α,β and γ-CD, adapted from [237]

Properties	α-CD	β-CD	γ-CD
Glucose units	6	7	8
Raw formula	$C_{36}H_{60}O_{30}$	$C_{42}H_{70}O_{35}$	$C_{48}H_{80}O_{40}$
Molecular mass [g/mol]	972	1135	1297
Cavity diameter [nm]	0.57	0.78	0.95
Periphery diameter [nm]	1.46-1.5	1.54-1.58	1.75-1.79
Cavity volume [nm³]	17.3	26.2	42.7
Solubility in water 25°C [g/L]	145	18.5	231

Native cyclodextrins are homogeneous, non-hygroscopic crystalline compounds. The diameter of the cavity varies with the number of glucose units in the molecule, while the height of the molecules is identical between different CDs. Thus, the external diameter of the cavity, and its volume, both increase from α-CD to γ-CD. The difference in water solubility between CDs is explained by the establishment of hydrogen bonds between the secondary hydroxyl groups, which are then linked in pairs. These intramolecular bonds strengthen the structure of the cyclodextrin and prevent its hydration. The small size of α-CDs and the large size of γ-CDs do not allow these bonds to appear and we observe a greater solubility for these two cyclodextrins compared to the β-CDs [238]. However, due to the size of its cavity, which is perfectly suited for complexation applications, and despite its low solubility, β-CD is the most produced CD [239]. β-CD solubility can be improved via chemical modifications. Indeed, substitution of any of the hydrogen bond-forming hydroxyl groups results in improvements in the aqueous solubility of the derivative [240].

III.1.3. MODIFIED Β-CYCLODEXTRINS

Native CDs can be chemically modified to improve their properties or to provide new functional groups, thanks to the hydroxyl groups at the C2, C3 (secondary hydroxyls) and C6 (primary hydroxyls) positions present on each glucose unit. However, the small difference in reactivity between the hydroxyl groups makes selective substitution difficult to achieve [241]. Another difficulty for the selective modification of CDs is the presence of the lipophilic cavity which can potentially interact with the different reagents. These difficulties

lead to a sharp increase in the price of cyclodextrins with the precision of the desired substitution, and commercial substituted cyclodextrins are generally composed of mixtures of substituted CDs that differ in the number of substituents but also in their position on the ring. Thus, while native cyclodextrins have a crystalline structure, this is not the case for modified cyclodextrins. Substituted cyclodextrins are characterized by their degree of substitution (DS), i.e. the mean number of substituted hydroxyls groups by cyclodextrin molecule. This DS can vary from 0 to 3n, n being the number of glucose units (6 for α-CD, 7 for β-CD and 8 for γ-CD). The high reactivity of the hydroxyl groups allows for a wide range of chemical modifications, and given the number of hydroxyls groups per cyclodextrin, the number of modification possibilities is almost unlimited. In 2004, Szejtli [234] estimated that thousands of CD derivatives were published and patented, however, the majority will never be industrially produced, because of the need for expensive, toxic and environment-polluting reagents, as well as complicated multi-step reactions. Finally, only a few dozen of modified CDs can be industrialized.

As there is a wide variety of modifications available, and the synthesis of these cyclodextrins is not the focus of this thesis project, we will only describe the modified cyclodextrins used in this project further in the text, presented in Figure I.26.

2-Hydroxypropyl β-Cyclodextrins (HP-β-CDs) : These derivatives are usually produced by the reaction of β-CDs with propylene oxide in alkaline medium [237]. The hydroxypropylation of cyclodextrins occurs in a random manner, with no preference on substitution site [242]. This results in products that are not well defined with respect to the position of the substituted group. HP-β-CDs are only characterized by their DS and the nature of the hydroxypropyl group. HP-β-CDs are highly water soluble and present an amorphous structure. Toxicological studies have been conducted and show that HP-β-CD is well tolerated by humans [243], making it one of the most produced and used cyclodextrin derivatives.

Carboxymethyl-β-Cyclodextrins : These derivatives are usually synthetized by reacting β-CDs with chloroacetic acid under alkaline condition [244], [245]. The carboxylic content introduced to the CDs offers new possibilities for grafting or adsorption of these derivatives onto substrates in order to bring the inclusion capabilities of cyclodextrins into different

application areas. These derivatives were first used for chiral analysis techniques [246], but studies on the use of these derivatives for biomedical applications are also being conducted, showing promising results [247].

Poly-β-CDs : the most common method used to polymerize cyclodextrins consists in their crosslinking using epichlorohydrin, resulting in an insoluble polymer [248]. The synthesis process, a one-step synthesis in water, is quite simple and easy to scale up. This kind of material could prove to be beneficial for e.g. remediation applications. However, epichlorohydrin is classified as a carcinogen reagent, thus important precautions must be taken when using it, and potential toxicity of the produced polymer is an obstacle to its use. Other routes of cross-linking have been studied with less harmful cross-linking reagents, such as polycarboxylic acids [249], resulting in water-soluble polymers. Having a chain of cyclodextrins rather than individual molecules can potentially have an impact on the interaction of CDs with the substrate in a functionalization, e.g. by increasing adsorption phenomena.

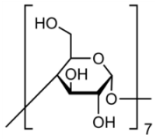

β-Cyclodextrin

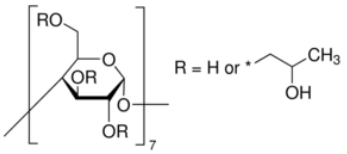

2-Hydroxypropyl-β-Cyclodextrin

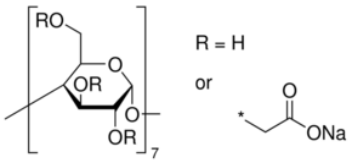

Carboxymethyl-β-Cyclodextrin Sodium Salt

Figure I.26: Schematic representations of the different β-CDs used.

III.2. CYCLODEXTRIN AND INCLUSION COMPLEX

III.2.1. PRINCIPLE AND PREPARATION

Thanks to its particular structure, CDs are widely used in supramolecular chemistry. In supramolecular chemistry, bonding between molecules is caused by weak and non-covalent interactions, such as electrostatic interactions, hydrogen bonds, hydrophobic interactions. Due to their hydrophobic cavity, CDs have been shown to perform host-guest interaction complexes with hydrophobic molecules, related to equilibrium between association and dissociation, as shown in Figure I.27.

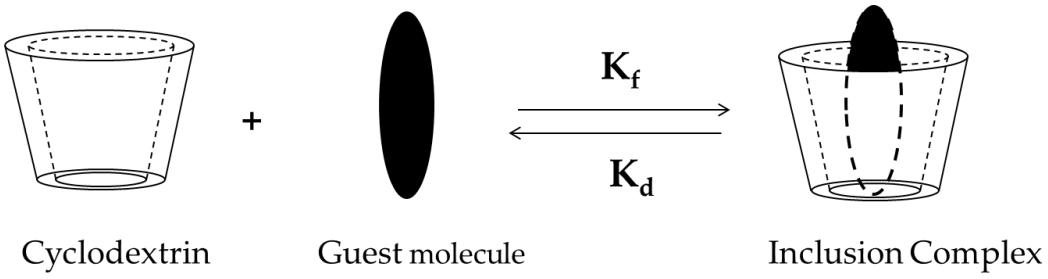

Figure I.27: Schematic representation of the inclusion process

Here, K_f and K_d are respectively the association and dissociation constant of the complex.

In 1956, the different steps of the formation of the inclusion complex was described by Cramer [238] :

1) The guest molecule approaches the cyclodextrin and the water molecules in the lipophilic cavity of the CD escape from it and place themselves in an energy level close to that of the gaseous state. 2) The guest molecule is free from the layer of water and acquires a different state. The layer of water then released disperses and rearranges itself. 3) The guest molecule, then in a state considered as that of perfect gases, penetrates inside the cavity and the complex is stabilized by Van der Waals and/or hydrogen interactions. 4) The expelled water molecules rearrange themselves and create hydrogen bonds between them. 5) Around the part of the guest molecule that has not entered the cavity, the structure of water is restored and integrated into the layer of water that moisturizes the CDs.

As reported, the forces and interactions driving the complexation process can be either i) Van der Waals interactions, ii) electrostatic interactions, iii) hydrophobic interactions or iv) hydrogen bonding. However, there is still no global consensus about the relative importance of each contribution.

The driving force of the complex formation is the release of water-molecules from the hydrophobic cavity. Water molecules are displaced by more hydrophobic molecules , forming apolar-apolar interactions with CDs, hence resulting in a more stable lower energy state [236], [250]. The stoichiometry of inclusion represented in Figure 28 is 1:1, i.e. one host molecule for one guest molecule. However, depending on the size of the guest molecule, different stoichiometries have been observed such as 1:2,2:1,2:2 [251], as displayed in Figure I.28.

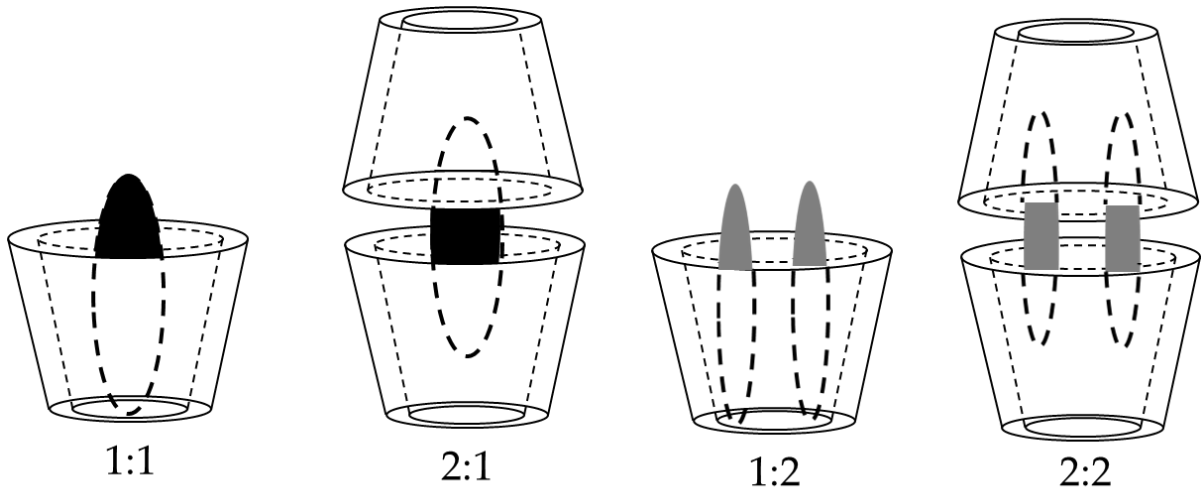

Figure I.28: various stoichiometries of inclusion complex.

When the stoichiometry of the complexation is known, it is then possible to determine the affinity constant between the host and the guest, with the following equations (Eq I.4).

$$aCD + bI \leftrightarrows CDa/Ib$$

$$Kf = \frac{[CDa/Ib]}{[CD]^a I^b} \qquad \text{(Eq. I.4)}$$

a and b being the stoichiometric coefficient of respectively the host and the guest. In the case of a stoichiometry 1:1, Eq. 4 becomes Eq.I.5:

$$CD + I \leftrightarrows CD/I$$

$$Kf = \frac{[CD/I]}{[CD][I]} \quad \text{(Eq.I.5)}$$

There are different processes for the preparation of inclusion complexes, allowing the preparation in solid or liquid medium [238]. Each preparation method has a particular influence on the physicochemical characteristics and must therefore be chosen carefully. The method used in the scope of this project to analyze the solid inclusion complex is the preparation by freeze-drying: the active ingredient in saturation is mixed with a specific amount of CDs in solution. The solution is mixed under controlled conditions (time, temperature). The solution is filtered with a 0.45 µm membrane in order to recover only what has been solubilized. The filtrate is then freeze-dried, in order to obtain the inclusion complexes in solid form.

III.2.2. CHARACTERIZATION

Some experimental methods to characterize the inclusion complexes are described, with a focus on the methods that were used during this project. Some methods allow fora direct measurement and characterization of the complexation process, such as phase solubility diagrams, isothermal titration calorimetry and nuclear magnetic resonance. Other methods, such as X-Ray diffraction, Fourier Transformed Infrared spectroscopy and thermal analysis (Differential Scanning calorimetry, Thermogravimetric analysis) are based on the modification of the physicochemical properties of cyclodextrins by the inclusion process, and make it possible, by comparison with the results obtained for cyclodextrins alone, to conclude on the formation of an inclusion or not, but do not allow to quantify the complexation equilibria. The following methods are the most used to characterize the inclusion complexes between cyclodextrins and a guest molecule.

PHASE SOLUBILITY DIAGRAM

By forming inclusion complexes with poorly soluble hydrophobic molecules, cyclodextrins increase the solubility of these molecules. This increase in solubility is linked to the concentration of cyclodextrins and to the stoichiometry of the host-guest interaction. In 1965, Higuchi and Connors [252] proposed a method to determine the affinity constant via a solubility diagram. This method can be summarized as follows: i) Solutions saturated with

active ingredients but with known cyclodextrin concentrations are prepared, with concentration within the solubility range of the CDs. ii) The solutions are placed under stirring and controlled humidity and temperature conditions for a suitable time (e.g. 24 hours). iii) The solutions are filtered with 0.45 µm filters and the filtrates are analyzed by UV spectroscopy, the concentration of active ingredient being calculated using calibration curves.

With this method, we can determine the solubilization effect of CDs due to the formation of inclusion complexes. Different behaviors can be observed, as shown in Figure I.29:

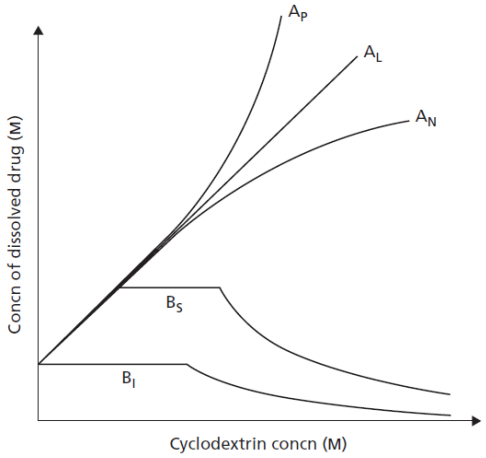

Figure I.29: Phase solubility diagram and classification according to Higuchi and Connors. Extracted from [253]

A-type curves corresponds to the formation of soluble inclusion complexes, while B-type curves are attributed to the formation of inclusion complexes with limited solubility [250]. A_L curves are representatives of a 1:1 complexation, with a linear increase in the drug solubility with the increase of the CD's concentration. Non-linear A-type curves are representative of inclusion complexes of higher stoichiometry. In the case of a 1:1 complexation, the stability constant of the complex can be calculated from the slope of the curve with the following equation (Eq I.6):

$$K_{1/1} = \frac{slope}{S_0(1-slope)} \quad \text{(Eq. I.6)}$$

Where S_0 is the solubility of the drug in the solvent without CD. This diagram is usually performed with UV-vis spectroscopy.

It is worth noting that the inclusion of the drug in the cyclodextrin can slightly modify the UV-response of the drug. To perform this characterization, filtrate should be mixed with ethanol at 1:1 proportion to ensure that no drug molecules remain in inclusion during UV-analysis.

Isothermal Titration Calorimetry

Isothermal titration calorimetry has been widely used for the characterization of inclusion complexes with natural CDs [254]. This polyvalent technique allows direct measurement of the association constant, the stoichiometry of the complex, the heat of reaction and hence the enthalpy of inclusion, allowing to calculate the thermodynamic values of the system such as enthalpy, entropy and free energy.

NMR

Nuclear Magnetic Resonance (NMR) allows the study of atomic nuclei capable of absorbing electromagnetic radiation in the radio frequency range when placed in an external magnetic field. The analysis of the interaction between CDs and active ingredients by NMR is based on the observation and interpretation of changes in the chemical environment of the CD protons during complexation [255]. As shown in Figure I.30, the CD's protons H3 and H5 are located inside the lipophilic cavity of the CD. Thus, a change in the resonance of these protons indicates complexation with the active ingredient. The study of the protons of the guest molecule also makes it possible to determine the portion of the molecule that interacts with CD. The development of 2D techniques, such as ROESY technique, allows a more detailed study of the interactions between CD and the molecule, especially for substituted cyclodextrins, which present more complex structures [256].

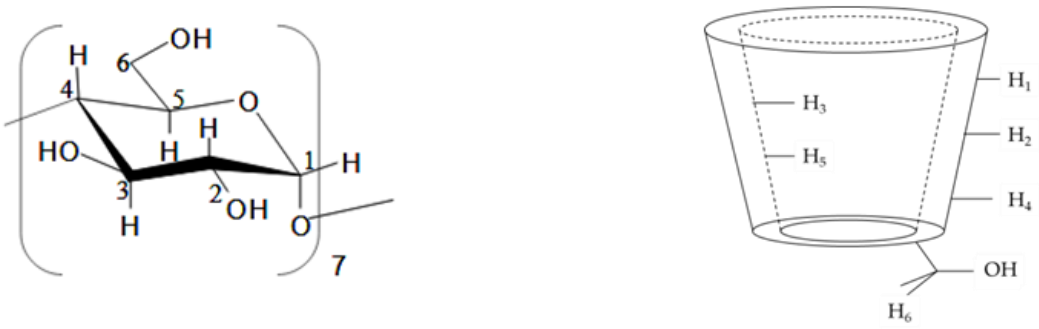

Figure I.30: Schematic representation of β-CD protons.

THERMAL METHODS: TGA/DSC

Differential Scanning Calorimetry (DSC) is used to demonstrate the formation of inclusion complexes in solid form. Following complexation, the thermodynamic properties of the compounds are modified, allowing for detection of the modification or disappearance of characteristic peaks of the guest molecules corresponding to their evaporation or melting following their encapsulation in CDs [257]. The modification of thermodynamic properties caused by the encapsulation could also be measured by thermogravimetric analysis, with the modification of fusion temperature between the raw compounds and the inclusion complex [258].

X-RAY DIFFRACTION

X-ray diffraction is a technique used for assessing the crystal structure of a compound. Natural CDs have a crystalline structure, and therefore show intense peaks in the diffractogram. When there is inclusion of an API in the CD, amorphisation of the API occurs, resulting in the appearance of a diffuse spectrum on the diffractogram of the complex. It should be noted that since substituted CDs are amorphous and show a diffuse spectrum, it is complicated to analyze the inclusion of an API in a substituted CD, as the change in the diffuse spectrum can be explained by the inclusion of the API but also by the mixing of the two amorphous compounds [259].

FTIR

Fourier-transformed infrared spectroscopy (FTIR) is used to identify directly and quickly the formation of an inclusion complex. This method is based on the comparison of the spectra of the individual molecules and the complex. The loss of vibrations and transitions of the guest molecule due to their change of environment and interactions with the CDs during their inclusion result in an alteration or even disappearance of their characteristic bands, while the spectrum of the CDs generally undergoes only a small change [260], [261].

III.2.3. APPLICATIONS

The development of cyclodextrin production on an industrial scale since the 1980s has enabled these molecules to be used in a wide range of applications in which their inclusion properties have proved to be of great value. A recent review by Crini et al. in 2019

[262] provides a global overview of the uses of cyclodextrins in different application areas, so this section will aim to provide a comprehensive summary of the different application areas.

PHARMACEUTICAL AND MEDICAL APPLICATIONS

The pharmaceutical field is the most studied for the use of cyclodextrins. In 2010, Loftson and Brewster [253] reported that while 40% of the drugs currently on sale could be characterized as poorly soluble, about 90% of the drugs being developed could be characterized as poorly soluble. This rises issues about the vectorization and bioavailabity of the drugs. The use of cyclodextrins and their inclusion complexes with poorly soluble API allows for increased stability of API, as well as an increase in their solubility and bioavailability. Furthermore, it has been proven that in some cases cyclodextrins can be applied to reduce the effect of irritating or bitter tasting of API [263]. Around 40 formulations have been commercialized since the 80's, mainly based on β-CD and HP-β-CD, but other cyclodextrins could be used, such as a modified γ-CD, as e.g. Sugammadex [264]. The following table presents some examples of approved and marketed drug-cyclodextrin complexes (see Table I.10). The use of cyclodextrins in the pharmaceutical field has now become so important that it is the industry with the highest consumption of CDs.

Table I.10: Examples of approved and marketed drug-cyclodextrin complexes, adapted from [265]

Cyclodextrin	Drug	Administration route	Trade name	Market
α-CD	Alprostadil (PGE1)	Intravenous	Prostavastin, Caverject,Edex	Europe,Japan, United States
	Cetofiam hexetil HCl	Oral	Pansorin T	Japan
β-CD	Nicotine	Sublingual	Nicorette	Europe
	Piroxicam	Oral	Brexin	Europe
	Dexamethasone	Dermal	Glymesason	Japan
	Iodine	Topical	Mena-Gargle	Japan
HP-β-CD	Cisapride	Rectal	Propulsid	Europe
	Hydrocortisone	Buccal	Dexocort	Europe
	Itraconazole	Oral, intravenous	Sporanox	Europe, United States
Randomly methylated-β-CD	Chloramphenicol	Eye drops	Clorocil	Europe

COSMETICS AND HYGIENE

CDs are commonly used in the fields of cosmetics and hygiene. CDs are used for multiple applications, such as for the preservation and stabilization of dyes, flavors or vitamins, the stabilization of emulsions, the increase in solubility of hydrophobic substances, the reduction of the volatility of perfumes, the transformation of liquid products into solid products, the controlled release of active ingredients or even the reduction of certain undesirable and irritating effects of certain molecules [266]. A well-known example of the use of CDs for hygiene is the Febreze household odor eliminator (Procter & Gamble), which has a formulation based on HP-β-CD to encapsulate odor molecules.

FOOD INDUSTRY

CDs are commonly used in the food industry for encapsulation of flavors, protection against oxidation, elimination of unpleasant odors and tastes, sequestration of cholesterol, preservation of foodstuffs or prolongation of the taste. It is worth noting that if the three native CDs, namely α-CD, β-CD and γ-CD, are approved as food ingredients, modified CDs that are approved as a drug excipient are not recognized as safe for food applications [267].

ENVIRONMENT

Cyclodextrins could be beneficial for environmental science, in terms of solubilizing organic contaminants and capturing pollutants such as heavy metals ions [268]. Cyclodextrines are also used in water treatments for removal of toxins [269].

III.3. PREVIOUS WORKS COMBINING CDS AND NANOCELLULOSIC MATERIALS

The association of CDs and wood-based nanocelluloses has not been extensively studied prior to this project. Below, a summary of the published work on this topic is given. The following table lists studies that have been published (Table I.11).

Table I.11: Previous work combining CDs and Nanocellulose

Nanocellulose	CD	Functionalization strategy	Application	Source
toCNFs	βCD	Direct grafting	Release of essential oil	[270]
CNFs	βCD	Cross linking with citric acid	Depollution	[271]
toCNFs	CMβCD	Amidation via EDC/NHS	Depollution	[272]
HP-CNFs	HPβCD	Electrospinning	Drug release	[273]
CNFs	βCD	Coating/Adsorption	Drug release	[190]
CNFs	βCD	Cross linking with citric acid	Antibacterial packaging	[274]
toCNFs	βCD	Non- covalent interaction	Drug Delivery/ Tissue Engineering	[275]
toCNCs	βCD / HPβCD	Direct grafting	Release of essential oil	[276]
CNCs	βCD	Grafting with epichlorohydrin	Tissue engineering	[277]
CNCs	βCD	Crosslinking with fumaric and succinic acid	Release of essential oil	[278]
CNCs	βCD	Ionic interaction	Drug delivery	[279]
CNCs	βCD	Grafting with epichlorohydrin	Supramolecular hydrogels	[280]

Different strategies have been implemented to functionalize nanocellulose with cyclodextrins, as illustrated in Figure I.31.

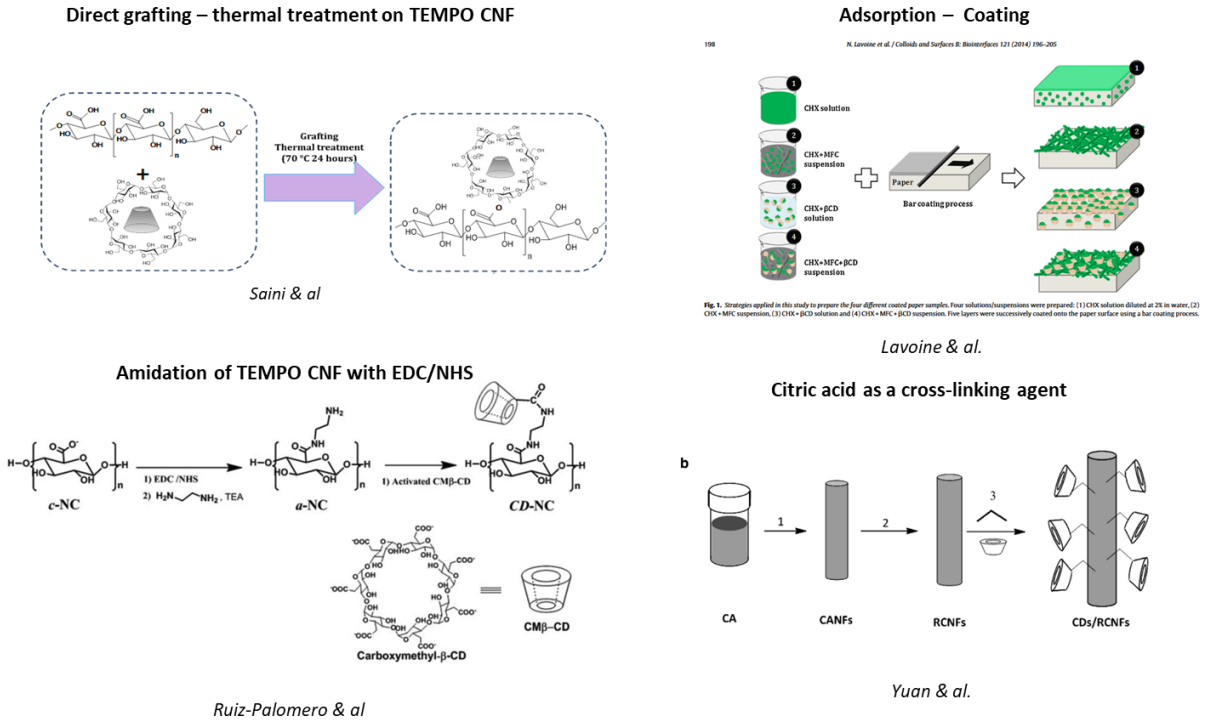

Figure I.31: Illustration of the different strategies of functionalization

One possible strategy is the use of a cross-linker between nanocellulose and cyclodextrins. Ruiz-Palomero et al. [272], reported the functionalization of toCNF with CM-β-CD, via EDC/NHS activation and used a diamine as cross-linker, for the adsorption of danofloxacin, an antibiotic in milk. Yuan et al. [271] used citric acid as a cross linker to graft β-CD and γ-CD on regenerated cellulose fibers for adsorption of toluene. Castro et al. [278] used different carboxylic acids as cross-linker between toCNF and β-CD and report better encapsulation of carvacrol for modified materials. Benefits of this strategy are the potential detection of the cross-linking agent, allowing an estimation of the yield of grafting. However, the potential traces of cross-linking agent can be an obstacle for biomedical applications.

Another strategy would be the grafting via thermal treatment. In 2016, Saini et al. [270] grafted β-CD on the carboxyls groups of toCNF via esterification by thermal treatment under vacuum, and reported a reduction in burst effect during release of carvacrol and an improvement in antimicrobial activity. The benefits of this strategy are the potential proof of esterification available with spectroscopic measurements. Additionally, the absence of cross-linking agent could be beneficial for medical applications.

Finally, a last strategy is the adsorption of cyclodextrins on nanocellulose with no further chemical reactions. Lavoine et al [190] reported the design of a controlled release system of chlorhexidine gluconate by coating onto a paper substrate a mixture of β-CD and micro-fibrillated cellulose. However, they pointed out the difficulty of assessing the adsorption and its characterization of it.

As mentioned earlier, the main difficulty with the combination of cyclodextrins and nanocelluloses is the chemical proximity of these two components. Both cellulose and cyclodextrins presents the same repeating units, linking β-1,4 glycosidic bonds in the case of cellulose and α-1,4 glycosidic bonds in the case of cyclodextrins, as illustrated in Figure I.32.

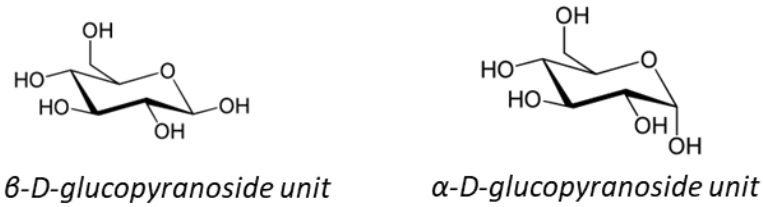

Figure I.32: Repeating units of cellulose (left) and cyclodextrins (right)

Additionally, when used in biomedical applications, it is necessary to avoid potential cross-linking with harmful agents or solvents.

The objective of this project is to design cyclodextrin/CNF materials without the use of toxic processes or molecules, while improving the release properties of a model active principal ingredient and find ways to characterize the adsorption between CDs and CNF. To achieve this, different cyclodextrins were used and methods to characterize the adsorption were set up in order to quantify the adsorbed cyclodextrins.

CONCLUSION

The advancement of technical and scientific knowledge has led to the development of biomaterials that offer increasingly effective therapeutic solutions, ranging from tissue reconstruction to controlled release of active ingredients. The current ecological and economic context requires, in addition to a reflection on the improvement of the properties of biomaterials, a questioning about their origin and their sustainability

Among the potential alternatives, cellulose is one of the most promising materials, being the most available biopolymer on earth but also a biocompatible polymer. In order to exploit this material for high value-added applications, nanomaterials are being extracted from it, offering exceptional physico-chemical characteristics. Moreover, these materials are bio-compatible, which makes them particularly suitable for use in biomedical applications. Their functionalization by molecules that can provide other properties is therefore particularly indicated.

The improvement of their active ingredient release properties, for the development of biobased wound dressings, can be envisaged by their functionalization with cyclodextrins, biobased cage-molecules which can form inclusion complexes with hydrophobic molecules. Although very promising, this approach presents many challenges, in particular the characterization of the functionalization or physisorption of CDs onto cellulose, complicated by the chemical proximity of CDs and cellulose.

This state of the art underlines the challenges on (i) the production and characterization of CDs/CNF materials, which has not been widely studied prior to this project, (ii) the fast and reliable production with various processing routes for these materials, and their structural characterization, since nanocellulose is a relatively recent field, (iii) provide antimicrobial properties and improve release properties through the formation of an inclusion complex between a poorly soluble active ingredient and different CDs.

Chapter 2 will present the methods used to characterize the adsorption of different cyclodextrins onto toCNFs, as well as the elaboration of CDs/toCNF films and cryogels and the impact of the functionalization on the mechanical properties of the materials

Chapter 3 will present a comprehensive study of the inclusion complexes formed between the different CDs and a model low-water soluble active ingredient, sulfadiazine, as well as the release and microbiology studies to demonstrate the beneficial impact of the use of cyclodextrins on the properties of our devices

LIST OF FIGURES

REFERENCES

[1] M. Y. Khan, P. Gupta, and V. K. Verma, 'A Review- Biomedical Engineering-Present and Future Prospective', vol. 3, no. 4, p. 6.

[2] G. Tiwari *et al.*, 'Drug delivery systems: An updated review', *Int J Pharm Investig*, vol. 2, no. 1, pp. 2–11, 2012, doi: 10.4103/2230-973X.96920.

[3] A. S. Hoffman, 'The origins and evolution of "controlled" drug delivery systems', *Journal of Controlled Release*, vol. 132, no. 3, pp. 153–163, Dec. 2008, doi: 10.1016/j.jconrel.2008.08.012.

[4] K. Park, 'Controlled drug delivery systems: Past forward and future back', *Journal of Controlled Release*, vol. 190, pp. 3–8, Sep. 2014, doi: 10.1016/j.jconrel.2014.03.054.

[5] Y. H. Yun, B. K. Lee, and K. Park, 'Controlled Drug Delivery: Historical perspective for the next generation', *Journal of Controlled Release*, vol. 219, pp. 2–7, Dec. 2015, doi: 10.1016/j.jconrel.2015.10.005.

[6] A. A. Chaudhari *et al.*, 'Future Prospects for Scaffolding Methods and Biomaterials in Skin Tissue Engineering: A Review', *Int. J. Mol. Sci.*, p. 31, 2016.

[7] A. C. de O. Gonzalez, T. F. Costa, Z. de A. Andrade, and A. R. A. P. Medrado, 'Wound healing - A literature review', *An. Bras. Dermatol.*, vol. 91, no. 5, pp. 614–620, Oct. 2016, doi: 10.1590/abd1806-4841.20164741.

[8] J. B. Shah, 'The History of Wound Care', *The Journal of the American College of Certified Wound Specialists*, vol. 3, no. 3, pp. 65–66, Sep. 2011, doi: 10.1016/j.jcws.2012.04.002.

[9] A. Demir and E. Cevher, 'Biopolymers as Wound Healing Materials: Challenges and New Strategies', in *Biomaterials Applications for Nanomedicine*, R. Pignatello, Ed. InTech, 2011. doi: 10.5772/25177.

[10] R. Langer and J. P. Vacanti, 'Tissue engineering', *Science*, vol. 260, no. 5110, pp. 920–926, May 1993, doi: 10.1126/science.8493529.

[11] D. Howard, L. D. Buttery, K. M. Shakesheff, and S. J. Roberts, 'Tissue engineering: strategies, stem cells and scaffolds', *Journal of Anatomy*, vol. 213, no. 1, pp. 66–72, Jul. 2008, doi: 10.1111/j.1469-7580.2008.00878.x.

[12] E. S. Place, N. D. Evans, and M. M. Stevens, 'Complexity in biomaterials for tissue engineering', *Nature Materials*, vol. 8, no. 6, pp. 457–470, Jun. 2009, doi: 10.1038/nmat2441.

[13] M. T. Cabeen and C. Jacobs-Wagner, 'Bacterial cell shape', *Nature Reviews Microbiology*, vol. 3, no. 8, pp. 601–610, Aug. 2005, doi: 10.1038/nrmicro1205.

[14] K. D. Young, 'Bacterial morphology: why have different shapes?', *Current Opinion in Microbiology*, vol. 10, no. 6, pp. 596–600, Dec. 2007, doi: 10.1016/j.mib.2007.09.009.

[15] C. Darpentigny, 'Nanocellulose-based materials functionalized in supercritical CO2 for antimicrobial wound dressing applications', p. 339.

[16] Weltgesundheitsorganisation, Ed., *Laboratory biosafety manual*, 3. ed. Geneva, 2004.

[17] J. W. Wilson, 'Mechanisms of bacterial pathogenicity', *Postgraduate Medical Journal*, vol. 78, no. 918, pp. 216–224, Apr. 2002, doi: 10.1136/pmj.78.918.216.

[18] G. Kapoor, S. Saigal, and A. Elongavan, 'Action and resistance mechanisms of antibiotics: A guide for clinicians', *J Anaesthesiol Clin Pharmacol*, vol. 33, no. 3, pp. 300–305, 2017, doi: 10.4103/joacp.JOACP_349_15.

[19] E. Etebu and I. Arikekpar, 'Antibiotics : Classification and mechanisms of action with emphasis on molecular perspectives', 2016.

[20] W. T. Langeveld, E. J. A. Veldhuizen, and S. A. Burt, 'Synergy between essential oil components and antibiotics: a review', *Critical Reviews in Microbiology*, vol. 40, no. 1, pp. 76–94, Feb. 2014, doi: 10.3109/1040841X.2013.763219.

[21] C. Darpentigny *et al.*, 'Antimicrobial cellulose nanofibril porous materials obtained by supercritical impregnation of thymol', *ACS Applied Bio Materials*, Mar. 2020, doi: 10.1021/acsabm.0c00033.

[22] S. Mittapally, R. Taranum, and S. Parveen, 'Metal ions as antibacterial agents', *J. Drug Delivery Ther.*, vol. 8, no. 6-s, pp. 411–419, Dec. 2018, doi: 10.22270/jddt.v8i6-s.2063.

[23] J. S. Möhler *et al.*, 'Enhancement of antibiotic-activity through complexation with metal ions - Combined ITC, NMR, enzymatic and biological studies', *Journal of Inorganic Biochemistry*, vol. 167, pp. 134–141, Feb. 2017, doi: 10.1016/j.jinorgbio.2016.11.028.

[24] R. J. Turner, 'Metal-based antimicrobial strategies', *Microb. Biotechnol.*, vol. 10, no. 5, pp. 1062–1065, Sep. 2017, doi: 10.1111/1751-7915.12785.

[25] C. J. Ioannou, G. W. Hanlon, and S. P. Denyer, 'Action of Disinfectant Quaternary Ammonium Compounds against Staphylococcus aureus', *AAC*, vol. 51, no. 1, pp. 296–306, Jan. 2007, doi: 10.1128/AAC.00375-06.

[26] C. P. Chauret, 'Sanitization', in *Encyclopedia of Food Microbiology (Second Edition)*, C. A. Batt and M. L. Tortorello, Eds. Oxford: Academic Press, 2014, pp. 360–364. doi: 10.1016/B978-0-12-384730-0.00407-9.

[27] J. Lei *et al.*, 'The antimicrobial peptides and their potential clinical applications', *Antimicrobial peptides*, p. 13.

[28] M. Vert *et al.*, 'Terminology for biorelated polymers and applications (IUPAC Recommendations 2012)', *Pure and Applied Chemistry*, vol. 84, no. 2, pp. 377–410, Jan. 2012, doi: 10.1351/PAC-REC-10-12-04.

[29] B. D. Ratner, 'Biomaterials: Been There, Done That, and Evolving into the Future', *Annu. Rev. Biomed. Eng.*, vol. 21, no. 1, pp. 171–191, Jun. 2019, doi: 10.1146/annurev-bioeng-062117-120940.

[30] B. D. Ratner and S. J. Bryant, 'Biomaterials: Where We Have Been and Where We Are Going', *Annu. Rev. Biomed. Eng.*, vol. 6, no. 1, pp. 41–75, Aug. 2004, doi: 10.1146/annurev.bioeng.6.040803.140027.

[31] M. Smyth, 'Nanocellulose based materials for Cell Culture', p. 334.

[32] P. Kumar, B. S. Dehiya, and A. Sindhu, 'Bioceramics for Hard Tissue Engineering Applications: A Review', vol. 13, no. 5, p. 9, 2018.

[33] M. Saini, 'Implant biomaterials: A comprehensive review', *WJCC*, vol. 3, no. 1, p. 52, 2015, doi: 10.12998/wjcc.v3.i1.52.

[34] A. J. Salinas and M. Vallet-Regí, 'Bioactive ceramics: from bone grafts to tissue engineering', *RSC Adv.*, vol. 3, no. 28, p. 11116, 2013, doi: 10.1039/c3ra00166k.

[35] K. Pajor, L. Pajchel, and J. Kolmas, 'Hydroxyapatite and Fluorapatite in Conservative Dentistry and Oral Implantology—A Review', *Materials*, vol. 12, no. 17, p. 2683, Aug. 2019, doi: 10.3390/ma12172683.

[36] G. A. dos Santos, 'The Importance of Metallic Materials as Biomaterials', *ATROA*, vol. 3, no. 1, Oct. 2017, doi: 10.15406/atroa.2017.03.00054.

[37] N. Eliaz, 'Corrosion of Metallic Biomaterials: A Review', *Materials*, vol. 12, no. 3, p. 407, Jan. 2019, doi: 10.3390/ma12030407.

[38] H. Hermawan, D. Ramdan, and J. R. P. Djuansjah, 'Metals for Biomedical Applications', *Biomedical Engineering - From Theory to Applications*, Aug. 2011, doi: 10.5772/19033.

[39] T. Srichana and A. J. Domb, 'Polymeric Biomaterials', in *Biomedical Materials*, Springer, 2009, pp. 83–19.

[40] V. DeStefano, S. Khan, and A. Tabada, 'Applications of PLA in modern medicine', *Engineered Regeneration*, vol. 1, pp. 76–87, 2020, doi: 10.1016/j.engreg.2020.08.002.

[41] K. J. Jem and B. Tan, 'The development and challenges of poly (lactic acid) and poly (glycolic acid)', *Advanced Industrial and Engineering Polymer Research*, vol. 3, no. 2, pp. 60–70, Apr. 2020, doi: 10.1016/j.aiepr.2020.01.002.

[42] T. G. Sahana and P. D. Rekha, 'Biopolymers: Applications in wound healing and skin tissue engineering', *Mol Biol Rep*, vol. 45, no. 6, pp. 2857–2867, Dec. 2018, doi: 10.1007/s11033-018-4296-3.

[43] R. Rebelo, M. Fernandes, and R. Fangueiro, 'Biopolymers in Medical Implants: A Brief Review', *Procedia Engineering*, vol. 200, pp. 236–243, 2017, doi: 10.1016/j.proeng.2017.07.034.

[44] 'Collagen Market Size, Trends | Industry Research Report 2027'. https://www.grandviewresearch.com/industry-analysis/collagen-market (accessed Mar. 01, 2021).

[45] F. Copes, N. Pien, S. Van Vlierberghe, F. Boccafoschi, and D. Mantovani, 'Collagen-Based Tissue Engineering Strategies for Vascular Medicine', *Front. Bioeng. Biotechnol.*, vol. 7, p. 166, Jul. 2019, doi: 10.3389/fbioe.2019.00166.

[46] S. Chattopadhyay and R. T. Raines, 'Collagen-based biomaterials for wound healing', *Biopolymers*, vol. 101, no. 8, pp. 821–833, Aug. 2014, doi: 10.1002/bip.22486.

[47] C. Dong and Y. Lv, 'Application of Collagen Scaffold in Tissue Engineering: Recent Advances and New Perspectives', *Polymers*, vol. 8, no. 2, p. 42, Feb. 2016, doi: 10.3390/polym8020042.

[48] J. Lee and G. Kim, 'Three-Dimensional Hierarchical Nanofibrous Collagen Scaffold Fabricated Using Fibrillated Collagen and Pluronic F-127 for Regenerating Bone Tissue', *ACS Appl. Mater. Interfaces*, vol. 10, no. 42, pp. 35801–35811, Oct. 2018, doi: 10.1021/acsami.8b14088.

[49] M. S. Manjari, K. P. Aaron, C. Muralidharan, and C. Rose, 'Highly biocompatible novel polyphenol cross-linked collagen scaffold for potential tissue engineering applications', *Reactive and Functional Polymers*, vol. 153, p. 104630, Aug. 2020, doi: 10.1016/j.reactfunctpolym.2020.104630.

[50] J. M. Hartinger *et al.*, 'Rifampin-Releasing Triple-Layer Cross-Linked Fresh Water Fish Collagen Sponges as Wound Dressings', *BioMed Research International*, vol. 2020, pp. 1–13, Oct. 2020, doi: 10.1155/2020/3841861.

[51] L. Ge *et al.*, 'Fabrication of Antibacterial Collagen-Based Composite Wound Dressing', *ACS Sustainable Chem. Eng.*, vol. 6, no. 7, pp. 9153–9166, Jul. 2018, doi: 10.1021/acssuschemeng.8b01482.

[52] W. Pon-On, N. Charoenphandhu, J. Teerapornpuntakit, J. Thongbunchoo, N. Krishnamra, and I.-M. Tang, 'In vitro study of vancomycin release and osteoblast-like cell growth on structured calcium phosphate-collagen', *Materials Science and Engineering: C*, vol. 33, no. 3, pp. 1423–1431, Apr. 2013, doi: 10.1016/j.msec.2012.12.046.

[53] O. C. M. Chan, K.-F. So, and B. P. Chan, 'Fabrication of nano-fibrous collagen microspheres for protein delivery and effects of photochemical crosslinking on release kinetics', *Journal of Controlled Release*, vol. 129, no. 2, pp. 135–143, Jul. 2008, doi: 10.1016/j.jconrel.2008.04.011.

[54] S. Municoy, P. E. Antezana, C. J. Pérez, M. G. Bellino, and M. F. Desimone, 'Tuning the antimicrobial activity of collagen biomaterials through a liposomal approach', *J Appl Polym Sci*, vol. 138, no. 18, p. 50330, May 2021, doi: 10.1002/app.50330.

[55] F. Howaili, M. Mashreghi, N. Mahdavi Sahri, A. Kompany, and R. Jalal, 'Development and evaluation of a novel beneficent antimicrobial bioscaffold based on animal waste-fish swim bladder (FSB) doped with silver nanoparticles', *Environmental Research*, p. 10, 2020.

[56] J. Liu, S. Willför, and C. Xu, 'A review of bioactive plant polysaccharides: Biological activities, functionalization, and biomedical applications', *Bioactive Carbohydrates and Dietary Fibre*, vol. 5, no. 1, pp. 31–61, Jan. 2015, doi: 10.1016/j.bcdf.2014.12.001.

[57] M. R. Kasaai, J. Arul, and G. Charlet, 'Fragmentation of Chitosan by Acids', *The Scientific World Journal*, vol. 2013, pp. 1–11, 2013, doi: 10.1155/2013/508540.

[58] S. Ahmed and S. Ikram, 'Chitosan Based Scaffolds and Their Applications in Wound Healing', *Achievements in the Life Sciences*, vol. 10, no. 1, pp. 27–37, Jun. 2016, doi: 10.1016/j.als.2016.04.001.

[59] R. Ramya, J. Venkatesan, S. K. Kim, and P. N. Sudha, 'Biomedical Applications of Chitosan: An Overview', *j biomat tissue engng*, vol. 2, no. 2, pp. 100–111, Jun. 2012, doi: 10.1166/jbt.2012.1030.

[60] Matica, Aachmann, Tøndervik, Sletta, and Ostafe, 'Chitosan as a Wound Dressing Starting Material: Antimicrobial Properties and Mode of Action', *IJMS*, vol. 20, no. 23, p. 5889, Nov. 2019, doi: 10.3390/ijms20235889.

[61] Blessing Aderibigbe and Buhle Buyana, 'Alginate in Wound Dressings', *Pharmaceutics*, vol. 10, no. 2, p. 42, Apr. 2018, doi: 10.3390/pharmaceutics10020042.

[62] K. Y. Lee and D. J. Mooney, 'Alginate: Properties and biomedical applications', *Progress in Polymer Science*, vol. 37, no. 1, pp. 106–126, Jan. 2012, doi: 10.1016/j.progpolymsci.2011.06.003.

[63] D. M. Hariyadi and N. Islam, 'Current Status of Alginate in Drug Delivery', p. 16.

[64] J. H. Sze, J. C. Brownlie, and C. A. Love, 'Biotechnological production of hyaluronic acid: a mini review', *3 Biotech*, vol. 6, no. 1, p. 67, Jun. 2016, doi: 10.1007/s13205-016-0379-9.

[65] A. Fakhari and C. Berkland, 'Applications and emerging trends of hyaluronic acid in tissue engineering, as a dermal filler and in osteoarthritis treatment', *Acta Biomaterialia*, vol. 9, no. 7, pp. 7081–7092, Jul. 2013, doi: 10.1016/j.actbio.2013.03.005.

[66] M. Dovedytis, Z. J. Liu, and S. Bartlett, 'Hyaluronic acid and its biomedical applications: A review', *Engineered Regeneration*, vol. 1, pp. 102–113, 2020, doi: 10.1016/j.engreg.2020.10.001.

[67] S. N. A. Bukhari *et al.*, 'Hyaluronic acid, a promising skin rejuvenating biomedicine: A review of recent updates and pre-clinical and clinical investigations on cosmetic and nutricosmetic effects', *International Journal of Biological Macromolecules*, vol. 120, pp. 1682–1695, Dec. 2018, doi: 10.1016/j.ijbiomac.2018.09.188.

[68] K. A. Sindhu, R. Prasanth, and V. K. Thakur, 'Medical Applications of Cellulose and its Derivatives: Present and Future', in *Nanocellulose Polymer Nanocomposites*, V. K. Thakur, Ed. Hoboken, NJ, USA: John Wiley & Sons, Inc., 2014, pp. 437–477. doi: 10.1002/9781118872246.ch16.

[69] 'Application of Cellulose and Cellulose Derivatives in Pharmaceutical Industries | IntechOpen'. https://www.intechopen.com/books/cellulose-medical-pharmaceutical-and-

electronic-applications/application-of-cellulose-and-cellulose-derivatives-in-pharmaceutical-industries (accessed May 12, 2021).

[70] H. Seddiqi *et al.*, 'Cellulose and its derivatives: towards biomedical applications', *Cellulose*, Jan. 2021, doi: 10.1007/s10570-020-03674-w.

[71] F. Rol, M. N. Belgacem, A. Gandini, and J. Bras, 'Recent advances in surface-modified cellulose nanofibrils', *Progress in Polymer Science*, Sep. 2018, doi: 10.1016/j.progpolymsci.2018.09.002.

[72] C. Darpentigny, S. Molina-Boisseau, G. Nonglaton, J. Bras, and B. Jean, 'Ice-templated freeze-dried cryogels from tunicate cellulose nanocrystals with high specific surface area and anisotropic morphological and mechanical properties', *Cellulose*, vol. 27, no. 1, pp. 233–247, Jan. 2020, doi: 10.1007/s10570-019-02772-8.

[73] T. Li *et al.*, 'Developing fibrillated cellulose as a sustainable technological material', *Nature*, vol. 590, no. 7844, pp. 47–56, Feb. 2021, doi: 10.1038/s41586-020-03167-7.

[74] A. Payen, 'Mémoire sur la composition du tissu propre des plantes et du ligneux', *Comptes rendus hebdomadaires des séances de l'académie des sciences*, vol. 7, pp. 1052–1056.

[75] Willstäter and Zechmeister, 'Zur Kenntnis der Hydrolyse von Cellulose I.', *Berichte der deutschen chemischen Gesellschaft*, vol. 46, pp. 2401–2412, 1913.

[76] D. Ciolacu and V. I. Popa, 'CELLULOSE ALLOMORPHS – OVERVIEW AND PERSPECTIVES', p. 39.

[77] F. M. Gírio, C. Fonseca, F. Carvalheiro, L. C. Duarte, S. Marques, and R. Bogel-Łukasik, 'Hemicelluloses for fuel ethanol: A review', *Bioresource Technology*, vol. 101, no. 13, pp. 4775–4800, Jul. 2010, doi: 10.1016/j.biortech.2010.01.088.

[78] M. Norgren and H. Edlund, 'Lignin: Recent advances and emerging applications', *Current Opinion in Colloid & Interface Science*, vol. 19, no. 5, pp. 409–416, Oct. 2014, doi: 10.1016/j.cocis.2014.08.004.

[79] I. A. Sacui *et al.*, 'Comparison of the Properties of Cellulose Nanocrystals and Cellulose Nanofibrils Isolated from Bacteria, Tunicate, and Wood Processed Using Acid, Enzymatic, Mechanical, and Oxidative Methods', *ACS Appl. Mater. Interfaces*, vol. 6, no. 9, pp. 6127–6138, May 2014, doi: 10.1021/am500359f.

[80] H. Suryanto, E. Marsyahyo, Y. S. Irawan, and R. Soenoko, 'Effect of Alkali Treatment on Crystalline Structure of Cellulose Fiber from Mendong (*Fimbristylis globulosa*) Straw', *KEM*, vol. 594–595, pp. 720–724, Dec. 2013, doi: 10.4028/www.scientific.net/KEM.594-595.720.

[81] 'Nanocellulose Market Size and Share | Industry Statistics – 2026', *Global Market Insights, Inc.* https://www.gminsights.com/industry-analysis/nanocellulose-market (accessed Apr. 21, 2021).

[82] J.-H. Kim *et al.*, 'Review of Nanocellulose for Sustainable Future Materials', *INTERNATIONAL JOURNAL OF PRECISION ENGINEERING AND MANUFACTURING*, vol. 2, no. 2, p. 17.

[83] J. Shojaeiarani, D. Bajwa, and A. Shirzadifar, 'A review on cellulose nanocrystals as promising biocompounds for the synthesis of nanocomposite hydrogels', *Carbohydrate Polymers*, vol. 216, pp. 247–259, Jul. 2019, doi: 10.1016/j.carbpol.2019.04.033.

[84] Y. Habibi, 'Key advances in the chemical modification of nanocelluloses', *Chem. Soc. Rev.*, vol. 43, no. 5, pp. 1519–1542, Feb. 2014, doi: 10.1039/C3CS60204D.

[85] A. F. Turbak and F. W. Snyder, '(54) MICROFIBRILLATED CELLULOSE', p. 9.

[86] O. Nechyporchuk, M. N. Belgacem, and J. Bras, 'Production of cellulose nanofibrils: A review of recent advances', *Industrial Crops and Products*, vol. 93, pp. 2–25, Dec. 2016, doi: 10.1016/j.indcrop.2016.02.016.

[87] T. Taipale, M. Österberg, A. Nykänen, J. Ruokolainen, and J. Laine, 'Effect of microfibrillated cellulose and fines on the drainage of kraft pulp suspension and paper strength', *Cellulose*, vol. 17, no. 5, pp. 1005–1020, Oct. 2010, doi: 10.1007/s10570-010-9431-9.

[88] S. Josset, P. Orsolini, G. Siqueira, A. Tejado, P. Tingaut, and T. Zimmermann, 'Energy consumption of the nanofibrillation of bleached pulp, wheat straw and recycled newspaper through a grinding process', *Nordic Pulp & Paper Research Journal*, vol. 29, no. 1, pp. 167–175, Jan. 2014, doi: 10.3183/npprj-2014-29-01-p167-175.

[89] H. Lee and S. Mani, 'Mechanical pretreatment of cellulose pulp to produce cellulose nanofibrils using a dry grinding method', *Industrial Crops and Products*, vol. 104, pp. 179–187, Oct. 2017, doi: 10.1016/j.indcrop.2017.04.044.

[90] M. Henriksson, G. Henriksson, L. A. Berglund, and T. Lindström, 'An environmentally friendly method for enzyme-assisted preparation of microfibrillated cellulose (MFC) nanofibers', *European Polymer Journal*, vol. 43, no. 8, pp. 3434–3441, Aug. 2007, doi: 10.1016/j.eurpolymj.2007.05.038.

[91] N. Lavoine, 'Conception, mise en oeuvre et caractérisation de nouveaux bio-nano-matériaux fonctionnels.', p. 411.

[92] M. Pääkkö *et al.*, 'Enzymatic Hydrolysis Combined with Mechanical Shearing and High-Pressure Homogenization for Nanoscale Cellulose Fibrils and Strong Gels', *Biomacromolecules*, vol. 8, no. 6, pp. 1934–1941, Jun. 2007, doi: 10.1021/bm061215p.

[93] A. Isogai, T. Saito, and H. Fukuzumi, 'TEMPO-oxidized cellulose nanofibers', *Nanoscale*, vol. 3, no. 1, pp. 71–85, 2011, doi: 10.1039/C0NR00583E.

[94] N. J. Davis and S. L. Flitscb, 'Selective Oxidation of Monosaccharide Derivatives to Uranic Acids', p. 4.

[95] T. Saito, Y. Nishiyama, J.-L. Putaux, M. Vignon, and A. Isogai, 'Homogeneous Suspensions of Individualized Microfibrils from TEMPO-Catalyzed Oxidation of Native Cellulose', *Biomacromolecules*, vol. 7, no. 6, pp. 1687–1691, Jun. 2006, doi: 10.1021/bm060154s.

[96] T. Saito and A. Isogai, 'TEMPO-Mediated Oxidation of Native Cellulose. The Effect of Oxidation Conditions on Chemical and Crystal Structures of the Water-Insoluble Fractions', *Biomacromolecules*, vol. 5, no. 5, pp. 1983–1989, Sep. 2004, doi: 10.1021/bm0497769.

[97] T. Saito and A. Isogai, 'Introduction of aldehyde groups on surfaces of native cellulose fibers by TEMPO-mediated oxidation', *Colloids and Surfaces A: Physicochemical and Engineering Aspects*, vol. 289, no. 1–3, pp. 219–225, Oct. 2006, doi: 10.1016/j.colsurfa.2006.04.038.

[98] T. Saito *et al.*, 'Individualization of Nano-Sized Plant Cellulose Fibrils by Direct Surface Carboxylation Using TEMPO Catalyst under Neutral Conditions', *Biomacromolecules*, vol. 10, no. 7, pp. 1992–1996, Jul. 2009, doi: 10.1021/bm900414t.

[99] Q. Tarrés, S. Boufi, P. Mutjé, and M. Delgado-Aguilar, 'Enzymatically hydrolyzed and TEMPO-oxidized cellulose nanofibers for the production of nanopapers: morphological, optical, thermal and mechanical properties', *Cellulose*, vol. 24, no. 9, pp. 3943–3954, Sep. 2017, doi: 10.1007/s10570-017-1394-7.

[100] D. Klemm *et al.*, 'Nanocelluloses as Innovative Polymers in Research and Application', in *Polysaccharides II*, D. Klemm, Ed. Berlin, Heidelberg: Springer, 2006, pp. 49–96. doi: 10.1007/12_097.

[101] A. Dufresne, *Nanocellulose: from nature to high performance tailored materials*. Berlin: de Gruyter, 2012.

[102] 'Bacterial nanocellulose from agro-industrial wastes: low-cost and enhanced production by Komagataeibacter saccharivorans MD1', p. 14.

[103] D. Klemm *et al.*, 'Nanocellulose as a natural source for groundbreaking applications in materials science: Today's state', *Materials Today*, vol. 21, no. 7, pp. 720–748, Sep. 2018, doi: 10.1016/j.mattod.2018.02.001.

[104] M. M. Abeer, M. C. I. Mohd Amin, and C. Martin, 'A review of bacterial cellulose-based drug delivery systems: their biochemistry, current approaches and future prospects', *Journal of Pharmacy and Pharmacology*, vol. 66, no. 8, pp. 1047–1061, Jul. 2014, doi: 10.1111/jphp.12234.

[105] A. F. Jozala *et al.*, 'Bacterial nanocellulose production and application: a 10-year overview', *Appl Microbiol Biotechnol*, vol. 100, no. 5, pp. 2063–2072, Mar. 2016, doi: 10.1007/s00253-015-7243-4.

[106] C. Sharma, 'Bacterial nanocellulose_ Present status, biomedical applications and future perspectives', *Materials Science*, p. 18, 2019.

[107] C. Zhong, 'Industrial-Scale Production and Applications of Bacterial Cellulose', *Frontiers in Bioengineering and Biotechnology*, vol. 8, p. 19, 2020.

[108] E. J. Foster *et al.*, 'Current characterization methods for cellulose nanomaterials', *Chemical Society Reviews*, vol. 47, no. 8, pp. 2609–2679, 2018, doi: 10.1039/C6CS00895J.

[109] H. Durand, 'Functionalization of cellulose nanofibrils for the development of biobased medical devices', p. 319, 2019.

[110] J. Desmaisons, E. Boutonnet, M. Rueff, A. Dufresne, and J. Bras, 'A new quality index for benchmarking of different cellulose nanofibrils', *Carbohydrate Polymers*, vol. 174, pp. 318–329, Oct. 2017, doi: 10.1016/j.carbpol.2017.06.032.

[111] M. A. Hubbe *et al.*, 'Nanocellulose in Thin Films, Coatings, and Plies for Packaging Applications: A Review', *BioResources*, vol. 12, no. 1, pp. 2143–2233, Feb. 2017, doi: 10.15376/biores.12.1.2143-2233.

[112] K. S. Kontturi *et al.*, 'Noncovalent Surface Modification of Cellulose Nanopapers by Adsorption of Polymers from Aprotic Solvents', *Langmuir*, vol. 33, no. 23, pp. 5707–5712, Jun. 2017, doi: 10.1021/acs.langmuir.7b01236.

[113] A. Dufresne, 'Nanocellulose: a new ageless bionanomaterial', *Materials Today*, vol. 16, no. 6, pp. 220–227, Jun. 2013, doi: 10.1016/j.mattod.2013.06.004.

[114] M. Herrera, J. Sirviö, A. Mathew, and K. Oksman, 'Environmental friendly and sustainable gas barrier on porous materials : Nanocellulose coatings prepared using spin- and dip-coating', *Materials & Design*, vol. 93, pp. 19–25, 2016.

[115] K. J. De France, T. Hoare, and E. D. Cranston, 'Review of Hydrogels and Aerogels Containing Nanocellulose', *Chemistry of Materials*, vol. 29, no. 11, pp. 4609–4631, Jun. 2017, doi: 10.1021/acs.chemmater.7b00531.

[116] S. Gupta, F. Martoïa, L. Orgéas, and P. Dumont, 'Ice-Templated Porous Nanocellulose-Based Materials: Current Progress and Opportunities for Materials Engineering', *Applied Sciences*, vol. 8, no. 12, p. 2463, Dec. 2018, doi: 10.3390/app8122463.

[117] N. Lavoine and L. Bergström, 'Nanocellulose-based foams and aerogels: processing, properties, and applications', *J. Mater. Chem. A*, vol. 5, no. 31, pp. 16105–16117, 2017, doi: 10.1039/C7TA02807E.

[118] J. P. Vareda, A. Lamy-Mendes, and L. Durães, 'A reconsideration on the definition of the term aerogel based on current drying trends', *Microporous and Mesoporous Materials*, vol. 258, pp. 211–216, Mar. 2018, doi: 10.1016/j.micromeso.2017.09.016.

[119] F. V. Ferreira *et al.*, 'Porous nanocellulose gels and foams: Breakthrough status in the development of scaffolds for tissue engineering', *Materials Today*, vol. 37, pp. 126–141, Jul. 2020, doi: 10.1016/j.mattod.2020.03.003.

[120] V. B. Bueno and D. F. S. Petri, 'Xanthan hydrogel films: Molecular conformation, charge density and protein carriers', *Carbohydrate Polymers*, vol. 101, pp. 897–904, Jan. 2014, doi: 10.1016/j.carbpol.2013.10.039.

[121] V. Sampatrao Ghorpade, A. Vyankatrao Yadav, R. Jacky Dias, and K. Krishnat Mali, 'Fabrication of citric acid crosslinked β-cyclodextrin/hydroxyethylcellulose hydrogel films for controlled delivery of poorly soluble drugs', *Journal of Applied Polymer Science*, vol. 135, no. 27, p. 46452, Jul. 2018, doi: 10.1002/app.46452.

[122] X. Shen, J. L. Shamshina, P. Berton, G. Gurau, and R. D. Rogers, 'Hydrogels based on cellulose and chitin: fabrication, properties, and applications', *Green Chem.*, vol. 18, no. 1, pp. 53–75, 2016, doi: 10.1039/C5GC02396C.

[123] R. Curvello, V. S. Raghuwanshi, and G. Garnier, 'Engineering nanocellulose hydrogels for biomedical applications', *Advances in Colloid and Interface Science*, vol. 267, pp. 47–61, May 2019, doi: 10.1016/j.cis.2019.03.002.

[124] A. Basu, J. Lindh, E. Ålander, M. Strømme, and N. Ferraz, 'On the use of ion-crosslinked nanocellulose hydrogels for wound healing solutions: Physicochemical properties and application-oriented biocompatibility studies', *Carbohydrate Polymers*, vol. 174, pp. 299–308, Oct. 2017, doi: 10.1016/j.carbpol.2017.06.073.

[125] O. Aarstad, E. Heggset, I. Pedersen, S. Bjørnøy, K. Syverud, and B. Strand, 'Mechanical Properties of Composite Hydrogels of Alginate and Cellulose Nanofibrils', *Polymers*, vol. 9, no. 12, p. 378, Aug. 2017, doi: 10.3390/polym9080378.

[126] M. Bakhshpour, N. Idil, I. Perçin, and A. Denizli, 'Biomedical Applications of Polymeric Cryogels', *Applied Sciences*, vol. 9, no. 3, p. 553, Feb. 2019, doi: 10.3390/app9030553.

[127] C. Darpentigny, G. Nonglaton, J. Bras, and B. Jean, 'Highly absorbent cellulose nanofibrils aerogels prepared by supercritical drying', *Carbohydrate Polymers*, vol. 229, p. 115560, Feb. 2020, doi: 10.1016/j.carbpol.2019.115560.

[128] D. Trache *et al.*, 'Nanocellulose: From Fundamentals to Advanced Applications', *Frontiers in Chemistry*, vol. 8, p. 392, 2020, doi: 10.3389/fchem.2020.00392.

[129] B. Thomas *et al.*, 'Nanocellulose, a Versatile Green Platform: From Biosources to Materials and Their Applications', *Chem. Rev.*, vol. 118, no. 24, pp. 11575–11625, Dec. 2018, doi: 10.1021/acs.chemrev.7b00627.

[130] P. Phanthong, P. Reubroycharoen, X. Hao, G. Xu, A. Abudula, and G. Guan, 'Nanocellulose: Extraction and application', *Carbon Resources Conversion*, vol. 1, no. 1, pp. 32–43, Apr. 2018, doi: 10.1016/j.crcon.2018.05.004.

[131] L. Bacakova *et al.*, 'Versatile Application of Nanocellulose: From Industry to Skin Tissue Engineering and Wound Healing', *Nanomaterials*, vol. 9, no. 2, p. 164, Jan. 2019, doi: 10.3390/nano9020164.

[132] M. Tavakolian, H. Wiebe, M. A. Sadeghi, and T. G. M. van de Ven, 'Dye Removal Using Hairy Nanocellulose: Experimental and Theoretical Investigations', *ACS Appl. Mater. Interfaces*, vol. 12, no. 4, pp. 5040–5049, Jan. 2020, doi: 10.1021/acsami.9b18679.

[133] Q. Xu, Y. Wang, L. Jin, Y. Wang, and M. Qin, 'Adsorption of Cu (II), Pb (II) and Cr (VI) from aqueous solutions using black wattle tannin-immobilized nanocellulose', *Journal of Hazardous Materials*, vol. 339, pp. 91–99, Oct. 2017, doi: 10.1016/j.jhazmat.2017.06.005.

[134] T. Shahnaz, V. Vishnu Priyan, S. Pandian, and S. Narayanasamy, 'Use of Nanocellulose extracted from grass for adsorption abatement of Ciprofloxacin and Diclofenac removal with phyto, and fish toxicity studies', *Environmental Pollution*, vol. 268, p. 115494, Jan. 2021, doi: 10.1016/j.envpol.2020.115494.

[135] H. Zhan *et al.*, 'UV-induced self-cleanable TiO2/nanocellulose membrane for selective separation of oil/water emulsion', *Carbohydrate Polymers*, vol. 201, pp. 464–470, Dec. 2018, doi: 10.1016/j.carbpol.2018.08.093.

[136] N. Keshavarzi *et al.*, 'Nanocellulose–Zeolite Composite Films for Odor Elimination', *ACS Appl. Mater. Interfaces*, vol. 7, no. 26, pp. 14254–14262, Jul. 2015, doi: 10.1021/acsami.5b02252.

[137] B. Piluharto, U. Salamah, and D. Indarti, 'Preparation of Alginate/Nanocellulose Nanocomposite for Protein Adsorption', *Macromol. Symp.*, vol. 391, no. 1, p. 1900141, Jun. 2020, doi: 10.1002/masy.201900141.

[138] N. Ferraz *et al.*, 'Haemocompatibility and ion exchange capability of nanocellulose polypyrrole membranes intended for blood purification', *J. R. Soc. Interface.*, vol. 9, no. 73, pp. 1943–1955, Aug. 2012, doi: 10.1098/rsif.2012.0019.

[139] G. Metreveli, L. Wågberg, E. Emmoth, S. Belák, M. Strømme, and A. Mihranyan, 'A Size-Exclusion Nanocellulose Filter Paper for Virus Removal', *Adv. Healthcare Mater.*, vol. 3, no. 10, pp. 1546–1550, Oct. 2014, doi: 10.1002/adhm.201300641.

[140] M. A. El-Samahy, S. A. A. Mohamed, M. H. Abdel Rehim, and M. E. Mohram, 'Synthesis of hybrid paper sheets with enhanced air barrier and antimicrobial properties for food packaging', *Carbohydrate Polymers*, vol. 168, pp. 212–219, Jul. 2017, doi: 10.1016/j.carbpol.2017.03.041.

[141] R. Koppolu, J. Lahti, T. Abitbol, A. Swerin, J. Kuusipalo, and M. Toivakka, 'Continuous Processing of Nanocellulose and Polylactic Acid into Multilayer Barrier Coatings', *ACS Appl. Mater. Interfaces*, vol. 11, no. 12, pp. 11920–11927, Mar. 2019, doi: 10.1021/acsami.9b00922.

[142] H. Spieser, A. Denneulin, D. Deganello, D. Gethin, R. Koppolu, and J. Bras, 'Cellulose nanofibrils and silver nanowires active coatings for the development of antibacterial packaging surfaces', *Carbohydrate Polymers*, vol. 240, p. 116305, Jul. 2020, doi: 10.1016/j.carbpol.2020.116305.

[143] V. Apostolopoulou-Kalkavoura, P. Munier, and L. Bergström, 'Thermally Insulating Nanocellulose-Based Materials', *Adv. Mater.*, p. 2001839, Aug. 2020, doi: 10.1002/adma.202001839.

[144] F. Carosio, K. Jose, M. Lilian, F. Cuttica, G. Camino, and L. Berglund, 'Nanocellulose/clay thin films and foams : Biobased nanocomposites with superior flame retardant properties', 2016.

[145] B. Wicklein *et al.*, 'Thermally insulating and fire-retardant lightweight anisotropic foams based on nanocellulose and graphene oxide', *Nature Nanotechnology*, vol. 10, no. 3, pp. 277–283, Mar. 2015, doi: 10.1038/nnano.2014.248.

[146] D. Wang *et al.*, 'Bioinspired Lamellar Barriers for Significantly Improving the Flame-Retardant Properties of Nanocellulose Composites', *ACS Sustainable Chem. Eng.*, vol. 8, no. 11, pp. 4331–4336, Mar. 2020, doi: 10.1021/acssuschemeng.9b07745.

[147] J. Chen *et al.*, 'Carbon nanofibril composites with high sulfur loading fabricated from nanocellulose for high-performance lithium-sulfur batteries', *Colloids and Surfaces A:*

Physicochemical and Engineering Aspects, vol. 603, p. 125249, Oct. 2020, doi: 10.1016/j.colsurfa.2020.125249.

[148] H. Kim, B. Endrődi, G. Salazar-Alvarez, and A. Cornell, 'One-Step Electro-Precipitation of Nanocellulose Hydrogels on Conducting Substrates and Its Possible Applications: Coatings, Composites, and Energy Devices', *ACS Sustainable Chem. Eng.*, vol. 7, no. 24, pp. 19415–19425, Dec. 2019, doi: 10.1021/acssuschemeng.9b04171.

[149] L. Song *et al.*, 'Water-Induced shape memory effect of nanocellulose papers from sisal cellulose nanofibers with graphene oxide', *Carbohydrate Polymers*, vol. 179, pp. 110–117, Jan. 2018, doi: 10.1016/j.carbpol.2017.09.078.

[150] J. A. Hernández-Flores *et al.*, 'Morphological and Electrical Properties of Nanocellulose Compounds and Its Application on Capacitor Assembly', *International Journal of Polymer Science*, vol. 2020, pp. 1–14, Apr. 2020, doi: 10.1155/2020/1891064.

[151] O. A. Hisseine, W. Wilson, L. Sorelli, B. Tolnai, and A. Tagnit-Hamou, 'Nanocellulose for improved concrete performance: A macro-to-micro investigation for disclosing the effects of cellulose filaments on strength of cement systems', *Construction and Building Materials*, vol. 206, pp. 84–96, May 2019, doi: 10.1016/j.conbuildmat.2019.02.042.

[152] M. F. F. Pego, M. L. Bianchi, and P. K. Yasumura, 'Nanocellulose reinforcement in paper produced from fiber blending', *Wood Sci Technol*, vol. 54, no. 6, pp. 1587–1603, Nov. 2020, doi: 10.1007/s00226-020-01226-w.

[153] J. L. Sanchez-Salvador *et al.*, 'Comparison Of Mechanical And Chemical Nanocellulose As Additives To Reinforce Recycled Cardboard', *Sci Rep*, vol. 10, no. 1, p. 3778, Dec. 2020, doi: 10.1038/s41598-020-60507-3.

[154] E. Doineau *et al.*, 'Adsorption of xyloglucan and cellulose nanocrystals on natural fibres for the creation of hierarchically structured fibres', *Carbohydrate Polymers*, vol. 248, p. 116713, Nov. 2020, doi: 10.1016/j.carbpol.2020.116713.

[155] R. M. Júnior, G. V. Cardoso, E. Ferreira, and H. Costa, 'Surface characterization, mechanical and abrasion resistance of nanocellulose-reinforced wood panels', 2020.

[156] X. Guo *et al.*, 'A novel fluorescent nanocellulosic hydrogel based on carbon dots for efficient adsorption and sensitive sensing in heavy metals', *J. Mater. Chem. A*, vol. 7, no. 47, pp. 27081–27088, 2019, doi: 10.1039/C9TA11502A.

[157] F. Tamaddon and D. Arab, 'Urease covalently immobilized on cotton-derived nanocellulose-dialdehyde for urea detection and urea-based multicomponent synthesis of tetrahydro-pyrazolopyridines in water', *RSC Adv.*, vol. 9, no. 71, pp. 41893–41902, 2019, doi: 10.1039/C9RA05240B.

[158] A. M. Mahmoud, M. H. Mahnashi, S. A. Alkahtani, and M. M. El-Wekil, 'Nitrogen and sulfur co-doped graphene quantum dots/nanocellulose nanohybrid for electrochemical sensing of anti-schizophrenic drug olanzapine in pharmaceuticals and human biological fluids', *International Journal of Biological Macromolecules*, vol. 165, pp. 2030–2037, Dec. 2020, doi: 10.1016/j.ijbiomac.2020.10.084.

[159] J. Wang *et al.*, 'Piezoelectric Nanocellulose Thin Film with Large-Scale Vertical Crystal Alignment', *ACS Appl. Mater. Interfaces*, vol. 12, no. 23, pp. 26399–26404, Jun. 2020, doi: 10.1021/acsami.0c05680.

[160] Aadland *et al.*, 'High-Temperature Core Flood Investigation of Nanocellulose as a Green Additive for Enhanced Oil Recovery', *Nanomaterials*, vol. 9, no. 5, p. 665, Apr. 2019, doi: 10.3390/nano9050665.

[161] E. B. Heggset, R. Aaen, T. Veslum, M. Henriksson, S. Simon, and K. Syverud, 'Cellulose nanofibrils as rheology modifier in mayonnaise – A pilot scale demonstration', *Food Hydrocolloids*, vol. 108, p. 106084, Nov. 2020, doi: 10.1016/j.foodhyd.2020.106084.

[162] T. Szlapak Franco *et al.*, 'Production and technological characteristics of avocado oil emulsions stabilized with cellulose nanofibrils isolated from agroindustrial residues', *Colloids and Surfaces A: Physicochemical and Engineering Aspects*, vol. 586, p. 124263, Feb. 2020, doi: 10.1016/j.colsurfa.2019.124263.

[163] L. Perrin, G. Gillet, L. Gressin, and S. Desobry, 'Interest of Pickering Emulsions for Sustainable Micro/Nanocellulose in Food and Cosmetic Applications', *Polymers*, vol. 12, no. 10, p. 2385, Oct. 2020, doi: 10.3390/polym12102385.

[164] F. Kuznik, K. Johannes, C. Obrecht, and D. David, 'A review on recent developments in physisorption thermal energy storage for building applications', *Renewable and Sustainable Energy Reviews*, vol. 94, pp. 576–586, Oct. 2018, doi: 10.1016/j.rser.2018.06.038.

[165] R. Sims, S. Harmer, and J. Quinton, 'The Role of Physisorption and Chemisorption in the Oscillatory Adsorption of Organosilanes on Aluminium Oxide', *Polymers*, vol. 11, no. 3, p. 410, Mar. 2019, doi: 10.3390/polym11030410.

[166] S. Lombardo and W. Thielemans, 'Thermodynamics of adsorption on nanocellulose surfaces', *Cellulose*, vol. 26, no. 1, pp. 249–279, Jan. 2019, doi: 10.1007/s10570-018-02239-2.

[167] M. Belhachemi and F. Addoun, 'Comparative adsorption isotherms and modeling of methylene blue onto activated carbons', *Appl Water Sci*, vol. 1, no. 3–4, pp. 111–117, Dec. 2011, doi: 10.1007/s13201-011-0014-1.

[168] M. Rodahl, F. Höök, A. Krozer, P. Brzezinski, and B. Kasemo, 'Quartz Cristal microbalance setup for frequency and Q-factor measurments in gaseous and liquid environments', *Review of Scientific Instruments*, vol. 66, no. 3924, 1995.

[169] M. V. Voinova, M. Rodahl, M. Jonson, and B. Kasemo, 'Viscoelastic Acoustic Response of Layered Polymer Films at Fluid-Solid Interfaces: Continuum Mechanics Approach', *Physica Scripta*, vol. 59, no. 5, pp. 391–396, May 1999, doi: 10.1238/physica.regular.059a00391.

[170] S. Lombardo, P. Chen, P. A. Larsson, W. Thielemans, J. Wohlert, and A. J. Svagan, 'Toward Improved Understanding of the Interactions between Poorly Soluble Drugs and Cellulose Nanofibers', *Langmuir*, vol. 34, no. 19, pp. 5464–5473, May 2018, doi: 10.1021/acs.langmuir.8b00531.

[171] N. Hasan *et al.*, 'Recent advances of nanocellulose in drug delivery systems', *J. Pharm. Investig.*, vol. 50, no. 6, pp. 553–572, Nov. 2020, doi: 10.1007/s40005-020-00499-4.

[172] S. Kamel, N. Ali, K. Jahangir, S. M. Shah, and A. A. El-Gendy, 'Pharmaceutical significance of cellulose: A review', *Express Polym. Lett.*, vol. 2, no. 11, pp. 758–778, 2008, doi: 10.3144/expresspolymlett.2008.90.

[173] C. Sharma and N. K. Bhardwaj, 'Bacterial nanocellulose: Present status, biomedical applications and future perspectives', *Materials Science and Engineering: C*, vol. 104, p. 109963, Nov. 2019, doi: 10.1016/j.msec.2019.109963.

[174] S. M. El-Hoseny *et al.*, 'Natural ECM-Bacterial Cellulose Wound Healing—Dubai Study', *JBNB*, vol. 06, no. 04, pp. 237–246, 2015, doi: 10.4236/jbnb.2015.64022.

[175] J. D. Fontana *et al.*, 'Acetobacter cellulose pellicle as a temporary skin substitute', *Appl Biochem Biotechnol*, vol. 24–25, no. 1, pp. 253–264, Mar. 1990, doi: 10.1007/BF02920250.

[176] W. Czaja, A. Krystynowicz, S. Bielecki, and R. Brownjr, 'Microbial cellulose—the natural power to heal wounds', *Biomaterials*, vol. 27, no. 2, pp. 145–151, Jan. 2006, doi: 10.1016/j.biomaterials.2005.07.035.

[177] D. Klemm, D. Schumann, U. Udhardt, and S. Marsch, 'Bacterial synthesized cellulose Ð arti®cial blood vessels for microsurgery', *Prog. Polym. Sci.*, p. 43, 2001.

[178] A. Müller *et al.*, 'The Biopolymer Bacterial Nanocellulose as Drug Delivery System: Investigation of Drug Loading and Release using the Model Protein Albumin', *Journal of Pharmaceutical Sciences*, vol. 102, no. 2, pp. 579–592, 2013, doi: https://doi.org/10.1002/jps.23385.

[179] M. Moniri *et al.*, 'Production and Status of Bacterial Cellulose in Biomedical Engineering', *Nanomaterials*, vol. 7, no. 9, p. 257, Sep. 2017, doi: 10.3390/nano7090257.

[180] N. Petersen and P. Gatenholm, 'Bacterial cellulose-based materials and medical devices: current state and perspectives', *Appl Microbiol Biotechnol*, p. 10, 2011.

[181] H. Du, W. Liu, M. Zhang, C. Si, X. Zhang, and B. Li, 'Cellulose nanocrystals and cellulose nanofibrils based hydrogels for biomedical applications', *Carbohydrate Polymers*, vol. 209, pp. 130–144, Apr. 2019, doi: 10.1016/j.carbpol.2019.01.020.

[182] J. Wu *et al.*, 'Structure and properties of cellulose/chitin blended hydrogel membranes fabricated via a solution pre-gelation technique', *Carbohydrate Polymers*, vol. 79, no. 3, pp. 677–684, Feb. 2010, doi: 10.1016/j.carbpol.2009.09.022.

[183] Letchford, Jackson, B. Wasserman, Ye, W. Hamad, and H. Burt, 'The use of nanocrystalline cellulose for the binding and controlled release of drugs', *IJN*, p. 321, Feb. 2011, doi: 10.2147/IJN.S16749.

[184] M. Jorfi and E. J. Foster, 'Recent advances in nanocellulose for biomedical applications', *Journal of Applied Polymer Science*, vol. 132, no. 14, p. n/a-n/a, Apr. 2015, doi: 10.1002/app.41719.

[185] N. Lin and A. Dufresne, 'Nanocellulose in biomedicine: Current status and future prospect', *European Polymer Journal*, vol. 59, pp. 302–325, Oct. 2014, doi: 10.1016/j.eurpolymj.2014.07.025.

[186] N. S. Sharip and H. Ariffin, 'Cellulose nanofibrils for biomaterial applications', *Materials Today: Proceedings*, vol. 16, pp. 1959–1968, 2019, doi: 10.1016/j.matpr.2019.06.074.

[187] K. Syverud, 'Tissue Engineering Using Plant-Derived Cellulose Nanofibrils (CNF) as Scaffold Material', in *ACS Symposium Series*, vol. 1251, U. P. Agarwal, R. H. Atalla, and A. Isogai, Eds. Washington, DC: American Chemical Society, 2017, pp. 171–189. doi: 10.1021/bk-2017-1251.ch009.

[188] R. Kolakovic, L. Peltonen, A. Laukkanen, J. Hirvonen, and T. Laaksonen, 'Nanofibrillar cellulose films for controlled drug delivery', *European Journal of Pharmaceutics and Biopharmaceutics*, vol. 82, no. 2, pp. 308–315, Oct. 2012, doi: 10.1016/j.ejpb.2012.06.011.

[189] R. Kolakovic *et al.*, 'Evaluation of drug interactions with nanofibrillar cellulose', *European Journal of Pharmaceutics and Biopharmaceutics*, vol. 85, no. 3, pp. 1238–1244, Nov. 2013, doi: 10.1016/j.ejpb.2013.05.015.

[190] N. Lavoine, N. Tabary, I. Desloges, B. Martel, and J. Bras, 'Controlled release of chlorhexidine digluconate using β-cyclodextrin and microfibrillated cellulose', *Colloids and Surfaces B: Biointerfaces*, vol. 121, pp. 196–205, Sep. 2014, doi: 10.1016/j.colsurfb.2014.06.021.

[191] H. Durand *et al.*, 'Pure cellulose nanofibrils membranes loaded with ciprofloxacin for drug release and antibacterial activity', *Cellulose*, May 2020, doi: 10.1007/s10570-020-03231-5.

[192] L. Alexandrescu, K. Syverud, A. Gatti, and G. Chinga-Carrasco, 'Cytotoxicity tests of cellulose nanofibril-based structures', *Cellulose*, vol. 20, no. 4, pp. 1765–1775, Aug. 2013, doi: 10.1007/s10570-013-9948-9.

[193] A. Rashad *et al.*, 'Responses and host tissue reactions to wood-based nanocellulose scaffolds', *Materials Science and Engineering: C*, Dec. 2018, doi: 10.1016/j.msec.2018.11.068.

[194] A. Rashad, K. Mustafa, E. B. Heggset, and K. Syverud, 'Cytocompatibility of Wood-Derived Cellulose Nanofibril Hydrogels with Different Surface Chemistry', *Biomacromolecules*, vol. 18, no. 4, pp. 1238–1248, Apr. 2017, doi: 10.1021/acs.biomac.6b01911.

[195] A. Rashad *et al.*, 'Inflammatory responses and tissue reactions to wood-Based nanocellulose scaffolds', *Materials Science and Engineering: C*, vol. 97, pp. 208–221, Apr. 2019, doi: 10.1016/j.msec.2018.11.068.

[196] Y. Alkhatib, M. Dewaldt, S. Moritz, R. Nitzsche, D. Kralisch, and D. Fischer, 'Controlled extended octenidine release from a bacterial nanocellulose/Poloxamer hybrid system', *European Journal of Pharmaceutics and Biopharmaceutics*, vol. 112, pp. 164–176, Mar. 2017, doi: 10.1016/j.ejpb.2016.11.025.

[197] L. Saïdi, C. Vilela, H. Oliveira, A. J. D. Silvestre, and C. S. R. Freire, 'Poly(N-methacryloyl glycine)/nanocellulose composites as pH-sensitive systems for controlled release of diclofenac', *Carbohydrate Polymers*, vol. 169, pp. 357–365, Aug. 2017, doi: 10.1016/j.carbpol.2017.04.030.

[198] M. Abba *et al.*, 'Transdermal Delivery of Crocin Using Bacterial Nanocellulose Membrane', *Fibers and Polymers*, vol. 20, no. 10, pp. 2025–2031, Oct. 2019, doi: 10.1007/s12221-019-9076-8.

[199] J. P. F. Carvalho *et al.*, 'Nanocellulose-Based Patches Loaded with Hyaluronic Acid and Diclofenac towards Aphthous Stomatitis Treatment', *Nanomaterials*, vol. 10, no. 4, p. 628, Mar. 2020, doi: 10.3390/nano10040628.

[200] J. Supramaniam, R. Adnan, N. H. Mohd Kaus, and R. Bushra, 'Magnetic nanocellulose alginate hydrogel beads as potential drug delivery system', *International Journal of Biological Macromolecules*, vol. 118, pp. 640–648, Oct. 2018, doi: 10.1016/j.ijbiomac.2018.06.043.

[201] U. G. T. M. Sampath, Y. C. Ching, C. H. Chuah, R. Singh, and P.-C. Lin, 'Preparation and characterization of nanocellulose reinforced semi-interpenetrating polymer network of chitosan hydrogel', *Cellulose*, vol. 24, no. 5, pp. 2215–2228, May 2017, doi: 10.1007/s10570-017-1251-8.

[202] T. Udeni Gunathilake, Y. Ching, and C. Chuah, 'Enhancement of Curcumin Bioavailability Using Nanocellulose Reinforced Chitosan Hydrogel', *Polymers*, vol. 9, no. 12, p. 64, Feb. 2017, doi: 10.3390/polym9020064.

[203] R. Poonguzhali, S. Khaleel Basha, and V. Sugantha Kumari, 'Synthesis of alginate/nanocellulose bionanocomposite for in vitro delivery of ampicillin', *Polym. Bull.*, vol. 75, no. 9, pp. 4165–4173, Sep. 2018, doi: 10.1007/s00289-017-2253-2.

[204] S. Fujisawa, E. Togawa, and K. Kuroda, 'Nanocellulose-stabilized Pickering emulsions and their applications', *Science and Technology of Advanced Materials*, vol. 18, no. 1, pp. 959–971, Dec. 2017, doi: 10.1080/14686996.2017.1401423.

[205] S. Hosseinzadeh, H. Hosseinzadeh, and S. Pashaei, 'Fabrication of nanocellulose loaded poly(AA- *co* -HEMA) hydrogels for ceftriaxone controlled delivery and crystal violet adsorption', *Polym. Compos.*, vol. 40, no. S1, pp. E559–E569, Jan. 2019, doi: 10.1002/pc.24875.

[206] C. Piotto and P. Bettotti, 'Surfactant mediated clofazimine release from nanocellulose-hydrogels', *Cellulose*, vol. 26, no. 7, pp. 4579–4587, May 2019, doi: 10.1007/s10570-019-02407-y.

[207] L. Ning, C. You, Y. Zhang, X. Li, and F. Wang, 'Synthesis and biological evaluation of surface-modified nanocellulose hydrogel loaded with paclitaxel', *Life Sciences*, vol. 241, p. 117137, Jan. 2020, doi: 10.1016/j.lfs.2019.117137.

[208] T. Md Abu *et al.*, 'Nanocellulose as drug delivery system for honey as antimicrobial wound dressing', *Materials Today: Proceedings*, vol. 31, pp. 14–17, 2020, doi: 10.1016/j.matpr.2020.01.076.

[209] S. Ilkar Erdagi, F. Asabuwa Ngwabebhoh, and U. Yildiz, 'Genipin crosslinked gelatin-diosgenin-nanocellulose hydrogels for potential wound dressing and healing applications', *International Journal of Biological Macromolecules*, vol. 149, pp. 651–663, Apr. 2020, doi: 10.1016/j.ijbiomac.2020.01.279.

[210] Y. Liu *et al.*, 'versatile vehicles for drug delivery and wound healing', *Carbohydrate Polymers*, p. 10, 2018.

[211] A. Basu, M. Strømme, and N. Ferraz, 'Towards Tunable Protein-Carrier Wound Dressings Based on Nanocellulose Hydrogels Crosslinked with Calcium Ions', *Nanomaterials*, vol. 8, no. 7, p. 550, Jul. 2018, doi: 10.3390/nano8070550.

[212] S. F. Plappert, 'Anisotropic nanocellulose gel–membranes for drug delivery_ Tailoring structure and interface by sequential periodate–chlorite oxidation', *Carbohydrate Polymers*, p. 9, 2019.

[213] K. L. O'Donnell, G. S. Oporto-Velásquez, and N. Comolli, 'Evaluation of Acetaminophen Release from Biodegradable Poly (Vinyl Alcohol) (PVA) and Nanocellulose Films Using a Multiphase Release Mechanism', *Nanomaterials*, vol. 10, no. 2, p. 301, Feb. 2020, doi: 10.3390/nano10020301.

[214] Y. Liu *et al.*, 'A physically crosslinked polydopamine/nanocellulose hydrogel as potential versatile vehicles for drug delivery and wound healing', *Carbohydrate Polymers*, vol. 188, pp. 27–36, May 2018, doi: 10.1016/j.carbpol.2018.01.093.

[215] J. Li, Y. Wang, L. Zhang, Z. Xu, H. Dai, and W. Wu, 'Nanocellulose/Gelatin Composite Cryogels for Controlled Drug Release', *ACS Sustainable Chem. Eng.*, vol. 7, no. 6, pp. 6381–6389, Mar. 2019, doi: 10.1021/acssuschemeng.9b00161.

[216] H.-J. Hong, J. Kim, D.-Y. Kim, I. Kang, H. K. Kang, and B. G. Ryu, 'Synthesis of carboxymethylated nanocellulose fabricated ciprofloxacine – Montmorillonite composite for sustained delivery of antibiotics', *International Journal of Pharmaceutics*, vol. 567, p. 118502, Aug. 2019, doi: 10.1016/j.ijpharm.2019.118502.

[217] V.-V. Auvinen *et al.*, 'Modulating sustained drug release from nanocellulose hydrogel by adjusting the inner geometry of implantable capsules', *Journal of Drug Delivery Science and Technology*, vol. 57, p. 101625, Jun. 2020, doi: 10.1016/j.jddst.2020.101625.

[218] H. Gao *et al.*, 'Construction of cellulose nanofibers/quaternized chitin/organic rectorite composites and their application as wound dressing materials', *Biomater. Sci.*, vol. 7, no. 6, pp. 2571–2581, 2019, doi: 10.1039/C9BM00288J.

[219] N. T. Lam, R. Chollakup, W. Smitthipong, T. Nimchua, and P. Sukyai, 'Utilizing cellulose from sugarcane bagasse mixed with poly(vinyl alcohol) for tissue engineering scaffold fabrication', *Industrial Crops and Products*, vol. 100, pp. 183–197, Jun. 2017, doi: 10.1016/j.indcrop.2017.02.031.

[220] W. Xu *et al.*, 'On Low-Concentration Inks Formulated by Nanocellulose Assisted with Gelatin Methacrylate (GelMA) for 3D Printing toward Wound Healing Application', *ACS Appl. Mater. Interfaces*, vol. 11, no. 9, pp. 8838–8848, Mar. 2019, doi: 10.1021/acsami.8b21268.

[221] N. Akhavan-Kharazian and H. Izadi-Vasafi, 'Preparation and characterization of chitosan/gelatin/nanocrystalline cellulose/calcium peroxide films for potential wound dressing applications', *International Journal of Biological Macromolecules*, vol. 133, pp. 881–891, Jul. 2019, doi: 10.1016/j.ijbiomac.2019.04.159.

[222] T. Abudula, U. Saeed, A. Memic, K. Gauthaman, M. A. Hussain, and H. Al-Turaif, 'Electrospun cellulose Nano fibril reinforced PLA/PBS composite scaffold for vascular tissue engineering', *J Polym Res*, vol. 26, no. 5, p. 110, May 2019, doi: 10.1007/s10965-019-1772-y.

[223] D. K. Patel, S. D. Dutta, W.-C. Shin, K. Ganguly, and K.-T. Lim, 'Fabrication and characterization of 3D printable nanocellulose-based hydrogels for tissue engineering', *RSC Adv.*, vol. 11, no. 13, pp. 7466–7478, 2021, doi: 10.1039/D0RA09620B.

[224] T. Kovacs *et al.*, 'An ecotoxicological characterization of nanocrystalline cellulose (NCC)', *Nanotoxicology*, vol. 4, no. 3, pp. 255–270, Sep. 2010, doi: 10.3109/17435391003628713.

[225] H. P. S. A. Khalil *et al.*, 'A Review on Micro- to Nanocellulose Biopolymer Scaffold Forming for Tissue Engineering Applications', *Polymers*, vol. 12, no. 9, p. 2043, Sep. 2020, doi: 10.3390/polym12092043.

[226] M. Čolić, S. Tomić, and M. Bekić, 'Immunological aspects of nanocellulose', *Immunology Letters*, vol. 222, pp. 80–89, Jun. 2020, doi: 10.1016/j.imlet.2020.04.004.

[227] G. Crini, 'Review: A History of Cyclodextrins', *Chem. Rev.*, vol. 114, no. 21, pp. 10940–10975, Nov. 2014, doi: 10.1021/cr500081p.

[228] A. Villiers, 'Sur la fermentation de la fécule par l'action du ferment butyrique', *Bull. Soc. Chim. Paris*, vol. 45, p. 468, 1891.

[229] F. Schardinger, Wien. Klin. Wochenschr., 1903.

[230] K. Freudenberg, E. Schaaf, G. Dumpert, and T. Ploetz, 'Neue ansichten uber die starke', *Naturwiss*, no. 27, pp. 850–953, 1939.

[231] K. Freudenberg and F. Cramer, 'Die Konstitution der Schardinger-Dextrine α, β und γ.', *Z. Naturforch.*, vol. 3b, p. 464.

[232] D. French, 'The Schardinger dextrins', *Advances in carbyhydrate history*, vol. 12, pp. 189–260, 1957.

[233] M. E. Brewster and T. Loftsson, 'Cyclodextrins as pharmaceutical solubilizers', *Advanced Drug Delivery Reviews*, vol. 59, no. 7, pp. 645–666, Jul. 2007, doi: 10.1016/j.addr.2007.05.012.

[234] J. Szejtli, 'Past, Present, and Future of Cyclodextrin Research', *ChemInform*, vol. 36, no. 17, Apr. 2005, doi: 10.1002/chin.200517261.

[235] J. Szejtli, 'Utilization of cyclodextrins in industrial products and processes', *Journal of Materials Chemistry*, vol. 7, no. 4, pp. 575–587, 1997, doi: 10.1039/a605235e.

[236] J. Szejtli, 'Introduction and General Overview of Cyclodextrin Chemistry', *Chem. Rev.*, vol. 98, no. 5, pp. 1743–1754, Jul. 1998, doi: 10.1021/cr970022c.

[237] M. Kfoury, 'Préparation, caractérisation physicochimique et évaluation des propriétés biologiques de complexes d'inclusion à base de cyclodextrines: applications à des principes actifs de type phénylpropanoïdes', p. 226.

[238] S. Fourmentin, N. Morin-Crini, and G. Crini, 'Cyclodextrines et complexes d'inclusion', in *Cyclodextrines, propriétés, chimie et applications*, Presse Universitaire de Franche-Comté, pp. 57–84.

[239] P. Blach, S. Fourmentin, D. Landy, F. Cazier, and G. Surpateanu, 'Cyclodextrins: A new efficient absorbent to treat waste gas streams', *Chemosphere*, vol. 70, no. 3, pp. 374–380, 2008, doi: https://doi.org/10.1016/j.chemosphere.2007.07.018.

[240] 'Cyclodextrins used as excipients', p. 16.

[241] A. R. Khan, P. Forgo, K. J. Stine, and V. T. D'Souza, 'Methods for Selective Modifications of Cyclodextrins', *Chemical Reviews*, vol. 98, no. 5, pp. 1977–1996, Jul. 1998, doi: 10.1021/cr970012b.

[242] C. Schönbeck, P. Westh, J. C. Madsen, K. L. Larsen, L. W. Städe, and R. Holm, 'Hydroxypropyl-Substituted β-Cyclodextrins: Influence of Degree of Substitution on the Thermodynamics of Complexation with Tauroconjugated and Glycoconjugated Bile Salts', *Langmuir*, vol. 26, no. 23, pp. 17949–17957, Dec. 2010, doi: 10.1021/la103124n.

[243] S. Gould and R. C. Scott, '2-Hydroxypropyl-β-cyclodextrin (HP-β-CD): A toxicology review', *Food and Chemical Toxicology*, vol. 43, no. 10, pp. 1451–1459, Oct. 2005, doi: 10.1016/j.fct.2005.03.007.

[244] A. Z. M. Badruddoza, G. S. S. Hazel, K. Hidajat, and M. S. Uddin, 'Synthesis of carboxymethyl-β-cyclodextrin conjugated magnetic nano-adsorbent for removal of methylene blue', *Colloids and Surfaces A: Physicochemical and Engineering Aspects*, vol. 367, no. 1–3, pp. 85–95, Sep. 2010, doi: 10.1016/j.colsurfa.2010.06.018.

[245] G. Shixiang, W. Liansheng, H. Qingguo, and H. Sukui, 'SOLUBILIZATION OF POLYCYCLIC AROMATIC HYDROCARBONS BY P-CYCLODEXTRIN AND CARBOXYMETHYL-fl-CYCLODEXTRIN', p. 7.

[246] N. H. Foda and R. B. Bakhaidar, 'Zaleplon', in *Profiles of Drug Substances, Excipients and Related Methodology*, vol. 35, Elsevier, 2010, pp. 347–371. doi: 10.1016/S1871-5125(10)35008-4.

[247] C. Su *et al.*, 'Carboxymethyl-β-cyclodextrin conjugated nanoparticles facilitate therapy for folate receptor-positive tumor with the mediation of folic acid', *International Journal of Pharmaceutics*, vol. 474, no. 1–2, pp. 202–211, Oct. 2014, doi: 10.1016/j.ijpharm.2014.08.026.

[248] N. Morin-Crini, P. Winterton, S. Fourmentin, L. D. Wilson, É. Fenyvesi, and G. Crini, 'Water-insoluble β-cyclodextrin–epichlorohydrin polymers for removal of pollutants from aqueous solutions by sorption processes using batch studies: A review of inclusion mechanisms', *Progress in Polymer Science*, vol. 78, pp. 1–23, Mar. 2018, doi: 10.1016/j.progpolymsci.2017.07.004.

[249] B. Martel, D. Ruffin, M. Weltrowski, Y. Lekchiri, and M. Morcellet, 'Water-soluble polymers and gels from the polycondensation between cyclodextrins and poly(carboxylic

acid)s: A study of the preparation parameters', *J. Appl. Polym. Sci.*, vol. 97, no. 2, pp. 433–442, Jul. 2005, doi: 10.1002/app.21391.

[250] E. M. M. Del Valle, 'Cyclodextrins and their uses: a review', *Process Biochemistry*, vol. 39, no. 9, pp. 1033–1046, May 2004, doi: 10.1016/S0032-9592(03)00258-9.

[251] K. A. Connors, 'The Stability of Cyclodextrin Complexes in Solution', *Chem. Rev.*, vol. 97, no. 5, pp. 1325–1358, Aug. 1997, doi: 10.1021/cr960371r.

[252] T. HIGUCHI, 'A phase solubility technique', *Adv. Anal. Chem. Instrum.*, vol. 4, pp. 117–211, 1965.

[253] T. Loftsson and M. E. Brewster, 'Pharmaceutical applications of cyclodextrins: basic science and product development: Pharmaceutical applications of cyclodextrins', *Journal of Pharmacy and Pharmacology*, vol. 62, no. 11, pp. 1607–1621, Nov. 2010, doi: 10.1111/j.2042-7158.2010.01030.x.

[254] M. Wszelaka-Rylik and P. Gierycz, 'Isothermal titration calorimetry (ITC) study of natural cyclodextrins inclusion complexes with tropane alkaloids', *Journal of Thermal Analysis and Calorimetry*, vol. 121, no. 3, pp. 1359–1364, Sep. 2015, doi: 10.1007/s10973-015-4658-1.

[255] F. B. T. Pessine, A. Calderini, and G. L. Alexandrino, 'Review: Cyclodextrin Inclusion Complexes Probed by NMR Techniques', *Magnetic Resonance Spectroscopy*, p. 29.

[256] H.-J. Schneider, F. Hacket, V. Rüdiger, and H. Ikeda, 'NMR Studies of Cyclodextrins and Cyclodextrin Complexes', *Chem. Rev.*, vol. 98, no. 5, pp. 1755–1786, Jul. 1998, doi: 10.1021/cr970019t.

[257] R. Ficarra *et al.*, 'Study of b-blockers/b-cyclodextrins inclusion complex by NMR, DSC, X-ray and SEM investigation_', *J. Pharm. Biomed. Anal.*, p. 8, 2000.

[258] R. L. Abarca, 'Characterization of beta-cyclodextrin inclusion complexes containing an essential oil component', *Food Chemistry*, p. 8, 2016.

[259] N. Mennini, M. Bragagni, F. Maestrelli, and P. Mura, 'Physico-chemical characterization in solution and in the solid state of clonazepam complexes with native and chemically-modified cyclodextrins', *Journal of Pharmaceutical and Biomedical Analysis*, vol. 89, pp. 142–149, Feb. 2014, doi: 10.1016/j.jpba.2013.11.009.

[260] K. Sambasevam, S. Mohamad, N. Sarih, and N. Ismail, 'Synthesis and Characterization of the Inclusion Complex of β-cyclodextrin and Azomethine', *IJMS*, vol. 14, no. 2, pp. 3671–3682, Feb. 2013, doi: 10.3390/ijms14023671.

[261] V. Crupi, R. Ficarra, M. Guardo, D. Majolino, R. Stancanelli, and V. Venuti, 'UV–vis and FTIR–ATR spectroscopic techniques to study the inclusion complexes of genistein with β-cyclodextrins', *Journal of Pharmaceutical and Biomedical Analysis*, vol. 44, no. 1, pp. 110–117, May 2007, doi: 10.1016/j.jpba.2007.01.054.

[262] G. Crini, S. Fourmentin, M. Fourmentin, and N. Morin-Crini, 'Principales applications des complexes d'inclusion cyclodextrine/substrat', p. 21, 2019.

[263] K. Frömming and J. Szetli, *Cycloedextrins in pharmacy. Topics in inclusion science.* Dordrecht : Kluwer Academic Publishers, 1994.

[264] T. Fuchs-Buder, C. Meistelman, and J. Raft, 'Sugammadex: clinical development and practical use', *Korean J Anesthesiol*, vol. 65, no. 6, p. 495, 2013, doi: 10.4097/kjae.2013.65.6.495.

[265] M. E. Davis and M. E. Brewster, 'Cyclodextrin-based pharmaceutics: past, present and future', *Nat Rev Drug Discov*, vol. 3, no. 12, pp. 1023–1035, Dec. 2004, doi: 10.1038/nrd1576.

[266] H.-J. Buschmann and E. Schollmeyer, 'Applications of cyclodextrins in cosmetic products: A review', *JOURNAL OF COSMETIC SCIENCE*, p. 7, 2002.

[267] É. Fenyvesi, M. Vikmon, and L. Szente, 'Cyclodextrins in Food Technology and Human Nutrition: Benefits and Limitations', *Critical Reviews in Food Science and Nutrition*, vol. 56, no. 12, pp. 1981–2004, Sep. 2016, doi: 10.1080/10408398.2013.809513.

[268] E. Kavitha, M. P. Rajesh, and S. Prabhakar, 'Removal and recovery of heavy metals from aqueous solution using b-cyclodextrin polymer and optimization of complexation conditions', *dwt*, vol. 122, pp. 219–230, 2018, doi: 10.5004/dwt.2018.22783.

[269] D. Gomez-Maldonado *et al.*, 'Cellulose-Cyclodextrin Co-Polymer for the Removal of Cyanotoxins on Water Sources', *Polymers*, vol. 11, no. 12, p. 2075, Dec. 2019, doi: 10.3390/polym11122075.

[270] S. Saini, D. Quinot, N. Lavoine, M. N. Belgacem, and J. Bras, 'β-Cyclodextrin-grafted TEMPO-oxidized cellulose nanofibers for sustained release of essential oil', *Journal of Materials Science*, vol. 52, no. 7, pp. 3849–3861, Apr. 2017, doi: 10.1007/s10853-016-0644-7.

[271] G. Yuan *et al.*, 'Cyclodextrin functionalized cellulose nanofiber composites for the faster adsorption of toluene from aqueous solution', *Journal of the Taiwan Institute of Chemical Engineers*, vol. 70, pp. 352–358, Jan. 2017, doi: 10.1016/j.jtice.2016.10.028.

[272] C. Ruiz-Palomero, M. L. Soriano, and M. Valcárcel, 'β-Cyclodextrin decorated nanocellulose: a smart approach towards the selective fluorimetric determination of danofloxacin in milk samples', *Analyst*, vol. 140, no. 10, pp. 3431–3438, May 2015, doi: 10.1039/C4AN01967A.

[273] Z. Aytac, H. S. Sen, E. Durgun, and T. Uyar, 'Sulfisoxazole/cyclodextrin inclusion complex incorporated in electrospun hydroxypropyl cellulose nanofibers as drug delivery system', *Colloids and Surfaces B: Biointerfaces*, vol. 128, pp. 331–338, Apr. 2015, doi: 10.1016/j.colsurfb.2015.02.019.

[274] N. Lavoine, C. Givord, N. Tabary, I. Desloges, B. Martel, and J. Bras, 'Elaboration of a new antibacterial bio-nano-material for food-packaging by synergistic action of cyclodextrin and microfibrillated cellulose', *Innovative Food Science & Emerging Technologies*, vol. 26, pp. 330–340, Dec. 2014, doi: 10.1016/j.ifset.2014.06.006.

[275] A. Fiorati *et al.*, 'TEMPO-Nanocellulose/Ca2+ Hydrogels: Ibuprofen Drug Diffusion and In Vitro Cytocompatibility', *Materials*, vol. 13, no. 1, p. 183, Jan. 2020, doi: 10.3390/ma13010183.

[276] D. O. de Castro, N. Tabary, B. Martel, A. Gandini, N. Belgacem, and J. Bras, 'Controlled release of carvacrol and curcumin: bio-based food packaging by synergism action of TEMPO-oxidized cellulose nanocrystals and cyclodextrin', *Cellulose*, vol. 25, no. 2, pp. 1249–1263, Feb. 2018, doi: 10.1007/s10570-017-1646-6.

[277] A. Jimenez, F. Jaramillo, U. Hemraz, Y. Boluk, K. Ckless, and R. Sunasee, 'Effect of surface organic coatings of cellulose nanocrystals on the viability of mammalian cell lines', *Nanotechnology, Science and Applications*, vol. Volume 10, pp. 123–136, Sep. 2017, doi: 10.2147/NSA.S145891.

[278] D. O. Castro, N. Tabary, B. Martel, A. Gandini, N. Belgacem, and J. Bras, 'Effect of different carboxylic acids in cyclodextrin functionalization of cellulose nanocrystals for prolonged release of carvacrol', *Materials Science and Engineering: C*, vol. 69, pp. 1018–1025, Dec. 2016, doi: 10.1016/j.msec.2016.08.014.

[279] G. M. A. Ndong Ntoutoume *et al.*, 'Development of curcumin–cyclodextrin/cellulose nanocrystals complexes: New anticancer drug delivery systems', *Bioorganic & Medicinal Chemistry Letters*, vol. 26, no. 3, pp. 941–945, Feb. 2016, doi: 10.1016/j.bmcl.2015.12.060.

[280] N. Lin and A. Dufresne, 'Supramolecular Hydrogels from In Situ Host–Guest Inclusion between Chemically Modified Cellulose Nanocrystals and Cyclodextrin', *Biomacromolecules*, vol. 14, no. 3, pp. 871–880, Mar. 2013, doi: 10.1021/bm301955k.

CHAPTER II. PRODUCTION OF β-CYCLODEXTRIN-FUNCTIONALIZED CELLULOSE NANOFIBRILS STRUCTURES

INTRODUCTION TO CHAPTER II

The use of cellulose nanofibrils as biomaterial implies improving its properties to match the needs of advanced applications in the medical field. Chapter I reviewed biomedical applications, such as drug delivery and tissue engineering, the different production routes of nanocellulosic materials as well as a promising way to improve them via combination with cyclodextrins. Multiple challenges were addressed, the main one being the physico-chemical characterization of the adsorption between β-cyclodextrins (β-CDs) and cellulose nanofibrils (CNFs). The aim of chapter II is to provide β-CD/CNF materials with a better understanding of (i) the adsorption phenomena occurring between the two components and (ii) the impact on mechanical properties of the β-CD/CNF nanostructured materials.

Thus, the **first part** of Chapter II deals with the production of TEMPO-oxidized cellulose nanofibrils (toCNF) films and cryogels, with a focus on the impact of different parameters such as filler content, process pH and introduction of β-CD on the physical properties of the hybrid materials. The variation in structure, water sorption and mechanical properties will be investigated in order to propose materials with suitable properties for biomedical applications.

The **second part** of this chapter is dedicated to the characterization and quantification of the adsorption of β-CD and also β-CD derivatives onto toCNFs. Isothermal Titration Calorimetry (ITC), Quartz Crystal Microbalance with dissipation (QCM-d) and a phenolphthalein-based protocol will be combined to determine the adsorption mechanism and binding capacities.

Finally, the **third part** consists of an evaluation of the impact of various types of β-CD derivatives regarding the physical properties of films and cryogels. This part provides us with the final design of the biomaterials comprised of the most suited combination of toCNF/ β-CD.

Figure II.1 summarizes the structure of Chapter II.

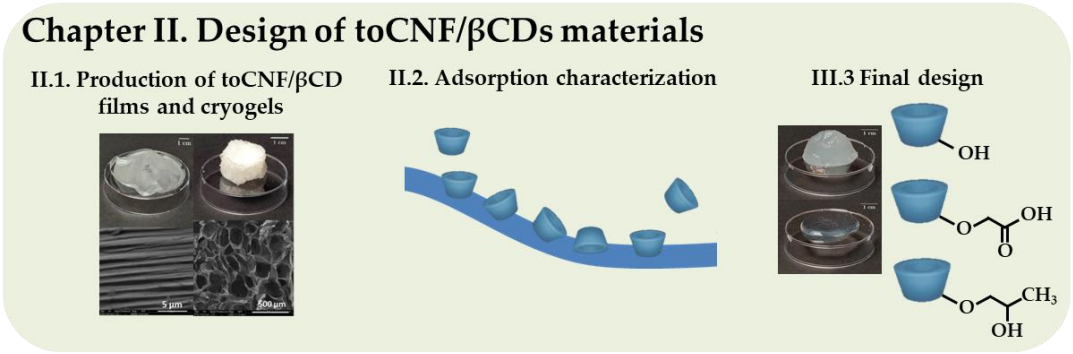

Figure II.1: Graphical representation of the structure of Chapter II

CHAPTER II.1 IMPACT OF PROCESS ON THE MECHANICAL PROPERTIES OF TEMPO-OXIDIZED CELLULOSE NANOFIBRILS/β-CYCLODEXTRIN FILMS AND CRYOGELS

Inspired from paper: ***Michel, B.;*** *Bras, J.; Dufresne, A.; Heggset, E. B.; Syverud, K. Production and Mechanical Characterisation of TEMPO-Oxidised Cellulose Nanofibrils/β-Cyclodextrin Films and Cryogels. Molecules* ***2020****, 25 (10), 2381.* https://doi.org/10.3390/molecules25102381.

Abstract: Wood-based TEMPO-oxidized cellulose nanofibrils (toCNF) are promising materials for biomedical applications. Cyclodextrins have the ability to form inclusion complexes with hydrophobic molecules and are considered as a method to bring new functionalities to these materials. Water sorption and mechanical properties are also key properties for biomedical applications such as drug delivery and tissue engineering. In this work, we report the modification with β-cyclodextrin (βCD) of toCNF samples with different carboxyl contents viz. 756 ± 4 μmol/g and 1048 ± 32 μmol/g. The modification was carried out at neutral and acidic pH (2.5) to study the effect of dissociation of the carboxylic acid group. Films processed by casting/evaporation at 40°C and cryogels prepared by freeze-drying were prepared from βCD-modified toCNF suspensions and compared with reference samples of unmodified toCNF. The impact of modification on water sorption and mechanical properties was assessed. It was shown that the water sorption behavior for films is driven by adsorption, with a clear impact of the chemical makeup of the fibers (charge content, pH, and adsorption of cyclodextrin). Modified toCNF cryogels (acidic pH and addition of cyclodextrins) showed lower mechanical properties linked to the modification of the cell wall porosity structure. Esterification between βCD and toCNF under acidic conditions was performed by freeze-drying, and such cryogels exhibited a lower decrease in mechanical properties in the swollen state. These results are promising for the development of scaffolds and films with controlled mechanical properties and added value due to the ability of cyclodextrin to form an inclusion complex with active principle ingredient (API) or growth factor (GF) for biomedical applications. Figure II.2 presents a graphical abstract of this study.

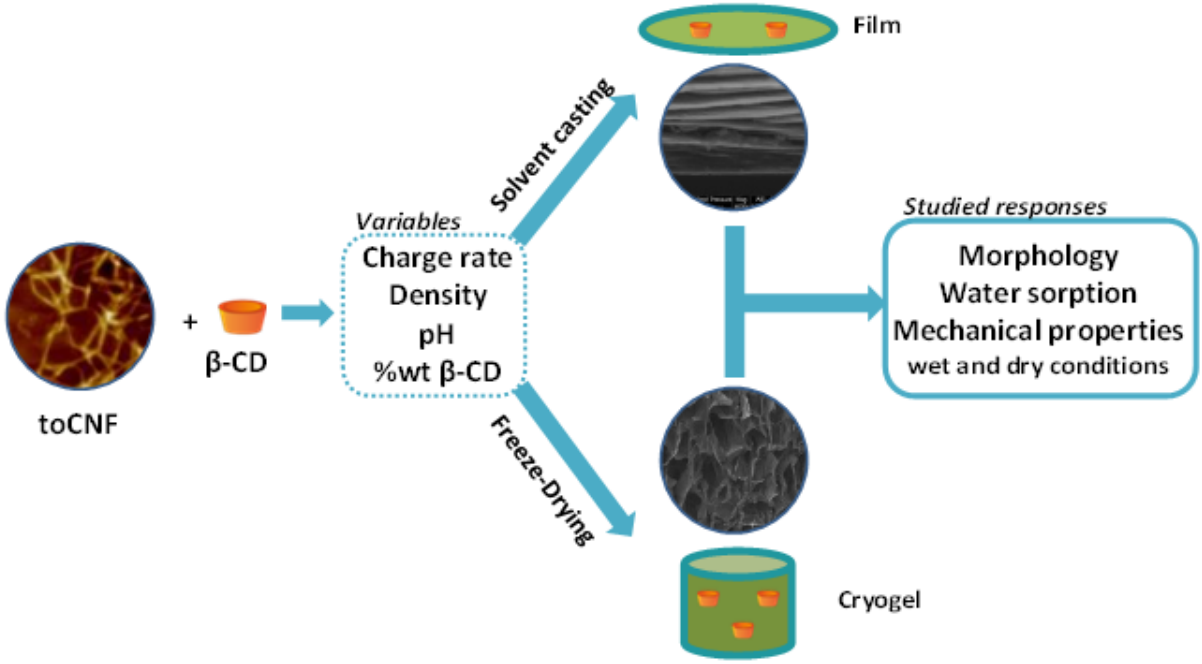

Figure II.2: Graphical abstract for Chapter II.1. as proposed in [1]

II.1.1. INTRODUCTION

Cellulose nanofibrils (CNFs) are high aspect ratio nanoparticles formed by bundles of cellulose chains that are a succession of glucose subunits linked by β-1-4 glycosidic bonds. CNFs are produced from a cellulosic raw material, usually wood, the most abundant and renewable polymer available on earth. CNFs are produced by a combination of chemical/enzymatic pre-treatments and mechanical treatment, usually using a homogenizer [2], a microfluidizer [3] or a grinder [4]. The variety of existing pre-treatments [5] allows for a variety of surface chemistries, making CNF materials suitable for many applications [6]. CNFs pre-treated with (2,2,6,6-tetramethyl-piperidin-1-yl)oxyl, also known as TEMPO, proposed by Saito et al., 2006, which consists in the regioselective oxidation of C6 primary hydroxyls of cellulose to C6 carboxylate groups have been considered in a wide variety of applications due to their carboxyl content and reduced size [7], [8]. CNFs are generally used in two different forms: either as films/nanopapers or as gels, and can be used as rheology modifier or emulsion stabilizer and additive in many applications. Films are obtained by solvent casting [9]–[11], and nanopapers are obtained by filtration [12], [13]. Three types of gels can be identified: hydrogels, cryogels obtained by freeze-drying and aerogels obtained by supercritical drying [14], [15]. For many applications, water sorption properties are important. TEMPO-oxidized cellulose nanofibrils (toCNF), like cellulose, are hygroscopic materials, meaning that they can attract and retain water molecules from their environment by absorption or adsorption [11]. The impact of process parameters on cryogel mechanical properties has been previously studied [15]–[20], highlighting the importance of density and preparation method on the mechanical properties.

As a natural, biodegradable and abundant polymer with reactive surface chemistry and good biocompatibility, nanocellulose is a promising material within the medical field. In recent years, applications in wound healing [21], [22], drug delivery [10] and tissue engineering [23] have been investigated. In tissue engineering, the scaffold should stimulate cells to differentiate, proliferate and form tissue. The interplay between the matrix and cells should be driven by the action of signals, which can be a mechanical stimulation, chemical compounds or growth factors (usually proteins) [24]. To be suited for tissue engineering applications, scaffolds need to exhibit a stiffness similar to that of the natural extra-cellular matrix (ECM) of the tissue to be repaired, measured by the elastic modulus E. Typical values

of stiffness of ECM are 0.1-1 kPa for brain tissue, 8-17 kPa for muscle tissue and 25-40 kPa for cross-linked collagen matrix [25], [26]. Another crucial aspect for tissue engineering application is the scaffold architecture. A high porosity is needed to promote the cellular penetration and adequate diffusion of nutrients to the cells [27].

The utilization of wood-based CNFs for tissue engineering applications is encouraged by recent studies that confirmed the safety of CNFs [28]–[31], the construction of cell-friendly porous structures [15] and the control of mechanical properties [32], [33]. In addition, CNFs, in the form of a highly entangled network, have shown the ability to retain an active principle ingredient up to several months [10]. However, major challenges for biomedical applications are yet to be overcome, such as increasing the bioavailability of drugs, as most new drugs are described as poorly soluble [34] and controlling the delivery kinetics of active principle ingredient (API). To address these issues, this research study proposes the use of cyclodextrins (CDs).

CDs are cyclic oligosaccharides consisting of glucose subunits linked by α-1-4 glycosidic bonds. Because of their conformation, with a hydrophobic interior and a hydrophilic exterior, these macromolecules exhibit cage-like properties and can form an inclusion complex with hydrophobic compounds [35], [36]. These properties have led to their use in various fields, such as cosmetics, food, environment and medicine [37]–[39]. Regarded as safe, they are widely used as an excipient in the pharmaceutical field [40], [41]. For such applications, βCD, a cyclodextrin with 7 glucose sub-units, and its derivatives are the most commonly used [34], [42]. βCDs are also of great interest for tissue engineering applications, with their lipophilic compound encapsulation properties proven to improve scaffold performance [43]–[45]. This property could also led to the immobilization of growth factors [46] or drug delivery [40] during cell growth to optimize the effect of the scaffold. Previous studies reported the association of cyclodextrin with various cellulose derivatives [47], [48]. The association between CDs and CNFs or cellulose nanocrystals (CNCs) has been attempted in a very small number of recent studies, summarized in Table II.1. To the best of our knowledge, no study presents the impact of βCD on both the sorption and the mechanical properties of toCNF substrates (films or cryogels).

The aim of the present study was to modify toCNF with βCD (preferably with covalent linkage) and to see what kind of effect this surface functionalization has on sorption and

mechanical properties. Thus, a comparison with the same structures using unmodified toCNF is necessary. For that purpose, two suspensions of toCNF with different charge contents were prepared. Fiber modification with cyclodextrins was carried out at neutral and acidic pH (2.5) to study the effect of the dissociation of the carboxylic acid group. Films, processed by casting/evaporation at 40°C and cryogels, processed by freeze-drying were prepared from βCD-modified toCNF and compared with reference samples of unmodified toCNF. Water sorption was evaluated gravimetrically for both films and cryogels. The impact of density on the mechanical properties of the cryogels was assessed for cryogels obtained from unmodified toCNFs and prepared by freeze-drying from suspensions at different dry matter contents for both charge contents. Compression tests in the dry and swollen state were performed for cryogels obtained from all suspensions and microscopic observation (SEM) was carried out to link the mechanical behavior to the microstructure of the materials.

Table II.1: Previous works on the association nanocellulose-cyclodextrin. CNFs: cellulose nanofibrils, toCNFs: tempo-oxidised cellulose nanofibrils, HP-CNFs: hydroxypropyl cellulose nanofibrils, CNCs: cellulose nanocrystals, βCD: β-cyclodextrin, CMβCD: carboxymethyl- β-cyclodextrin, HPβCD : hydroxypropyl-β-cyclodextrin

Nanocellulose	CD	Functionalization strategy	Application	Source
toCNFs	βCD	Direct grafting	Release of essential oil	[49]
CNFs	βCD	Cross linking with citric acid	Depollution	[50]
toCNFs	CMβCD	Amidation via EDC/NHS	Depollution	[51]
HP-CNFs	HPβCD	Electrospinning	Drug release	[52]
CNFs	βCD	Coating/Adsorption	Drug release	[53]
CNFs	βCD	Cross linking with citric acid	Antibacterial packaging	[54]
toCNFs	βCD	Non- covalent interaction	Drug Delivery/ Tissue Engineering	[30]
toCNCs	βCD / HPβCD	Direct grafting	Release of essential oil	[55]
CNCs	βCD	Grafting with epichlorohydrin	Tissue engineering	[56]
CNCs	βCD	Crosslinking with fumaric and succinic acid	Release of essential oil	[57]
CNCs	βCD	Ionic interaction	Drug delivery	[58]
CNCs	βCD	Grafting with epichlorohydrin	Supramolecular hydrogels	[59]

II.1.2.MATERIALS AND METHODS

II.1.2.1. MATERIALS

A mixture of bleached and never-dried spruce (Picea abies (ca. 75 %) and pine (Pinus sylvestries, ca. 25%) cellulose pulp from Södra (Växjö, Sweden) was used as raw material. All chemicals used in this study were of laboratory grade quality purchased from Sigma-Aldrich.

II.1.2.2. METHODS

II.1.2.2.1. PREPARATION OF TOCNF WITH TWO DIFFERENT CHARGE CONTENTS

TEMPO-oxidized cellulose nanofibrils were produced according to a protocol adapted from [7]. Never-dried cellulose (110 g) was suspended in water (3 L) and stored overnight at 4°C. The suspension was dispersed with a blender and mixed with a solution (400 mL) containing TEMPO (1.375 g) and sodium bromide (13.75 g). Water was added to obtain a total volume of 8250 mL (75 mL/$g_{cellulose}$). TEMPO-mediated oxidation of cellulose started by adding different amounts of 13% NaClO: 2.5 mmol/$g_{cellulose}$ for a charge content of 750 μmol/g (that will be used to prepare L-toCNF) and 3.3 mmol/$g_{cellulose}$ for a charge content of 1100 μmol/g (that will be used to prepare H-toCNF). NaClO was added gradually and the pH was maintained at 10.5 by adding 0.5M NaOH. The slurry was stirred for 15 min after complete addition of NaClO, and the pH was then dropped to 7 with 0.1 M HCl. Methanol (100 mL) was then added to the slurry. The product was thoroughly washed with water by filtration until the conductivity of the filtrate was below 5 μS/cm. Homogenization was conducted using a Rannie 15 type 12.56X homogenizer (APV, SPX Flow Technology, Silkeborg, Denmark). The suspension was diluted to 1.2 wt% and dispersed with an electric mixer. The fibers underwent two passes in the homogenizer at 600 bar and 1000 bar, respectively. The final suspensions were stored at 4°C.

II.1.2.2.2. DETERMINATION OF THE CHARGE CONTENT

The carboxyl group content was determined by conductometric titration as described in previous studies (eg. [8], [33], [60]). 5 mL of 0.1M NaCl was added to a toCNF dispersion with 0.2 g solid content in 450 mL. The pH was adjusted to approximately 2.5 by adding 0.1M HCl and further diluted with water to a total volume of 500 mL. The dilution was titrated with 0.05M NaOH solution added at a rate of 0.15 mL/min under stirring up to a pH of 11. An automatic titrator (902 Titrando, Methrom AG, Herisau, Switzerland) was used and

the conductivity of the sample was automatically measured (856 Conductivity Module, Methrom AG, Herisau, Switzerland) for increments of 0.02 mL. Data were recorded by Tiamo Titration software. The carboxyl content was calculated from the titration curve using the Gran plot. Duplicates were made for both suspensions and NaOH titration (control).

II.1.2.2.3. Material processing

II.1.2.2.3.1. Film processing

0.40g of dry toCNF was weighed and diluted with water to a total volume of 50 mL. The suspension was dispersed for 2 min at 7000 rpm with an UltraTurrax at room temperature. βCD (0.025 g) and 0.1M HCl (2 mL) were added to the relevant samples. The suspensions were magnetically stirred for 1 hour and placed in an ultra-sonic bath for 3 min. The suspension was then cast in Petri dishes (9 cm diameter) and stored in an oven at 40°C for 18h. The resulting films were stored in closed Petri dishes at room temperature.

II.1.2.2.3.2 Cryogel processing

Impact of pH, cyclodextrin and comparison dry/swollen

50 mL of 0.8 wt% toCNF suspension was prepared and dispersed 2 min at 7000 rpm with an UltraTurrax. βCD (0.04 g) and 0.1M HCl (3 mL) were added if required. The suspensions were magnetically stirred for 1 hour and placed in an ultra-sonic bath for 3 min. The suspensions were poured into a 24-well plate (3mL per well) and freeze-dried for 24h at -20°C and 0.3 mbar (BK FD12S, Biobase Biodustry). The resulting cryogels were stored in closed well-plates.

Impact of density

50 mL of 1 wt%, 0.8 wt%, 0.6 w% and 0.4 wt% L-toCNF and H-toCNF suspensions were prepared and dispersed for 2 min at 7000 rpm with an UltraTurrax. The suspensions were magnetically stirred for 1 h and placed in an ultra-sonic bath for 3 min. The suspensions were then poured into a 24-well plate (3mL per well) and put in a freezer at -20°C for 24 h before freeze-drying (ALPHA 2-4 LDplus, Christ ®).

II.1.2.2.4. Water sorption analysis

Water sorption tests on films were carried out gravimetrically in a Percival climatic chamber at 25°C and 90% RH (relative humidity). The samples were weighted every hour at the beginning of the experiment and at selected times thereafter. Water sorption experiments

were conducted after 48 hours, with at least 3 replicates for each sample. The samples were put in a desiccator for 16 h prior to the experiment. The water sorption was characterized by the weight change between the initial sample weight (m_0) and the weight after a certain time t (m_t), according to equation II.1:

$$Water\ sorption\ [\%] = \frac{m_t - m_0}{m_0} \times 100 \qquad \text{(Eq. II.1)}$$

Water sorption tests on cryogels were conducted gravimetrically. The cryogels were weighted and immersed in distilled water, and then removed at different times. Excess water was removed before weighting.

II.1.2.2.5. MICROSCOPY

Atomic Force Microscopy images were recorded on a Dimension icon® (Bruker, USA). The concentration of the suspension was adjusted to 10^{-3} wt% by diluting the CNF dispersion using high shear mixer Ultra-Turrax (IKA). A drop of this suspension was deposited on freshly cleaved mica plate before drying overnight under fume hood at room temperature. The acquisition was performed in tapping mode using a silica coated cantilever (OTESPA® 300 kHz – 42 N/m, Bruker, USA). Zones of 1.1*1.1 μm² were analyzed.

Scanning Electron Microscopy images were recorded with ESEM (Quanta 200, FEI, Japan). Film and cryogel cross sections were cut with a razor blade. SEM observation was carried out on cross-sections after carbon sputter coating of 5 nm, with a tension of 10 kV and a spot size of 3.5. The working distance was set between 9.5 mm and 11.5 mm depending on the sample.

For both microscopy techniques, at least 5 different images were performed to check the consistency in various zones of the sample and the most representatives were selected for the discussion.

II.1.2.2.6. MECHANICAL CHARACTERIZATION

Impact of density

Compression tests were performed using a TA Instruments RSA 3 (New Castle, Delaware, USA) dynamic mechanical analyser fitted with a 100 N load cell. Samples prepared as cylinders were individually measured and compressed with a crosshead speed

of 0.1 mm/s at room temperature. At least triplicates were performed and the average is presented.

Impact of pH, cyclodextrin and comparison dry/swollen

Compression tests were performed with a Stable Micro Systems TA-XT2 texture-analyzer equipped with a P/35 probe and with a crosshead speed of 0.1 mm/s as previously described by Heggset et al., 2018 [60].

A minimum of 6 cryogels were tested for each sample. The compression modulus was calculated in the elastic region at half the strain of the beginning of the plateau region and the stress at 70 % strain was directly read from the data. The normalized compression modulus was calculated by dividing the compression modulus by the cryogel density. The cryogel density ϱ was determined by dividing the mass of each cryogel by its volume. The volume of produced cryogels was measured from height and diameter measurements using a calliper. For each sample, the two extreme values were removed. The relative density of cryogels was calculated from the ratio ϱ/ ϱc , where ϱc is the density of cellulose, 1.5 g/cm^3 [62]. The porosity was calculated from Equation II.2:

$$Porosity\ [\%] = \left(1 - \frac{\rho}{\rho_C}\right) * 100 \qquad \text{(Eq. II.2)}$$

II.1.2.2.8. FOURIER-TRANSFORM INFRARED SPECTROSCOPY (FTIR)

FTIR spectra were recorded in Attenuated Total Reflectance (ATR) mode, using a Perkin Elmer Spectrum 65. Spectra were recorded between 4000 and 600 cm^{-1}, with 16 scans and a resolution of 4 cm^{-1}. Since this technique is used to determine the possible esterification between the cyclodextrins and toCNF, and given the proximity between the carboxylic peak and the ester peak (≈1720 cm^{-1} and ≈1750 cm-^{1}, respectively), each cryogel was dipped in 0.05M NaOH for 10s to convert the carboxylic acid groups into carboxylate groups (1600 cm-^{1}) and dried in oven for 30 min prior to analysis. As control sample, neat samples and neat samples after 30 min drying in oven were also analysed to ensure that esterification was only due to the freeze-drying process. At least 5 different zones of the sample were analyzed and the most representative spectra was used for discussion.

II.1.3. RESULTS AND DISCUSSION

TEMPO-oxidized cellulose nanofibrils suspensions were successfully produced. The amounts of carboxylic groups were determined to be 756 ± 4 μmol/g and 1048 ± 32 μmol/g. Films and cryogels were processed from the two different toCNFs suspensions in four different conditions presented in Table II.2.

Table II.2: Samples codes

Sample code	βCD	pH
1	0	Neutral
2		Acidic
3	10 wt%	Neutral
4		Acidic

The suspension with 756 μmol/g carboxyl content will be referred as L-toCNF in the text, hence samples from L-toCNF will be labelled L1, L2, L3, L4. Similarly, the suspension with 1048 μmol/g carboxyl content will be referred as H-toCNF, i.e. samples from H-toCNF will be labelled H1, H2, H3, H4. Figure II.3. shows AFM images of the nanofibers obtained for both charge contents. Similar and slightly thinner fibrils were obtained for the most oxidized cellulose, as expected.

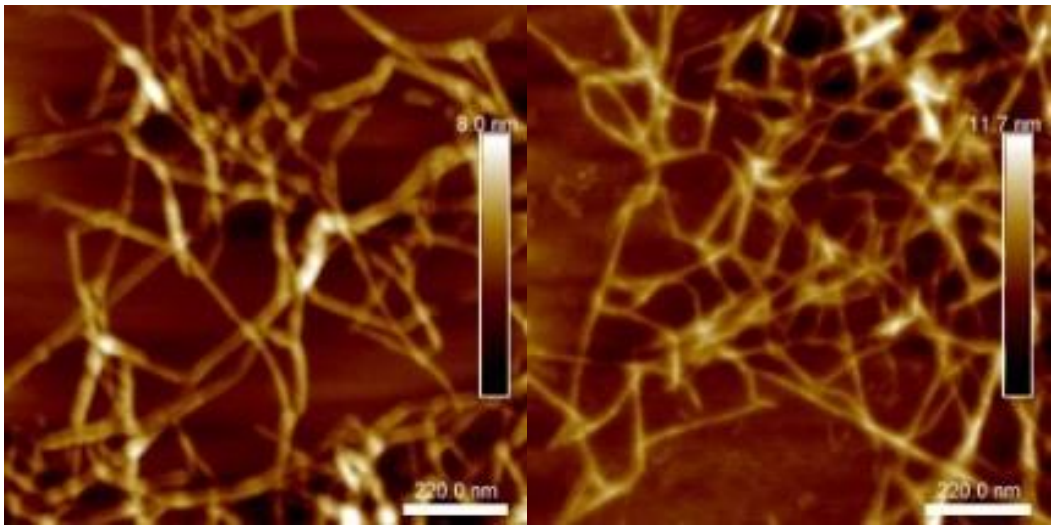

Figure II.3: AFM images of L-toCNF (left) and H-toCNF (right)

II.1.3.1. WATER SORPTION ANALYSIS

II.1.3.1.1. FILMS

Water sorption of films was assessed gravimetrically in a Percival climatic chamber at 25°C and 90% RH for 48h. Figure II.4. displays the time dependence of water sorption for films with various carboxyl contents and casting conditions (casting pH, amount of cyclodextrin).

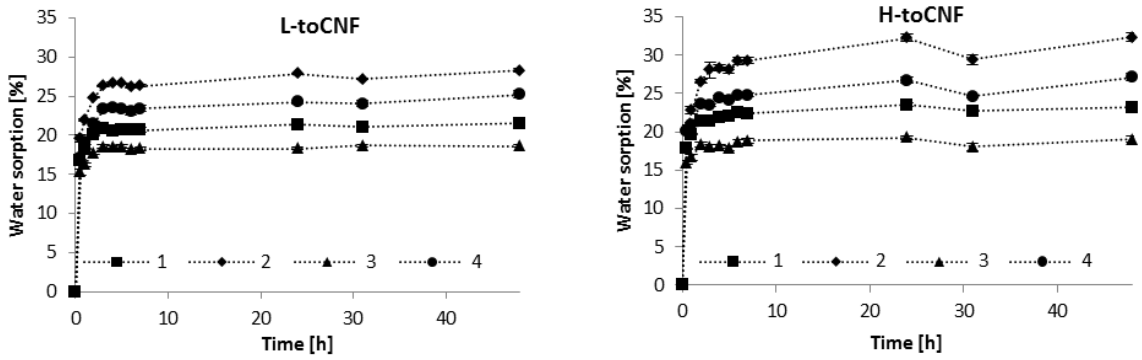

Figure II.4 : Water sorption as a function of time of conditioning at 25°C-90%RH for L-toCNF (left) and H-toCNF (right)

Table II.3: Sorption equilibrium after 48h and % of sorption after 30 min for L-toCNF films and H-toCNF films

Sample	Water sorption equilibrium after 48h [wt%]		% of sorption after 30 min	
	L-toCNF	*H-toCNF*	*L-toCNF*	*H-toCNF*
1	21.5 ± 0.2	23.2 ± 0.2	77.6 ± 0.2	76.7 ± 1.2
2	28.3 ± 0.3	32.3 ± 0.6	69.3 ± 2.0	62.9 ± 2.1
3	18.6 ± 0.1	19.0 ± 0.4	82.0 ± 1.5	83.9 ± 0.9
4	25.2 ± 0.5	27.1 ± 0.5	67.9 ± 2.0	74.1 ± 0.5

For each sample of both L-toCNF and H-toCNF, sorption equilibrium was reached after approximately 4h, indicating that this property is not dependent on any of the variable parameters in this study. Table 3 reports the sorption equilibrium obtained after 48h. It is slightly higher for H-toCNF samples compared to L-toCNF: + 1.9% for raw suspension samples (condition 1) , +4% for pH 2.5 samples (condition 2), +0.4% for 10 wt% CD samples (condition 3) and +1.9% for 10 wt% CD/pH 2.5 samples (condition 4). For both charge contents, the same dynamic between the different casting conditions was observed: sample 3 < 1 < 4 < 2. The carboxylic content at acidic pH is in its carboxylic acid form, hence increasing

the water sorption by forming more H-bonds with water molecules than in neutral conditons. Cyclodextrins, by adsorbing onto toCNF fibers, decrease the water sorption ability. For hygroscopic cellulosic materials, the two mechanisms of sorption, namely adsorption and absorption, need to be considered. In addition, depending on the surface chemistry of the fibers, sorption can be either slow or fast [63]. For toCNF, due to their hydroxyl and carboxylic surface groups, sorption occurs quite fast. Two mechanism of sorption can also be distinguished: direct sorption, which corresponds to water molecules forming hydrogen bonds directly with toCNF, and indirect sorption, which corresponds to water molecules binding with already bound water molecules [11]. Interfibril interactions, on the other hand, may inhibit swelling [64] because the volume increase of hydrated nanofibrils can be slowed down by other nanofibrils, and water binding to nanofibrils reduces interfibril binding. While adsorption is a fast process, absorption occurs more slowly, with less water molecules penetrating the inner surface and amorphous regions [65].

SEM images of the cross-section of films presented in Figure II.5 show the same laminar structure with a similar density, regardless of the carboxyl content and casting conditions.

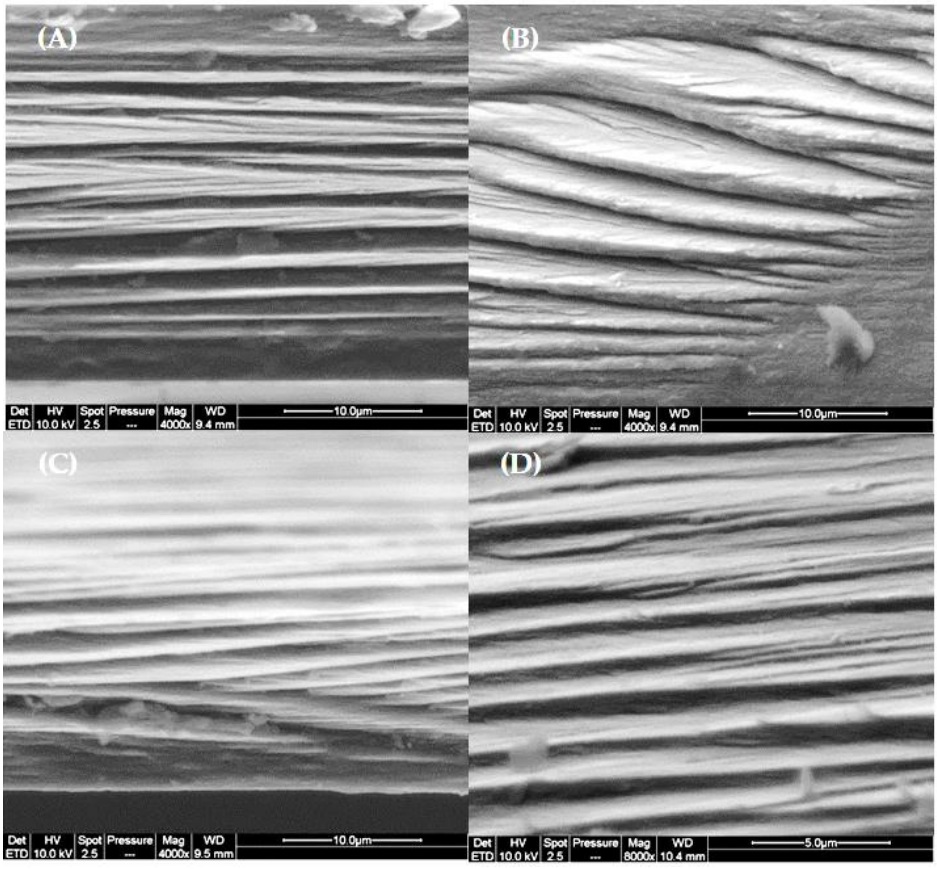

Figure II.5: SEM images of the cross-section of films. (A) H1, (B) H2 (C) H3, (D) H4

In addition, the sorption equilibrium was achieved within a relatively short period of time, with about 65% of the sorption equilibrium reached after 30 min for films cast in acidic conditions, up to around 80% for films containing cyclodextrins. The difference in sorption equilibrium observed between L-toCNF and H-toCNF can be linked to the number of carboxylic functions prone to form H-bonds with water molecules, which is higher for H-toCNF than for L-toCNF. The increase in sorption for films prepared under acidic conditions is explained by the acid form of the carboxylic groups, which is more prone to form H-bonds with water molecules than the carboxylate form at neutral pH. Finally, the decrease in sorption when adding cyclodextrin is thought to be due to the adsorption of β-CD on the surface of the fibers, which could decrease the amount of water bounded to the fibers. Water sorption is mainly driven by adsorption and chemical makeup dependent. For a given drying temperature, water sorption can be slightly tuned by varying the process parameters, which is an interesting property for drug delivery applications, where swelling and sorption properties are important for the delivery kinetics.

II.1.3.1.2. CRYOGELS

Water sorption tests for cryogels were conducted gravimetrically. The cryogels were weighted and immersed in distilled water, and then removed at different time intervals. Tissue paper was used to remove excess water prior to weighing. For both charge contents, the swelling equilibrium was reached after the first measurement at 15 minutes, as shown in Figure II.6. The swelling equilibrium after 3h was 4871 % ± 471% and 4890 % ± 141 % for L-toCNF and H-toCNF samples, respectively. According to these results, cryogels were immersed 1h before compression to study the mechanical properties of swollen cryogels so that they would be at swelling equilibrium. It also appeared that the charge content does not have a significant impact on the sorption equilibrium, suggesting that the absorption mechanism in immersion is mainly driven by the porosity and the pore morphology which are not strongly affected by the charge content.

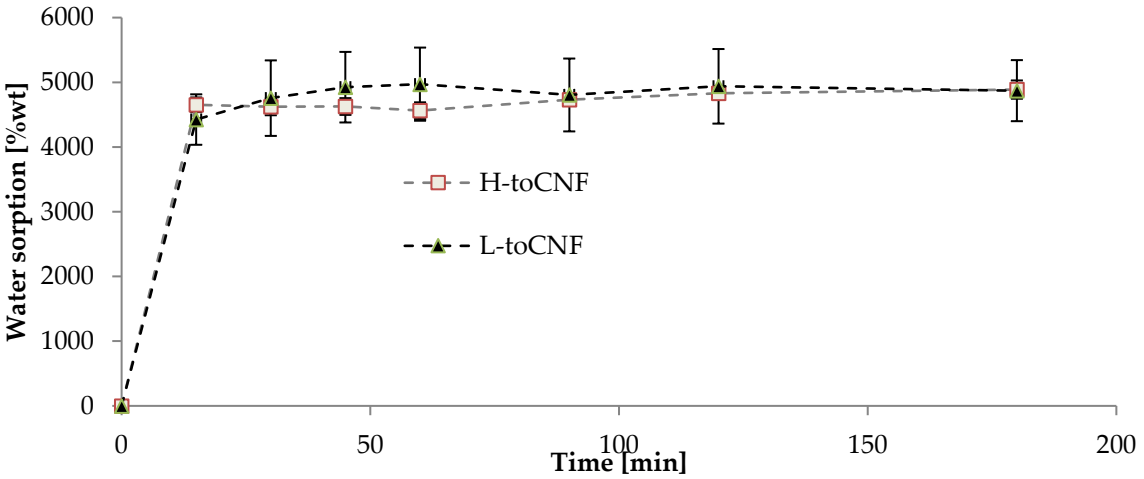

Figure II.6: Water sorption for toCNF cryogels in immersion

II.1.3.2. MECHANICAL CHARACTERIZATION

Compression tests were carried out on cylindrically shaped cryogels. The density of each sample was determined by dividing the mass of each cryogel by its volume. The volume of the cryogels was measured from height and diameter measurements using a calliper. In each case, the compression curve can be divided into 3 different regions:

- For low strain values, the compression stress increases linearly with the strain in the elastic domain up to the yield point. The compression modulus was calculated at a strain corresponding to half the yield stress in order to be reproducible between all samples.
- For strains higher than the yield point, the plastic region was reached. In this region, the stress increases with the strain with significant residual deformation after unloading.
- For high compressive strains, the curves exhibit a sharp increase in the compressive stress, typical of a densification regime.

This behaviour has previously been reported for cellulose-based foam materials [16], [17], [19], [20]. The obtained cryogels are closed-cell wall foams, as observed in Figure II.7. In such materials, elasticity is caused by the stretching of the cell walls, plastic deformation occurs when the cells start to lose their integrity and densification occurs when cells collapse on themselves, reducing porosity and causing the cryogels to behave like the solid itself [66], [67].

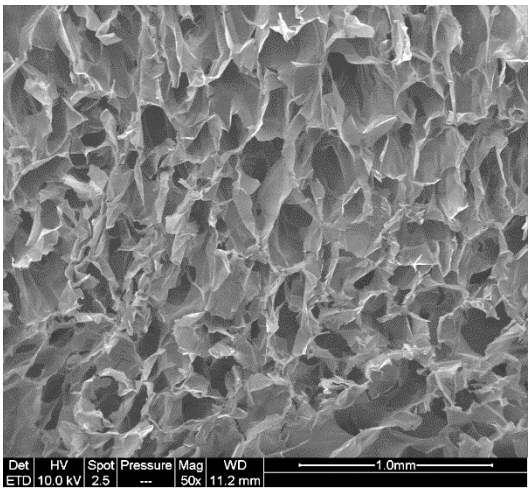

Figure II.7: SEM images of the cross-section for toCNF cryogel

II.1.3.2.1. IMPACT OF DENSITY

Compression tests were carried out on cryogels with four different densities prepared from toCNF with both charge densities. The variation of the different parameters (compression modulus, normalized compression modulus, maximum stress at 70% deformation) with the relative density is presented in Figure II.8 and numerical values are summarized in Table II.4. The results for L-toCNF and H-toCNF are similar for all densities, indicating that the charge content has no major impact on the mechanical properties under process conditions tested. All the properties increased with the density, quite linearly for the compression modulus and the maximum stress at 70% deformation, while the normalized compression modulus seems to stabilize for densities higher than 15 mg/cm^3 (which corresponds to a relative density of 0.01). It is worth noting that the normalized compression modulus withstands a huge decrease for relative densities lower than 0.008. Density is of major importance for the mechanical behavior of cryogels, and by controlling the density it is possible to tailor the mechanical properties of the cryogel.

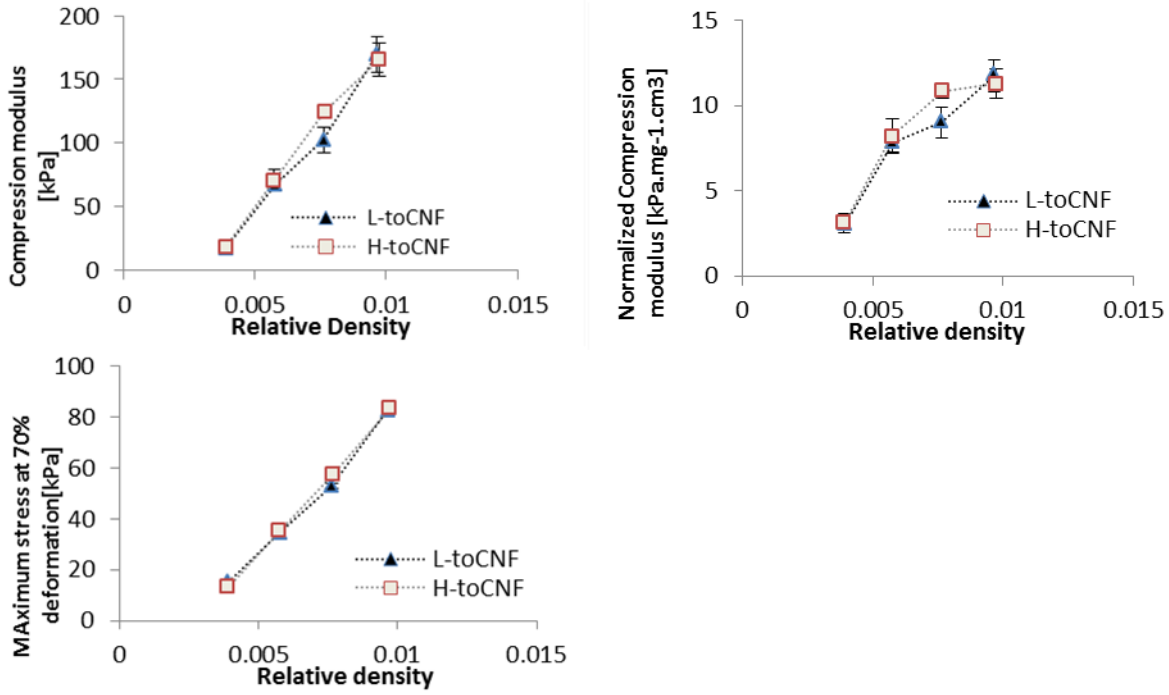

Figure II.8: Relative density dependence of compression modulus, normalized compression modulus and maximum stress at 70% deformation for L-toCNF and H-toCNF cryogels

Table II.4: Mechanical properties for toCNF at various densities

Initial dry content	Porosity [%]		Compression modulus [kPa]		Normalized compression modulus [kPa.mg-1.cm³]		Maximum stress at 70% deformation [kPa]	
	L-toCNF	*H-toCNF*	*L-toCNF*	*H-toCNF*	*L-toCNF*	*H-toCNF*	*L-toCNF*	*H-toCNF*
0.4 wt%	99.6	99.6	17 ± 2	18 ± 3	3.0 ± 0.3	3.1 ± 0.6	15 ± 1	13 ± 1
0.6 wt%	99.4	99.4	68 ± 5	71 ± 9	7.8 ± 0.6	8.2 ± 1.0	35 ± 1	35 ± 1
0.8 wt%	99.2	99.2	102 ± 10	125 ± 4	9.0 ± 0.9	10.9 ± 0.4	53 ± 1	57 ± 2
1 wt%	99.0	99.0	170 ± 14	165 ± 13	11.8 ± 0.9	11.3 ± 0.9	83 ± 1	84 ± 1

II.1.3.2.2 Impact of pH and cyclodextrins on dry cryogels

Cryogels were prepared from the four compositions by freeze-drying the nanofibrils suspensions. SEM images of the cross-section of the cryogels are presented in Figure II.9. For all cryogels, closed-cell wall structures are observed, organized as an alveolar structure.

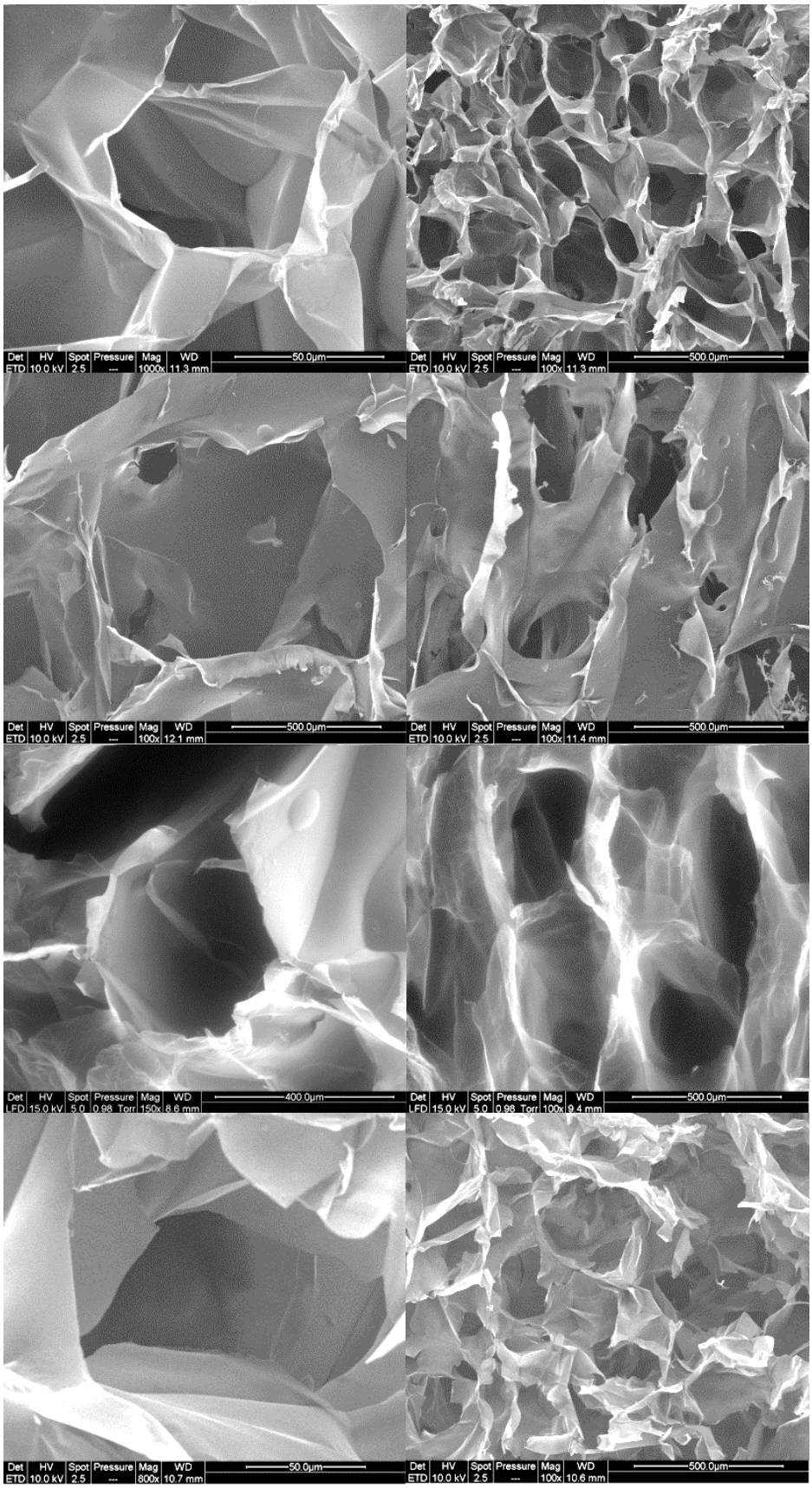

Figure II.9: SEM images for toCNF cryogels. From Top to down: 1 / 2 / 3 / 4

This specific orientation of the porosity is due to the freeze-drying process. Indeed, freezing occurred from the bottom part of the freeze-dryer, resulting in the growth of ice in a specific direction, leading to anisotropy in pore orientation.

In addition, we can observe that the structure of the cell walls for modified-toCNF cryogels presents more structural deflects (holes, folds) than for unmodified-toCNF. Compression tests were carried out on cryogels prepared from the four compositions for both charge contents. Typical stress-strain curves for each composition are presented in Figure II.10.

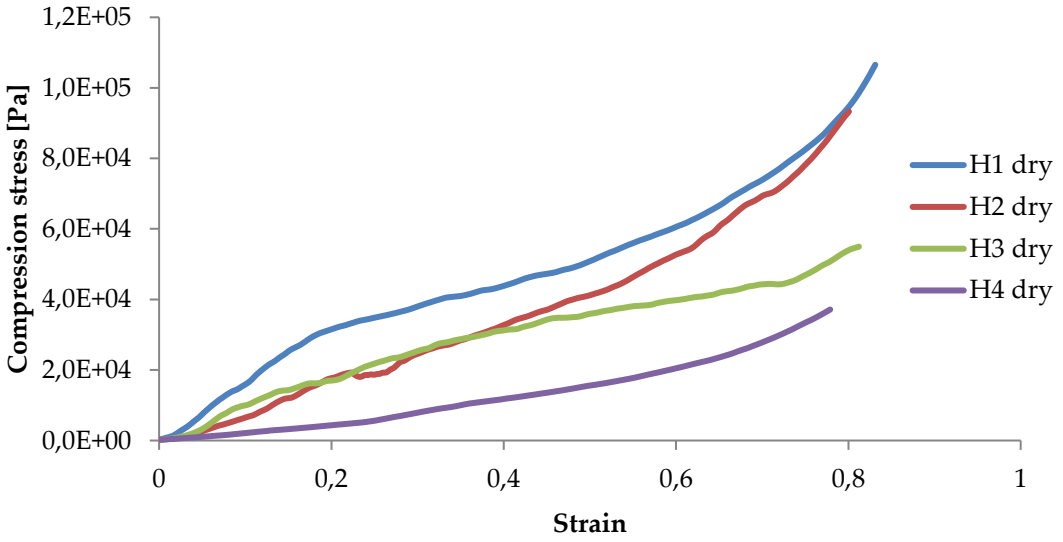

Figure II.10: Representative compression curves for H-toCNF cryogels

Unmodified toCNF cryogels (H1 and H2) exhibit a clear elastomeric behavior, with a well-defined linear elastic zone up to a strain of about 0.2, followed by a compression plateau and a densification for higher strains. For modified toCNF cryogels (H3 and H4), the linear elastic zone is restrained to lower strain values and the yield point is less marked. The deflects observed in Figure II. in the cell walls for modified toCNF cryogels oppose the elastic buckling of the cells, explaining the small elastic region for modified cryogels. The density, compression modulus, normalized compression modulus and maximum stress at 70% deformation for each type of cryogel and for both charge contents are summarized in Table II.5.

Table II.5: Mechanical properties for to-CNF cryogels of different compositions

	Cryogel Density [mg/cm3]		**Compression modulus [kPa]**		**Normalized compression modulus [kPa.mg-1.cm3]**		**Maximum stress at 70% deformation [kPa]**	
	L-toCNF	*H-toCNF*	*L-toCNF*	*H-toCNF*	*L-toCNF*	*H-toCNF*	*L-toCNF*	*H-toCNF*
1	14.89 ± 0.47	16.07 ± 0.57	104 ± 13	150 ± 10	7.0 ± 0.8	9.4 ± 0.8	64 ± 3	65 ± 3
2	25.32 ± 0.84	20.82 ± 1.08	34 ± 6	76 ± 6	1.4 ± 0.2	3.7 ± 0.3	58 ± 7	63 ± 3
3	17.91 ± 0.60	18.45 ± 1.66	59 ± 10	84 ± 13	3.3 ± 0.5	4.7 ± 0.3	42 ± 2	43 ± 2
4	20.85 ± 0.96	26.41 ± 2.19	37 ± 3	17 ± 3	1.8 ± 0.2	0.6 ± 0.1	59 ± 5	24 ± 4

An increase in density can be observed for cryogels cast under acidic pH and with cyclodextrins. The carboxyl content increases the interactions between the fibers in their carboxylic form, as it forms a denser structure. The adsorption of cyclodextrins on the surface of the fibers also increases the interaction between fibers or creates local deflects in the fiber arrangement. Both mechanisms impact the mechanical properties. The mechanical properties decrease when the density increases and the elastic region in the stress-strain curve also decreases for cryogels cast under acidic pH or when containing cyclodextrins. It is also worth noting that the yield point is lower for modified cryogels (pH, cyclodextrins) than for unmodified ones, and that the plateau is less pronounced. Since elasticity of foams is linked to the stretching of the cell walls and the plastic behavior prior to densification is linked to the compression of cells, the modification of fiber-fiber interaction under acidic pH and/or with adsorption of cyclodextrin on the fiber surface is responsible for the modification of the cell wall, thus the mechanical properties. Both charge contents exhibit a similar behavior for toCNF, toCNF pH 2.5 and toCNF 10wt%CD, but a noticeable difference is observed for toCNF 10wt%CD pH 2.5. For L-toCNF, the density decreases between pH 2.5 and 10wt%CD pH2.5, while the normalized compression modulus and the maximum stress at deformation are quite similar. For H-toCNF, the density increases between pH2.5 and 10wt%CD pH2.5, while the normalized compression modulus and the maximum stress at 70% deformation decrease. Under these conditions (10wt%CD and pH2.5), esterification

occurred between the carboxylic acid of toCNF and hydroxyl groups of cyclodextrins, as evidenced by the ATR-FTIR spectra shown in Figure II.11.

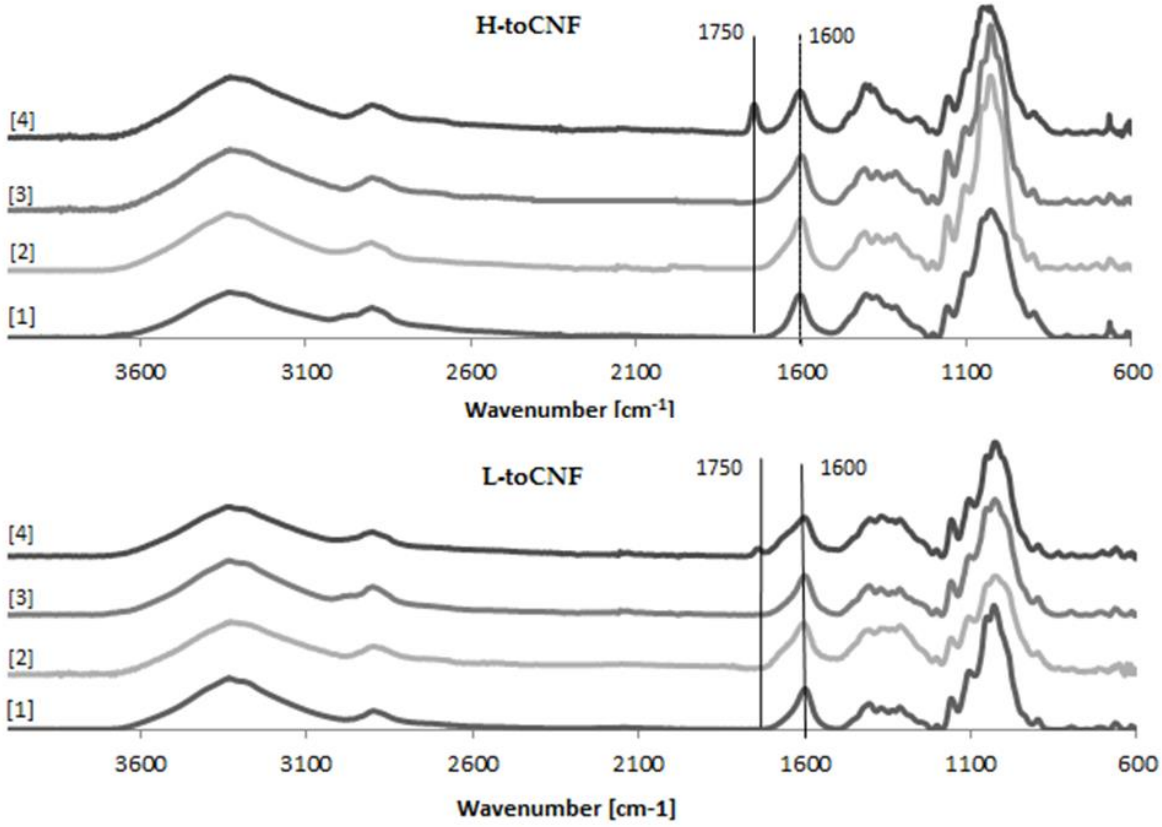

Figure II.11: ATR-FTIR spectra for toCNF cryogels

The peak observed at 1600 cm^{-1} corresponds to the carboxylate ions present on the surface of the fibers introduced during TEMPO-mediated oxidation. For toCNF 10%CD pH 2.5, a peak at 1750 cm^{-1} can be observed which corresponds to the ester groups. The presence of this esterification peak only for toCNF 10%CD pH2.5 indicates that the esterification reaction occurred between the hydroxyl groups of the cyclodextrins and the carboxylic acid groups of toCNF under acidic pH, suggesting that the freeze-drying process allows the reaction by removal of water. Considering the respective charge contents for L-toCNF and H-toCNF, the efficiency of esterification might be higher for H-toCNF, which can explain the decrease in mechanical properties observed for H4.

II.1.3.2.3 Difference between dry and swollen cryogels

Cryogels were immersed in water for 1h prior to the experiment and tissue paper was used to remove excess water before compression. The changes in mechanical properties between the dry and swollen states are summarized in Table II.6. Comparison of typical

stress-strain curves for dry and swollen cryogels are presented in Figure II.12. For swollen cryogels no clear elastic zone is observed. The water molecules, by binding to the fibrils, inhibit interfibrillar interactions, and thus largely reduce the elastic behavior. As a result, a significant decrease in mechanical properties is observed for each sample tested, as illustrated in Table II.6.

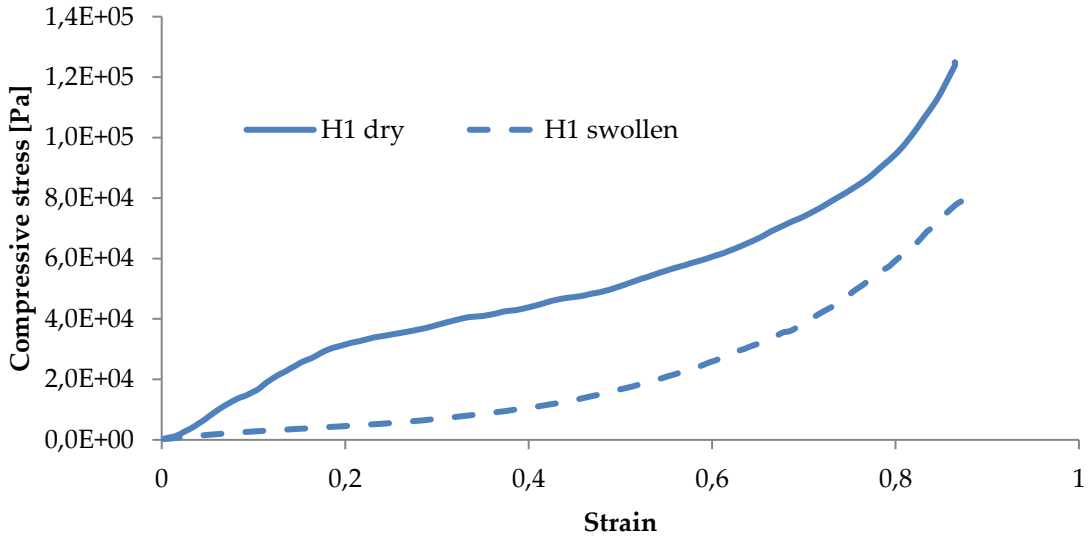

Figure II.12: Representative compression curves for dry and swollen H-toCNF cryogels

Table II.6: Diminution of mechanical properties between dry and swollen states

	Compression modulus [kPa]		**Diminution of compression modulus [%]**		**Diminution of maximum stress at 70% deformation [%]**	
Casting conditions	*L-toCNF*	*H-toCNF*	*L-toCNF*	*H-toCNF*	*L-toCNF*	*H-toCNF*
1	45 ± 4	33 ± 4	-57 %	-78%	-4%	-54%
2	9 ± 1	8 ± 1	-75 %	-90%	-82%	-90%
3	6 ± 1	7 ± 1	-89%	-92%	-90%	-89%
4	9 ± 1	9 ± 4	-77%	-49%	-82%	-73%

Since no clear elastic deformation zone can be observed for swollen cryogels, the compression modulus was calculated at low-strain (<0.1) for comparison with dry cryogels. The decrease in mechanical properties is more significant for H-toCNF (H1, H2 and H3 cryogels), which can be explained by the higher charge content, making the fibers more sensitive to adsorption of water molecules. It is also worth noting that the decrease in mechanical properties is reduced for H4 in comparison with L4, with respectively -49% and -77% decrease in compression modulus compared to their dry state. This behavior could be explained by the esterification between cyclodextrin and toCNF, cross-linking the fibers and making the structure less sensitive to water ad/absorption.

Esterification of βCD with toCNF under acidic conditions by freeze-drying was proven. Nevertheless, some questions remain about the yield of grafting and the adsorption mechanism between unbound cyclodextrins and toCNF. Given the chemical similarity between toCNF and βCD, direct characterization and quantification of grafting seems impossible, as a cyclodextrin with several hydroxyl functions is likely to bind with the carboxylic acid of toCNF. Nevertheless, the presence of multiple hydroxyl functions on both toCNF and βCD indicates a strong adsorption between these two components. However, some cyclodextrins might be trapped in the ice phase during the freezing process and therefore not available for esterification reaction during the freeze-drying phase. In order to better quantify this adsorption and to be able to confirm that no material will be released from the materials produced, further studies, in particular with the means of QCM-D and

Isothermal Titration Calorimetry, will be conducted. Additionally, a method adapted from [57] will be implemented, with the use of phenolphthalein (PhP). The interactions between PhP and βCD, described by [68], could led to an indirect estimation of βCD available in the materials, and release measurements of βCD could led to an estimation of the portion of cyclodextrins linked (adsorbed/grafted) to toCNF.

The compression modulus for swollen modified toCNF cryogels ranges between 6 and 9 kPa, i.e. in the range of mechanical stiffness of muscle tissue, and the high porosities obtained (> 99% for all conditions), which are mandatory to promote a good vascularization, the diffusion of nutrients to the cells and tissue growth, make them structurally suited for tissue engineering applications. Further studies will be focused on the mechanical properties of such materials under successive stress. Nevertheless, to confirm the potential for tissue engineering applications, cytotoxicity and degradation studies need to be done in further work. However, βCD -toCNF materials could be of a great interest for other applications, such as filtration or depollution, using cyclodextrins to capture molecules of interest rather than releasing.

II.1.4. CONCLUSION

In this work, films and cryogels of β-cyclodextrin-modified TEMPO-oxidized cellulose nanofibrils were produced. Water sorption analysis and mechanical characterization were conducted on both modified and unmodified materials, under dry and wet conditions. Two unmodified nanofibril suspensions were prepared with different charge contents (750 µmol/g and 1050 µmol/g), and modification was carried out under neutral and acidic conditions. The sorption equilibrium was reached after 4h for all tested films but charge content and acidic casting pH were shown to increase the water sorption, while cyclodextrins decreased it. Density, process pH and addition of cyclodextrins had a major impact on the mechanical properties, related to the modification of the cell wall structure. Finally, covalent esterification binding between β-cyclodextrin and toCNF under acidic pH by freeze-drying was achieved and had an interesting impact on the mechanical properties in the swollen state. This study is a step towards the production of mechanically tailored cryogels containing cyclodextrin, making them promising materials for sustained delivery of active principle ingredients.

After these promising results, it is then crucial to understand the adsorption phenomena between CD and toCNF but also check if any CD derivatives could emphasize such adsorption.

CHAPTER II.2. ADSORPTION CHARACTERIZATION OF VARIOUS MODIFIED β-CYCLODEXTRINS ONTO TEMPO-OXIDIZED CELLULOSE NANOFIBRILS.

Inspired from paper: ***Michel, B.;*** *Imberty, A.; Heggset, E. B.; Syverud, K; Bras, J; Dufresne, A.. Adsorption characterization of various modified β-cyclodextrins onto TEMPO-oxidized cellulose nanofibrils membranes and cryogels. Published in Sustainable Chemistry and Pharmacy (Elsevier) in September 2021* https://doi.org/10.1016/j.scp.2021.100523.

Abstract: TEMPO-Oxidized cellulose nanofibrils (toCNF), in the form of highly entangled network such as membrane or cryogels, have proven to be of interest for various applications, including drug release or purification by pollutant adsorption. β-Cyclodextrins (β-CDs) have the ability to form inclusion complexes with a large number of hydrophobic molecules, and are considered as a promising way to bring new functionalities to these materials, by reducing drug burst release effect or improving the pollutant adsorption properties. The study of the adsorption of β-CDs onto toCNF is then crucial to design toCNF/β-CDs materials, but it is very complex due to the chemical proximity between these compounds. In this study, we develop toCNF cryogels containing various types of β-CD derivatives by physical adsorption. Different protocols for analyzing the interactions between these compounds, such as Isothermal Titration Calorimetry (ITC), Quartz-Crystal Microbalance with dissipation monitoring (QCM-d) and a Phenolphthalein-based protocol (PhP protocol) have been performed. Adsorption between β-CD and toCNF was proven at two different temperatures with ITC. QCM-d measurements allowed measuring adsorption of different β-CD derivatives onto toCNF, with higher adsorption measured for modified β-CDs, and with estimated binding capacity ranging from 13.4 to 47.6 μmol/g toCNF. PhP protocol allowed us to monitor the amount of β-CDs released in aqueous environment, highlighting a lower release for modified β-CDs onto toCNF, and the results were consistent with the estimated binding capacity. This quantification of the binding adsorption capacity of various β-CDs is a key result for optimizing the design of toCNF/β-CD materials. Figure II.13 presents the graphical abstract of this chapter.

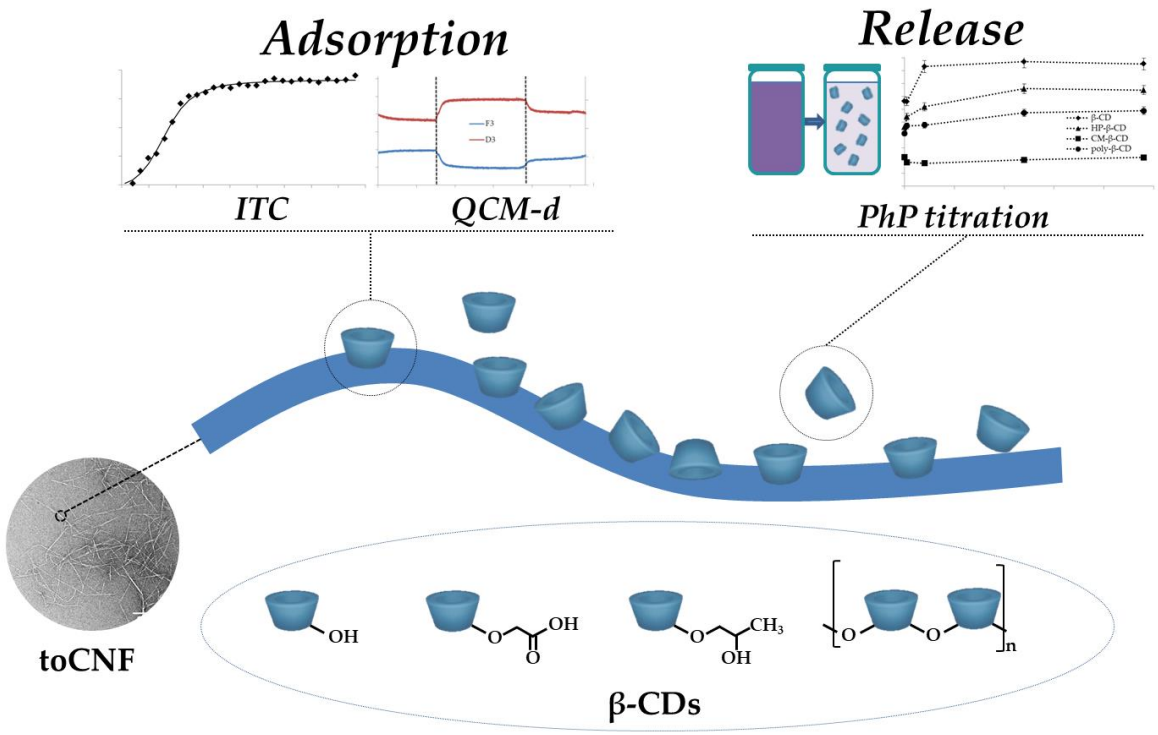

Figure II.13: Graphical abstract for Chapter II.2.

II.2.1. INTRODUCTION

Through the combination of various chemical and/or enzymatic pretreatments and mechanical treatments, cellulose nanofibrils (CNFs) can be isolated from cellulose fibers [69]. CNFs are high aspect ratio nanoparticles, formed by bundles of cellulose chains, which consist of repeating anhydroglucose units (AGU) linked by β-1-4 glycosidic bonds. Among the various pre-treatments used, is the so-called TEMPO-oxidation, proposed by Saito et al. in 2006 [70]. TEMPO-oxidation consists of regioselective oxidation of C6 primary hydroxyls of cellulose to C6 carboxylate groups in the presence of (2,2,6,6-tetramethyl-piperidin-1-yl)oxyl, also known as TEMPO. TEMPO-oxidized cellulose nanofibrils (toCNFs) exhibit high carboxylic group contents and reduced size, making them interesting for specific applications. More generally, the excellent properties of CNFs have made them a material of choice for a wide variety of applications, as shown by recent reviews [6], [9], [71]. The ability of CNFs and toCNFs to form entangled networks, their chemical surface tunability, their sorption properties and biocompatibility have made them particularly suited for drug release [10] or filtration applications, such as water purification [72]. Even if these materials have been proven to be promising for such applications, there is still huge room for improvements, more specifically reducing the burst release effect for drug release applications or improving the entrapment properties for filtration. Among the various improvement strategies envisaged, the use of cyclodextrins (CDs) seems to be one of the most promising.

CDs are macromolecules enzymatically derived from starch, composed of AGU linked by α-1-4 glycosidic bonds. The 3 most frequently encountered CDs are α-CD, β-CD and γ-CD, composed of 6, 7 and 8 AGU, respectively. These cyclic oligosaccharides exhibit cage-like properties linked to their specific conformation. Indeed, with their hydrophilic outer surface and hydrophobic central core, CDs have the property to form inclusion complexes with lipophilic compounds. Due to this feature, CDs have been widely used for numerous applications [38], such as drug excipient [34] or selective extraction of pollutants [37]. Because of its specific cavity size, β-CD can form inclusion complexes with aromatic compounds, making it suitable for a high number of molecules of interest. Despite its low solubility in water (around 18g/L), β-CD is the most produced CD [73]. β-CD solubility can be improved via chemical modification. Indeed, substitution of any of the hydrogen bond-

forming hydroxyl group results in improved aqueous solubility [74]. Additionally, the chemical modification of CDs, made possible through the presence of hydroxyl groups in the C2, C3 (secondary hydroxyls) and C6 (primary hydroxyls) positions available on each glucose unit, can also bring new functionalities to the produced CDs. Of these derivatives, the most common is 2-Hydroxypropyl β-Cyclodextrin (HP-β-CD). HP-β-CD is usually produced by the reaction of β-CD with propylene oxide in alkaline medium [75]. This derivative is highly soluble and has been proven to be non-toxic [76], making HP-β-CD one of the most produced β-CD derivatives. Another interesting derivative is Carboxymethyl-β-Cyclodextrin (CM-β-CD). This derivative is usually synthetized by reacting β-CD with chloroacetic acid under alkaline condition [77], [78]. The carboxylic groups introduced to CD offer new possibilities for grafting or adsorption of these derivatives onto substrates in order to bring the inclusion capabilities of β-CD into different application areas. These derivatives were first used for chiral analysis techniques [79], but studies on the use of these derivatives for biomedical applications are also being conducted, showing promising results [80]. There have been attempts also to cross-link cyclodextrins, to obtain a polymer of β-CDs. Different protocols exist, using various cross-linkers, such as epichlorohydrin, resulting in insoluble polymers [39], or poly-carboxylic acids, resulting in water-soluble polymers [81]. Thus, the functionalization of materials with native or modified cyclodextrins can be considered in order to combine the original properties of the materials with the complexing properties of cyclodextrins.

If the combination of cellulose-derivatives and cyclodextrins has raised some interest, as shown by a recent review from Cova et al. [82], the combination of β-CDs with nanocellulose is reported in only few recent studies [1], [30], [49]–[53], [55]–[57], [83], [84]. One possible strategy is the use of a cross-linker between nanocellulose and cyclodextrins .Ruiz-Palomero et al. [51] reported the functionalization of toCNF with CM-β-CD, via *N*-ethyl-*N*′-(3-(dimethylamino)propyl)carbodiimide/*N*-hydroxysuccinimide (EDC/NHS) activation and used a diamine as cross-linker, for the adsorption of danofloxacin, an antibiotic contained in milk. Yuan et al. [50] used citric acid as a cross linker to graft βCD and γ-CD on regenerated cellulose fibers for adsorption of toluene. Castro et al. [57] used different carboxylic acids as cross-linker between toCNF and β-CD and reported better encapsulation of carvacrol for modified materials. Benefits of this strategy are the potential

detection of the cross-linking agent, allowing an estimation of the grafing yield. However, the potential trace of cross-linking agent can be an obstacle for biomedical applications. Another strategy would be the grafting via thermal treatment. In 2016, Saini et al. [49] grafted β-CD on the carboxyls groups of toCNF via esterification by thermal treatment under vacuum, and reported a reduction in burst effect for the release of carvacrol and an improvement in antimicrobial activity. The benefits of this strategy are the potential proof of esterification available with spectroscopic measurements. Additionally, the absence of cross-linking agent could be beneficial for medical applications. Finally, a last strategy is the adsorption of cyclodextrins on nanocellulose with no further chemical reaction. Lavoine et al. [53] reported the design of a controlled release system forf chlorhexidine gluconate by coating onto a paper substrate with a mixture of β-CD and micro-fibrillated cellulose. However, they pointed out the difficulty of assessing the adsorption and its characterization.

The main difficulty with the combination of β-CDs and nanocellulose is the chemical similarity of these two components. Both cellulose and cyclodextrins have the same repeating units, linked by β-1, 4 glycosidic bonds in the case of cellulose and α-1, 4 glycosidic bonds in the case of β-CD. Different experimental methods can be considered to study the adsorption between cyclodextrins and nanocellulose. Quartz Cristal Microbalance with dissipation monitoring (QCM-d) has been used to assess the functionalization of cellulose nanofibrils with β-CD and polyβ-CD by Gomez-Maldonado et al. [84], but they highlighted the challenges of assessing the amount of cyclodextrins attached to CNF. A protocol to quantify the amount of cyclodextrins grafted onto toCNFs has been proposed by de Castro et al. [55], based on the use of phenolphthalein. A recent work studied the thermodynamics of absorption of molecules on nanocellulose by Isothermal Titration Calorimetry (ITC) [85]–[87], which make it conceivable to measure the absorption of cyclodextrins by this method.

The aim of this study is to characterize the adsorption between toCNF and cyclodextrins by using different protocols. The implementation of three different protocols, namely ITC, QCM-d and PhP, will allow the characterization of the possible adsorption phenomena in a complete way and to obtain a quantification of the adsorbed CDs. The use of different cyclodextrins (β-CD, HP-β-CD, CM-β-CD and polyβ-CD) will allow us to verify whether the chemical makeup of the modified cyclodextrins has an impact on the quantity of

adsorbed cyclodextrins. Finally, the combination of the three protocols for the different cyclodextrins will help us to identify the best way to design materials for controlled release applications.

II.2.2. MATERIALS AND METHODS

II.2.2.1. MATERIALS

Aqueous toCNF suspension was purchased from the University of Maine (Lot # 2019-FPL-CNF-123). ToCNF were extracted from TEMPO-pretreated wood pulp and was received as a 1%wt suspension in water at neutral pH. β-Cyclodextrin (β-CD, M = 1134.98 g/mol), 2-Hydroxypropyl-β-Cyclodextrin (HP-β-CD, DS = 3, M = 1380 g/mol) and a β-CD polymer (polyβ-CD, M ≈ 1190 g/mol) were purchased from Sigma-Aldrich. Carboxymethyl- β-Cyclodextrin Sodium Salt (CM- β-CD, DS = 3.5, M = 1415 g/mol) was purchased from CycloLab. The degree of substitution of the different cyclodextrins is given for one cyclodextrin molecule. Other chemicals were of laboratory grade and purchased from Sigma-Aldrich.

II.2.2.2. METHODS

II.2.2.2.1. CONDUCTOMETRIC TITRATION

Conductometric titration was carried out to measure the total amount of carboxyl groups in neat toCNF suspension. 0.2g of dry content of toCNF was dispersed in 200mL of distilled water. The pH was then adjusted to approximately 2.5 by adding 0.1M HCl. Then, the suspension was titrated with 0.05M NaOH by adding 0.1 mL every 30s until the pH was up to 11. The total carboxylate content was calculated on the basis of NaOH volume with equation II.3.

$$Charge\ rate = \frac{C_{NaOH} \times V_{eq}}{m} \quad \text{(Eq. II.3)}$$

Where C_{NaOH} is the concentration of the NaOH solution, V_{eq} the volume of NaOH corresponding to the volume consumed in the second intersection point for weak acids, and m is the toCNF dry content. This measurement was done in triplicate.

II.2.2.2.2.CRYOGEL PROCESSING

Material processing used in the study is similar to the one reported in a previous study [1]. Suspensions at 0.8 %wt toCNF were prepared in a 50 mL volume of distilled water (0.4 g of dry matter). The suspensions were dispersed for 2 min at 7000 rpm with an UltraTurrax at room temperature. Cyclodextrins (0.04 g) were added and the suspensions were magnetically stirred for 1h and placed in an ultra-sonic bath for 3 min. The suspensions

were poured into a 24-well plate (3mL per well) and put in a freezer at -20°C for 24h before freeze-drying for 48 h at 0.04 mbar (ALPHA 2-4 LDplus, Christ ®). The resulting cryogels were stored in closed well-plates under controlled conditions (23°C with 50%RH).

II.2.2.2.3. Isothermal Titration Calorimetry

Isothermal Titration Calorimetry experiments were performed with a VP-ITC (Microcal Inc.). A sample cell with a volume of 1.8 mL was filled with aqueous toCNF suspensions (concentration 2 mg/mL in MilliQ water). ITC experiments were carried out at 25°C and 35°C by injecting 10µL of aqueous β-CD (and derivatives) solution (1 mM in MQ water) from a 280 µL injection syringe into the sample cell, which was stirred at 307 rpm to ensure optimal mixing efficiency. To determine the heat of dilution of β-CD, blank titrations were made by injecting the β-CD solution into the cell filled with MQ water. The heat enthalpy curve of the dilutions was then subtracted from the interaction curves between toCNF and β-CD. Data were fitted with one site model of interaction with MicroCal PEAQ-ITC Analyzer Software, according to standard procedures. Fitted data yielded the stoichiometry (N), the dissociation constant (K_D), and the binding enthalpy (ΔH). Two independent titrations were performed for each ligand tested.

II.2.2.2.4. Quartz Cristal Microbalance with dissipation

The principle of QCM-d was first described by Rodahl et al. [88]. It is based on the changes in frequency of a piezoelectric sensor. The sensor has a base resonance of 5MHz and its respective overtones. These frequencies are monitored as the sensor is in contact with a material flow. When the mass of the sensor changes, i.e. molecules are adsorbed on its surface, the frequency changes and the shift in frequency is linked to the mass of material adsorbed. This mass can be calculated according to the Sauerbrey equation (Eq. II.4):

$$\Delta m = -C\frac{\Delta f}{n} \qquad \text{(Eq. II.4)}$$

Where C is a constant related to the density and thickness of the quartz crystals (C = 17.7 ng/cm²), Δf is the shift in frequency and n is the overtone number. It is worth noting that this model is valid if the created films are rigid, uniform and if the mass is small compared to the mass of the crystal. Other models have been developed [89] but for our systems we will use Sauerbrey's model.

In situ formation of toCNF surfaces on gold sensors and the adsorption of CDs were studied with a QSense Analyzer from Biolin Scientific. QCM-d sensors were cleaned by dipping them 30 min in a Piranha bath (1:3 H_2O_2 / 2/3 H_2SO_4). After cleaning, the sensors were rinsed by successive immersions in distilled water and dried with nitrogen. Sensors were then spin-coated with polyethyleneimine (PEI), the anchoring polymer. After spin coating, the sensors were placed in the QCM-d apparatus and stabilized under a 100 µL/min distilled water flow, for a minimum of 10 min for stabilization before toCNF flow (adsorption step), followed by a rinsing step with distilled water. toCNFs and CD solutions were prepared at 0.1wt% in distilled water and flowed at a rate of 100 µL/min. A minimum of 10 min of stabilization time was done after each step (rinsing step, adsorption step). Calculations were made using the third overtone. The good coverage of the sensor with toCNF (first step) has been checked by AFM. At least duplicate were performed.

II.2.2.2.5.PHENOLPHTHALEIN PROTOCOL

Phenolphthalein is a phenolate ion which is colored purple in alkaline solution but loses its color when forming an inclusion complex with β-CD [90]. The decrease in absorbance when increasing the β-CD content has been proved to follow an exponentially decreasing curve [91]. A calibration curve of the concentration of β-CDs according to the absorbance of a PhP solution with known concentration can therefore be built by UV spectrophotometry by plotting the logarithmic concentration of β-CD against the logarithmic absorbance value at 554 nm.

II.2.2.2.5.1 CALIBRATION CURVES

A working solution of 375 µM PhP in EtOH, a 28 mM Na_2CO_3 solution in distilled water, a 15 mM CDs stock solution in distilled water, and a pH 12.5 buffer were prepared. The calibration curves were built by preparing solutions composed of 1 mL PhP: 1 mL Na2CO3: x mL CDs: 8-x mL distilled: 50 µL pH 12.5 buffer, with x varying between 2.5 mL and 50 µL. The absorbance was measured at 554 nm with a UV-vis spectrophotometer (SHIMADZU, Japan). Each calibration curve was done in triplicate.

II.2.2.2.5.2. DETERMINATION OF THE CONCENTRATION OF CYCLODEXTRINS RELEASED

0.02g of samples was immersed in 5 mL of distilled water for various durations. 3 mL of releasing solutions was retrieved and mixed with 50 µL PhP: 50 µL Na2CO3: 1 mL distilled

water and 50 µL buffer pH 12.5. The absorbance of the solutions was measured at 554 nm, and the concentration of cyclodextrins was calculated according to the calibration curves.

II.2.3. RESULTS AND DISCUSSION

For ITC experiments, an estimated molar mass for toCNF is needed. Since the molar mass of regular AGU ($C_6H_{10}0_5$) is 162.1 mol/g, and the molar mass of oxidized AGU ($C_6H_8O_6$) is 176.1 mol/g, the molar mass of the toCNF suspension, according to the charge level, is 164.60 ± 0.03 mol/g. The molar mass of the cyclodextrins was calculated according to the degree of substitution provided by the different suppliers. For polyβ-CD, which consists of β-CD linked through epoxy linkage, the molar mass of the repeating unit was estimated considering the molar mass of β-CD and the one of the epoxide functional group. Figure II.14.A presents a schematic representation of β-CD, while figure II.14.B shows the modified cyclodextrins used in this study.

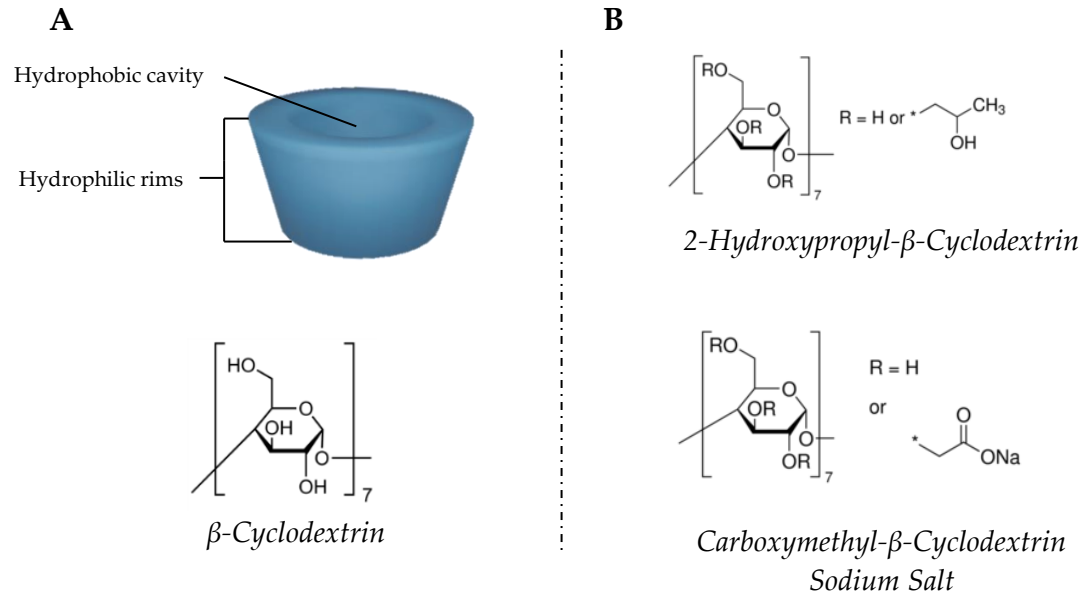

Figure II.14: β-CD and its derivatives. A) Schematic representation and formula of β-CD. B) Formula of HP-β-CD and CM-β-CD.

Both hydroxyl (-OH) and carboxylate ($-COO^-$) groups on the surface of toCNF are prone to form hydrogen bonds [92], [93]. Hence, the presence of multiple hydroxyl groups on the rims of β-CD should allow the formation of H-bonds with toCNF functional groups, thus its adsorption. The addition of hydroxyl groups to HP- β-CD and carboxylate groups to CM-β-CD is then supposed to increase the adsorption capacity of the β-CD derivatives onto toCNF by adding more reactive functional groups. Additionally, the presence of a spacer on the β-CD derivatives could also increase the accessibility of these functional groups. Given these

elements, we can formulate the hypothesis that β-CD can be adsorbed onto toCNF, and that β-CD derivatives should displays a higher adsorption capacity, with the adsorption phenomena driven by hydrogen bonding.

II.2.3.1. PHYSICO-CHEMICAL ADSORPTION

A series of ITC measurements were conducted in order to further understand the adsorption mechanism occurring between toCNF and β-CD. However, the measurements for this kind of system present some difficulties. ITC is a method developed to determine the thermodynamic parameters during the interaction between two molecules. This method is based on the measurement of the heat released during the interaction between the two molecules during a titration. First developed for molecules in solution, this method has recently been used to measure interactions between a molecule in solution and a molecule in suspension, in particular nanocellulose suspensions [85]. As toCNFs are non-soluble in water and give quite viscous suspensions at low concentrations, tests have been made to determine the ideal toCNF concentration for the suspension. They should not be too viscous to ensure a good homogeneity and mobility of cyclodextrins during the titration. The concentration used in this study was 2 mg/mL. Additionally, to be able to perform calculations according to the Langmuir adsorption isotherm, which is included in the MicroCal PEAK ITC analysis software, to calculate the binding parameters (enthalpy ΔH, entropy ΔS, binding constant K_D, stoichiometry N), the molar ratio between the two molecules of interest needs to be known. Since no specific interactions should occur, the hypothesis that was chosen is to consider that the adsorption of cyclodextrins on toCNFs is mainly linked to the presence of hydroxyl groups on the C2, C3 and C6 carbons of the AGU units, as well as on the carboxylic functions present at C6 on oxidized AGU unit. Hence the estimated molar mass of toCNF taking into account its charge level was used for the calculations. The concentration of 2 mg/mL used will then correspond to a molar concentration of 12.1 mM. Finally, since the interactions between CDs and toCNF are non-specific interactions, ΔH can be too weak to be measured. The concentrations of β-CD and toCNF need to be adjusted in order to be able to obtain a measurement. The use of β-CD at 1mM and toCNF at 2 mg/mL (12.1 mM) were found to be the best compromise. Figure II.15 shows typical titration data of β-CD to toCNF. The thermogram is represented at the top, where each peak corresponds to one injection of the β-CD solution. Integration of this curve and subtraction of the dilution enthalpy obtained

after the blank experiments lead to the titration represented in the bottom curve, with the fit calculated using the analysis software. Additionally, the binding capacity was calculated by dividing the stoichiometry N by the molar mass of toCNF. The results of the analysis of the binding isotherms are summarized in Table II.7.

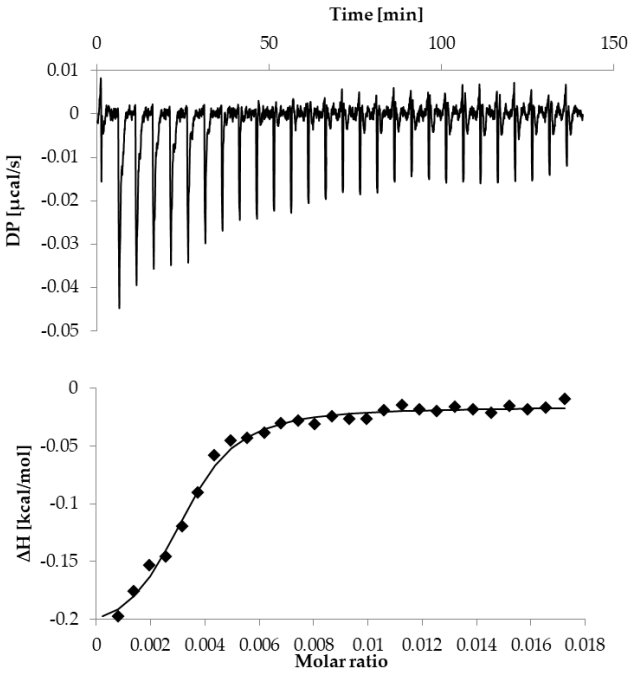

Figure II.15: Raw thermogram (at the top) and enthalpic curves (at the bottom) of an ITC titration for toCNF suspension (2 mg/mL) by a solution of β-CD (1 mM) at 25°C.

Table II.7 : Calculated thermodynamic parameters from ITC measurements

Temperature	N	Binding capacity [µmol/g]	Calculated K_D [M]	ΔH [kcal/mol]
25°C	3.2e-3 ± 9.2e-5	19.4 ± 0.4	4.58e-6 ± 0.85e-6	-0.204±0.01
35°C	3.1e-3 ± 8.9e-4	18.8 ± 0.6	17.1e-6 ± 1.2e-6	-0.161±0.02

The weak values of enthalpy observed, as well as the dissociation constant in the micromolar range, indicate that non-specific interactions occur between β-CD and toCNF. The enthalpy is weaker at 35°C than at 25°C, and the calculated K_D value is slightly higher at 35°C than at 25°C, with value of 17.1e-6 M and 4.58e-6 M, respectively. Since the physical adsorption decreases with temperature, this is consistent with the hypothesis that cyclodextrins are physically adsorbed on the surface of the fibrils. The stoichiometry is similar between the two tested temperatures, and indicates that approximately 300 toCNF anhydroglucose

subunits (AGU) are needed for binding one cyclodextrin. To the best of our knowledge, this is the first detailed report of ITC measurement between CNF and cyclodextrins; hence there is no literature to compare these values with existing data. However, the estimated binding capacity, 19.4 μmol/g at 25°C and 18.8 μmol/g at 35°C, can be compared to the binding capacity of some drugs onto CNF materials reported by Kolakovic et al. [94]. Our values are significantly higher than those reported in this study (a few μmol/g depending on the drug compared to about 20μmol/g for our system).The estimated value for the binding capacity needs to be considered with cautions. Indeed, these calculations were made using Langmuir isotherm. This isotherm is based on three assumptions: i) no multilayer adsorption, ii) identical binding sites and homogeneous surfaces and iii) no interaction between adsorbed molecules. The toCNF/β-CDs system studied here does not fully respect these assumptions, since potential interaction can occur between β-CDs or between toCNF by hydrogen bonding, and that we might not have identical binding sites. However, as explained by Lombardo et al. [85], this model has been the most widely used in the literature for adsorption studies on nanocellulose surface, and has been shown to fit quite well the experimental data, while other, more complicated models, have shown other limitations. Thus, this can be considered as a good approach to obtain an order of magnitude for the binding capacity of β-CDs on toCNF. This measurement leads to the conclusion that β-CDs do adsorb onto toCNF under the tested conditions, and that the strength of adsorption is relatively low and mainly driven by electrostatic forces. Given the charges present in the toCNF suspension, it would be interesting to perform these measurements at acidic pH. However, at the concentrations tested, acidic pH greatly increases the viscosity of the suspension, making the measurement impossible. Nevertheless, this first adsorption measurement between β-CDs and toCNF is a great step towards a better characterization of this system using an innovative tool for cellulose nanofibrils suspension.

II.2.3.2. Influence of type of β-CD derivative in adsorption onto to-CNF

To test the capacity of toCNF in adsorbing the various CDs, surfaces were generated in situ on the QCM-d by flowing the substrate and once stabilized, flowing the CDs until stabilization. Gold sensors were cleaned and activated with a piranha bath, followed by a spin-coating of PEI as anchoring polymer on which the toCNF were then adsorbed. The sensograms were split to facilitate discussion, with the first part being the surface generation,

presented in Figure II.16, and the second part being the adsorption of the various β-CDs, presented in Figure II.18. Only the third overtone is presented here.

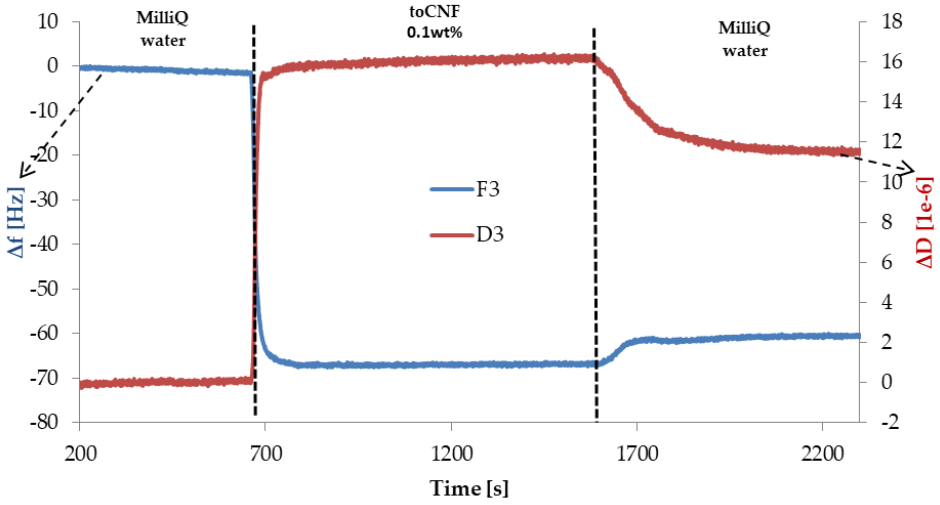

Figure II.16: QCM-d sensograms of the in-situ surface generation from toCNF

The coverage of the sensor with toCNFs by the in-situ preparation method was checked with AFM, as presented in Figure II.17.

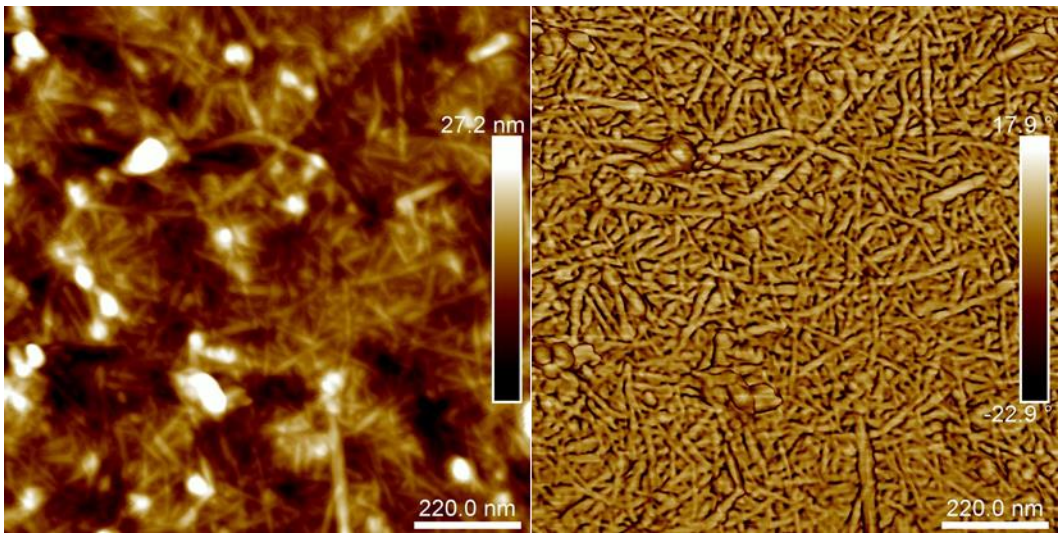

Figure II.17: AFM images of toCNF mat on gold sensor via in-situ preparation method. Left: Topographical image. Right: Phase image

A toCNF mat is clearly visible on the AFM images, validating the preparation via the in-situ method. For all surfaces generated in situ, the frequency change during toCNF flow was observed to be between -50Hz and -65Hz, and a dissipation shift ranging from 12 to 18 ppm, showing good consistency in the approach. It can also be observed that during the rinsing

step following the adsorption of toCNF, there was a diminution in the frequency shift of few Hz, as well as a decrease in the dissipation shift, which is linked to the loss of some toCNF materials that were not strongly adsorbed on PEI. A double flow protocol, i.e. flowing a second time the toCNF suspension after the rinsing phase, has been tested but did not show any beneficial impact or improvement in the quantity of toCNF adsorbed. The assumption that the sensor is homogeneously covered by toCNF has been checked by AFM. The method presented here has already been used in the literature, the first rinsing phase allows to evacuate the toCNF materials not bound to PEI, and the values of frequency and dissipation shift for the surface functionalization are consistent with those reported in the literature [84], [95]. The advantages of this method compared with an ex-situ preparation by spin coating is that it enables the calculation of the adsorbed mass on the sensors using the Sauerbrey equation, thus calculation of the binding capacity of the adsorbate, in this case CDs. The frequency shift used for the calculations is the frequency shift after the rinsing step.

Sensograms corresponding to the adsorption of CDs are presented in Figure II.18. The frequency shift and dissipation shift after the rinsing step are displayed in Table II.8, along with the calculated adsorbed mass of CDs and an estimated binging capacity, obtained by dividing the adsorbed mass by the molar mass of the corresponding cyclodextrin.

Table II.8: Frequency shift (Δf), dissipation shift (ΔD), adsorbed mass and estimated binding capacity for the adsorption of various β-CDs on toCNF surfaces.

CDs	Δf after rinsing [Hz]	ΔD after rinsing [ppm]	Adsorbed mass [mg/g_{toCNF}]	Estimated binding capacity [μmol/g_{toCNF}]
β-CD	-0.7	0.6	15.2	13.4
HP-β-CD	-1.7	2.48	42.4	30.7
CM-β-CD	-4.05	1.35	67.3	47.6
Polyβ-CD	-1.3	1.05	25	21.0

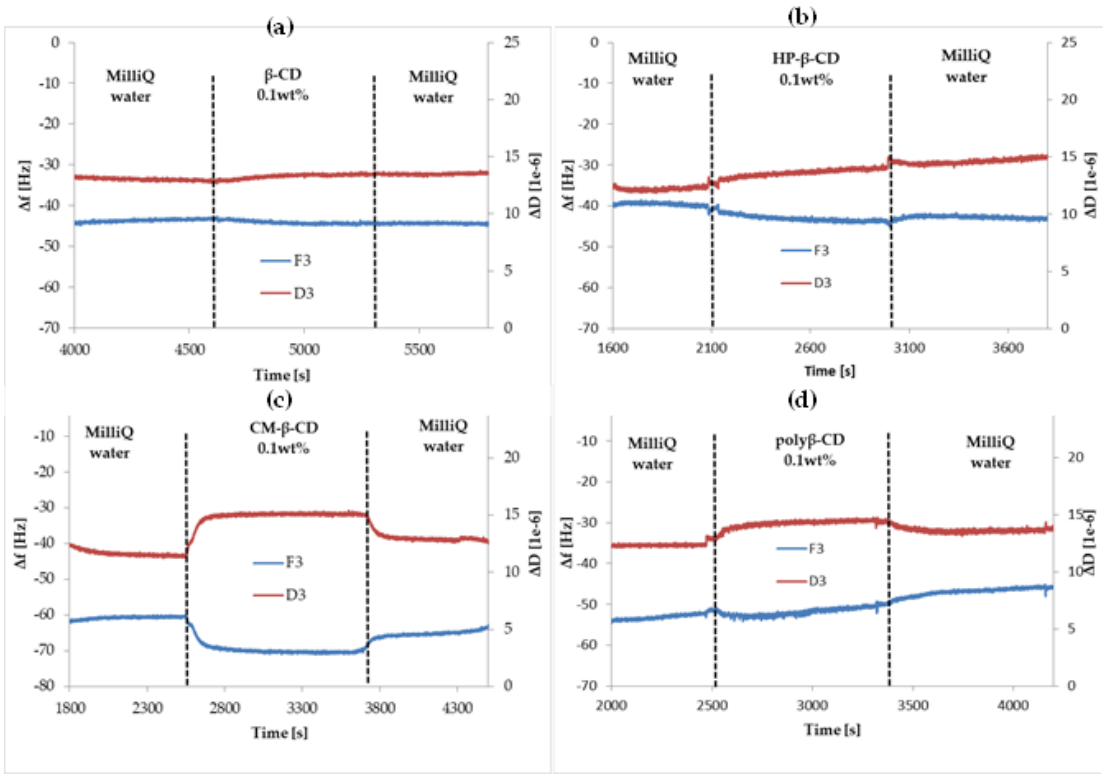

Figure II.18: QCM-d sensograms for the adsorption of (a) β-CD, (b) HP-β-CD, (c) CM-β-CD and (d) polyβ-CD on toCNF surfaces

For the adsorption of β-CDs on the toCNF surface (Figure II.18.a), the frequency shift amounted to only -0.7Hz, which corresponds to 15.2 mg/g_{toCNF} and can be regarded too low to consider that an adsorption phenomenon occurred. However, a dissipation shift higher than 0.5 ppm indicates that molecular adsorption occurred even if it is a low amount. The estimated binding capacity of 13.4 µmol/ g_{toCNF} for β-CD is of the order of magnitude of the one estimated from ITC experiments. This proves that adsorption, although weak, is occurring between β-CD and toCNF under the tested conditions. The polyβ-CD displayed slightly higher adsorption, with an adsorbed mass of 25 mg/$g_{toCNF,}$ a dissipation shift of 1.05 ppm and an estimated binding capacity of 22.0 µmol/ g_{toCNF}. The difference between β-CD and polyβ-CD can be explained by the polymerized form of polyβ-CD. Indeed, by adsorbing cyclodextrin units of the polyβ-CD, the material can retain the cyclodextrin units linked to the adsorbed one. The chemical makeup of CDs seems to be an important parameter towards the adsorption phenomena occurring between CDs and toCNF, as displayed by the estimated binding capacity for HP-β-CD and CM-β-CD, with 30.7 µmol/ g_{toCNF} and 47.6 µmol/ $g_{toCNF,}$ respectively. The presence of added chemical functions for these β-CDs derivatives increases the possibility of forming H-bonds with toCNF, hence increasing the

adsorption. It is worth noting that for CM-β-CD, the rinsing step has more impact on the frequency shift, meaning that the flow of water removes a higher proportion of adsorbed CM-β-CDs than for other CDs, which can be due to some repulsion between the carboxylate functions of both CM-β-CD and toCNF. However, these measurements show that β-CDs are adsorbed onto toCNF and that the modified β-CDs displayed much higher adsorption capacity, meaning that the adsorption phenomena are at least partially driven by chemical interactions.

II.2.3.3. CYCLODEXTRIN RELEASE FROM NANOCELLULOSE STRUCTURE

It is difficult to estimate the quantity of cyclodextrins still present in cryogels after contact or immersion in the liquid medium. Hence, it was decided to use a phenolphthalein-based method, previously reported by Basappa et al. [91] and adapted by De Castro et al. [55]. Phenolphthalein is a phenolate ion which is purple in alkaline conditions and loses its color when included inside a β-CD cavity. The absorbance intensity at 554 nm for a PhP solution depends on the alkalinity of the medium, hence the mixing of PhP with a Na_2CO_3 solution of controlled concentration to ensure consistency between the measurements [45]. Calibration curves were built by measuring the absorbance at 554 nm for PhP/Na2CO3 solutions with various amounts of CDs. It appeared that linear zones were obtained by plotting

$$Log(Abs\ 554\ nm) = A \times Log([CD]) + B$$

With A being the slope and B the intercept. For each individual β-CD, the calibration curves were performed in triplicate. Figure II.19 presents for each β-CD the mean calibration curve obtained by averaging the values obtained for each triplicate. Standard deviations are displayed but too low to be visible. Table II.9 presents the data obtained for the linear ranges.

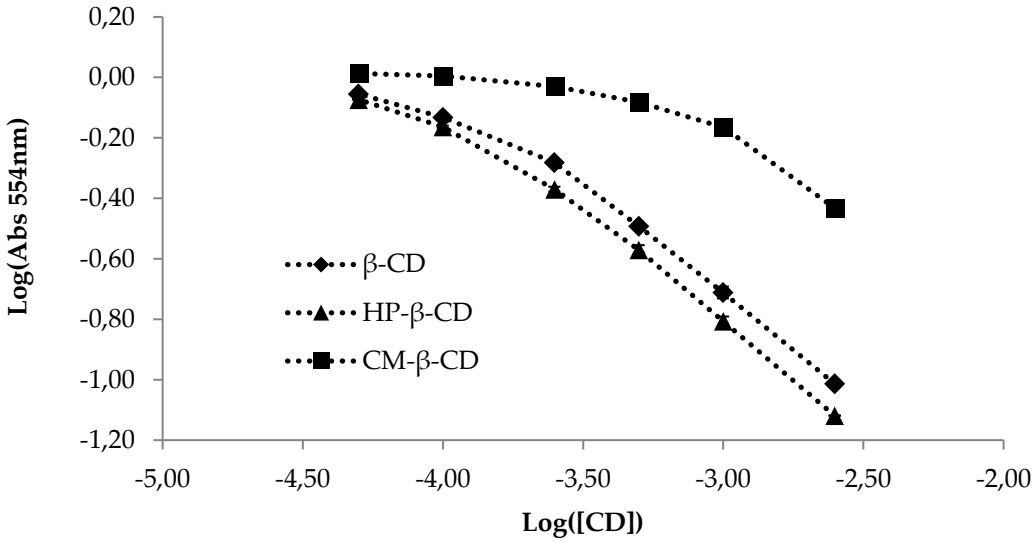

Figure II.19: Calibration curves for the various CDs with PhP. Standard deviations are displayed but too low to be visible.

Table II.9: Data obtained from the calibration plots for the various CDs estimated by the PhP protocol. Slope and intercept values are for the linear portion of the curve.

CDs	Linear range [mM]	Slope	Intercept	Mean SD	Correlation coefficient
β-CD	0.1-2.5	-0.643	-2.650	0.008	0.9827
HP-β-CD	0.1-2.5	-0.690	-2.884	0.002	0.9917
CM-β-CD	/	/	/	0.009	/

It can be observed that the calibration curves obtained for β-CD and HP-β-CD show a great similarity, with a linear range for β-CDs concentration between 0.1 mM and 2.5 mM and a good correlation coefficient. The low standard deviation obtained also proves a good consistency of the method. These calibrations curves can therefore be used for the calculation of the concentrations of β-CD and HP-β-CD in a solution mixed with the working solution of PhP. For CM-β-CD, in the concentration range used, no linear zone can be observed, therefore no slope and intercept can be calculated. This can be explained by the presence of carboxylate ions at basic pH. This leads to a modification of the inclusion properties, which was not observed for β-CD and HP-β-CD. However, the low standard deviation obtained proves a good consistency, meaning that this curve can be used to approximate the concentration of cyclodextrins in the solutions mixed with the working solution of PhP by framing the values obtained with reference values.

These data were used to calculate the amount of β-CD released from cryogels upon immersion for various release times in distilled water. The release volume was chosen based on the mass of CD in the cryogels so that the CD concentrations were in the linear range of the calibration curves. The release medium was then sampled and mixed with the PhP working solution and the absorbance was measured at 554 nm. The concentrations of β-CD and HP-β-CD were calculated using the data from their respective calibration curves. The poly-β-CD concentration was calculated using the calibration data for β-CD. The CM-β-CD concentration was approximated using the reference values of the calibration curve. The percentage of CD released was calculated from the initial mass of CD in the cryogel, the volume of release medium, the volume of the sampled released medium, the volume of the analyzed solution and the measured or approximated concentration. The results are displayed in Figure II.20.

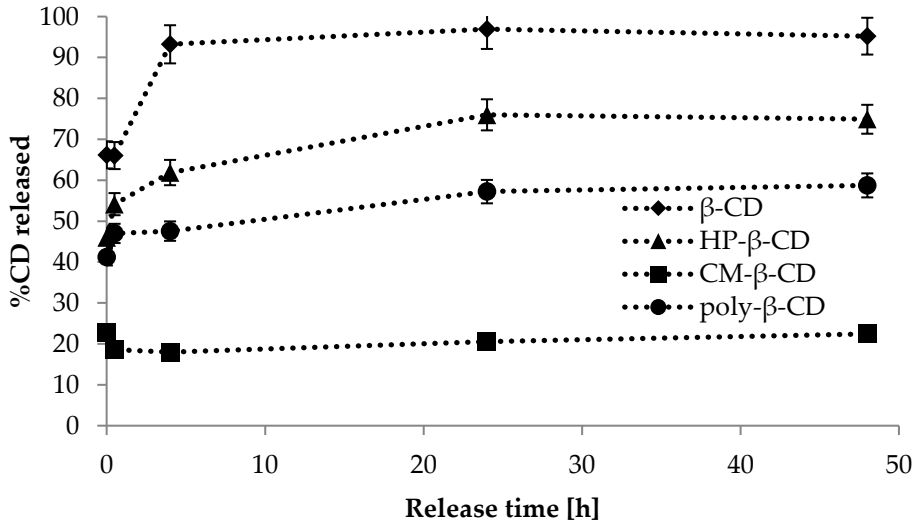

Figure II.20: Release profile for β-CDs from toCNF cryogels

β-CD is the most released CDs, with around 65% of the total amount released after 1 min and up to 95% after 24h. The increase in the amount of cyclodextrins release with time can be explained by the swelling of the cryogels. This increase with the release time is observed for HP-β-CD, with around 45% of CD released after 1 min up to 75% after 24h, and for polyβ-CD, with around 40% after 1 min up to 58% after 24h. It is worth noting that the values of %CD released do not vary much between 24h and 48h of release time, meaning that a plateau is reached. For CM-β-CD, the approximated amount of CD released remains roughly

constant with the release time, and it is estimated around 20%. These results indicate that the adsorption is much stronger between modified cyclodextrins and toCNF than between raw β-CD and toCNF, confirming the observation made with QCM-d. Since the quantity of CDs introduced in the cryogels is known, as well as their respective molar mass, it is possible to calculate the amount of CD in μmol/g for each type of CD. By comparing this quantity with the estimated binding capacity determined by QCM-d, an estimation of the percentage of cyclodextrin released can also be calculated. These data are presented in Table II.10.

Table II.10: Estimation of β-CDs release from toCNF cryogels

CDs	Amount of CD in the sample [μmol/g_{toCNF}]	Estimated binding capacity by QCM-d [μmol/g_{toCNF}]	Estimated %CD released (QCM-d)
β-CD	88.1	13.4	84.8
HP-β-CD	72.5	30.7	57.6
CM-β-CD	70.7	47.6	32.7
Polyβ-CD	84.0	22.0	73.8

The comparison between these calculations and the results obtained with the PhP protocol are presented in Figure II.21. These results need to be considered with cautions. Indeed, the values of binding capacity determined by QCM-d are calculated according to a mass of CD adsorbed on a thin film, while the PhP protocol was used on cryogels. Additionally, the adsorbed mass was calculated in QCM-d with the Sauerbrey equation and considering low frequency drop, which can induce some uncertainties in the calculations. Considering this, we can observe that the estimated percentage of CD released is quite close to the measured one, confirming the very good correlation between each characterization and the adsorption between toCNF and CDs, with stronger adsorption for modified CDs, especially for CM-β-CD.

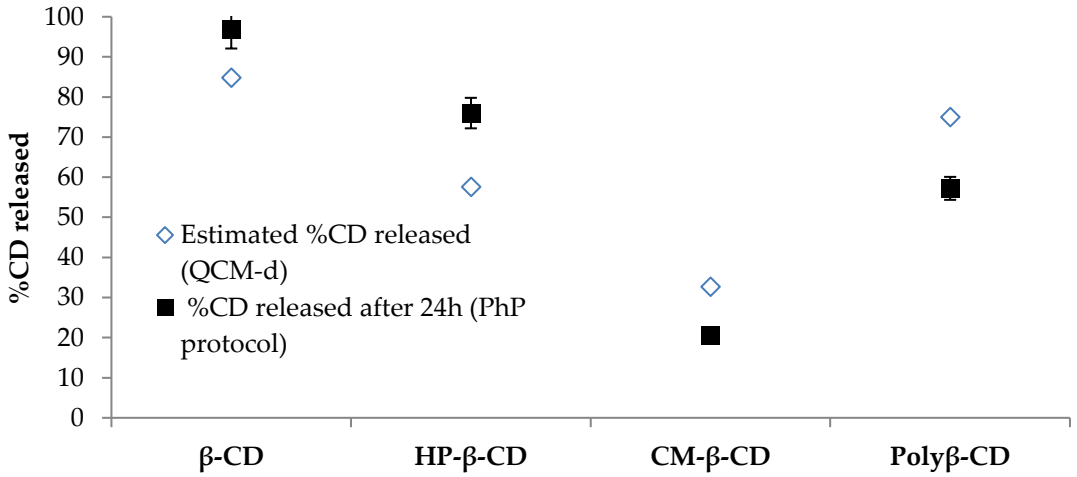

Figure II.21: Comparison between estimated and measured β-CD release from toCNF cryogels

For polyβ-CD, the increased adsorption in comparison with β-CD can be explained by the potential entanglement of the long chains with the nanofibers. For modified β-CDs, the difference in adsorption is supposed to be chemically driven, with difference in the accessibility of hydroxyl groups, which is higher for modified CDs due to the added functional groups. In order to go further in the understanding of the observed phenomena, it would be relevant to set up measurements allowing to compare this accessibility of the hydroxyl groups between the CDs, but also to evaluate the strength of the resulting hydrogen bonds.

II.2.4. CONCLUSION

In this study, we have investigated the adsorption of various β-CDs onto toCNF materials via different experimental means. The adsorption of β-CD onto toCNFs in suspension was investigated via Isothermal Titration Calorimetry, which has, to the best of our knowledge, not been reported previously. The affinity constant measured between β-CD and toCNFs at neutral pH led to an estimated binding capacity around 19 $\mu mol/g_{toCNF}$. This order of magnitude was confirmed by QCM-d experiments. Additionally, different types of CD derivatives, namely HP-β-CD and CM-β-CD, had binding capacities higher than natural β-CD, with values up to 47.6 $\mu mol/g_{toCNF}$ for CM-β-CD. This confirmed that the adsorption phenomenon was driven by H-bonding and that the introduction of hydroxyl and carboxyl groups on β-CDs as well as the presence of a spacer increased the availability of these functional groups and led to an important increase in the number of CD molecules adsorbed on toCNFs. This observation was confirmed by measuring the percentage of cyclodextrin released from toCNF/CD cryogels, assessed with a phenolphthalein based titration method. toCNF/β-CD released up to 95% of CD content after 24h, while cryogels with CM-β-CD released only around 20% of the CD content after the same period of time. These different methods contribute to a better understanding and quantification of the adsorption of β-CDs onto toCNFs, and will help to design optimized toCNF/β-CD materials with lasting functionalization without the use of any cross-linker or harmful solvent. Such materials could be beneficial for numerous applications, such as biomedical drug release system, depollution filtration or scavenger devices.

As the CD derivatives are promising when adsorption phenomena are considered, it was then obvious to check their impact onto mechanical properties and water adsorption in a final design of biomaterials using toCNF and CD derivatives

CHAPTER II.3. FINAL DESIGN AND CHARACTERIZATION OF INDUSTRIAL TOCNF/β-CYCLODEXTRIN DERIVATIVE MATERIALS

Abstract: Two types of wood-based TEMPO-oxidized cellulose nanofibrils (toCNFs), one industrially produced (I-toCNFs) and one produced in our lab (H-toCNFs) were compared to choose the most suited one for the final design of toCNF/β-CD materials. Both suspensions have similar carboxylic content (1088 ± 14 μmol/g_{toCNF} and 1048 ± 32 μmol/g_{toCNF} for I-toCNF and H-toCNF, respectively), but present notable differences in term of opacity and viscosity. A more heterogeneous dispersion with increased fiber length and presence of residual fibers was observed in the sample of H-toCNFs compared to I-toCNFs, using analyses of turbidity, nanosize fraction and TEM images. Impact on water sorption properties for films and cryogels, as well as mechanical properties, were investigated. The reduced size of I-toCNFs increases its water sorption properties in the form of cryogels, while not having a major impact on mechanical properties. Subsequently, the I-toCNF quality was chosen as the most suitable suspension to design toCNF/β-CD materials for biomedical applications, and the impact of the introduction of β-CD and β-CD derivatives to the toCNF structure was assessed, confirming the interesting results previously reported. Figure II.22 presents the graphical abstract of the study.

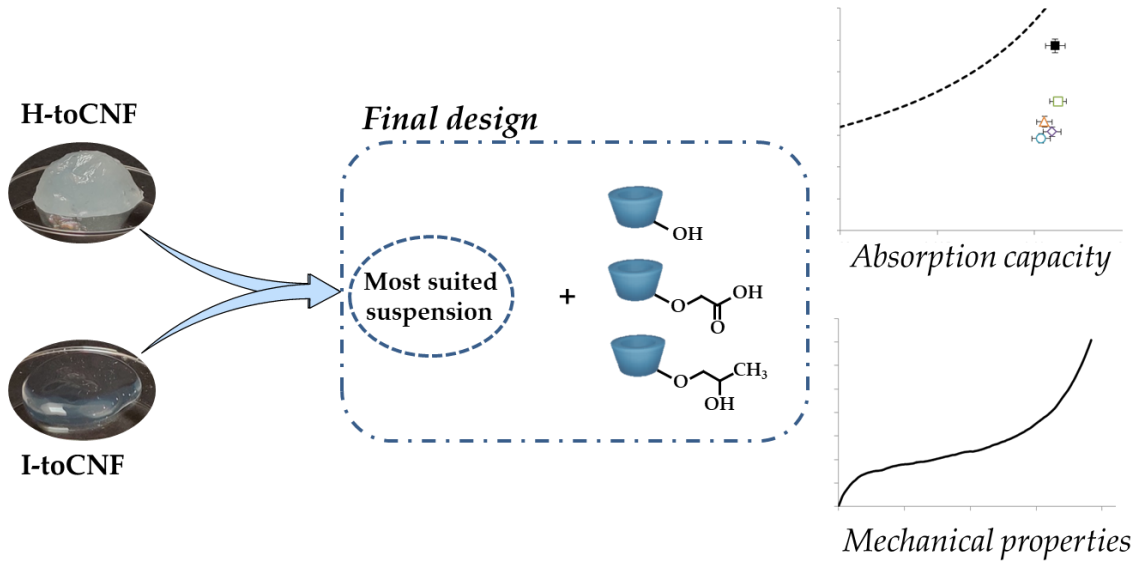

Figure II.22: Graphical abstract for Chapter II.3.

II.3.1. INTRODUCTION

Cellulose nanofibrils have received increasing interest during the last decade, with numerous possibilities in pretreatment and process. By using the same raw materials, more than 60 different types of CNFs can be produced [69], with various properties and morphologies. When considering TEMPO-oxidized CNFs (toCNFs), the degree of substitution reached after the pretreatment, as well as the post treatment for purification and the method for mechanical fibrillation strongly influences the toCNF quality. Several researchers have tried to find protocols for characterization and comparison of different CNF or toCNF qualities [97], [98]. However, this is still a challenge, and it is always necessary to control or adapt the quality of toCNFs in each research study and for each application. Furthermore, the industrialization of toCNFs is recent, and trading such material is clearly of great interest. Due to confidentiality issues, no detailed information can be provided by the supplier regarding production process, and it is therefore important to characterize the new industrial batches and compare them with the samples of laboratory grade.

Laboratory made toCNF suspensions, viz. L-toCNF and H-toCNF used in chapter II.1 [1], were produced to study the impact of the charge content on various properties such as water sorption or mechanical properties. The design of β-CD/toCNF materials in the form of films and cryogels was reported and the impact of the charge content, pH of process and introduction of β-CD to the toCNF structure were highlighted. Adsorption of β-CD and β-CD derivatives onto an industrial suspension toCNF suspension (I-toCNF), which is more suited for the experimental means used, such as ITC and QCM-d, was reported in Chapter II.2. The interest in using β-CD derivatives was highlighted with higher binding capacities than natural β-CD. The objective of this part of the study is to select the most suited suspension for the final design of toCNF/β-CD materials for biomedical applications.

Several methods were used to compare I-toCNFs and H-toCNFs. Turbidity measurements were done to evaluate the size of the nanofibrils in each suspension. This test measures the light scattered by a suspension at an angle of 90° to the incident light, which is directly related to the shape, size and refractive index of the considered suspension [97]. As such, a poorly fibrillated suspension will display high turbidity, while a homogeneous suspension of nanoscale elements will display low turbidity. The presence of residual fibers

in both suspensions was assessed by measuring the nanosized fraction by separating nanosized cellulose nanofibrils from larger entities or aggregates by centrifugal forces, with a method proposed by Naderi et al. [99]. TEM images were used to measure the dimensions of toCNFs as well as their homogeneity. The impact on water sorption and mechanical properties was investigated to allow the selection of the most suited suspension.

Very recently (chapter II.2), use of β-CD derivatives were considered very promising compared to natural β-CD, due to their higher binding capacities Previous studies have also used CD derivatives but with solvents and crosslinkers which were not biocompatible. Up to our knowledge, no previous study deals with physical adsorption of such material and it was therefore important to check the impact of these CD derivatives on mechanical properties before use in biomedical applications. Finally, the production and characterization of toCNF/β-CD derivatives using the selected toCNF suspension will be reported to propose a final material which can be used in suitable biomedical applications.

II.3.2. MATERIALS AND METHODS

II.3.2.1. MATERIALS

Two different toCNF suspensions were considered for this study, one industrially available (I-toCNF) and the other one produced in this project (H-toCNF).

Aqueous I-toCNF suspension was purchased from the University of Maine (Lot # 2019-FPL-CNF-123). I-toCNF were extracted from TEMPO-pretreated wood pulp and was received as a 1 wt% suspension in water at neutral pH.

The production of H-toCNF is thoroughly described in section II.1.2.2.1.

β-Cyclodextrin (β-CD, M = 1134.98 g/mol), 2-Hydroxypropyl-β-Cyclodextrin (HP-β-CD, DS = 3, M = 1380 g/mol) and β-CD polymer (polyβ-CD, M ≈ 1190 g/mol) were purchased from Sigma-Aldrich. Carboxymethyl- β-Cyclodextrin Sodium Salt (CM- β-CD, DS = 3.5, M = 1415 g/mol) was purchased from CycloLab. The degree of substitution of the different cyclodextrins is given for one cyclodextrin molecule. Other chemicals were of laboratory grade and purchased from Sigma-Aldrich.

II.3.2.2.METHODS

II.3.2.2.1. CHARACTERIZATION OF THE SUSPENSIONS

II.3.2.2.1.1. CONDUCTOMETRIC TITRATION

Conductometric titration was carried out to measure the total amount of carboxyl groups in the neat toCNF suspension. 0.2 g toCNF (dry content) was dispersed in 200 mL distilled water. The pH was then adjusted to approximately 2.5 by adding 0.1 M HCl. Then, the suspension was titrated with 0.05 M NaOH by adding 0.1 mL every 30 s until pH reached 11. The total carboxylate content was calculated on the basis of NaOH volume (equation II.5).

$$Charge\ rate = \frac{C_{NaOH} \times V_{eq}}{m} \quad \text{(Eq.II.5)}$$

, where C_{NaOH} is the concentration of the NaOH solution, V_{eq} the volume of NaOH corresponding to the volume consumed in the second intersection point for weak acids, and m is the toCNF dry content. This measurement was done in triplicate.

II.3.2.2.1.2. Transmission Electron Microscopy (TEM)

Transmission electron microscopy (TEM) images were performed with a JEOL JEM 2100-Plus microscope operating at 200 kV. Samples were deposited on copper grids, and uranyl acetate was used as negative staining.

At least 10 images were acquired for each sample and the most representative was used for the discussion.

Morphological properties of toCNFs (length and diameter) were measured from TEM images with ImageJ software. 10 different pictures with 10 measurement for each property were considered, and the range of results are presented in [Minimum]-[Maximum] form.

II.3.2.2.1.3. Turbidity measurement

toCNF suspensions were diluted to 0.1wt% and 1 wt% and stirred for 3 min with Ultra Turrax (IKA T-25). The turbidity of the subsequent suspensions was measured with a portable turbidimeter (Aqualytic, AL-250, wavelength 860 nm). Turbidity is measured in Nephelometric Turbidity Units (NTU). The turbidity is linked to the presence of nanoscale material in the suspensions. At least triplicate measurements on 2 suspensions were performed for the two suspensions.

II.3.2.2.1.4. Nanosized Fraction

toCNF suspensions were diluted to 0.02 wt% and centrifuged at 1000 g for 15 min to segregate larger fibers. After centrifugation, the supernatant was collected and the concentration was measured gravimetrically after 24h at 105°C. The nanosized fraction, i.e. the quantity of nanoscale particles in the suspension, was determined with Eq. II.6 :

$$Nanosized\ fraction\ \left(\frac{w}{w}\%\right) = \frac{Cfinal}{C_{initial}} \times 100 \qquad \text{(Eq.II.6)}$$

,where $C_{initial}$ and C_{final} are the mass concentration of the suspension before and after centrifugation, respectively. As reported by Desmaisons et al. [97], the nanosized fraction corresponds to individual toCNFs and aggregates, but also to larger entities that exhibit resistance to phase separation by centrifuge force.

II.3.2.2.2. Film and cryogel processing and characterization

II.3.2.2.2.1. Material processing

Films: 0.4 g of dry toCNF were weighed and diluted with water to a total volume of 50 mL. The suspension was dispersed for 2 min at 7000 rpm with an UltraTurrax. βCD (0.025 g) and 0.1M HCl (2 mL) were added to the relevant samples. The suspensions were magnetically stirred for 1h, placed in an ultra-sonic bath for 3 min, and further casted in Petri dishes (9 cm diameter) and incubated at 40°C for 18h. The resulting films were stored in closed petri dishes at room temperature.

Cryogels: Suspensions of 0.8 wt% toCNF were prepared in a 50 mL volume of distilled water (0.4 g of dry matter). The suspensions were dispersed for 2 min at 7000 rpm with an UltraTurrax. Cyclodextrins (0.04 g) were added and the suspensions were magnetically stirred for 1h and incubated in an ultra-sonic bath for 3 min. The suspensions were poured into a 24-well plate (3 mL per well; 1.5 cm height) and incubated in a freezer at -20 °C for 24 h before freeze drying for 48 h at 0.04 mbar (ALPHA 2-4 LDplus, Christ ®). The resulting cryogels were stored in closed well-plates under controlled conditions (23 °C with 50 %RH).

II.3.2.2.2.2. Water sorption

Water sorption tests on films were carried out gravimetrically in a Percival climatic chamber at 25°C and 90% RH. The samples were weighted every hour in the beginning of the experiment and at selected times thereafter. Water sorption experiments were conducted after 48h, with at least 3 replicates for each sample. The samples were put in a desiccator for 16h prior to the experiment. The water sorption was characterized by the weight change between the initial sample weight (m_0) and the weight after a certain time t (m_t), according to equation II.7:

$$Water\ sorption\ [\%] = \frac{m_t - m_0}{m_0} \times 100 \qquad \text{(Eq.II.7)}$$

Water sorption tests on cryogels were conducted gravimetrically. The cryogels were weighted and immersed in distilled water, and then removed at different times. Excess water was removed before weighting.

II.3.2.2.2.3. Absorption capacity

Absorption capacity tests on cryogels were conducted gravimetrically on triplicates. The cryogels were weighted and immersed in distilled water at room temperature, and then removed at different time intervals. Excess water was removed with absorbent paper before weighting. Water sorption was calculated using equation II.8.

$$Absorption\ capacity\ [g/g] = \frac{m_{swollen} - m_{dry}}{m_{dry}} \quad \text{(Eq.II.8)}$$

The volume of produced cryogels was measured from height and diameter measurements using a calliper without compression. The relative density of cryogels was calculated from the ratio ϱ/ ϱc , where ϱc is the density of cellulose, 1.5 g/cm^3 [62]. The porosity was calculated from equation II.9.

$$Porosity\ = \left(1 - \frac{\rho}{\rho_C}\right) \quad \text{(Eq. II.9)}$$

II.3.2.2.2.4. Scanning Electron microscopy

Scanning electron microscopy (SEM) images were performed with ESEM (Quanta 200, FEI, Japan). Cryogels were cut with a razor blade. SEM analysis were carried out on cross-sections after carbon sputter coating of 5 nm, with a tension of 10 kV and a spot size of 3.5. The working distance was set between 9.5 mm and 11.5 mm depending on the sample.
At least 10 images were acquired at different zones of each sample and the most representative was used for the discussion.

II.3.2.2.2.5. Mechanical properties

Compression tests were performed using a TA Instruments RSA 3 (New Castle, Delaware, USA) dynamic mechanical analyser fitted with a 100 N load cell. Samples prepared as cylinders were individually measured and compressed with a crosshead speed of 0.1 mm/s at room temperature. At least triplicates were performed and the average value was presented. A minimum of 6 cryogels were tested for each sample. The compression modulus was calculated in the elastic region at half the strain of the beginning of the plateau region. The stress at 70 % strain was directly read from the data. The normalized compression modulus was calculated by dividing the compression modulus by the cryogel density. The cryogel density (ϱ) was determined by dividing the mass of each cryogel by its volume. The volume of produced cryogels was measured from height and diameter measurements using a calliper. For each sample, the two extreme values were removed.

II.3.3. Results and discussion

II.3.3.1. Differences between industrial and laboratory grade toCNF suspensions

Both toCNF suspensions, despite having similar carboxylic content, with 1088 ± 14 μmol/g_{toCNF} for I-toCNF and 1048 ± 14 μmol/g_{toCNF} for H-toCNF, display completely different properties in suspension, even at the same concentration and pH, as shown in Figure II.23.A and II.23.B.

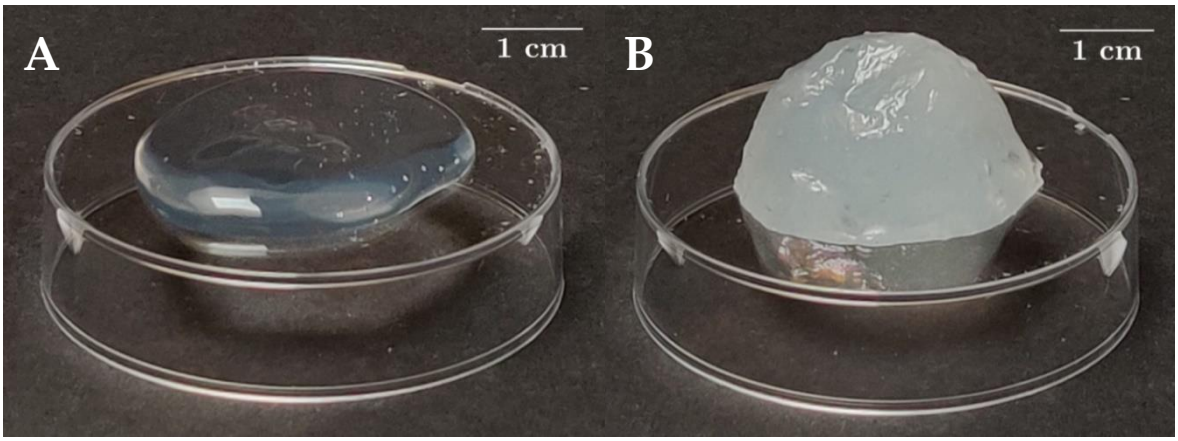

Figure II.23: Morphological aspect of toCNFs suspensions at 1 wt% and pH 7. A) I-toCNF B) H-toCNF

Notable differences in transparency and viscosity were observed, with the I-toCNF suspension being transparent and out of low viscosity, while H-toCNF is more opaque and retains a solid shape due to higher viscosity. These behaviors could be explained by the size of the nanofibrils in each suspension, but also by the presence of large residual fibers. We assume that the post-treatment of purification is slightly different between the two materials Turbidity of both suspensions was investigated, and the values obtained for 1 wt% suspensions, 25 + 7 NTU for I-toCNF and 488 ± 10 NTU for H-toCNF, indicate that the I-toCNF suspension presents smaller nanofibrils than H-toCNF. Additionally, the experiments indicate that I-toCNF is composed of 76 ± 5 % nanoscale elements, compared to 46 ± 3 % recorded for H-toCNF. To obtain a more in-depth comparison between the two suspensions, TEM images were recorded (Fig.II.24.A and Fig.II.24.B) and the diameter and length of the nanofibrils were measured, with at least 100 measurements per suspension. The distribution of lengths are presented in Figure II.24.C.

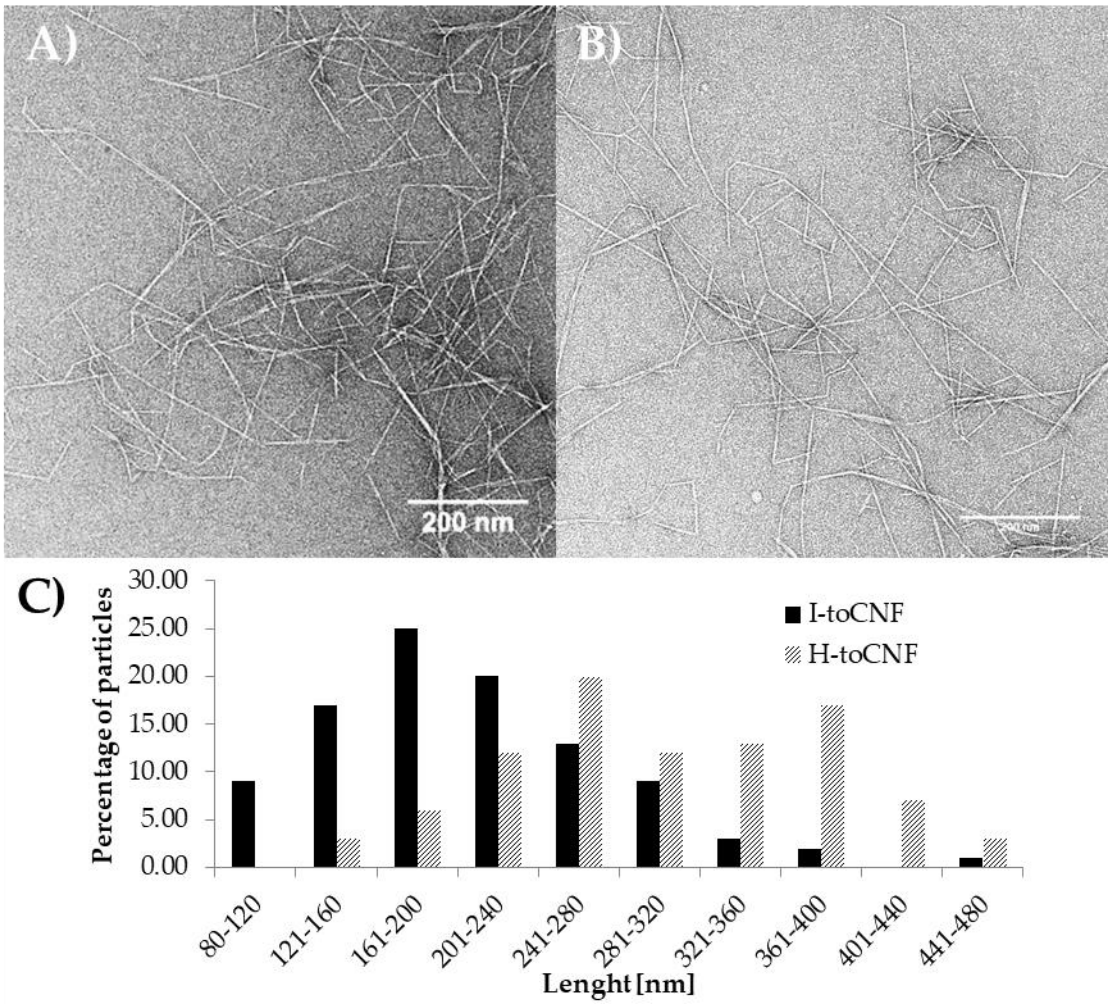

Figure II.24: Morphological aspect of individual toCNF A) TEM image for I-toCNF B) TEM image for H-toCNF C) Length distribution

While both suspensions present nanofibers of similar diameter (4.5 ± 1.1 nm and 4.3 ± 0.9 nm for I-toCNF and H-toCNF, respectively), it can be observed that the I-toCNF suspension presents smaller fibers in terms of length (average of 207 ± 75 nm) than H-toCNF (average of 317 ± 102 nm). Additionally, as displayed in Figure II.24.C, the length distribution is much more homogeneous for I-toCNF than for H-toCNF. A summary of the different measured characteristics for both suspensions is presented in Table II.11.

Table II.11: Characterization of properties. Comparison between I-toCNF and H-toCNF

Characterization	I-toCNF	H-toCNF
Carboxyl content [μmol/g_{toCNF}]	1088 ± 14	1048 ± 32
Length [nm]	207 ± 75	317 ± 102
Diameter [nm]	4.5 ± 1.1	4.3 ± 0.9
Turbidity at 0.1 wt% [NTU]	/	18 ± 5
Turbidity at 1 wt% [NTU)	25 + 7	488 ± 10
Nanosized Fraction [%]	76 ± 5	46 ± 3

Films and cryogels were processed to assess the impact of the morphological properties (nanofiber dimensions) on the properties of the produced structures. Figure II.25 presents the water sorption properties for films and cryogels produced with both suspensions.

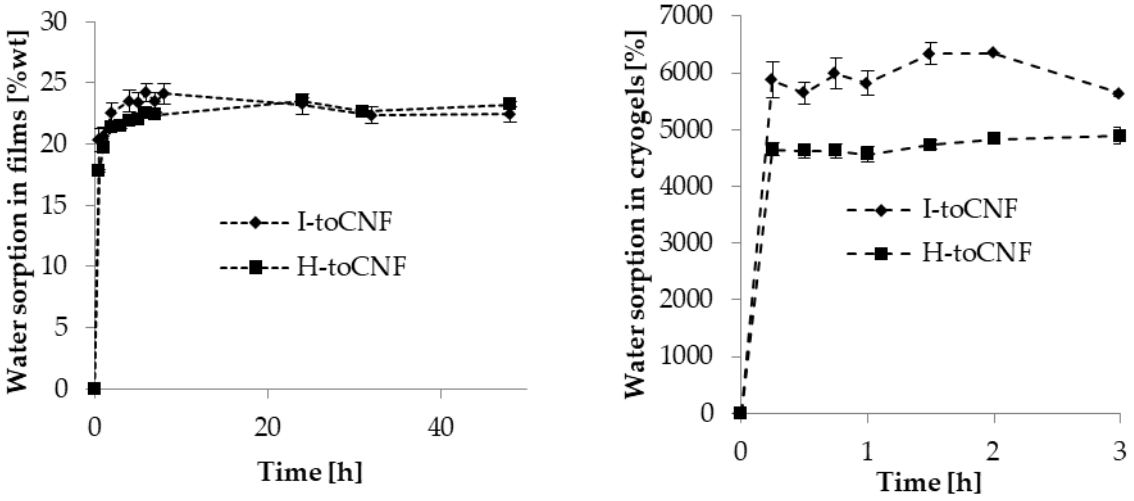

Figure II.25: Water sorption properties for A) films and B) cryogels

Water sorption properties for films are relatively similar, and sorption equilibrium were reached after 4h. After 48 h, values of sorption equilibrium were 22.4 ± 0.6 %wt and 23.2 ± 0.2 %wt for I-toCNF and H-toCNF, respectively. As shown in Chapter II.1, due to their densely packed structure, water sorption in films is mainly driven by the chemical makeup of toCNF; hence the difference in toCNF dimensions does not have an impact on these properties. The almost identical amount of charges between the two suspensions explains the proximity between the sorption equilibrium values. However, difference in toCNF dimensions should have an impact on water sorption of cryogels, since the sorption mechanism in this case mainly is driven by capillary forces linked to the porosity of the material. It can be observed in Figure II.25.B that water sorption value for I-toCNF cryogels is higher than for H-toCNF.

The heterogeneity as well as the presence of residual fibers in H-toCNF suspension cause deflects and shrinkage of some cell walls in the cryogel structure, hence reducing its water sorption properties. The mechanical properties of cryogels were assessed and the main results are presented in Table II.12.

Table II.12: Cryogel characteristics

Cryogel properties	I-toCNF	H-toCNF
Density [mg/cm^3]	13.4 ± 0.7	16.1 ± 0.6
Compression modulus [kPa]	133 ± 10	150 ± 10
Normalized compression modulus [kPa.mg^{-1}.cm^3]	9.9 ± 0.2	9.4 ± 0.8
Maximum stress at 70% deformation [kPa]	62 ± 3	65 ± 3

Moreover, both cryogels present mechanical properties with the same order of magnitude. All these results led us to consider I-toCNF as the most suitable suspension for use in the final design of toCNF/β-CD. Its smaller size and more homogeneous distribution in terms of fiber length, meaning a higher specific surface area, led to less residual fiber and higher water sorption properties while being still in line with suitable mechanical properties. In addition, the fact that this suspension is commercially available could be beneficial for any potential scale-up. Adsorption of different β-CD derivatives onto I-toCNF suspensions was reported in Chapter II.2. The results indicate that the addition of β-CDs to I-toCNF structures should have an impact on the mechanical properties of the material.

II.3.3.2. Impact of β-CD derivatives on physical properties

Various β-CD derivatives have been selected based on previous adsorption studies to to-CNF to study their influence on the physical properties of nanocellulose cryogels. The molar mass of the cyclodextrins was calculated according to the degree of substitution provided by the different suppliers. For polyβ-CD, which consists of β-CD linked through epoxy linkage, the molar mass of the repeating unit was estimated considering the molar mass of β-CD and the one of the epoxide functional group. Figure II.26 presents a schematic representation of β-CD and its derivatives.

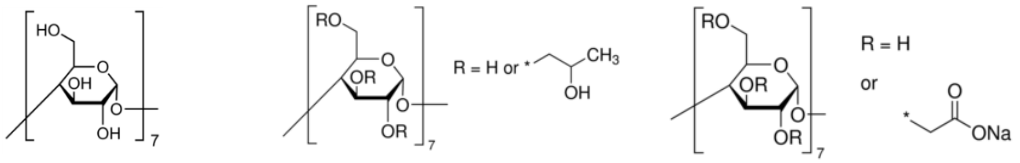

β-Cyclodextrin
(M = 1134.98 g/mol)

2-Hydroxypropyl-β-Cyclodextrin
(M = 1380 g/mol)

Carboxymethyl-β-Cyclodextrin
Sodium Salt
(M= 1415 g/mol)

Figure II.26: β-CD and its derivatives.

The porosity of the cryogels and their absorption capacity were measured at room temperature. Absorption capacity of cryogels is linked to their capillary forces and porosity and are the driving mechanisms of the absorption of liquid in the structure, in addition to the potential swelling of the fibers. Hence, a theoretical curve can be plotted, corresponding to the theoretical case where all the porosity of the material is occupied with water, calculated using equation II.10

$$Absorption\ capacity = \left(\frac{Porosity}{1-Porosity}\right) \times \frac{\rho_{water}}{\rho_{cellulose}} \quad \text{(Eq. II.10)}$$

According to Sayeb et al. [100], a result below this curve indicates that there is a collapse of the porous structure, decreasing the absorption capacity of the porous material, while the results above this curve indicate that the sorption properties of the structure are not only due to capillary forces, but also to the swelling of the fibers. Both theoretical curve and experimental results are presented in Figure II.27.

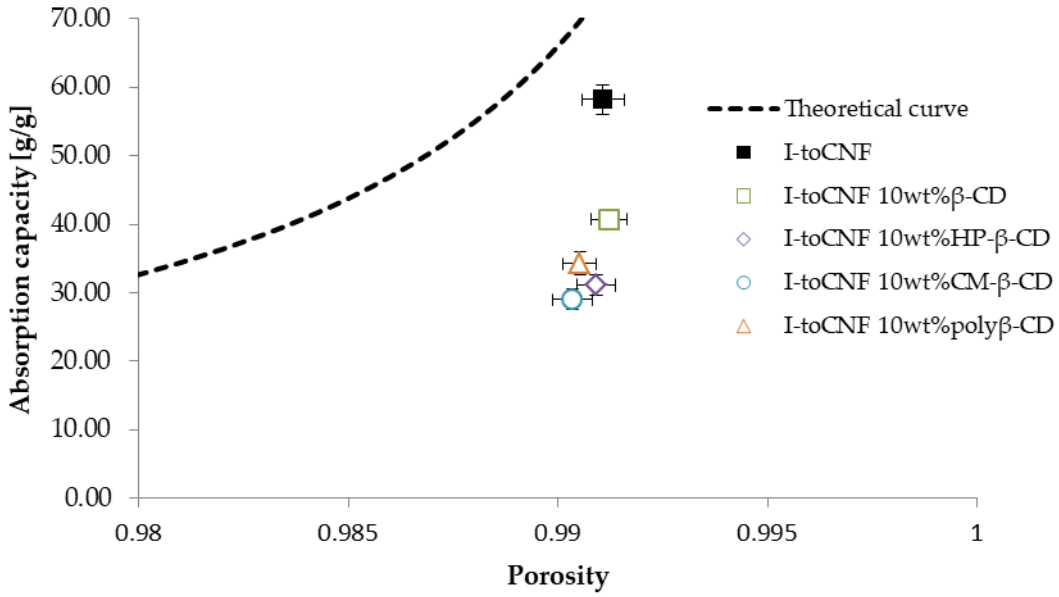

Figure II.27: Absorption capacity of toCNF cryogels with various β-cyclodextrins.

All cryogels displayed porosity values higher than 99%, meaning that the addition of cyclodextrins does not have a negative impact, or only slightly impact, on the macroscopic arrangement of toCNFs and further the porosity of the structure. Such values of porosity, higher than 99%, and high absorption capacity are typical for CNF cryogels and aerogels and are in line with toCNF constructs reported in the literature [15], [18], [101]. All cryogels are below the theoretical curve, meaning that there is some collapse of the cell wall structure, linked to deflection in the cell wall arrangement. However, it can be noted that the pure toCNF sample exhibits a much higher absorption capacity (58.2 ± 2.1 g/g) than modified aerogels and is much closer to the theoretical curve. In this case, the collapse of some pores can be linked to the presence of residual fibers. The comparison of the porosity for the different cryogels was investigated with SEM and the images are presented in Figure II.27. While the porosity present in pure toCNF cryogels is quite homogeneous (Fig. II.28.A), the porosity in modified cryogels exhibits more heterogeneity and confirm the presence of collapsed porosity (Fig. II.28.B, C,D and E).

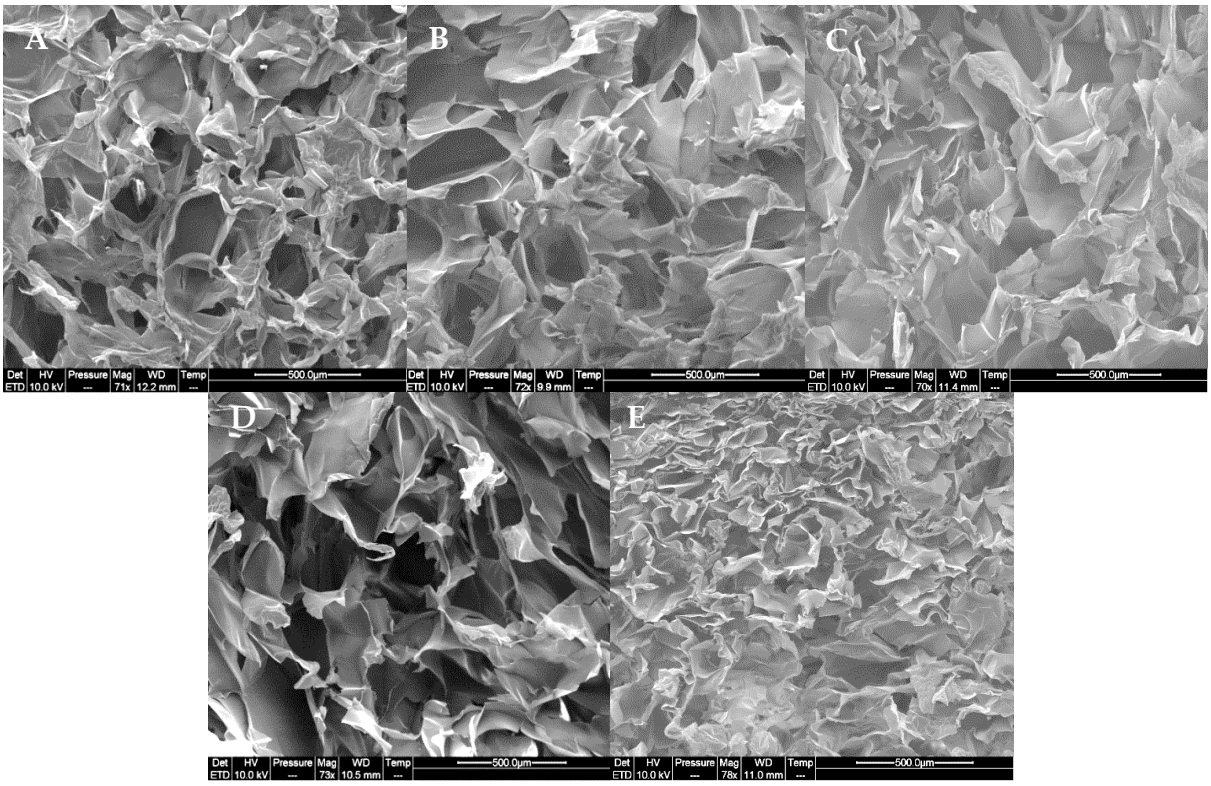

Figure II.28: SEM images of the porous structure of cryogels. A) toCNF B) toCNF-β-CD C) toCNF-HP-β-CD D) toCNF-CM-β-CD E) toCNF-poly- β-CD

The modified cryogels present a lower absorption capacity, which can be linked to the adsorption of CDs on the surface of the nanofibrils, creating small defects in the cell wall. This adsorption of β-CD to toCNFs and its impact over water sorption properties and mechanical properties of cryogels have been discussed in details in our previous study [1]. The absorption capacity for toCNFs with β-CD is slightly higher (40.8 ± 1.5 g/g) than for the samples with HP-β-CD (31.1 ± 1.3 g/g), CM-β-CD (29.0 ± 1.2 g/g) and polyβ-CD (34.3 ± 1.7 g/g). This is a clear indication that there is slightly more adsorption for β-CD derivatives on toCNF than for the native one. Modification of water sorption properties and porosity of cryogels with the addition of β-CD and derivatives are in line with the hypothesis of adsorptions via H-bonding and confirm the conclusions in Chapter II.2. The impact of β-CD adsorption on mechanical properties of toCNFs was reported in Chapter II.1. Compression tests were conducted on I-toCNF cryogels with 10 wt% β-CD derivatives, and the main results are reported in Table II.13.

Table II.13: Mechanical properties for I-toCNF cryogels with various β-CD derivatives

Sample	Compression Modulus [kPa]	Normalized compression modulus [kPa.mg-1.cm3]	Maximum stress at 70% deformation [kPa]
I-toCNF	133 ± 10	9.9 ± 0.2	63 ± 3
I-toCNF-β-CD	101 ± 15	6.8 ± 0.4	61 ± 3
I-toCNF-HP-β-CD	94 ± 13	6.9 ±0.4	61 ± 2
I-toCNF-CM-β-CD	87 ± 17	5.9 ± 0.4	64 ± 3
I-toCNF-polyβ-CD	90 ± 20	5.7 ± 0.5	60 ±3

As discussed in Chapter II.1, it is believed that adsorption of cyclodextrin on the fiber surface is responsible for the slight modification of the cell wall, thus impacting the mechanical properties and especially the elastic behavior. A decrease in the compression modulus upon adsorption of both natural β-CD and β-CD derivatives is observed, but it is nevertheless of the same order of magnitude when considering the standard deviation. However, the maximum stress at 70% deformation, i.e. in the densification regime, is almost identical for all cryogels (around 60 kPa). This is yet another confirmation of adsorption of β-CDs on toCNF fibers. I-toCNF/β-CD derivative cryogels also display mechanical properties in line with the desired biomedical applications.

As a clear conclusion, these results proved that the addition of β-CD derivatives have globally the same impact as regular β-CD onto CNF structure and mechanical properties, meaning that such biomaterial have properties suited for biomedical application.

II.3.4. CONCLUSION

In this study, two toCNF suspensions with similar charge content, one industrially available (I-toCNFs) and one lab-made (H-toCNFs), have been characterized. The nanofibril size and presence of residual fibers have been investigated via turbidity, nanosize fraction and TEM observations. The H-toCNF quality has longer fibers and a less homogeneous size distribution, as well as a greater presence of residual fibers, resulting in higher opacity and viscosity than for I-toCNFs. The size of toCNFs also impact on the water sorption properties of the cryogels, with I-toCNFs displaying water uptake up to 5500 wt% against 4600 wt% for H-toCNFs. All these considerations led to select I-toCNF as the ideal suspension for the design of toCNF/β-CD materials.

The impact of adsorption of β-CD and β-CD derivatives onto I-toCNF fibers on the water sorption and mechanical properties of cryogel was assessed and the measured properties are in line with desired properties for subsequent biomedical applications, which will be described in detail in the next chapter.

CONCLUSION OF CHAPTER II

The aim of chapter II was to provide the most suitable β-CDs/CNF combination for producing biomaterials (cryogel and membrane), with a better understanding of adsorption phenomena occurring between these two components.

In Chapter II.1, β-CD/toCNF films and cryogels were produced. Water sorption analysis and mechanical characterization were conducted for both modified and unmodified materials, under dry and wet conditions. Two unmodified nanofibrils suspensions were prepared with different charge contents (750 μmol/g and 1050 μmol/g), and modification was carried out under neutral or acidic conditions. The sorption equilibrium was reached after 4h for all tested films but higher charge content and acidic casting pH were shown to increase the water sorption, while cyclodextrins decreased it. Density, process pH and addition of cyclodextrins had actually a major impact on the mechanical properties, mainly related to the modification of the H-bond interactions and consequently the cell wall structure.

In Chapter II.2, the adsorption of various β-CD derivatives to toCNF materials was investigated. The adsorption of β-CD onto toCNFs in suspension was investigated using ITC, with an affinity constant measured between β-CD and toCNFs at neutral pH leading to an estimated binding capacity around 19 $\mu mol/g_{toCNF}$. This order of magnitude was confirmed by QCM-d experiments. Different β-CD derivatives, HP-β-CD and CM-β-CD, had binding capacities higher than natural β-CD, with values up to 47.6 $\mu mol/g_{toCNF}$ for CM-β-CD. It was confirmed that the adsorption phenomenon is driven by H-bonding and that the introduction of hydroxyl and carboxyl groups on β-CDs as well as the presence of a spacer increased the availability of these functional groups and led to an important increase in the number of CD molecules adsorbed to toCNFs. The percentage of cyclodextrin released from toCNF/CD cryogels was then measured with a phenolphthalein based titration method. toCNF/β-CD released up to 95% of CD content after 24h, while cryogels with CM-β-CD released only around 20% of the CD content after the same period of time. It was clearly proved that using CM-β-CD instead of β-CD increased the number of CD cavities available as well as improving the anchoring to the nanocellulose structure considerably. Indeed, considering the release, with similar amount of CDs introduced in the cryogel or film, the

number of CD "available" in the structure after 24h release was only around 5 μmol/g_{toCNF} for β-CD against 55 μmol/g_{toCNF} for CM-β-CD.

In Chapter II.3, two toCNF suspensions with similar charge content, one industrially available (I-toCNF) and one lab-made (H-toCNF), have been characterized. H-toCNF presented longer fibers and a less homogeneous size distribution, as well as a greater presence of residual fibers, leading to higher opacity and viscosity compared to I-toCNF. The size of toCNFs also impacted the water sorption properties of the cryogels, with I-toCNF cryogel displaying water uptake up to 5500 wt% against 4600 wt% for H-toCNF cryogel. All these considerations led to a preference for I-toCNF as the ideal suspension for the design of toCNF/β-CD materials. Adsorption of β-CD and β-CD derivatives to I-toCNF impacted water sorption and mechanical properties. It was pointed out that while β-CD derivatives had increased adsorption onto toCNF in comparison with unmodified β-CD, the resulting mechanical properties of the cryogels were in line with the desired properties for biomedical applications such as tissue engineering or topical drug delivery.

In summary, these results contribute to a better understanding and quantification of the adsorption of β-CDs onto toCNFs, and will help to design optimized toCNF/β-CD materials with lasting functionalization without the use of any crosslinker or harmful solvent. Additionally, the use of industrially available toCNF suspensions could be of interest for any potential scale up. Such materials could be beneficial for numerous applications, such as biomedical drug release system, depollution filtration or scavenger devices.

The next chapter will deal with the use of this final design of toCNF/β-CD materials for drug release and antimicrobial applications.

LIST OF FIGURES

REFERENCES

[1] B. Michel, J. Bras, A. Dufresne, E. B. Heggset, and K. Syverud, 'Production and Mechanical Characterisation of TEMPO-Oxidised Cellulose Nanofibrils/β-Cyclodextrin Films and Cryogels', *Molecules*, vol. 25, no. 10, p. 2381, May 2020, doi: 10.3390/molecules25102381.

[2] A. F. Turbak and F. W. Snyder, '(54) MICROFIBRILLATED CELLULOSE', p. 9.

[3] T. Taipale, M. Österberg, A. Nykänen, J. Ruokolainen, and J. Laine, 'Effect of microfibrillated cellulose and fines on the drainage of kraft pulp suspension and paper strength', *Cellulose*, vol. 17, no. 5, pp. 1005–1020, Oct. 2010, doi: 10.1007/s10570-010-9431-9.

[4] S. Josset, P. Orsolini, G. Siqueira, A. Tejado, P. Tingaut, and T. Zimmermann, 'Energy consumption of the nanofibrillation of bleached pulp, wheat straw and recycled newspaper through a grinding process', *Nordic Pulp & Paper Research Journal*, vol. 29, no. 1, pp. 167–175, Jan. 2014, doi: 10.3183/npprj-2014-29-01-p167-175.

[5] F. Rol, M. N. Belgacem, A. Gandini, and J. Bras, 'Recent advances in surface-modified cellulose nanofibrils', *Progress in Polymer Science*, Sep. 2018, doi: 10.1016/j.progpolymsci.2018.09.002.

[6] T. Abitbol *et al.*, 'Nanocellulose, a tiny fiber with huge applications', *Current Opinion in Biotechnology*, vol. 39, pp. 76–88, Jun. 2016, doi: 10.1016/j.copbio.2016.01.002.

[7] T. Saito, Y. Nishiyama, J.-L. Putaux, M. Vignon, and A. Isogai, 'Homogeneous Suspensions of Individualized Microfibrils from TEMPO-Catalyzed Oxidation of Native Cellulose', *Biomacromolecules*, vol. 7, no. 6, pp. 1687–1691, Jun. 2006, doi: 10.1021/bm060154s.

[8] A. Isogai, T. Saito, and H. Fukuzumi, 'TEMPO-oxidized cellulose nanofibers', *Nanoscale*, vol. 3, no. 1, pp. 71–85, 2011, doi: 10.1039/C0NR00583E.

[9] M. A. Hubbe *et al.*, 'Nanocellulose in Thin Films, Coatings, and Plies for Packaging Applications: A Review', *BioResources*, vol. 12, no. 1, pp. 2143–2233, Feb. 2017, doi: 10.15376/biores.12.1.2143-2233.

[10] R. Kolakovic, L. Peltonen, A. Laukkanen, J. Hirvonen, and T. Laaksonen, 'Nanofibrillar cellulose films for controlled drug delivery', *European Journal of Pharmaceutics and Biopharmaceutics*, vol. 82, no. 2, pp. 308–315, Oct. 2012, doi: 10.1016/j.ejpb.2012.06.011.

[11] J. Ø. Torstensen *et al.*, 'Swelling and Free-Volume Characteristics of TEMPO-Oxidized Cellulose Nanofibril Films', *Biomacromolecules*, vol. 19, no. 3, pp. 1016–1025, Mar. 2018, doi: 10.1021/acs.biomac.7b01814.

[12] K. S. Kontturi *et al.*, 'Noncovalent Surface Modification of Cellulose Nanopapers by Adsorption of Polymers from Aprotic Solvents', *Langmuir*, vol. 33, no. 23, pp. 5707–5712, Jun. 2017, doi: 10.1021/acs.langmuir.7b01236.

[13] P. Orsolini, B. Michen, A. Huch, P. Tingaut, W. R. Caseri, and T. Zimmermann, 'Characterization of Pores in Dense Nanopapers and Nanofibrillated Cellulose Membranes: A Critical Assessment of Established Methods', *ACS Appl. Mater. Interfaces*, vol. 7, no. 46, pp. 25884–25897, Nov. 2015, doi: 10.1021/acsami.5b08308.

[14] C. Darpentigny, G. Nonglaton, J. Bras, and B. Jean, 'Highly absorbent cellulose nanofibrils aerogels prepared by supercritical drying', *Carbohydrate Polymers*, vol. 229, p. 115560, Feb. 2020, doi: 10.1016/j.carbpol.2019.115560.

[15] K. J. De France, T. Hoare, and E. D. Cranston, 'Review of Hydrogels and Aerogels Containing Nanocellulose', *Chemistry of Materials*, vol. 29, no. 11, pp. 4609–4631, Jun. 2017, doi: 10.1021/acs.chemmater.7b00531.

[16] N. Buchtová, C. Pradille, J.-L. Bouvard, and T. Budtova, 'Mechanical properties of cellulose aerogels and cryogels', *Soft Matter*, vol. 15, no. 39, pp. 7901–7908, 2019, doi: 10.1039/C9SM01028A.

[17] C. Darpentigny, S. Molina-Boisseau, G. Nonglaton, J. Bras, and B. Jean, 'Ice-templated freeze-dried cryogels from tunicate cellulose nanocrystals with high specific surface area and anisotropic morphological and mechanical properties', *Cellulose*, vol. 27, no. 1, pp. 233–247, Jan. 2020, doi: 10.1007/s10570-019-02772-8.

[18] N. Lavoine and L. Bergström, 'Nanocellulose-based foams and aerogels: processing, properties, and applications', *J. Mater. Chem. A*, vol. 5, no. 31, pp. 16105–16117, 2017, doi: 10.1039/C7TA02807E.

[19] S. Gupta, F. Martoïa, L. Orgéas, and P. Dumont, 'Ice-Templated Porous Nanocellulose-Based Materials: Current Progress and Opportunities for Materials Engineering', *Applied Sciences*, vol. 8, no. 12, p. 2463, Dec. 2018, doi: 10.3390/app8122463.

[20] F. Martoïa, T. Cochereau, P. J. J. Dumont, L. Orgéas, M. Terrien, and M. N. Belgacem, 'Cellulose nanofibril foams: Links between ice-templating conditions, microstructures and mechanical properties', *Materials & Design*, vol. 104, pp. 376–391, Aug. 2016, doi: 10.1016/j.matdes.2016.04.088.

[21] A. Rees *et al.*, '3D Bioprinting of Carboxymethylated-Periodate Oxidized Nanocellulose Constructs for Wound Dressing Applications', *BioMed Research International*, vol. 2015, pp. 1–7, 2015, doi: 10.1155/2015/925757.

[22] T. Hakkarainen *et al.*, 'Nanofibrillar cellulose wound dressing in skin graft donor site treatment', *Journal of Controlled Release*, vol. 244, pp. 292–301, Dec. 2016, doi: 10.1016/j.jconrel.2016.07.053.

[23] E. Campodoni *et al.*, 'Polymeric 3D scaffolds for tissue regeneration: Evaluation of biopolymer nanocomposite reinforced with cellulose nanofibrils', *Materials Science and Engineering: C*, vol. 94, pp. 867–878, Jan. 2019, doi: 10.1016/j.msec.2018.10.026.

[24] D. Howard, L. D. Buttery, K. M. Shakesheff, and S. J. Roberts, 'Tissue engineering: strategies, stem cells and scaffolds', *Journal of Anatomy*, vol. 213, no. 1, pp. 66–72, Jul. 2008, doi: 10.1111/j.1469-7580.2008.00878.x.

[25] D. E. Discher, 'Tissue Cells Feel and Respond to the Stiffness of Their Substrate', *Science*, vol. 310, no. 5751, pp. 1139–1143, Nov. 2005, doi: 10.1126/science.1116995.

[26] A. J. Engler, S. Sen, H. L. Sweeney, and D. E. Discher, 'Matrix Elasticity Directs Stem Cell Lineage Specification', *Cell*, vol. 126, no. 4, pp. 677–689, Aug. 2006, doi: 10.1016/j.cell.2006.06.044.

[27] F. J. O'Brien, 'Biomaterials & scaffolds for tissue engineering', *Materials Today*, vol. 14, no. 3, pp. 88–95, Mar. 2011, doi: 10.1016/S1369-7021(11)70058-X.

[28] L. Alexandrescu, K. Syverud, A. Gatti, and G. Chinga-Carrasco, 'Cytotoxicity tests of cellulose nanofibril-based structures', *Cellulose*, vol. 20, no. 4, pp. 1765–1775, Aug. 2013, doi: 10.1007/s10570-013-9948-9.

[29] A. Basu, G. Celma, M. Strømme, and N. Ferraz, 'In Vitro and in Vivo Evaluation of the Wound Healing Properties of Nanofibrillated Cellulose Hydrogels', *ACS Appl. Bio Mater.*, vol. 1, no. 6, pp. 1853–1863, Dec. 2018, doi: 10.1021/acsabm.8b00370.

[30] A. Fiorati *et al.*, 'TEMPO-Nanocellulose/Ca2+ Hydrogels: Ibuprofen Drug Diffusion and In Vitro Cytocompatibility', *Materials*, vol. 13, no. 1, p. 183, Jan. 2020, doi: 10.3390/ma13010183.

[31] A. Rashad, K. Mustafa, E. B. Heggset, and K. Syverud, 'Cytocompatibility of Wood-Derived Cellulose Nanofibril Hydrogels with Different Surface Chemistry', *Biomacromolecules*, vol. 18, no. 4, pp. 1238–1248, Apr. 2017, doi: 10.1021/acs.biomac.6b01911.

[32] K. Syverud, H. Kirsebom, S. Hajizadeh, and G. Chinga-Carrasco, 'Cross-linking cellulose nanofibrils for potential elastic cryo-structured gels', *Nanoscale Research Letters*, vol. 6, no. 1, p. 626, 2011, doi: 10.1186/1556-276X-6-626.

[33] K. Syverud, S. R. Pettersen, K. Draget, and G. Chinga-Carrasco, 'Controlling the elastic modulus of cellulose nanofibril hydrogels—scaffolds with potential in tissue engineering', *Cellulose*, vol. 22, no. 1, pp. 473–481, 2015, doi: 10.1007/s10570-014-0470-5.

[34] T. Loftsson and M. E. Brewster, 'Pharmaceutical applications of cyclodextrins: basic science and product development: Pharmaceutical applications of cyclodextrins', *Journal of Pharmacy and Pharmacology*, vol. 62, no. 11, pp. 1607–1621, Nov. 2010, doi: 10.1111/j.2042-7158.2010.01030.x.

[35] S. V. Kurkov and T. Loftsson, 'Cyclodextrins', *International Journal of Pharmaceutics*, vol. 453, no. 1, pp. 167–180, Aug. 2013, doi: 10.1016/j.ijpharm.2012.06.055.

[36] J. Szejtli, 'Introduction and General Overview of Cyclodextrin Chemistry', *Chem. Rev.*, vol. 98, no. 5, pp. 1743–1754, Jul. 1998, doi: 10.1021/cr970022c.

[37] E. M. M. Del Valle, 'Cyclodextrins and their uses: a review', *Process Biochemistry*, vol. 39, no. 9, pp. 1033–1046, May 2004, doi: 10.1016/S0032-9592(03)00258-9.

[38] G. Crini, S. Fourmentin, M. Fourmentin, and N. Morin-Crini, 'Principales applications des complexes d'inclusion cyclodextrine/substrat', p. 21, 2019.

[39] N. Morin-Crini, P. Winterton, S. Fourmentin, L. D. Wilson, É. Fenyvesi, and G. Crini, 'Water-insoluble β-cyclodextrin–epichlorohydrin polymers for removal of pollutants from aqueous solutions by sorption processes using batch studies: A review of inclusion

mechanisms', *Progress in Polymer Science*, vol. 78, pp. 1–23, Mar. 2018, doi: 10.1016/j.progpolymsci.2017.07.004.

[40] F. J. Otero-Espinar, J. J. Torres-Labandeira, C. Alvarez-Lorenzo, and J. Blanco-Méndez, 'Cyclodextrins in drug delivery systems', *Journal of Drug Delivery Science and Technology*, vol. 20, no. 4, pp. 289–301, 2010, doi: 10.1016/S1773-2247(10)50046-7.

[41] S. S. Jambhekar and P. Breen, 'Cyclodextrins in pharmaceutical formulations I: structure and physicochemical properties, formation of complexes, and types of complex', *Drug Discovery Today*, vol. 21, no. 2, pp. 356–362, Feb. 2016, doi: 10.1016/j.drudis.2015.11.017.

[42] O. Cusola, N. Tabary, M. N. Belgacem, and J. Bras, 'Cyclodextrin functionalization of several cellulosic substrates for prolonged release of antibacterial agents', *Journal of Applied Polymer Science*, vol. 129, no. 2, pp. 604–613, Jul. 2013, doi: 10.1002/app.38748.

[43] J. Lukášek *et al.*, 'Cyclodextrin-Polypyrrole Coatings of Scaffolds for Tissue Engineering', *Polymers*, vol. 11, no. 3, p. 459, Mar. 2019, doi: 10.3390/polym11030459.

[44] V. Venuti *et al.*, 'Tuning structural parameters for the optimization of drug delivery performance of cyclodextrin-based nanosponges', *Expert Opinion on Drug Delivery*, vol. 14, no. 3, pp. 331–340, Mar. 2017, doi: 10.1080/17425247.2016.1215301.

[45] C. Alvarez-Lorenzo, C. A. García-González, and A. Concheiro, 'Cyclodextrins as versatile building blocks for regenerative medicine', *Journal of Controlled Release*, vol. 268, pp. 269–281, Dec. 2017, doi: 10.1016/j.jconrel.2017.10.038.

[46] W. K. Grier, A. S. Tiffany, M. D. Ramsey, and B. A. C. Harley, 'Incorporating β-cyclodextrin into collagen scaffolds to sequester growth factors and modulate mesenchymal stem cell activity', *Acta Biomaterialia*, vol. 76, pp. 116–125, Aug. 2018, doi: 10.1016/j.actbio.2018.06.033.

[47] A. A. Nada, F. H. H. Abdellatif, E. A. Ali, R. A. Abdelazeem, A. A. S. Soliman, and N. Y. Abou-Zeid, 'Cellulose-based click-scaffolds: Synthesis, characterization and biofabrications', *Carbohydrate Polymers*, vol. 199, pp. 610–618, Nov. 2018, doi: 10.1016/j.carbpol.2018.07.049.

[48] K. O. Kim, G. J. Kim, and J. H. Kim, 'A cellulose/β-cyclodextrin nanofiber patch as a wearable epidermal glucose sensor', *RSC Adv.*, vol. 9, no. 40, pp. 22790–22794, 2019, doi: 10.1039/C9RA03887F.

[49] S. Saini, D. Quinot, N. Lavoine, M. N. Belgacem, and J. Bras, 'β-Cyclodextrin-grafted TEMPO-oxidized cellulose nanofibers for sustained release of essential oil', *Journal of Materials Science*, vol. 52, no. 7, pp. 3849–3861, Apr. 2017, doi: 10.1007/s10853-016-0644-7.

[50] G. Yuan *et al.*, 'Cyclodextrin functionalized cellulose nanofiber composites for the faster adsorption of toluene from aqueous solution', *Journal of the Taiwan Institute of Chemical Engineers*, vol. 70, pp. 352–358, Jan. 2017, doi: 10.1016/j.jtice.2016.10.028.

[51] C. Ruiz-Palomero, M. L. Soriano, and M. Valcárcel, 'β-Cyclodextrin decorated nanocellulose: a smart approach towards the selective fluorimetric determination of

danofloxacin in milk samples', *Analyst*, vol. 140, no. 10, pp. 3431–3438, May 2015, doi: 10.1039/C4AN01967A.

[52] Z. Aytac, H. S. Sen, E. Durgun, and T. Uyar, 'Sulfisoxazole/cyclodextrin inclusion complex incorporated in electrospun hydroxypropyl cellulose nanofibers as drug delivery system', *Colloids and Surfaces B: Biointerfaces*, vol. 128, pp. 331–338, Apr. 2015, doi: 10.1016/j.colsurfb.2015.02.019.

[53] N. Lavoine, N. Tabary, I. Desloges, B. Martel, and J. Bras, 'Controlled release of chlorhexidine digluconate using β-cyclodextrin and microfibrillated cellulose', *Colloids and Surfaces B: Biointerfaces*, vol. 121, pp. 196–205, Sep. 2014, doi: 10.1016/j.colsurfb.2014.06.021.

[54] N. Lavoine, C. Givord, N. Tabary, I. Desloges, B. Martel, and J. Bras, 'Elaboration of a new antibacterial bio-nano-material for food-packaging by synergistic action of cyclodextrin and microfibrillated cellulose', *Innovative Food Science & Emerging Technologies*, vol. 26, pp. 330–340, Dec. 2014, doi: 10.1016/j.ifset.2014.06.006.

[55] D. O. de Castro, N. Tabary, B. Martel, A. Gandini, N. Belgacem, and J. Bras, 'Controlled release of carvacrol and curcumin: bio-based food packaging by synergism action of TEMPO-oxidized cellulose nanocrystals and cyclodextrin', *Cellulose*, vol. 25, no. 2, pp. 1249–1263, Feb. 2018, doi: 10.1007/s10570-017-1646-6.

[56] A. Jimenez, F. Jaramillo, U. Hemraz, Y. Boluk, K. Ckless, and R. Sunasee, 'Effect of surface organic coatings of cellulose nanocrystals on the viability of mammalian cell lines', *Nanotechnology, Science and Applications*, vol. Volume 10, pp. 123–136, Sep. 2017, doi: 10.2147/NSA.S145891.

[57] D. O. Castro, N. Tabary, B. Martel, A. Gandini, N. Belgacem, and J. Bras, 'Effect of different carboxylic acids in cyclodextrin functionalization of cellulose nanocrystals for prolonged release of carvacrol', *Materials Science and Engineering: C*, vol. 69, pp. 1018–1025, Dec. 2016, doi: 10.1016/j.msec.2016.08.014.

[58] G. M. A. Ndong Ntoutoume *et al.*, 'Development of curcumin–cyclodextrin/cellulose nanocrystals complexes: New anticancer drug delivery systems', *Bioorganic & Medicinal Chemistry Letters*, vol. 26, no. 3, pp. 941–945, Feb. 2016, doi: 10.1016/j.bmcl.2015.12.060.

[59] N. Lin and A. Dufresne, 'Supramolecular Hydrogels from In Situ Host–Guest Inclusion between Chemically Modified Cellulose Nanocrystals and Cyclodextrin', *Biomacromolecules*, vol. 14, no. 3, pp. 871–880, Mar. 2013, doi: 10.1021/bm301955k.

[60] H. Orelma, I. Filpponen, L.-S. Johansson, M. Österberg, O. J. Rojas, and J. Laine, 'Surface Functionalized Nanofibrillar Cellulose (NFC) Film as a Platform for Immunoassays and Diagnostics', *Biointerphases*, vol. 7, no. 1, p. 61, Dec. 2012, doi: 10.1007/s13758-012-0061-7.

[61] E. B. Heggset, B. L. Strand, K. W. Sundby, S. Simon, G. Chinga-Carrasco, and K. Syverud, 'Viscoelastic properties of nanocellulose based inks for 3D printing and mechanical properties of CNF/alginate biocomposite gels', *Cellulose*, Nov. 2018, doi: 10.1007/s10570-018-2142-3.

[62] R. Weishaupt *et al.*, 'TEMPO-Oxidized Nanofibrillated Cellulose as a High Density Carrier for Bioactive Molecules', *Biomacromolecules*, vol. 16, no. 11, pp. 3640–3650, Nov. 2015, doi: 10.1021/acs.biomac.5b01100.

[63] S. Okubayashi, U. J. Griesser, and T. Bechtold, 'A kinetic study of moisture sorption and desorption on lyocell fibers', *Carbohydrate Polymers*, vol. 58, no. 3, pp. 293–299, 2004.

[64] A. Dufresne, *Nanocellulose: from nature to high performance tailored materials*. Berlin: de Gruyter, 2012.

[65] S. Belbekhouche *et al.*, 'Water sorption behavior and gas barrier properties of cellulose whiskers and microfibrils films', *Carbohydrate Polymers*, vol. 83, no. 4, pp. 1740–1748, Feb. 2011, doi: 10.1016/j.carbpol.2010.10.036.

[66] L. A. Gibson and M. Ashby, *MF.(1999) Cellular Solids, Structure and Properties*. Cambridge University Press, Cambridge.

[67] N. Mills, *Polymer Foams Handbook: Engineering and Biomechanics Applications and Design Guide*. Elsevier, 2007.

[68] A. Goel and S. N. Nene, 'Modifications in the Phenolphthalein Method for Spectrophotometric Estimation of Beta Cyclodextrin', *Starch - Stärke*, vol. 47, no. 10, pp. 399–400, 1995, doi: 10.1002/star.19950471006.

[69] O. Nechyporchuk, M. N. Belgacem, and J. Bras, 'Production of cellulose nanofibrils: A review of recent advances', *Industrial Crops and Products*, vol. 93, pp. 2–25, Dec. 2016, doi: 10.1016/j.indcrop.2016.02.016.

[70] T. Saito and A. Isogai, 'Introduction of aldehyde groups on surfaces of native cellulose fibers by TEMPO-mediated oxidation', *Colloids and Surfaces A: Physicochemical and Engineering Aspects*, vol. 289, no. 1–3, pp. 219–225, Oct. 2006, doi: 10.1016/j.colsurfa.2006.04.038.

[71] D. Klemm *et al.*, 'Nanocellulose as a natural source for groundbreaking applications in materials science: Today's state', *Materials Today*, vol. 21, no. 7, pp. 720–748, Sep. 2018, doi: 10.1016/j.mattod.2018.02.001.

[72] P. R. Sharma, S. K. Sharma, T. Lindström, and B. S. Hsiao, 'Nanocellulose-Enabled Membranes for Water Purification: Perspectives', *Adv. Sustainable Syst.*, vol. 4, no. 5, p. 1900114, May 2020, doi: 10.1002/adsu.201900114.

[73] P. Blach, S. Fourmentin, D. Landy, F. Cazier, and G. Surpateanu, 'Cyclodextrins: A new efficient absorbent to treat waste gas streams', *Chemosphere*, vol. 70, no. 3, pp. 374–380, 2008, doi: https://doi.org/10.1016/j.chemosphere.2007.07.018.

[74] European Medicine Agency, 'Cyclodextrins used as excipient', EMA/CHMP/4957472013,October 2017

[75] M. Kfoury, 'Préparation, caractérisation physicochimique et évaluation des propriétés biologiques de complexes d'inclusion à base de cyclodextrines: applications à des principes actifs de type phénylpropanoïdes', p. 226.

[76] S. Gould and R. C. Scott, '2-Hydroxypropyl-β-cyclodextrin (HP-β-CD): A toxicology review', *Food and Chemical Toxicology*, vol. 43, no. 10, pp. 1451–1459, Oct. 2005, doi: 10.1016/j.fct.2005.03.007.

[77] A. Z. M. Badruddoza, G. S. S. Hazel, K. Hidajat, and M. S. Uddin, 'Synthesis of carboxymethyl-β-cyclodextrin conjugated magnetic nano-adsorbent for removal of methylene blue', *Colloids and Surfaces A: Physicochemical and Engineering Aspects*, vol. 367, no. 1–3, pp. 85–95, Sep. 2010, doi: 10.1016/j.colsurfa.2010.06.018.

[78] G. Shixiang, W. Liansheng, H. Qingguo, and H. Sukui, 'SOLUBILIZATION OF POLYCYCLIC AROMATIC HYDROCARBONS BY P-CYCLODEXTRIN AND CARBOXYMETHYL-fl-CYCLODEXTRIN', p. 7.

[79] N. H. Foda and R. B. Bakhaidar, 'Zaleplon', in *Profiles of Drug Substances, Excipients and Related Methodology*, vol. 35, Elsevier, 2010, pp. 347–371. doi: 10.1016/S1871-5125(10)35008-4.

[80] C. Su *et al.*, 'Carboxymethyl-β-cyclodextrin conjugated nanoparticles facilitate therapy for folate receptor-positive tumor with the mediation of folic acid', *International Journal of Pharmaceutics*, vol. 474, no. 1–2, pp. 202–211, Oct. 2014, doi: 10.1016/j.ijpharm.2014.08.026.

[81] B. Martel, D. Ruffin, M. Weltrowski, Y. Lekchiri, and M. Morcellet, 'Water-soluble polymers and gels from the polycondensation between cyclodextrins and poly(carboxylic acid)s: A study of the preparation parameters', *J. Appl. Polym. Sci.*, vol. 97, no. 2, pp. 433–442, Jul. 2005, doi: 10.1002/app.21391.

[82] T. F. Cova, D. Murtinho, A. A. C. C. Pais, and A. J. M. Valente, 'Combining Cellulose and Cyclodextrins: Fascinating Designs for Materials and Pharmaceutics', *Front. Chem.*, vol. 6, 2018, doi: 10.3389/fchem.2018.00271.

[83] N. Tabary *et al.*, 'A chlorhexidine-loaded biodegradable cellulosic device for periodontal pockets treatment', *Acta Biomaterialia*, vol. 10, no. 1, pp. 318–329, Jan. 2014, doi: 10.1016/j.actbio.2013.09.032.

[84] D. Gomez-Maldonado *et al.*, 'Cellulose-Cyclodextrin Co-Polymer for the Removal of Cyanotoxins on Water Sources', *Polymers*, vol. 11, no. 12, p. 2075, Dec. 2019, doi: 10.3390/polym11122075.

[85] S. Lombardo and W. Thielemans, 'Thermodynamics of adsorption on nanocellulose surfaces', *Cellulose*, vol. 26, no. 1, pp. 249–279, Jan. 2019, doi: 10.1007/s10570-018-02239-2.

[86] Y. Navon, H. Radavidson, J.-L. Putaux, B. Jean, and L. Heux, 'pH-Sensitive Interactions between Cellulose Nanocrystals and DOPC Liposomes', *Biomacromolecules*, vol. 18, no. 9, pp. 2918–2927, Sep. 2017, doi: 10.1021/acs.biomac.7b00872.

[87] S. Lombardo, P. Chen, P. A. Larsson, W. Thielemans, J. Wohlert, and A. J. Svagan, 'Toward Improved Understanding of the Interactions between Poorly Soluble Drugs and Cellulose Nanofibers', *Langmuir*, vol. 34, no. 19, pp. 5464–5473, May 2018, doi: 10.1021/acs.langmuir.8b00531.

[88] M. Rodahl, F. Höök, A. Krozer, P. Brzezinski, and B. Kasemo, 'Quartz Cristal microbalance setup for frequency and Q-factor measurments in gaseous and liquid environments', *Review of Scientific Instruments*, vol. 66, no. 3924, 1995.

[89] M. V. Voinova, M. Rodahl, M. Jonson, and B. Kasemo, 'Viscoelastic Acoustic Response of Layered Polymer Films at Fluid-Solid Interfaces: Continuum Mechanics Approach', *Physica Scripta*, vol. 59, no. 5, pp. 391–396, May 1999, doi: 10.1238/physica.regular.059a00391.

[90] K. Taguchi, 'Transient binding of phenolphthalein-.beta.-cyclodextrin complex: an example of induced geometrical distortion', *Journal of the American Chemical Society*, vol. 108, no. 10, pp. 2705–2709, May 1986, doi: 10.1021/ja00270a032.

[91] C. Basappa, P. Rao, D. N. Rao, and Divakar, 'A modified colorimetric method for the estimation of β-cyclodextrin using phenolphthalein', *International Journal of Food Science & Technology*, vol. 33, no. 6, pp. 517–520, Dec. 1998, doi: 10.1046/j.1365-2621.1998.00216.x.

[92] J. Lin, E. Pozharski, and M. A. Wilson, 'Short Carboxylic Acid–Carboxylate Hydrogen Bonds Can Have Fully Localized Protons', *Biochemistry*, vol. 56, no. 2, pp. 391–402, Jan. 2017, doi: 10.1021/acs.biochem.6b00906.

[93] C. H. Görbitz and M. C. Etter, 'Hydrogen bonds to carboxylate groups. The question of three-centre interactions', *J. Chem. Soc., Perkin Trans. 2*, no. 1, pp. 131–135, 1992, doi: 10.1039/P29920000131.

[94] R. Kolakovic *et al.*, 'Evaluation of drug interactions with nanofibrillar cellulose', *European Journal of Pharmaceutics and Biopharmaceutics*, vol. 85, no. 3, pp. 1238–1244, Nov. 2013, doi: 10.1016/j.ejpb.2013.05.015.

[95] S. Ahola, M. Österberg, and J. Laine, 'Cellulose nanofibrils—adsorption with poly(amideamine) epichlorohydrin studied by QCM-D and application as a paper strength additive', *Cellulose*, vol. 15, no. 2, pp. 303–314, Apr. 2008, doi: 10.1007/s10570-007-9167-3.

[96] M. Mikel, 'Colorimetric determination of/3-cyclodextrin" two assay modifications based on molecular complexation of phenolphtalein', p. 8.

[97] J. Desmaisons, E. Boutonnet, M. Rueff, A. Dufresne, and J. Bras, 'A new quality index for benchmarking of different cellulose nanofibrils', *Carbohydrate Polymers*, vol. 174, pp. 318–329, Oct. 2017, doi: 10.1016/j.carbpol.2017.06.032.

[98] E. J. Foster *et al.*, 'Current characterization methods for cellulose nanomaterials', *Chemical Society Reviews*, vol. 47, no. 8, pp. 2609–2679, 2018, doi: 10.1039/C6CS00895J.

[99] A. Naderi, T. Lindström, and J. Sundström, 'Repeated homogenization, a route for decreasing the energy consumption in the manufacturing process of carboxymethylated nanofibrillated cellulose?', *Cellulose*, vol. 22, no. 2, pp. 1147–1157, Apr. 2015, doi: 10.1007/s10570-015-0576-4.

[100] S. Sayeb, M. B. Hassen, and F. Sakli, 'Modelling Absorption Capacity Performance of Hygienic Product', *OJAppS*, vol. 03, no. 02, pp. 169–173, 2013, doi: 10.4236/ojapps.2013.32023.

[101] F. Jiang and Y.-L. Hsieh, 'Super water absorbing and shape memory nanocellulose aerogels from TEMPO-oxidized cellulose nanofibrils via cyclic freezing–thawing', *J. Mater. Chem. A*, vol. 2, no. 2, pp. 350–359, 2014, doi: 10.1039/C3TA13629A.

Chapter III. β-cyclodextrin-functionalized nanocellulose for drug release applications

INTRODUCTION TO CHAPTER III

Chapter II focused on the production and characterization of toCNF/β-CD structures with various geometries (films and cryogels) and different types of β-CDs. Adsorption of β-CDs was assessed, and the produced materials displayed promising properties suited for biomedical applications. The aim of chapter III is to provide a proof of concept for the beneficial use of toCNFs functionalized with β-CDs for specific medical applications, i.e. drug release and antimicrobial activity in a wound dressing. To bring antimicrobial activity to these materials a prophylactic molecule used in the prevention of infections, sulfadiazine, was selected. This was done to validate the potential of the loading and prolonged release of low-water soluble active principal ingredient (API) through complexation with β-CDs.

The first part of chapter III deals with characterization of the inclusion complex formation between sulfadiazine and the various types of β-CDs via different experimental techniques. The effects of complexation with β-CDs on the physico-chemical properties, e.g. the increase in solubility of this poorly water-soluble API and association/dissociation constant of the complexes will be measured. Mechanism of the adsorption/inclusion and orientation of the molecules inside the β-CDs cavity, as well as the impact of the chemical modifications of β-CD derivatives will be investigated.

The second part of this chapter is dedicated to the production of toCNF/ β-CDs/SD materials and their characterization in terms of (i) release properties in sink conditions (i.e. release in volume of release medium 5 times superior to the saturated solution of API) and (ii) antimicrobial activity. The impact of the process (pH of casting) as well as the toCNF network structure and a variety of β-CDs will be investigated to verify if the potential seen at the end of chapter II is confirmed.

Figure III.I summarizes the structure of Chapter III.

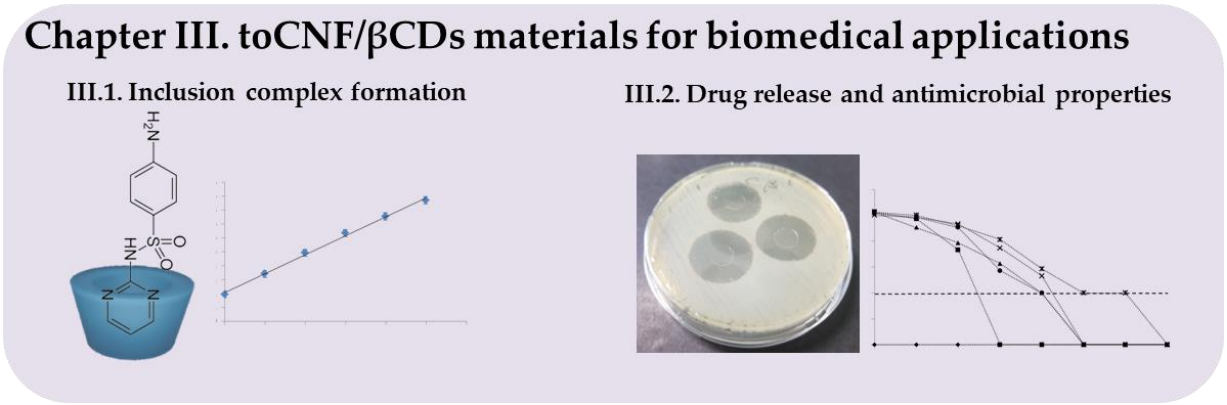

Figure III.1: Graphical representation of the structure of Chapter III

CHAPTER III.1. INCLUSION COMPLEX FORMATION BETWEEN SULFADIAZINE AND VARIOUS MODIFIED Β-CYCLODEXTRINS AND CHARACTERIZATION OF THE COMPLEXES

Inspired from paper: ***B. Michel,*** *E.B. Heggset, K. Syverud, A. Dufresne, J. Bras, Inclusion complex formation between sulfadiazine and various modified β-cyclodextrin. Submitted to Journal of Drug Delivery Science and Technology (Elsevier) in March 2022.*

Abstract: β-Cyclodextrin (β-CD) and its derivatives are cyclic oligosaccharides which present the ability to form inclusion complexes with hydrophobic molecules and can bring new functionalities to a wide range of materials. As of today, the most used prophylactic drugs for wound dressing applications are sulfadiazine (SD) and its derivatives silver sulfadiazine (SSD). These drugs are used to prevent infections of the wounds; however, their low intrinsic water-solubility is a hindrance to their use. In this study, the inclusion complex formation between SD/SSD and the various β-CDs were assessed with various protocols. Isothermal Titration Calorimetry (ITC) experiments led to the conclusion that the formation constants measured for SD and SSD are sufficiently similar meaning that SD can be considered as a satisfactory model molecule. Phase Solubility Diagram (PSD) were built for SD and the various β-CDs, highlighting a 1:1 stoichiometry of inclusion and a linear increase in solubility of SD with increasing concentration of β-CDs- The formation constant ranged from 197 M^{-1} to 245 M^{-1} for the different β-CDs. X-Ray diffraction (XRD) and Differential Scanning Calorimetry (DSC) experiments revealed the different physico-chemical properties affected by the formation of an inclusion complex. Finally, Nuclear Magnetic Resonance (NMR) experiments confirmed the depth of penetration of SD inside the β-CDs cavity as well as the orientation of SD, highlighting the fact that CM-β-CDs induce a deeper penetration than other β-CDs. The graphical abstract of this study is presented in Figure III.2.

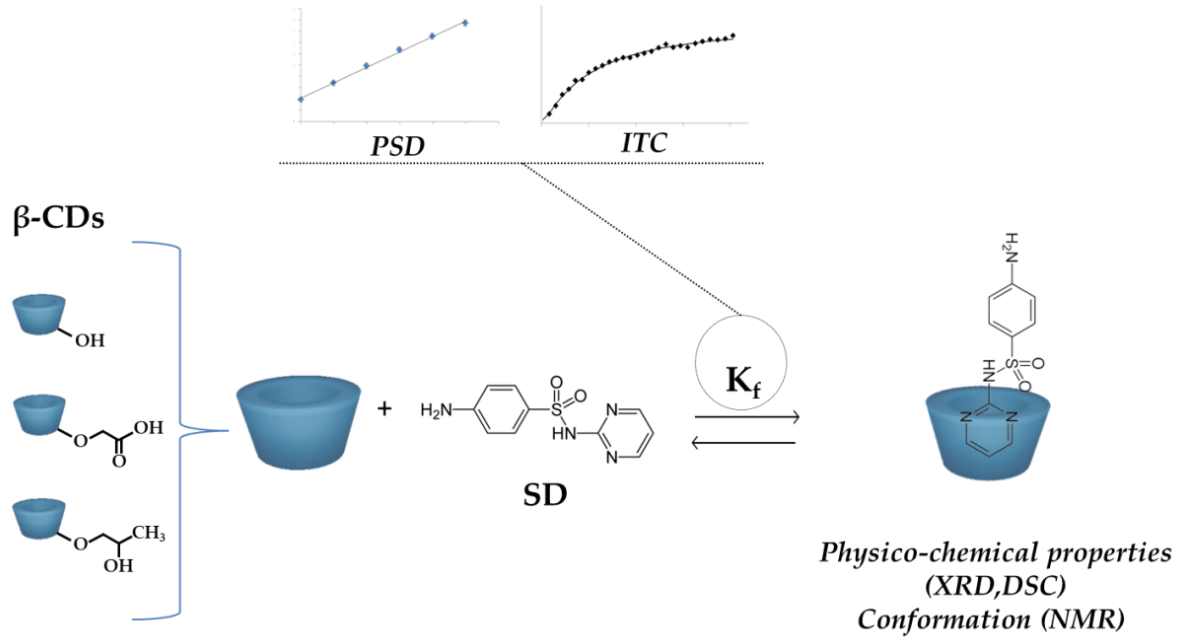

Figure III.2: Graphical abstract for Chapter III.1

III.1.1. INTRODUCTION

Wound dressings are materials used to fulfill two principal functions: (i) protect the wound and (ii) facilitate the healing process. [1]. To facilitate the healing process, wound dressing materials should display characteristics such as i) control the moisture content around the wound, ii) allow the transmission of gases between the wound and the surroundings, iii) prevent infections of the wound, iv) be biocompatible, and v) be easily handled with low adherence to the skin [1]. With their intrinsic biocompatibility, tunable nanostructure and surface chemistry, and good water retention properties, CNFs have proven to be beneficial for wound dressing/wound healing applications, in the form of hydrogels or membranes [2]–[5]. Recently, it has been demonstrated that the oxidized form of CNFs (toCNFs) developed by Isogai et al. [6] are particularly suitable for such applications. However, toCNF materials does not exhibit any intrinsic antibacterial activity, implying that toCNFs-only would not be sufficient to protect the wound from the risk of infections. Multiples strategies have been implemented to provide antimicrobial properties to such nanocellulose materials, as described in a recent review by Li et al. [7]. The main strategies identified are the surface modification of nanocellulose with quaternary ammonium compounds [8], addition of an antibiotic to nanocellulose [9], combination with nanomaterials such as silver nanoparticles [10] or combination with antibacterial polymer [11]. However, these strategies present some limitations, such as the lack of selectivity for surface modification, burst effect for impregnation of antibiotics, cost for nanomaterials to cite a few. Another strategy which can be promising for solving these issues would be the combination with cyclodextrins. Cyclodextrins have been used previously as pharmaceutical excipients to increase the bioavailabity of low water-soluble active principal ingredients (APIs). Due to their ability to form inclusion complex with a wide range of molecules, they can be adapted for numerous applications [12]. As such, the objective of this study is to evaluate the potential inclusion complex formations between cyclodextrins and APIs of interest for the specific application of burn wound dressing.

Sulfadiazine (SD) is a drug classically used in the treatment of infections from Gram-positive and Gram-negative micro-organisms. It is also used for the treatment of toxoplasmosis [13]. Its silver derivative, silver sulfadiazine (SSD), is used for the prevention of infections of burn wound [14]–[16]. However, the major issue with SD and its derivatives

is their low water solubility (7.4 mg/mL at 25°C) [17], which limits their bioavailabity and applications. As an illustration, SSD is typically used in the form of a 1wt% cream in combination with gauze for the treatment of burn wound. Its low bioavailabity imposes a frequent application of antibiotic ointment, implying a change of dressing and thus a significant amount of discomfort for the patient as well as a risk to degrade the wound. β-CD and some of its derivatives are used to encapsulate, solubilize and stabilize hydrophobic drugs [18], [19]. Studies involving the complexation of SD and SSD with β-CD and some derivatives have been reported in the literature [17], [20]–[23]. These studies have shown that the complexation between SD/SSD and β-CDs and Hydroxypropyl-β-Cyclodextrin (HP-β-CD) is feasible and that it improves the aqueous solubility of the drugs. However, to the best of our knowledge, there is no study reporting on the characterization of the inclusion complex formation between SD and Carboxymethyl-β-Cyclodextrin (CM-β-CD).

The principal forces and interactions involved in the complexation process have been widely discussed in the literature [24]–[28] and is suggested to consist of Van der Waals interactions, electrostatic interactions, hydrophobic interactions or hydrogen bonding. Nevertheless, there is currently no certainty about the contribution of each of these interactions in the complexation phenomenon. The inclusion of a molecule within a cyclodextrin has an impact on its solubility, but also on the other physico-chemical properties, such as e.g. thermal stability, resistance to oxidation and hydrolysis as well as crystallinity of the host-cyclodextrins. Thus, the study of the formation of complexes can be done by a great variety of physicochemical characterization. However, the most common ones are Phase Solubility Diagram (PSD) [29], UV-vis spectroscopy [30], Isothermal Titration Calorimetry (ITC) [31], Fourier Transform Infrared Spectroscopy (FTIR) [32] and Nuclear Magnetic Resonance (NMR) [33] to name only a few.

Accordingly, the objective of this part of the project will be to characterize the inclusion complex between sulfadiazine and its silver derivative and the various cyclodextrins used in the project, namely β-CD, 2-Hydroxypropyl-β-Cyclodextrin (HP-β-CD) and Carboxymethyl-β-Cyclodextrin (CM-β-CD) by several different methods such as PSD, ITC, FTIR, X-Ray diffraction (XRD) and NMR in order to validate its utilization to characterize toCNF/β-CDs structures for biomedical applications.

III.1.2. Materials and Methods

III.1.2.1. Materials

Sulfadiazine (SD, M = 250.28 g/mol), silver sulfadiazine (SSD, M = 357.14 g/mol), β-Cyclodextrin (β-CD, M = 1134.98 g/mol), 2-Hydroxypropyl-β-Cyclodextrin (HP-β-CD, DS = 3, M = 1380 g/mol) were purchased from Sigma-Aldrich. Carboxymethyl-β-Cyclodextrin Sodium Salt (CM- β-CD, DS = 3.5, M = 1415 g/mol) was purchased from CycloLab (Hungary). The degree of substitution (DS) of the different cyclodextrins is given for one cyclodextrin molecule. The two active principle ingredients (APIs), SD and SSD, as well as the cyclodextrins used in the project are presented in Figure III.3. HCl, KH_2PO_4 and NaOH were of laboratory grade and purchased from Sigma-Aldrich.

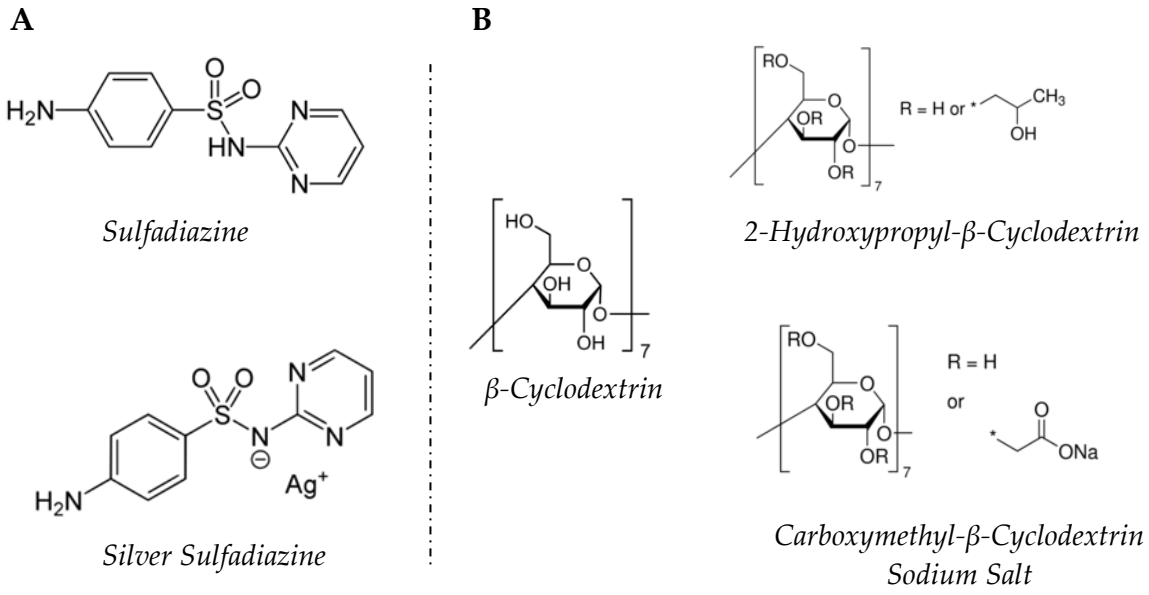

Figure III.3: APIs and β-CDs. A) Formula of SD and SSD. B) Formula of β-CD, HP-β-CD and CM-β-CD.

III.1.2.2. Methods

III.1.2.2.1. Isothermal titration Calorimetry

Isothermal Titration Calorimetry experiments were performed with a VP-ITC (Microcal Inc.). A sample cell with a volume of 1.8 mL was filled with 40 µM SD or SSD solution in a KH_2PO_4/NaOH buffer, pH 6. ITC experiments were carried out at 25°C by injecting 10 µL of aqueous β-CD solution (15-20 mM in KH_2PO_4/NaOH buffer at pH 6) from a 280 µL injection syringe into the sample cell. To ensure optimal mixing efficiency the

solution was stirred at 307 rpm throughout the titration process. To determine the heat of dilutions of β-CDs, blank titrations were made by injecting the β-CD solution into the cell filled with KH_2PO_4/NaOH buffer, pH 6. The enthalpy curve of heat for the dilutions was then subtracted from the curves of interactions between SD and β-CDs. Data were fitted with one site model of interaction with MicroCal PEAQ-ITC Analyzer Software, according to standard procedures. Two independent titrations were performed for each cyclodextrin tested.

III.1.2.2.2. Phase solubility diagram

The effect of each β-CDs on the solubility of SD was studied according to the method of Phase Solubility Diagram (PSD) proposed in 1965 by Higuchi and Connors [34]. Excess amounts of SD were added to deionized water containing different amounts of β-CDs, corresponding to concentrations 0 mM, 3 mM, 6 mM, 9 mM, 12 mM and 15 mM. The suspensions were homogenized by magnetic stirring for 1h and further incubated at 25 °C regulated chamber under orbital shaking (100 rpm) for 24h. Once the equilibrium was reached, the suspensions were filtered through a 0.45 µm membrane filter (Millipore) and mixed with ethanol in 1:1 proportion. The subsequent solutions were analyzed by UV-vis spectrophotometry at 261.5 nm. The concentrations of SD in the solutions were calculated according to a calibration curve of SD in EtOH:H_2O at 261.5 nm and the final concentrations were determined with the dilution factors. Each PSD was done in triplicate and the results reported are the mean values. The association constant of the SD:β-CD complex (K_F) and the complexation efficiency (CE) were calculated from the slope of the PSD and the solubility S_0 according to equation III.1 and III.2 [35]:

$$K_F = \frac{slope}{S_0(1-slope)} \quad \text{(Eq.III.1)}$$

$$CE = K_F \times S_0 = \frac{slope}{(1-slope)} \quad \text{(Eq.III.2)}$$

Both the slope and S_0 value are determined by linear regression on the mean values of the triplicate measurements for each cyclodextrin.

III.1.2.2.3. Preparation of the solid inclusion complex

SD and β-CDs were added in excess in MilliQ water. The subsequent suspension was homogenized by magnetic stirring for 1h and incubated at 25 °C in a regulated chamber under orbital shaking (100 rpm) for 24h. After reaching equilibrium, the suspension was

filtered through a 0.45 µm membrane filter (Millipore) and the filtrate was frozen for 24h at -20°C, prior to freeze-drying for 48h at 0.01 mbar (ALPHA 2-4 LDplus, Christ ®). The resulting powdered complexes were stored in airtight containers and kept away from the light under controlled conditions before use.

III.1.2.2.4. X-RAY DIFFRACTION

X-Ray diffraction (XRD) analysis was performed on freeze-dried samples deposited on a zero-background silicon substrate. Both individual products and complexes were analyzed. A diffractometer X'Pert Pro MPD (PANalytical, Netherlands) was used, equipped with a Bragg-Brentano geometry and copper anode ($K\alpha$ = 1.5149 Å). The angle 2θ ranged from 4° to 70° with a 0.05° integral. Duplicate measurements were performed for each sample.

III.1.2.2.5. DIFFERENTIAL SCANNING CALORIMETRY

Differential Scanning Calorimetry was performed on freeze-dried samples for both pure materials and inclusion complexes. The thermal behavior was studied by heating the 3-5 mg samples in closed aluminum pans from 25°C to 350 °C under nitrogen flow at 10°C/min. Experiments were duplicated and carried out with DSC TA Q100.

III.1.2.2.6. NUCLEAR MAGNETIC RESONANCE (NMR)

^{1}H NMR spectra were recorded on an Avance III 400 MHz spectrometer at 24.85°C (298K). Complexes were prepared using the freeze-drying method. All products were re-solubilized in D_2O except the non-miscible SD for which CD_3OD was used. Residual signals of the solvents were used to calibrate the spectra: 4.8 ppm for protons in D_2O and 3.31 ppm for protons in CD_3DO. A 30° pulse was applied to acquire the proton spectrum with a spectral width of 4000 Hz, 65536 points, 1 s relaxation time and 16 scans. Drug inclusion into the β-CDs cavities was studied using a two-dimensional rotating frame Overhauser experiments (2D ROESY), with the following pulse sequence: roesygppph19 with ROESY spinlock p15 = 200ms as pulse, D1: 2s and ns at 128 scans.

III.1.3. RESULTS AND DISCUSSION

III.1.3.1. SD COMPLEXATION MODEL AND SOLUBILITY ENHANCEMENT WITH CDS

Phase-solubility diagrams for the systems β-CD:SD, HP-β-CD:SD and CM-β-CD:SD in water at pH 7 are presented in Figure III.4. For the three cyclodextrins, it is shown that the solubility of SD increases linearly with β-CDs concentration. As such, the three systems could be classified as A_L type in the range of concentrations tested according to the classifications given by Higuchi and Connor [34], indicating that the complexation occurs in a 1:1 stoichiometry. Subsequently, by performing a linear regression on the data sets, and with the slope and the intersect (i.e. S_{int}), the affinity constant K_F and the complexation efficiency CE are calculated. These data are presented in Table III.1.

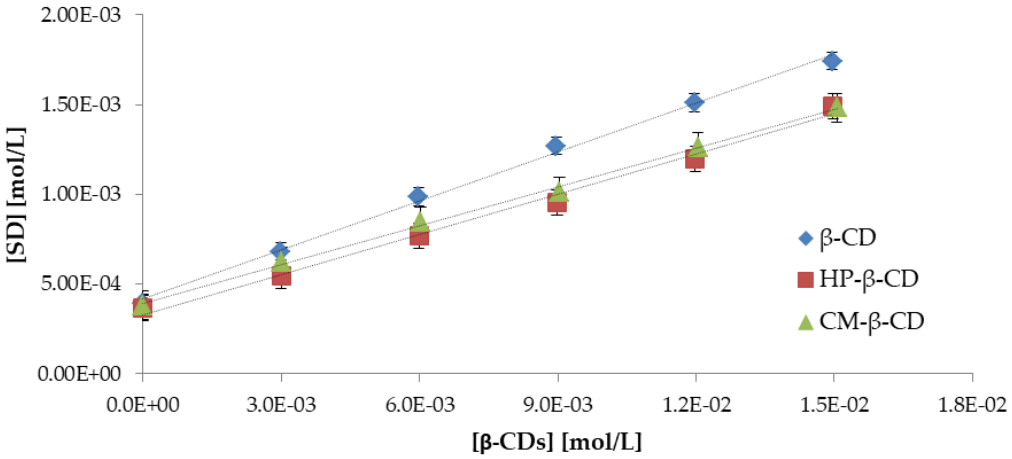

Figure III.4: Phase-solubility diagram for the three different systems.

Table III.1: Data obtained with PSD method allowing the calculation of the association constant.

Cyclodextrin	Slope	S_{int} [M]	R^2	K_F [M^{-1}]	C.E.
β-CD	9.11e-2	4.16e-4	0.997	241 ± 7	0.10
HP-β-CD	7.45e-2	3.29e-4	0.993	245 ± 5	0.08
CM-β-CD	7.20e-2	3.93e-4	0.998	197 ± 10	0.08

The values of K_F calculated for the system β-CD:SD of 241 ± 7 M^{-1} is in agreement with the values determined by Delrivo et al. of 282 ± 11 M^{-1} via the PSD method in water at pH6 [20]. It can be observed that the value determined for HP-β-CD:SD system of 245 ± 5 M^{-1} is similar to the one of the β-CD:SD system, suggesting that the hydroxypropylation of the β-CD does not impact the complexation properties of the derivation, whereas the carboxymethylated groups in the CM- β-CD might have an impact. Indeed, the value of K_F

for the CM-β-CD:SD system is slightly lower than for the two other systems, with 197 ± 10 M^{-1}.

It can be noted that S_{int} is different compared to the intrinsic solubility S_0 of SD, which is generally the case for poorly soluble drugs [18]. Thus, the complexation efficiency is often considered as a better measure for comparison of solubilization effect of CDs [36]. In this case, a C.E. of 0.1 indicates that 10 CD molecules are needed to solubilize one molecule of SD, while a C.E. of 0.08 indicates that 12.5 CD molecules are needed. The values of formation/dissociation constant measured are enough to consider that β-CDs have a beneficial impact over the solubility and thus bioavailabity of SD for subsequent biomedical applications.

III.1.3.2. Influence of SD:β-CDs inclusion on properties of the complex

The inclusion of SD in β-CDs can be observed with other physico-chemical characterizations such as X-ray diffraction (XRD) or Differential Scanning Calorimetry (DSC). The changes in physicochemical properties of the host and guest molecules other than solubilization caused by the formation of inclusion complexes can thus be studied. When API is included in the CD, amorphization of the API occurs, resulting in a diffuse spectrum on the diffractogram of the complex. Since the characterization of the inclusion complex with XRD relies on the amorphization of both the CD and the API, this technique is not pertinent for modified β-CDs. Indeed, β-CD derivatives consist of a mix of derivatives with different degrees of substitution. This, with the addition of chemical functions, prevents a crystalline arrangement. Thus, diffraction patterns for modified β-CDs, with no defined peaks, do not allow to identify a crystalline phase. However, a series of large signals was observed, indicating a semi-crystalline material. Figure III.5 presents the diffraction pattern for pure β-CD (Fig III.5.A.), pure SD (Fig III.5.B.) and the inclusion complex prepared by freeze drying (Fig III.5.C). The diffraction pattern obtained for β-CD indicates a crystalline substance with well-defined characteristic peaks present. The diffraction pattern obtained for SD displays a crystalline structure with defined peaks of high intensity. In the diffraction pattern for the freeze-dried inclusion complex, a decrease in the degree of crystallinity can be observed, although some characteristic β-CD peaks could still be observed. This is due to the host-guest interactions between SD and β-CD in the solid state, which is an indication of the formation of the inclusion complex.

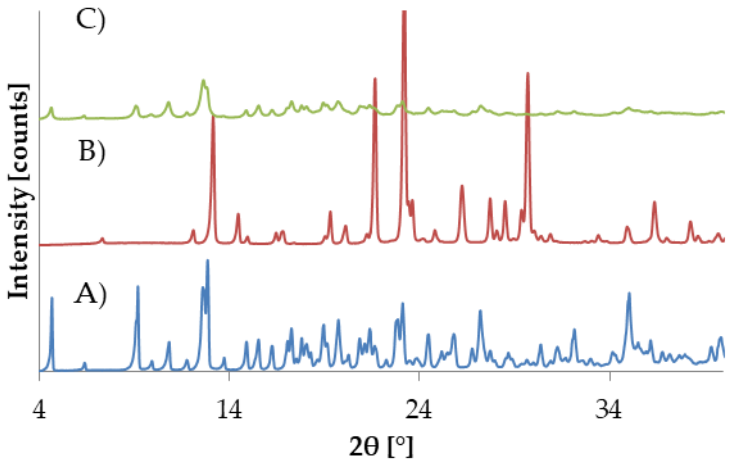

Figure III.5: Diffractograms for A) β-CD B) SD C) β-CD:SD

Thermal analysis methods such as DSC are often used for studying complexation. It can provide information about thermodynamic and physical properties of the produced complex, as well as proving inclusion. As an illustration, DSC curves for β-CD, SD and the freeze-dried inclusion complex are presented in Figure III.6.

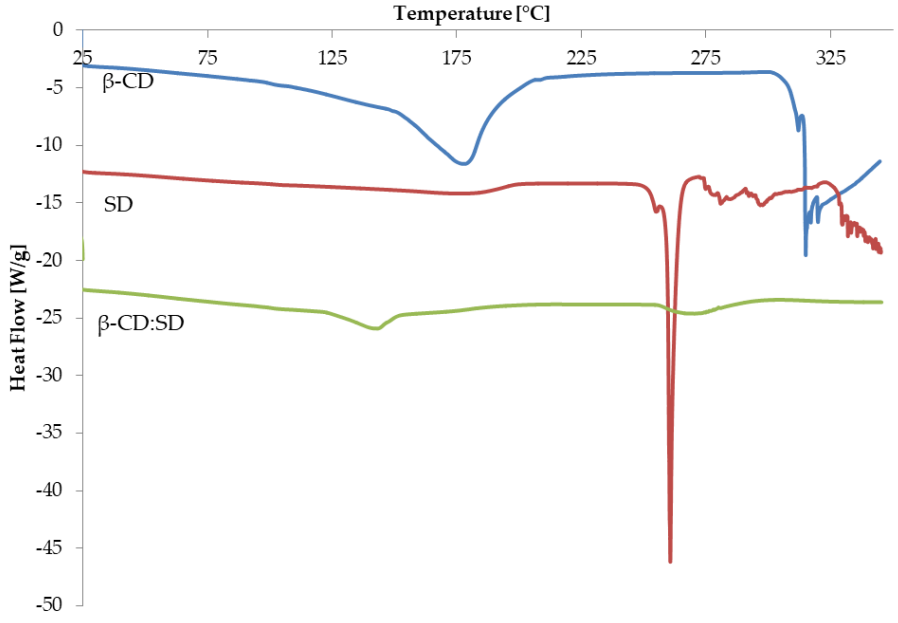

Figure III.6: Thermograms obtained by DSC for β-CD, SD, β-CD:SD

The DSC trace for β-CD shows a broad endothermic effect around 180°C which is associated with water release from the cyclodextrin's cavity. The DSC trace for SD displays a sharp endothermic event at 260.7 °C, which corresponds to its melting point, while β-CD degrades

at temperatures above 300 °C. The disappearance of the SD melting point in the thermogram for the freeze-dried complex is an indication that confirms the presence of inclusion complex. Additionally, the reduction of the broad endothermic effect associated with the release of water molecules from the cavity in the freeze-dried product in comparison with the pure β-CD also lead to confirmation of the inclusion process.

These two techniques (DSC and XRD) illustrate how basic characterization of inclusion complex formation can be performed with a wide variety of experimental methods. However, these methods do not provide information on the stability and association/dissociation constant of the complexes, such as ITC or PSD, or conformational indication, like Nuclear Magnetic Resonance.

III.1.3.3. Depth of penetration of SD in inclusion complex

To analyze more thoroughly the inclusion complex, ^{1}H-NMR experiments were performed. NMR is one of the most useful analytical techniques to investigate the interactions between CDs and the guest molecules. Indeed, NMR can provide information on the specific orientation of the guest molecule inside the CD cavity, which no other techniques can provide [37]. The simplest way to obtain complex characterization using NMR is to observe the differences in the chemical shift of protons from the free molecules and the complexed molecules. For that purpose, inclusion complexes were prepared by freeze-drying to obtain solid powders which subsequently were dissolved in D_2O to perform ^{1}H-NMR experiments. The proton identification for SD is presented in Figure III.7.A. and was done according to the literature [17], [23]. The proton identification for β-CD is presented in Figure III.7.B. and performed as previously described [33], [38], [39].

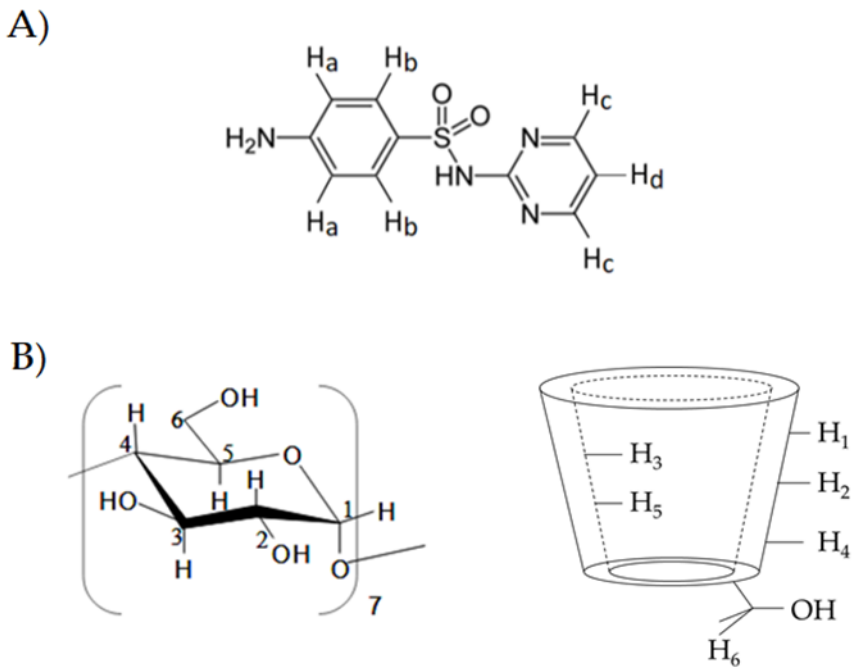

Figure III.7: Schematic representation of a) SD protons b) β-CD protons

The impact of the modification of β-CD was assessed by comparing the H1-NMR spectra between 5.5 ppm and 3.1 ppm for the three different β-CDs, as presented in Figure III.8.

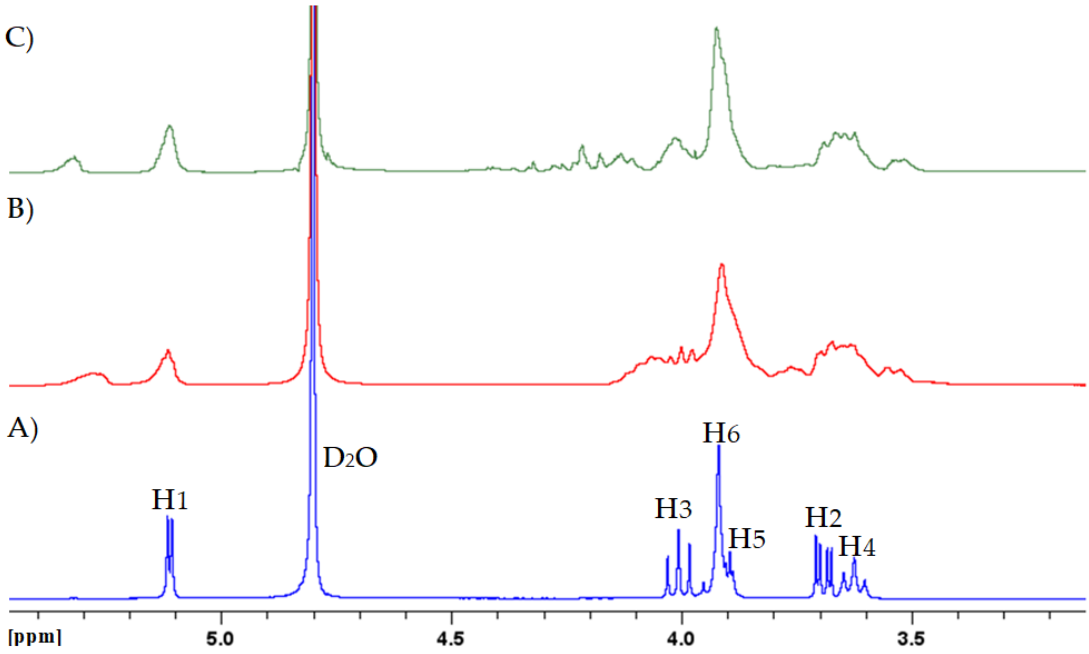

Figure III.8: ^{1}H-NMR spectra for A) β-CD B) HP-β-CD C) CM-β-CD

The ^{1}H spectrum of β-CD (Fig.III.8.A.) displays clear and distinct signals, allowing an assignation of each signal to its corresponding proton. Commercial HP-β-CD and CM-β-CD

contain mixtures of hydroxypropyl-β-CDs and carboxymethyl-β-CDs with various degrees of substitution and with potential modification on carbon C2, C3 or C6 of the anhydroglucose units of the cyclodextrins. Therefore, they are characterized by presence of signals spreading over a range of chemical displacement values, as illustrated by Figure III.8.B. and III.8.C., making the exact measurement of the chemical displacement of each protons less precise.

The inclusion of SD into the various β-CD cavities was first evaluated by the changes in the chemical shifts of protons H3 and H5, located inside the cavity of the β-CDs. For that purpose, Figure III.9 presents a comparison of ^{1}H-NMR spectra between the complex and the free β-CD for the three β-CDs used.

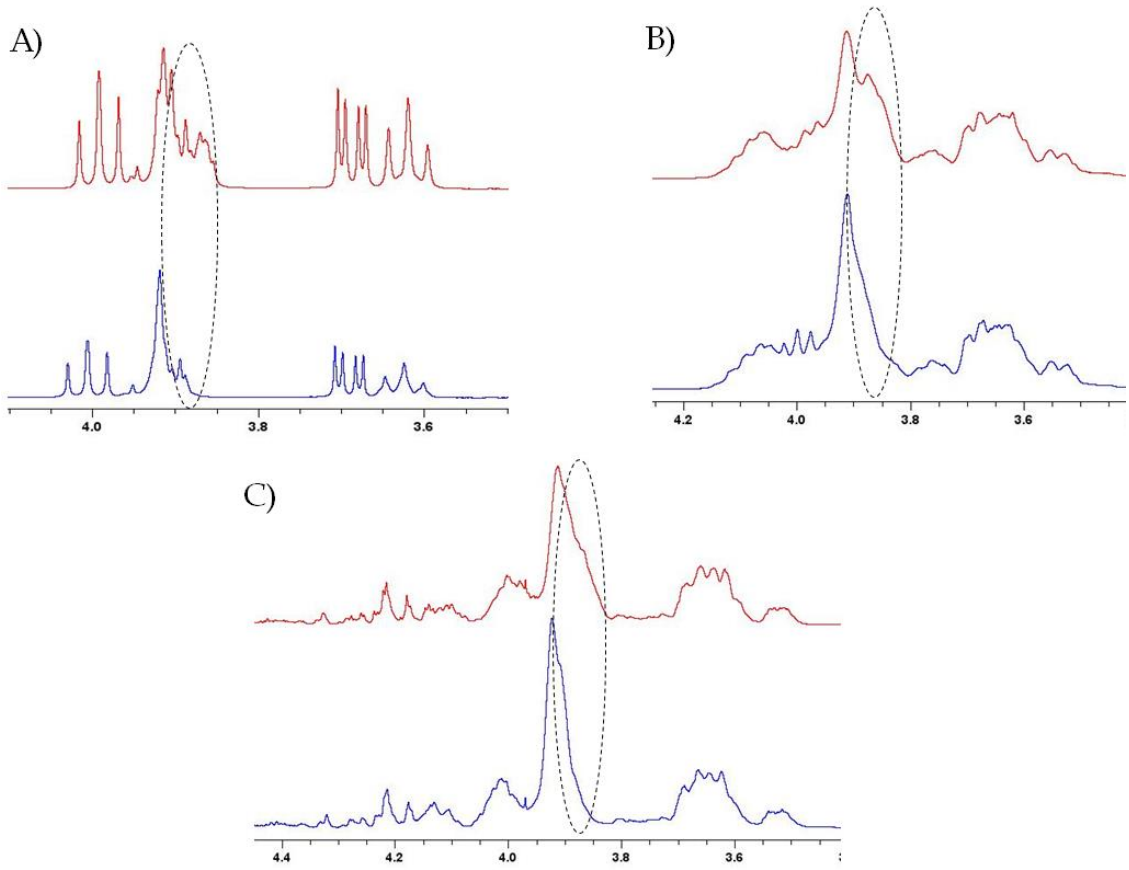

Figure III.9: Comparison between ^{1}H-NMR spectra for pure β-CDs (bottom spectra) and β-CDs:SD (top spectra) for A) β-CD B), HP-β-CD, and C) CM-β-CD

On first glance, it can be noted that for all cyclodextrins considered there is a notable modification of the H5 peak between free cyclodextrins and the complex (circled area on the spectra), indicating that the chemical environment of the H5 protons is significantly

modified, suggesting that the guest molecules enters the cavity. To determine the depth of penetration of the SD inside the β-CDs cavity, chemical displacements of protons for free β-CDs (δ0), complex (δc) and the chemical shifts ($\Delta\delta = \delta_0 - \delta_c$) are reported in Table III.2.

Table III.2: Chemical shift for the protons of β-CDs in the free and complex state with SD

	β-CD:SD			HP-β-CD:SD			CM-β-CD:SD		
Protons	δ_0	δ_C	Δδ	δ_0	δ_C	Δδ	δ_0	δ_C	Δδ
H1	5.112	5.109	-0.003	5.119	5.115	-0.004	5.111	5.105	-0.006
H2	3.690	3.688	-0.002	3.656	3.654	-0.002	3.652	3.650	-0.002
H3	4.004	3.992	-0.012	4.002	3.988	-0.014	4.013	3.986	-0.027
H4	3.624	3.621	-0.003	3.542	3.539	-0.003	3.528	3.525	-0.003
H5	3.894	3.867	-0.027	3.901	3.873	-0.028	3.907	3.868	-0.039
H6	3.918	3.914	-0.004	3.913	3.915	0.002	3.925	3.917	-0.008

It can be noted that for all β-CDs, the only protons that undergo a notable shift between the free and complex states are H3 and H5. Additionally, the chemical shift related to H3 is lower than the one related to H5. As illustrated in Figure III.7.B., H3 and H5 protons are located inside the cyclodextrin's cavity, with H3 protons near the wide extremity of the β-CDs and H5 protons near the narrow side. In this case, Δδ(H5) > Δδ(H3), which indicates that we have a deep penetration of the guest molecules inside the cyclodextrin cavity [40], [41]. Additionally, it can be noted that Δδ(H3) and Δδ(H5) are similar for β-CD and HP-β-CD (Δδ(H3) = -0.012ppm and -0.014ppm, Δδ(H5)= - 0.027ppm and -0.028 ppm, respectively), while slightly higher for CM-β-CD (Δδ(H3) = - 0.027, Δδ(H5)= - 0.039 ppm), which can indicate a deeper penetration of SD inside CM-β-CD than for the two other β-CDs considered. One hypothesis to explain this particularity would be the extension of the lipophilic cavity due to the presence of carboxymethyl groups grafted on the C6 carbons of the CM-β-CD, located on the narrow side of the CD. To determine the orientation of SD molecules inside the cyclodextrin cavity, the chemical shift of the specific SD peak between 8.8 ppm and 6.4 ppm for the free species and the complex was analyzed. The corresponding spectra are presented in Figure III.10 and the chemical displacements of protons for SD (δ0), complex (δc) and the chemical shifts ($\Delta\delta = \delta_0 - \delta_c$) are reported in Table III.3.

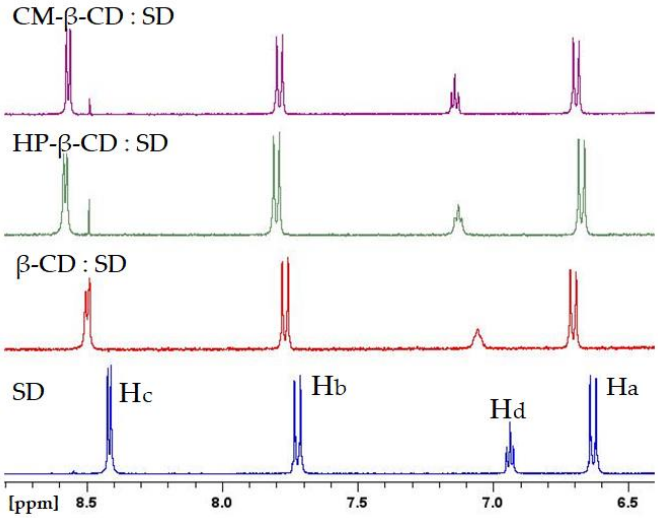

Figure III.10: H¹-NMR spectra for A) SD B) β-CD:SD C) HP-β-CD:SD D) CM-β-CD:SD

Table III.3: Chemical shift for the protons of SD in the free and complex state with native and modified β-CDs

	SD	β-CD:SD		HP-β-CD:SD		CM-β-CD:SD	
Protons	δ_0	δ_C	$\Delta\delta$	δ_C	$\Delta\delta$	δ_C	$\Delta\delta$
Ha	6.630	6.681	0.051	6.674	0.044	6.693	0.063
Hb	7.722	7.787	0.065	7.804	0.082	7.789	0.067
Hc	8.415	8.551	0.136	8.581	0.166	8.567	0.152
Hd	6.935	7.128	0.193	7.132	0.197	7.141	0.206

The SD protons with the largest chemical displacement when in complexations for all βCDs are Hc and Hd, with 0.136 ppm and 0.193 ppm for β-CD:SD, 0.166 and 0.197 ppm for HP-β-CD:SD and 0.152 ppm and 0.206 pm for CM-β-CD:SD, respectively. As illustrated in Figure III.7.A., Hc and Hd protons are located on the pyrimidine ring. If we consider that the higher the chemical displacement of a proton, the deeper it is included into the cyclodextrin, it can be concluded that the pyrimidine moiety is included inside the lipophilic cavity during the inclusion process.

Drug inclusion into the β-CDs cavity was attempted to be observed by two-dimensional rotating frame Overhauser experiments (2D ROESY), but it was not conclusive, hence, no special correlation stain could be observed under the experimental conditions tested. The main hypothesis to explain why no correlation stains were observed while ^{1}H-NMR proved deep inclusion of SD in β-CDs with interactions between H3/H5 β-CD's protons and Hc/Hd SD's protons, is the sample preparation. Indeed, the inclusion complexes were prepared by

freeze-drying in order to have only complexed or naturally solubilized SD (hence no saturation of SD that could precipitate). With the freeze-drying protocol used, the cyclodextrin solutions were prepared at saturation to solubilize a maximum amount of SD. However, by preparing it in this way, there is a significant surplus of β-CDs compared to SD, resulting in important background noises due to β-CD- β-CD interactions. To obtain results with 2D-NMR, it would be necessary to optimize the preparation of the inclusion complex.

III.1.3.4. Role of ionic charge with test of SSD

One method to characterize the inclusion complex formation and their stability in solution is Isothermal Titration Calorimetry. This technique was specifically developed to study the molecular interactions, which differentiates it from other characterization techniques, such as PSD. Using PSD, the measurement of stability is based on non-direct observations of changes in the physicochemical properties of host and guest molecules (solubility in the case of PSD). In 1978, Bender and Komiyama [26] reported that the complexation process is characterized by a gain of enthalpy and a loss of entropy of the host-guest system, making ITC perfectly suited for the characterization of the inclusion complex formation in solution [42]. To conduct ITC experiments, the concentrations of molecules in the sample cell should be below the saturated concentrations, thus the SD and SSD solutions were prepared at 40 μM. The β-cyclodextrin solutions in the syringe (15 mM) were close to the maximal solubility of β-CD. The ITC experiments were conducted at 25 °C and pH 6 in a KH_2PO_4/NaOH buffer. Figure III.12. shows typical β-CD titration data in SD and SSD. Thermograms are represented at the top, where each peak corresponds to one injection of the β-CD solution. Integration of this curve and subtraction of the dilution enthalpy for the control sample are shown in the bottom curve, with the fit calculated using the analysis software and with the hypothesis that the inclusion occurs with a 1:1 stoichiometry as previously reported in the literature [17], [22]. The calculated K_D and K_F values are presented in Table III.4.

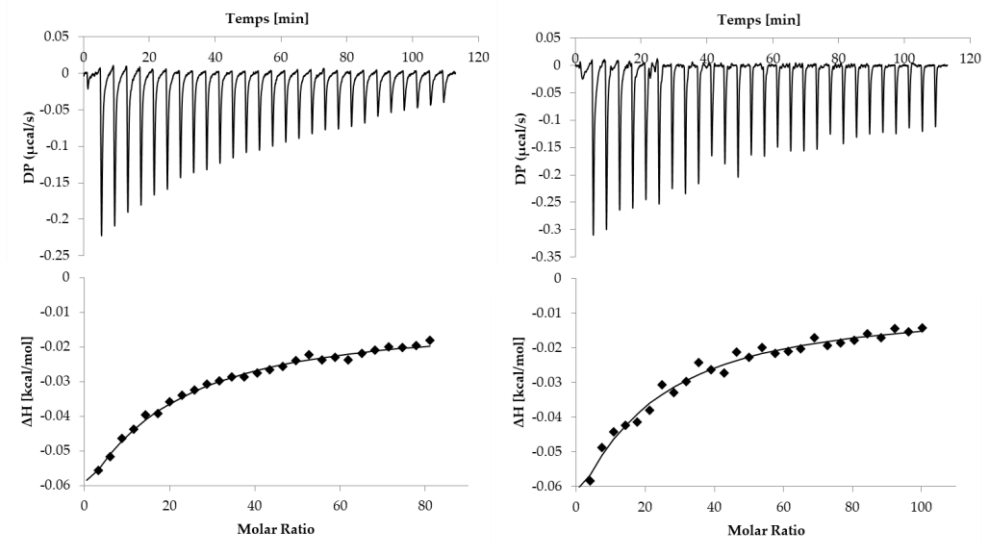

Figure III.11: Raw thermogram (at the top) and enthalpic curves (at the bottom) of an ITC titration for (Right) SD solution (40 µM) with a solution of β-CD (15 mM) at 25°C and pH 6 (Left) SSD solution (40 µM) with a solution of β-CD (15 mM) at 25°C and pH 6.

Table III.4: Association/Dissociation constant determined by ITC for β-CDs:APIs inclusion complexes

Buffer pH 6	Sulfadiazine (SD)		Silver sulfadiazine (SSD)	
Cyclodextrin	K_D [M]	Estimated K_F [M^{-1}]	K_D [M]	Estimated K_F [M^{-1}]
β-CD	2.00E-03 ± 0.20E-03	505 ± 51	2.16E-3 ± 0.28E-03	470 ± 61
HP-β-CD	2.19E-03 ± 0.34E-03	467 ± 72	1.92E-3 ± 0.27E-03	532 ± 77
CM-β-CD	0.93E-3 ± 0.10E-03	1087 ± 116	1.52E-3 ± 0.22E-03	672 ± 97

The titration curves obtained confirm that complexation occurs between the β-CDs and the selected APIs. It should be noted that the values of the formation constant for β-CD and HP-β-CD with SD (505 ± 51 M^{-1} and 467 ± 72 M^{-1}, respectively) and SSD (470 ± 61 M^{-1} and 532 ± 77 M^{-1}, respectively) are very close to each other, showing that the presence of the hydroxypropyl function on HP-β-CD does not impact the inclusion driving force. For CM-β-CD, the value of the formation constant K_F with SD (1087 ± 51 M^{-1}) at pH 6 is much higher (almost doubled).

Additionally, it is worth noting that the formation constant of CM-β-CD with SSD is lower (672 ± 97 M^{-1}) compared to CM-β-CD with SD (1087±116). This can be explained by the potential interactions between the negative charges present in both CM-β-CD and SSD at the pH considered. Moreover, this indicates that the presence of charges on CM-β-CD has an impact, although limited, on the complexation process with the selected APIs. It should also be noted that the values of association/dissociation constant measured for β-CDs:SD and β-

CDs:SSD systems are in the same order of magnitude, indicating that a single API can be considered as a model molecule to study the beneficial impact of β-CDs for both SD and SSD in further studies.

III.1.3.5. Comparison of the methods

The values of the formation constant determined by PSD are slightly lower than those determined by ITC. This can be explained by several factors. First, the pH and solvent used were different for the two analyses (buffer pH 6 for ITC and MilliQ water at pH7 for PSD). This can impact the complexation process, especially for charged molecules. Hence the most notable difference was observed for CM-β-CD:SD systems, where carboxylate groups were grafted on the primary face of the β-CDs (i.e. on primary hydroxyls in C6 position). Secondly, since both experimental methods do not rely on the same physicochemical properties, a direct comparison might not be pertinent. As shown by the difference in association constants between CM-β-CD:SD and CM-β-CD:SSD (due to the repulsion between the negative surface charges of CM-β-CD and SSD), ITC is sensitive to both complexation and adsorption. PSD is only sensitive to the increase in solubility of the guest molecule, and not to molecules potentially adsorbed on the β-CD surface. However, both experiments proved that SD and the various β-CDs form inclusion complexes in the liquid state, that β-CD and HP-β-CD exhibit similar behavior while chemical modifications of CM-β-CD induce a slightly different complexation mechanism.

III.1.4. CONCLUSION

In this study, we investigated the formation of inclusion complexes between SD and various β-CDs. The Phase Solubility Diagram (in water at pH 7) confirmed the 1:1 inclusion stoichiometry, with a formation constant ranging from 197 to 245 M^{-1}. Even though the values are low, they are significant enough to consider that the use of β-CDs is beneficial for increasing solubility and bioavailability of SD. The impact of complexation on properties other than solubility was illustrated with X-ray diffraction and Differential Scanning Calorimetry. The ^{1}H-NMR spectra for pure molecules and freeze-dried inclusion complexes were used to elucidate the penetration depth of SD inside the β-CDs cavities as well as the orientation of SD in this complex, highlighting that CM-β-CDs induce deeper penetration than other β-CDs. Finally, Isothermal Titration Calorimetry measurements also highlighted the impact of chemical modifications of β-CDs, with β-CD and HP-β-CD exhibiting similar behavior while CM-β-CD was more sensible to pH due to its ionic charges.

All these results were necessary to validate the choice of SD as a model molecule in the following studies, and was crucial for the characterization of release as well as antimicrobial properties (described in the next sub-chapter).

Functionalization of toCNFs with various β-CDs was characterized in the previous sections of the manuscript, as well as the inclusion complex formation between β-CDs and Sulfadiazine (SD). The objective of the next sub chapter is then to assess the release properties and antibacterial activity of toCNF/ β-CD/SD materials in the form of films and cryogels.

CHAPTER III.2. DRUG RELEASE AND ANTIMICROBIAL PROPERTIES OF TOCNF/Β-CDS/SULFADIAZINE FILMS AND CRYOGELS.

Inspired from paper: ***B. Michel,*** *E.B. Heggset, K. Syverud, A. Dufresne, J. Bras, Drug release and antimicrobial properties of TEMPO-CNF/β-CDs/Sulfadiazine films and cryogels. Submitted to Carbohydrate Polymers (Elsevier) in March 2022.*

Abstract: Active Principal Ingredient (API) encapsulation through adsorption and physical entrapment onto TEMPO-oxidized cellulose nanofibrils (toCNFs) is possible, but challenges such as burst release and use of low water-soluble API such as sulfadiazine (SD) are yet to be addressed. The objective of this study is to assess the release properties and antibacterial activity of toCNF/ β-CD/SD materials in the form of films and cryogels. Release in sink conditions was achieved with a release of ≈ 95 % SD after 60 min for films casted at neutral pH and ≈85 % SD after 120 min for films processed at acidic pH, indicating the impact of pH for the release of SD from the films. This result highlights the importance of the toCNF network structure, which is tightened at acidic pH for toCNFs due to its carboxylic content, reducing the burst effect phenomena. Antibacterial activity against *Staphylococcus aureus* (*S. aureus*) and *Escherichia coli (E. coli)* was assessed and the results showed a clear beneficial impact using β-CDs. An antibacterial effect for toCNF/SD films is confirmed for 3 successive applications whereas an antibacterial effect for a toCNF/CMβCD/SD film is prolonged up to 7 successive applications. The use of a porous structure such as cryogels allows sustaining antibacterial activity up to a minimum of 18 successive applications. These toCNF materials functionalized with β-CDs without any use of cross linker were found to be beneficial for topical delivery of a low water soluble API and thus could be used as a novel wound dressing. The graphical abstract of this study is presented in Figure III.12.

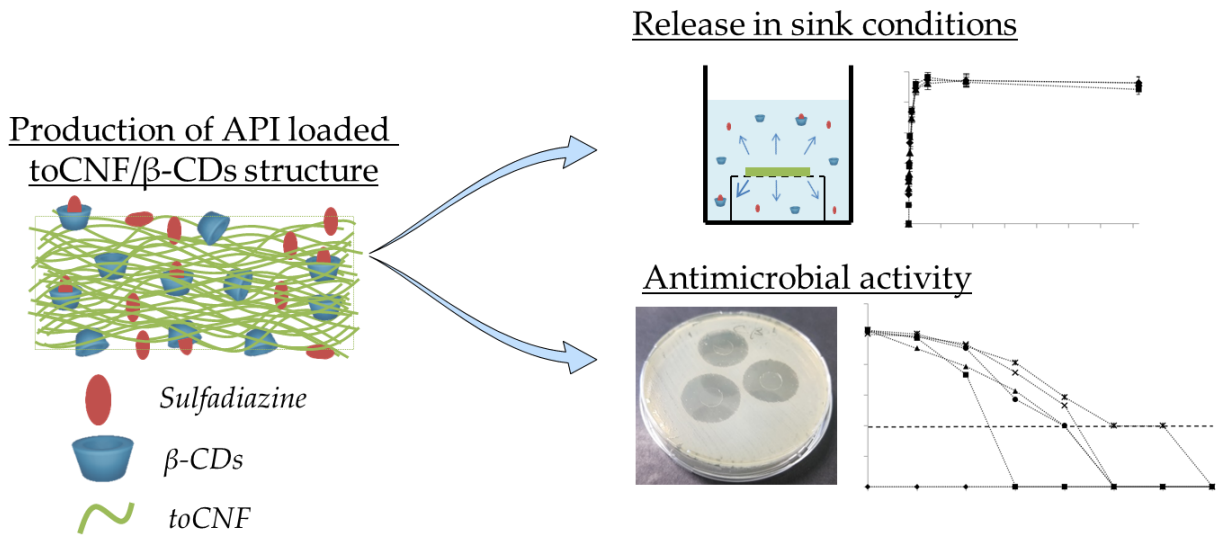

Figure III.12: Graphical abstract for Chapter III.2.

III.2.1. INTRODUCTION

Cellulose nanofibrils (CNFs) have recently been considered as promising materials for biomedical applications. These materials present many qualities for such applications, such as their biobased nature, chemical tunability, water sorption and mechanical properties, and most interestingly their biocompatibility and their ability to form an entangled nanosized network. As such, recent reviews have been published covering the use of CNFs as biomaterials for tissue engineering or drug release [2], [43]–[46]. CNFs can be used in drug release either as drug excipients (film formers, binding agents or stabilizers for example) or as drug delivery matrix (carrier system) [47]. The major challenges for drug release applications are (i) the loading of the active principle ingredient (API), (ii) the reduction of the burst effect (i.e. the almost immediate release of the loaded API), but also (iii) the increase of the bioavailability of poorly water-soluble APIs. The first use of CNF materials in a film-like matrix system for drug release was reported by Kolakovic et al. in 2012 [48]. They reported drug loading with a filtration method in the range of 20-40 % with films exhibiting excellent mechanical properties and sustained release up to 90 days, explained by the tight fiber network around the API molecules. This sustained release due to physical entrapment of APIs was also reported by Lavoine et al. [49], who obtained a prolonged and controlled release of various APIs by coating CNFs onto a paper substrate. Durand et al. [9] successfully loaded APIs into CNF membranes and highlighted the importance of films thickness. Other loading routes for API have been studied, such as impregnation using supercritical CO_2 conditions [50]. Additionally, the different grades of CNFs available through various pretreatments and production methods [51] make a wide variety of chemical modifications of CNF materials with APIs possible. TEMPO-oxidized CNFs (toCNFs), obtained via the regioselective oxidation of the C6 primary hydroxyls of cellulose into C6 carboxylates in the presence of (2,2,6,6-tetramethyl-piperidin-1-yl)oxyl, also known as TEMPO, first proposed by Saito et al. [52], is therefore an interesting platform for API immobilization with the presence of carboxylic groups. As such, Durand et al. [53] proposed the covalent grafting of a pro-drug onto such toCNF for controlled drug release.

The β-cyclodextrins, cyclic oligosaccharides composed of 7 anhydroglucose units (AGU) with α-1,4 glycosidic linkages, have the property of forming inclusion complexes with

lipophilic molecules, which is an interesting strategy to entrap active molecules onto a toCNF-based drug release device. Functionalization of CNFs with β-CDs have been reported with various strategies, such as the use of a cross-linker [54]–[57], esterification with thermal treatments [58] or adsorption/coatings [59]. However, all previous studies pointed out the challenge in measuring and characterizing CNF/β-CD interactions due to their chemical proximity. The characterization and quantification of the functionalization of toCNFs with various β-CDs are reported in Chapter II.2, while the production and characterization toCNF/β-CDs films and cryogels are reported in Chapters II.1 and II.3. The results indicate that the functionalization by physical adsorption of toCNF matrixes with β-CDs was carried out efficiently with higher adsorption for modified β-CDs compared to unmodified β-CDs. Additionally, it showed that the water sorption and mechanical properties of toCNF/β-CDs materials, alongside with the potential to form inclusion complex with lipophilic API, make these materials promising for drug release applications. To our knowledge, this is the first study on topical delivery from toCNF structures with low water-soluble API, Sulfadiazine (SD), one of the most widely used prophylactic drugs (i.e., used to prevent infections). Chapter III.1 provides an extensive study of the inclusion complex formation between SD and β-CDs, justifying the use of SD as a model molecule for this study.

The aim of this work is to prepare an enhanced toCNF/β-CD-based carrier system for topical release of sulfadiazine. Different protocols were implemented to highlight the impact of process parameters on SD release from toCNF/ β-CDs materials. Release protocols in sink conditions (i.e. a release medium volume of at least three to ten times the saturation volume [60]) were performed to assess the impact of process parameters over the sulfadiazine release. Due to the large volume of medium release, the beneficial impact of β-CDs due to inclusion complex formation with SD might not be observable. In order to more appropriately mimic the application conditions of our devices, namely as a wound dressing for topical delivery, microbiology experiments, adapted from the Kirby-Bauer disk diffusion susceptibility tests [61], were conducted.

III.2.2. MATERIALS AND METHODS

III.2.2.1. MATERIALS

A 1 wt% toCNF suspension was purchased from the University of Maine (Lot # 2019-FPL-CNF-123). Sulfadiazine (SD, M = 250.28 g/mol), β-Cyclodextrin (β-CD, M = 1134.98 g/mol), 2-Hydroxypropyl-β-Cyclodextrin (HP-β-CD, DS = 3, M = 1380 g/mol) were purchased from Sigma-Aldrich. Carboxymethyl- β-Cyclodextrin Sodium Salt (CM- β-CD, DS = 3.5, M = 1415 g/mol) was purchased from CycloLab (Hungary). The degree of substitution of the different cyclodextrins is given for one cyclodextrin molecule meaning that the Maximal DS is 21. Mueller-Hinton agar was purchased from Sigma-Aldrich and was composed of 2.0 g/L beef infusion solids, 1.5g/L starch, 17.5 g/L casein hydrolysate and 17.0 g/L agar. Nutrient broth was purchased from WVR, and was composed of 15.0 g/L pepton, 3.0 g/L beef extract, 6.0 g/L NaCl and 1.0 g/L glucose. *S. aureus* (ATCC 6538 Q+) and *E.coli* (ATCC 8739 Q+ KT/100 TST) were purchased from ThermoScientific and stored at 4°C prior to utilization.

III.2.2.2. METHODS

III.2.2.2.1. toCNF FILMS AND CRYOGELS PROCESSING

The preparation of the suspensions followed the same first steps for both films and cryogels:

0.40 g of dry toCNFs were weighed and diluted with water to a total volume of 50 mL. The suspension was dispersed for 2 min at 7,000 rpm with an UltraTurrax at room temperature. β-CDs (0.04g), SD (0.02g) and 0.1M HCl (2 mL) were added to the relevant samples. The suspensions were magnetically stirred for 1h and placed in an ultra-sonic bath for 3 min.

For films, the suspension was then cast in petri dishes (9 cm diameter) and stored in an oven at 40°C for 18h. The resulting films (60 g/m²) were stored in closed petri dishes at room temperature.

For cryogels, the suspensions were then poured into a 24-well plate (3mL per well, 1.5 cm height) and put in a freezer at -20°C for 24 h before freeze-drying (ALPHA 2-4 LDplus, Christ ®). The resulting cryogels were stored in closed petri dishes at room temperature.

III.2.2.2.2 Drug Release in liquid

III.2.2.2.2.1 Continuous release

The samples were immersed in a 600 mL volume of deionized water in order to achieve sink conditions. They were placed on a metal mesh inside the container to ensure equivalent diffusion of the released molecules as well as to limit the physical degradation of the samples. The containers incubated at 37 °C under stirring (100 rpm) to ensure constant agitation and homogenization of the release medium. 2 mL aliquots were withdrawn from the release medium at predetermined time intervals, mixed with 2 mL EtOH to ensure that the SD molecules will not be present in the inclusion complex under UV-spectrophotometry analysis, as this may impact the spectral response. The amount of sulfadiazine was measured by UV spectroscopy at a wavelength of 261 nm using a SD calibration curve in a $1{:}1_{volume}$ H_2O/EtOH solution:

$$Absorbance\ at\ 261\ nm = 18711 \times C\ (R^2 = 0.9967)$$

where C is the concentration of sulfadiazine in mol/L. Blank experiments were performed to measure the impact of toCNF release on the spectral response at 261 nm and absorbance linked to this release was suppressed from the SD release experiments. Each sample was analyzed in triplicate.

III.2.2.2.2.2. Intermittent release

Samples were pinned to a lightweight polystyrene support and set to float on the surface of a 600 mL volume of deionized water. The containers were incubated at 37°C, 100 rpm to ensure a constant agitation and homogenization of the release medium. Every ten minutes, samples were transferred to a new release medium, while 2 mL samples were withdrawn from the previous release media and mixed with 2 mL EtOH. Quantification of SD released was performed similarly as in the continuous release protocol. Each experiment was done in triplicate.

III.2.2.2.3. Antimicrobial properties onto Agars

All microbiological experiments were performed in a class-2 laboratory under a biological safety cabinet. All consumables, equipments and chemicals were either

individually packed in sterile packaging or sterilized in autoclave at 120°C for 15 min before use.

III.2.2.2.3.1. Preparation of the pre-inoculum

The bacterial strain of *E. coli* and *S. aureus* are initially in lyophilized form. The strains were rehydrated and 10 µL aliquots of the rehydrated products were added to 20 mL of nutrient broth in a previously sterilized flask and incubated for 24h at 37 °C under 100 rpm orbital shaking. 10 µL of this solution were then collected with an inoculation loop to transfer the bacterial colony to nutrient agar. The bacterial strains were then transplanted every 2 weeks onto freshly prepared nutrient agar. The pre-inoculum was prepared by adding 1 CFU (colony forming units) from transplanted bacteria in 20mL of nutrient broth in a sterilized flask. Cultures were grown overnight at 37°C under horizontal shaking at 100 rpm.

III.2.2.2.3.2. Zone of inhibition 24h

Zone of Inhibition (ZOI) measurements were designed with reference to the CA-SFM recommendations for the implementation of antibiograms [62]. Mueller-Hinton agars were prepared by adding 10 mL of the autoclaved commercial preparation onto sterile Petri dishes (d = 9 cm). Inoculums at 0.5 McFarland were prepared by diluting the pre-inoculum with nutrient broth. Turbidity measurements were performed using a densitometer Biosan DEN-1. Mueller-Hinton agar plates were inoculated with swab in 2 directions to form the bacterial mat. Samples were cut into 1 cm diameter discs (for films) and used as produced (for cryogels) and deposited on freshly inoculated MH-agar surface. The Petri dishes were subsequently incubated for 24h at 37 °C. Inoculum preparation, inoculation and incubation were performed within a 15 min period. For each samples presenting an antibacterial behavior, the diameter of the inhibition zone was measured with a ruler (± 0.5 mm). At least 5 diameter measurements were performed for each sample, and each sample was done in triplicate.

III.2.2.2.3.3. Successive zone of inhibition

For successive ZOI, bacterial mats were prepared as previously described. The samples were put in contact with the bacterial mat and incubated for 1h at 37 °C. After 1h, the samples were collected and deposited on a freshly prepared bacterial mat and put in

incubation 1h at 37°C, while the precedent media in contact with the sample was incubated at 37°C for 23h. This operation was repeated to obtain a number of successive release. All analysis was done in triplicate.

III.2.2.2.4 Scanning Electron Microscopy

Scanning electron microscopy (SEM) images were performed with ESEM (Quanta 200, FEI, Japan). Cryogel cross-sections were cut with a razor blade. SEM observation was carried out on cross-sections after carbon sputter coating of 5 nm, with a tension of 10 kV and a spot size of 3.5. The working distance was set between 9.5 mm and 11.5 mm depending on the sample. At least 10 images were acquired for each sample and the most representative is used for the discussion.

III.2.3. RESULTS AND DISCUSSION

III.2.3.1. IMPACT OF CASTING PROCESS ON RELEASE PROFILES

Based on recent literature, CNF-based nanostructured network seems to be a valid candidate for loading and release of API. Here, the release profiles of SD from toCNF membranes were investigated. The first protocols implemented were the release profiles in sink conditions, i.e. samples immersed in high volume of deionized water under controlled conditions (37 °C and under 100 rpm orbital shaking). Release profiles from both cryogels and films were investigated, however, cryogels undergo more physical degradation under shaking, causing an arbitrary release of CNFs into the release medium, which impacts the UV-measurements used to determine the amounts of sulfadiazine released. Conversely, the films retain structural integrity when immersed under agitation. For this reason, the release profiles presented here are those obtained only for films. Since Durand et al. [9] highlighted the impact of the thickness of the CNF membrane on the release profiles, all films were produced with a similar grammage of approximately 60 g/m². Due to the presence of carboxylic groups on the surface of toCNF, the impact of pH of casting on the release profiles were investigated by processing films at neutral pH and at acidic pH with the addition of HCl. One of our recent study prove that pH influenced the structure and entanglement of toCNFs [63]. Finally, to discuss the beneficial impact of various types of β-CDs over the release in sink conditions, films containing β-CDs were analyzed. The two types of β-CDs considered for this part are natural β-CD and CM-β-CD, which was proven in Chapter II.2 to adsorb the most to toCNF. The final release profiles are presented in Figure III.13.

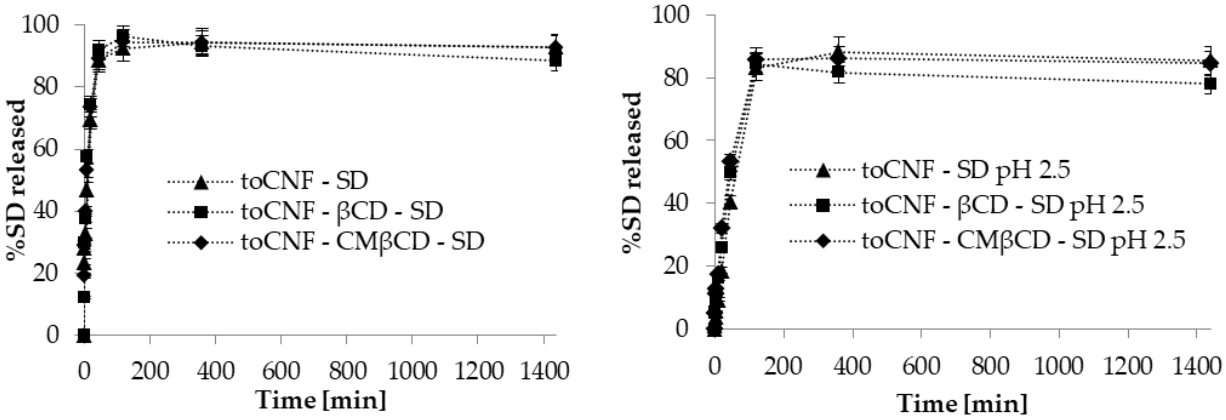

Figure III.13: Continuous release in sink condition for SD from films cast at neutral pH (left) and acidic pH (right)

The release profiles for films casted at neutral pH indicate a delayed burst effect, with a regular release of SD and with a plateau at around 95% of SD released reached after 60 min. For films casted at acidic pH, the release appears to be sustained for a longer period, with a plateau at around 85% reached after 120 min. These results confirm the influence of pH on the structure of the toCNF films with CD. According to these release profiles, a schematic description of the release of SD from films is proposed in Figure III.14. Fig III.14.A proposes a schematic description of the experimental setup, and highlights the multiple release directions available as well as the potential release of individual CD, individual SD or the complex itself. As illustrated in Figure III.14.B., SD molecules can be either (i) adsorbed on the surface of a nanofiber at the surface of the film, (ii) physically entrapped into the toCNF network or (iii) in inclusion complex with a cyclodextrin. When immersed in the release medium, the SD molecules, βCDs and the complexes not strongly adsorbed on the surface of the films are the first to be released. This explains the initial burst release observed on the release profiles in Figure III.13. Finally, swelling of the films occurs over time and allows the release of the previously entrapped molecules, as shown in Figure III.14.C.

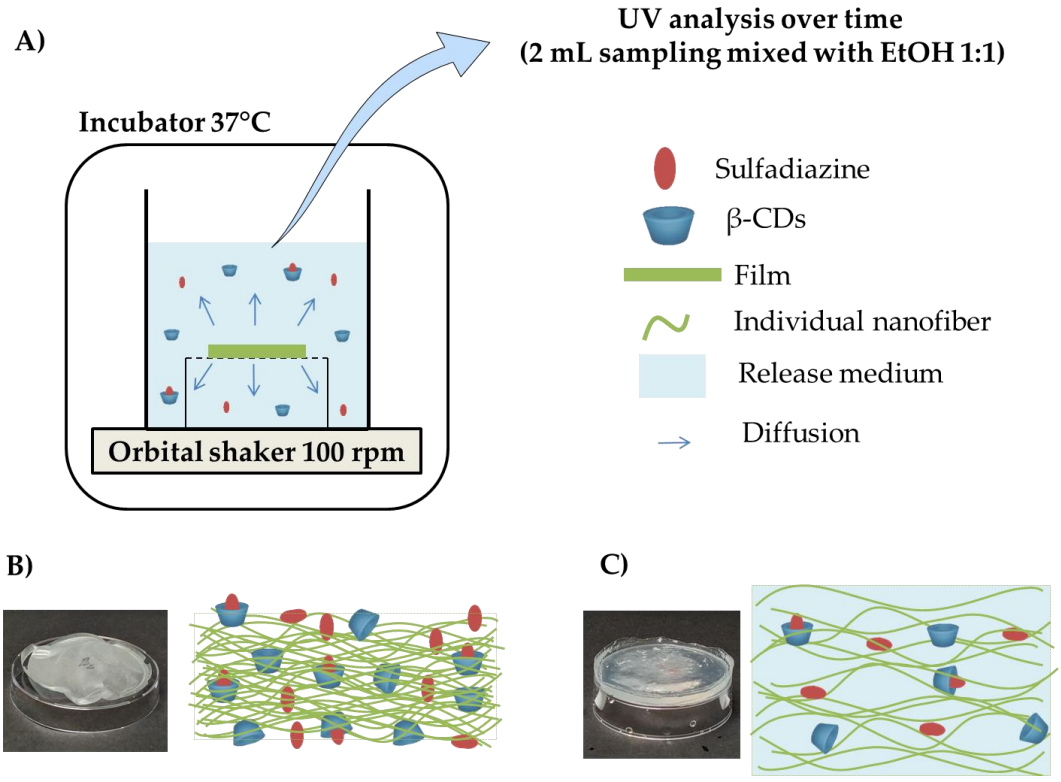

Figure III.14: A) Schematic representation of continuous release protocol B) Photo and schematic representation of a dry film C) Photo and schematic representation of a swollen film

To better understand the impact of the various parameters, the amounts of SD released after specific time intervals are given in Table III.5.

Table III.5: Sulfadiazine released after given time from toCNF/β-CD films.

	%SD released				
	1 min	**10 min**	**45 min**	**2h**	**24h**
Cast at neutral pH					
toCNF - SD	23 ± 2	47 ± 4	89 ± 5	93 ± 2	93 ± 5
toCNF - βCD - SD	12 ± 2	58 ± 3	92 ± 5	96 ± 3	88 ± 3
toCNF - CMβCD - SD	15 ± 3	53 ± 4	89 ± 6	95 ± 5	93 ± 5
Cast at acidic pH					
toCNF - SD pH 2.5	1 ± 1	10 ± 2	41 ± 4	83 ± 4	86 ± 5
toCNF - βCD - SD pH 2.5	6 ± 2	16 ± 2	49 ± 6	84 ± 2	78 ± 2
toCNF - CMβCD - SD pH 2.5	5 ± 1	18 ± 3	53 ± 4	86 ± 4	84 ± 3

For films casted at either neutral or acidic pH, it can be observed that the addition of β-CDs on the nanostructured toCNF network does not cause any significant impact on the release profiles, both for the release kinetics and for the value of the final plateau. This result was expected considering the sink conditions in which these experiments were conducted. Indeed, the two main benefits using cyclodextrins, the increase in SD solubility and the encapsulation of API molecules, are not observable in such a high volume of water corresponding to 5 times the volume of the saturated solution. Hence, as displayed by the differences between films casted at neutral or acidic pH, the release in these particular experimental conditions is mainly driven by the physical entrapment into the toCNF matrix. The acidic pH turns the carboxylic content of toCNFs to be in its carboxylic acid groups, and this functionality induces more hydrogen bonding between the nanofibrils, which tightens the network and limit the release. As an illustration, for films casted at neutral pH, after 45 min of release, around 90% of the SD was released for all samples whereas only around 50% of the SD was released for films cast at acidic pH. To put this results in perspective, Durand et al. [9] reported 70% of ciprofloxacin released from a CNF membrane of similar grammage after 30 minutes. Additionally, it was expected that 100% of SD would be released for each sample, which was not observed here. This may be explained by the irreversible adsorption of some SD molecules onto toCNFs via hydrogen bonding, favored for films presenting carboxylic acid rather than carboxylate groups.

This first protocol highlighted the impact of the structured toCNF network (strengthened through an acidic pH of the process) on the continuous release of SD in sink conditions. However, no significant beneficial impact of β-CDs over the release properties was observed under these experimental conditions. With this in mind, a second protocol of release was implemented.

An intermittent release protocol was set up to simulate repeated washings. Samples were pinned to a polystyrene support and put to float on a large volume of deionized water to meet the sink conditions, with a renewal of the release medium every 10 min to promote the SD release by altering the molecule balance. Each renewal of the release medium will be referred as "washing step". The amount of SD released during each washing step and a cumulative release over the number of washing steps are presented in Figure III.15.

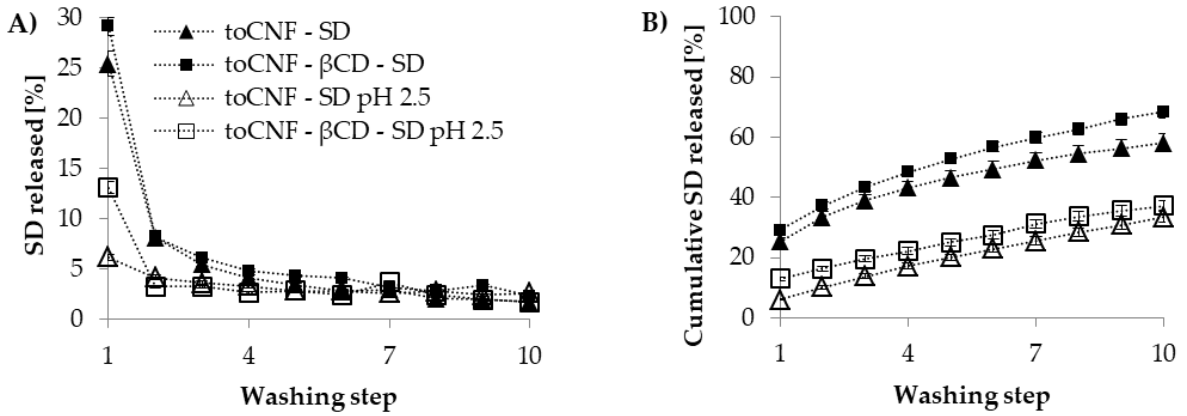

Figure III.15: Suldiazine amount (%) released at each washing step (A) and cumulative release (B).

For all samples, it can be seen that there is a decrease in the amount of SD released from the first washing steps leading to stabilization after about 5 washing steps. According to the release profiles, a schematic illustration of the intermittent release of SD from the films is proposed in Figure III.16. This high initial release corresponds to SD molecules present on the surface of the samples or those not strongly adsorbed to the matrix, (Figure III.16.A). After a few washing steps and renewal of the release medium, the films have swollen and the toCNF structures are less densely packed, and the water molecules act as a plasticizer. This swelling allow the diffusion of SD, β-CDs and inclusion complexes through the film, as displayed in Figure III.16.B. Cumulative SD release values after 1 and 10 washing steps are reported in Table III.6.

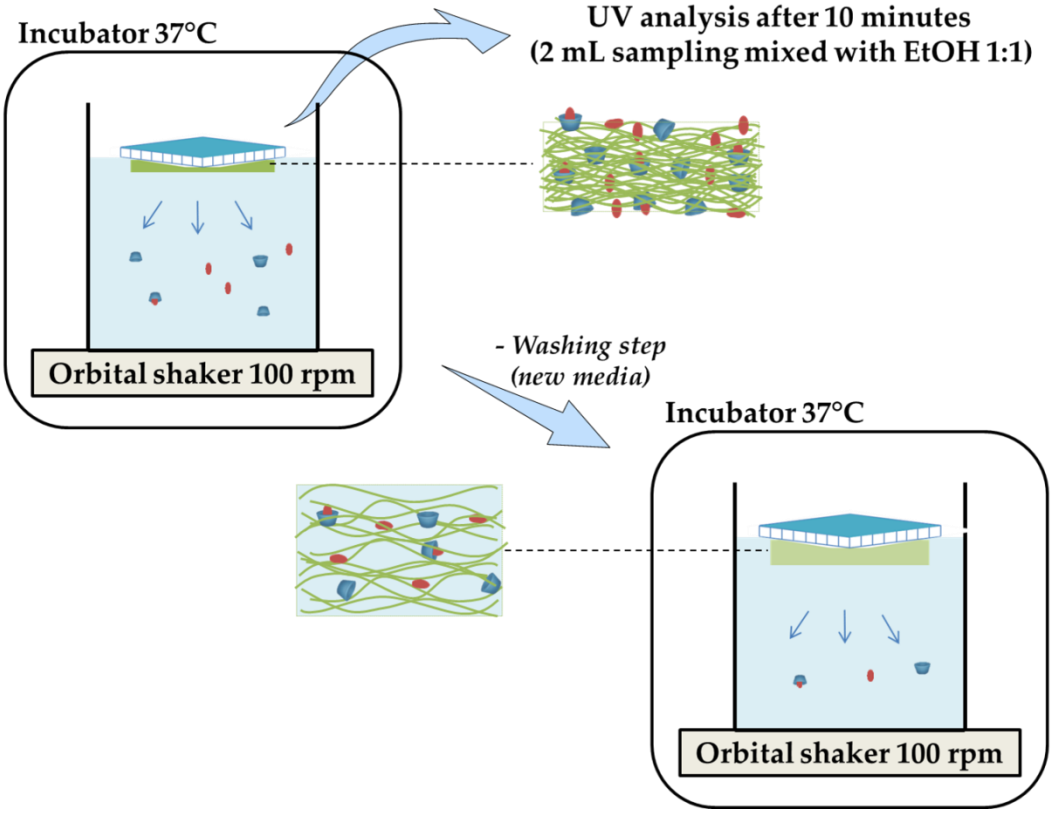

Figure III.16: A) Initial release from toCNF/β-CD/SD films B) Swelling of the films and reduced release after few washing steps.

Table III.6: Amount of sulfadiazine released after 1 and 10 washing steps

	%SD release	
	1 step	**10 steps**
Cast at neutral pH		
toCNF - SD	25 ± 2	58 ± 3
toCNF - βCD - SD	29 ± 2	68 ± 4
Cast at acidic pH		
toCNF - SD pH 2.5	6 ± 2	33 ± 2
toCNF - βCD - SD pH 2.5	13 ± 2	37 ± 4

The amount of SD released after 1 washing step is significantly different between films casted at acidic pH and neutral pH, with around 10 % and 30 % release, respectively. This confirms the observation made previously for the continuous release experiments and can be explained by the tighter toCNF network obtained at acidic pH as well as by the increased molecular interaction of SD with the carboxylic content. The amount of SD released after 1 washing step, i.e. 10 min of release, is slightly lower than the amount released after the same time for the continuous release experiments (25% and 29 % for toCNF-SD and toCNF-βCD-

SD at neutral conditions, and 6% and 13% for toCNF-SD and toCNF-βCD-SD acidic pH, respectively). This is explained by the different arrangements of the films in the release medium, i.e. full immersion for the continuous release protocols, in contact with the release medium surface for intermittent release. In complete immersion, the release of the molecules of interest can occur in all directions, while in the intermittent release protocol, only one face of the film is in contact with the release medium, implying that molecules not present on this surface initially must first diffuse through the toCNF structure prior to release. Such diffusion will prolong the release of drug or model molecule, as previously described [48], [49]. Swelling of the films during the experiments influenced their mechanical properties and the arrangement of the films on the polystyrene devices allowed the flotation to be maintained for about ten washing steps.

Both release protocols revealed that the pH and subsequent toCNF matrix structure had impact on SD release properties in sink conditions, confirming the potential of toCNF structures for drug release applications. However, no significant synergistic effect of toCNFs and β-CDs was observed. Consequently, protocols closer to the end applications of these materials, namely topical antimicrobial activity, were performed.

III.2.3.2. Antimicrobial properties: Successive zone of inhibition to assess beneficial impact of CDs.

The antibacterial activity of SD and its derivatives was previously reported [64]–[66]. SD, like all sulfonamides, is a competitive inhibitor of the bacterial enzyme dihydropteroase synthetase, and as such inhibits bacterial multiplication by disrupting the production of folic acid, which is necessary for the growth of all cells [67]. Sulfonamides have a broad spectrum of activity against most gram-positive and gram-negative species and, as a class, tend to have the same range of therapeutic actions [68]. The antibacterial activity of the produced materials was investigated on two bacterial strains *E. coli* (gram-negative) and *S. aureus* (gram-positive), which are the main pathogens in healthcare related infections [69]. It has been reported that the minimum inhibitory concentration (MIC), i.e. the minimum quantity of sulfonamide needed to inhibit the bacterial growth, is higher for *S. aureus* than for *E. coli* [70]. Antibacterial activity was assessed by the disk diffusion test, which is the most common test to evaluate the leaching on an API from a material to an agar medium, and mimics wet skin wound. A zone of inhibition (ZOI), i.e. no bacterial growth, is observed as a clear zone

around the tested materials, as illustrated in Figure III.17. The size of this ZOI depends on the diffusion of the antibiotics into the agar surface and its inherent activity against the bacterial strain. On the surfaces where release and API diffusion did not occur, or where the API concentration was not high enough to inhibit bacterial growth, dense bacterial growth is observed, as shown in Figure III.17.

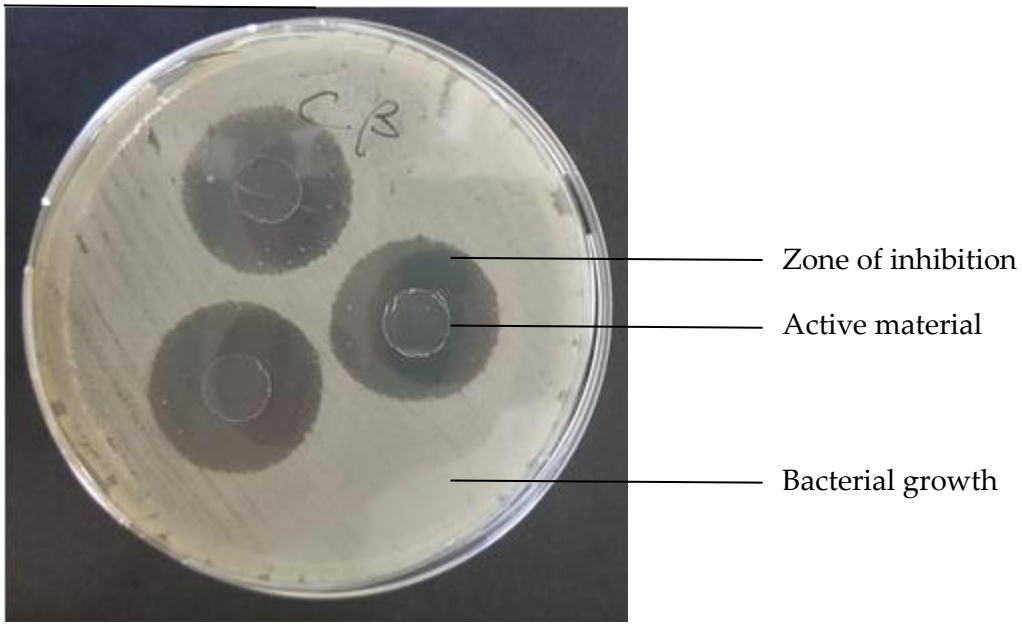

Figure III.17: Photograph of an MH2-agar medium inoculated with *E. coli* for the determination of the zone of inhibition induced by contact with an active material.

The zones of inhibition after 24h of contact in incubator at 37 °C is a quick qualitative analysis of the capacity for a medical device to release drug, as shown in other studies [9], [50]. Such ZOI are presented in Figure III.18. Reference materials, i.e. toCNFs and the different β-CDs, were individually tested and displayed no antibacterial behavior. As such, any antibiotic behavior observed is due to the antibacterial activity of SD.

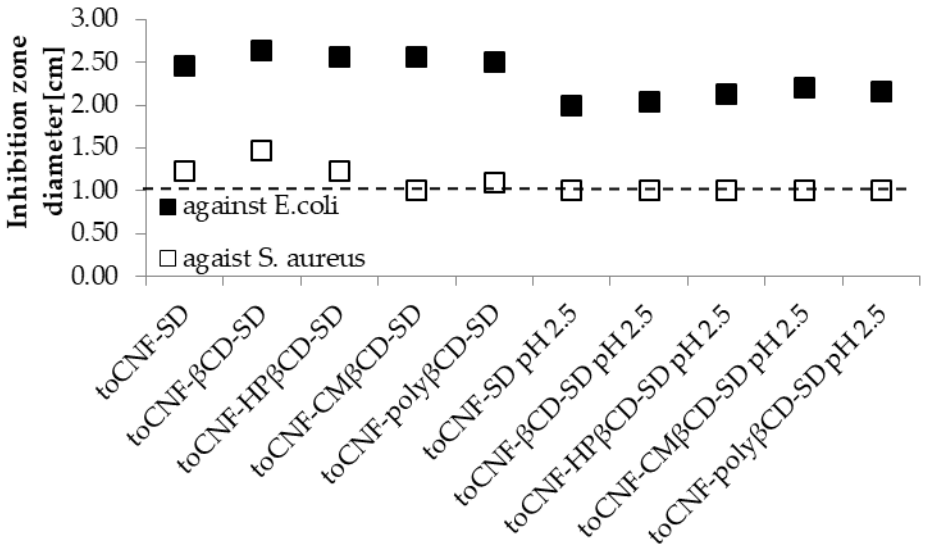

Figure III.18: ZOI against *S. aureus* and *E. coli*. Dotted line represents the diameter of the sample.

It can first be noted that the ZOIs are much larger for materials tested against *E. coli* than against *S. aureus*. This was expected since the MIC of sulfonamides is higher for *S. aureus* than for *E. coli.* A schematic representation of the diffusion phenomena at the agar surface and how it corresponds with the MIC is proposed in Figure III.19. The SD concentration at the agar surface is considered constant below the sample surface and modeled as an exponential curve decreasing with radial distance from the sample center as reported in the literature [71]. When the surface concentration is higher than the MIC of the bacterial species, growth inhibition is observed.

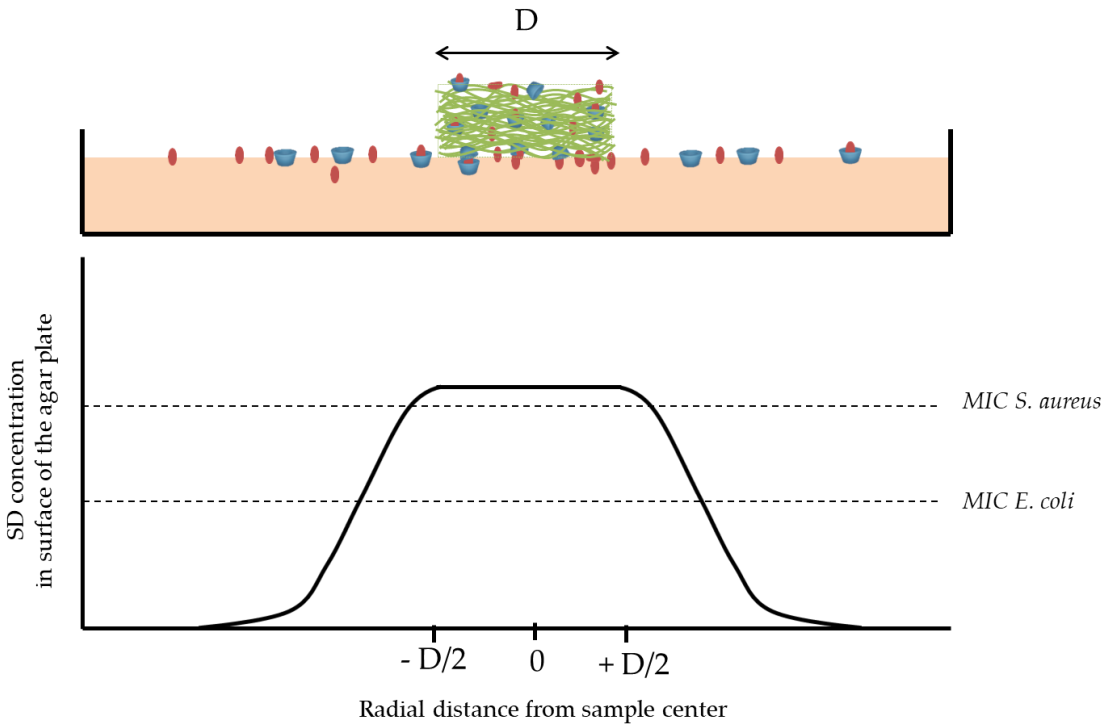

Figure III.19: Schematic representation of the API diffusion on agar surface and its link with MIC

The ZOI measured against *S. aureus* are close to 1 cm in diameter, which is the sample diameter, meaning that the diffusion of SD does not reach the minimum concentration to have a bactericidal effect outside the sample surface. For samples cast at acidic pH, which display low ZOI corresponding to the sample surface, the insufficient SD diffusion may be related to the tighter toCNF network and increased adsorption, similar to the previous release protocols.

For samples cast at neutral pH, it can be noted that toCNF-SD, toCNF-βCD-SD and toCNF-HPβCD-SD exhibited ZOIs larger than 1 cm (1.2 cm, 1.5 cm and 1.2 cm, respectively), while only toCNF-CMβCD-SD had a ZOI of 1 cm. As illustrated in Figure III.19, the antibacterial effect is (i) due to the release of SD molecules that were either adsorbed onto or entrapped within the toCNF network, but also (ii) the release from an inclusion complex while the cyclodextrin is still adsorbed on the toCNF network, or (iii) the release as inclusion complex with cyclodextrin. When released with cyclodextrin in an inclusion complex, the maximum solubility of SD is increased, thereby increasing its diffusivity on aqueous gel surface.

As reported in Chapter II.2, the adsorption strength of βCDs onto toCNF is not the same for the different CDs. It was shown that modified βCDs are more strongly adsorbed onto the

toCNF structure, especially CM-β-CD, while natural βCD undergo faster release. The hypothesis to explain the larger ZOI for toCNF-βCD-SD against *S. aureus* is the important release of the inclusion complex in addition to individual SD molecules, while the inclusion complex with CM-β-CD is strongly adsorbed onto the toCNF nanofibrils and thus does not immediately release.

For the ZOIs against *E. coli*, no significant difference was observed between the different βCD since the release of SD molecules only is sufficient to reach the MIC.

To observe a possible beneficial impact of the functionalization of toCNF with modified cyclodextrins, successive zones of inhibition were performed. These tests are known to enhance the difference between samples by visualizing the capacity to release a molecule in a novel agar media. Additionally, this test also mimics the use of wound healing dressing repetitively after cleaning of the wound. These successive ZOI tests were conducted against *E. coli*, as large ZOIs were observed for all samples against this strain, and on films casted at neutral pH, in order to highlight the impact of βCDs rather than the network structure. The ZOI measured after each successive application is presented in Figure III.20.

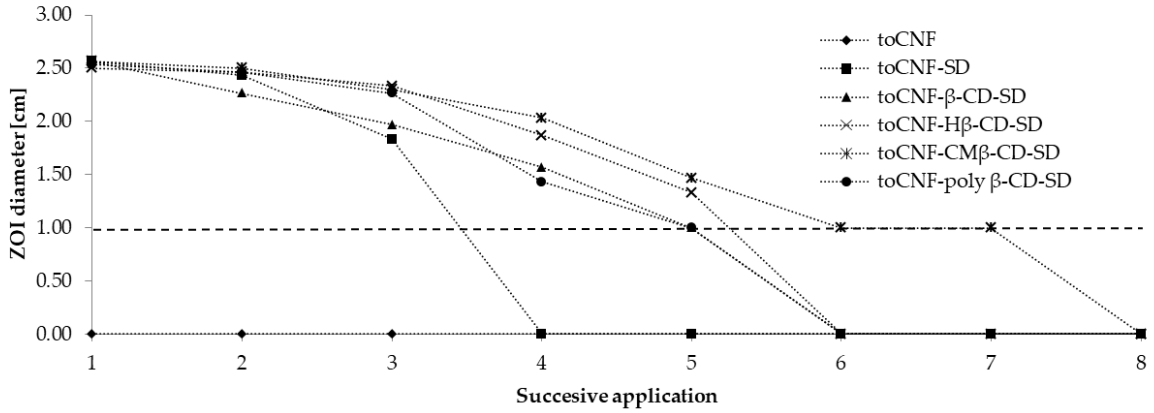

Figure III.20: Successive ZOI against *E. coli* for toCNF/β-CDs/SD films

toCNF-alone displayed no antibacterial activity, with bacterial growth even below the sample (ZOI=0). toCNF-SD showed antibacterial activity up to 3 successive applications, indicating that the toCNF structure is sufficient to limit the burst release of SD and favor a prolonged release, confirming the observation made with release in sink conditions. Materials functionalized with cyclodextrins exhibited improved antibacterial activity, up to 5

successive applications for β-CD, HP-β-CD and poly β-CD, and up to 7 successive applications for CM-β-CD.

This result is of great interest and is a confirmation that the inclusion complex formation between β-CDs and SD, reported in sub-chapter III.1, is an efficient way to enhance loading and release of this API. This confirms that the adsorption of β-CDs on toCNF structures is driving the release mechanism of toCNF-β-CDs-SD for films, as the use of CM-β-CD, which is the β-CD that adsorbs best onto toCNFs (as reported in chapter II.2 and illustrated in Table III.7), improve the release properties best. This proves for the first time that the use of CD derivatives is an innovative and efficient way to control the prolonged release of low soluble API.

Table III.7. : Comparison between adsorption, release and antibacterial activity

Sample	Estimated binding capacity by QCM-d [$\mu mol/g_{toCNF}$]	Estimated %CD released (QCM-d)	Antibacterial activity against E. coli [successive ZOI]
toCNF	/	/	0
toCNF-SD	/	/	3
toCNF-β-CD-SD	13.4	84.8	5
toCNF-HP-β-CD-SD	30.7	57.6	5
toCNF-CM-β-CD-SD	**47.6**	**32.7**	**7**
toCNF-Polyβ-CD-SD	22.0	73.8	5

III.2.3.3. IMPACT OF THE MACROSCOPIC STRUCTURE

The functionalization of toCNFs with β-CDs has a clear impact on the topical SD release from films that exhibit a densely packed and laminar structure, making them suitable for wound dressing applications. The impact of β-CDs on SD release for a more open toCNF structure was investigated by assessing successive ZOIs for cryogels, presented in Figure III.21.

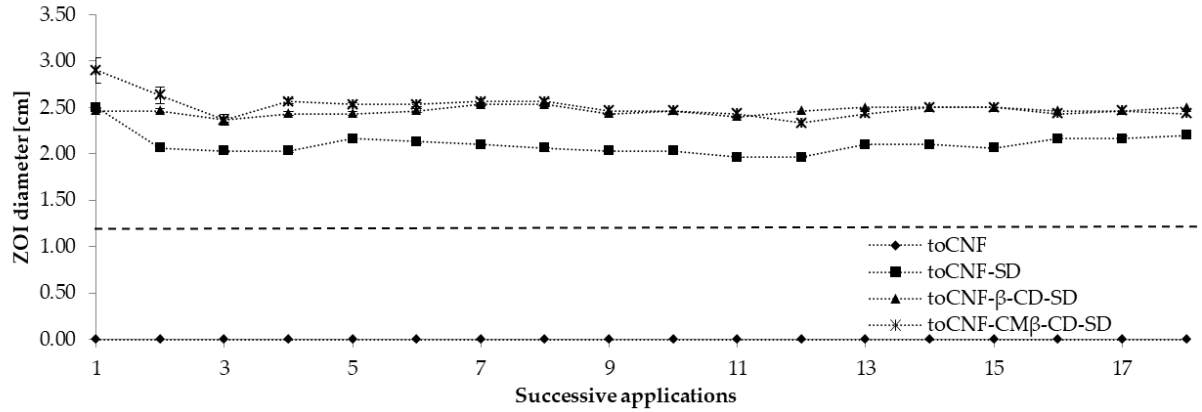

Figure III.21: Successive ZOI against *E. coli* for toCNF/β-CDs/SD cryogels

Cryogels were tested for up to 18 successive applications, after which they were no longer handeable due to decreased mechanical properties linked to water sorption from the agar.

All cryogels containing SD displayed ZOIs up to 18 successive applications. Samples containing β-CDs displayed slightly larger ZOIs, linked to the solubilization of SD molecules released in inclusion complex. As reported in Chapter II.1 [67] and illustrated in Figure III.22, films and cryogels present different structures, cryogels having an open porous structure while films have a densely packed laminar structure.

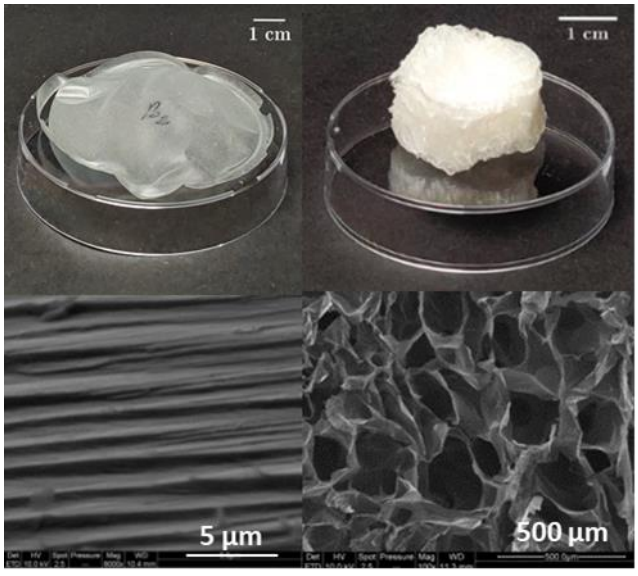

Figure III. 22: Macroscopic (photographs) and microscopic (SEM images) structure of films (left) and cryogels (right)

This difference in structure has two main impacts. Firstly, the specific surface area of cryogels is higher than that of films, inducing increased molecular interactions between toCNFs and both SD and β-CDs. Secondly, due to its open porous structure, the diffusion of

molecules through the toCNF network is easier for cryogels than for films. The limiting factor for evaluation of the cryogels is the mechanical properties of the swollen cryogels, preventing more than 18 successive applications. However, the higher release properties of cryogels, demonstrated here, combined with the improved release properties obtained by functionalization of toCNF with βCDs demonstrated for films, are extremely promising for the design of toCNF/ β-CDs materials for wound dressing applications.

III.2.4. CONCLUSION

toCNF/β-CDs/SD structures were produced in the form of films and cryogels. Release in sink conditions was conducted with two different protocols, namely continuous and intermittent release. Continuous release of ≈ 95% SD after 60 min for films casted at neutral pH and ≈85% SD after 120 min for films processed at acidic pH showed the impact of the pH in the production process on the release of SD from films, demonstrating the importance of the toCNF network structure. This was denser at acidic pH for toCNF due to its carboxylic content, which reduced the burst effect phenomena. These observations were confirmed by the intermittent release protocols. However, such protocols in sink conditions are not suitable for characterizing the impact of β-CDs. Consequently, disk diffusion assays were implemented to test the antimicrobial properties against two bacterial strains *S. aureus* and *E.coli.* An increase in the antibacterial activity was assessed by successive zone of inhibitions, with antibacterial effect lasting for 3 successive applications for toCNF/SD films, 5 for toCNF/β-CD/SD films and up to 7 with toCNF/CM-β-CD/SD films. This improvement is linked to the formation of inclusion complexes between SD and the various β-CDs, which improve the solubility of SD as well as delay the release of SD molecules in inclusion complex. CM-β-CD, by adsorbing more strongly onto toCNF, held the SD molecules for a longer period of time, resulting in a more durable antibacterial activity. Functionalization of toCNF structures with various modified β-CDs improvement of the topical release of a low water-soluble prophylactic agent, without the use of any cross-linker agent or harmful solvent. They are thus promising materials for biomedical applications such as wound dressings.

CONCLUSION OF CHAPTER III

The aim of this chapter was to obtain proof of concept of beneficial toCNF/β-CDs structures for biomedical applications such as wound dressing and drug release.

In chapter III.1, the formation of inclusion complexes between sulfadiazine and its silver derivative, and various β-CDs was investigated. Sulfadiazines are poorly water-soluble prophylactic agents frequently used in the prevention of infections for burn wound. Various protocols were implemented to assess the inclusion complex formation, which confirmed the 1:1 stoichiometry of the inclusion. The complex formation constant were determined and the results showed that the use of β-CDs is beneficial for increasing the solubility and bioavailability of SD. The penetration depth of SD inside the β-CDs cavity, as well as the orientation of SD in this complex, were investigated. It was demonstrated that CM-β-CDs induce a deeper penetration than other β-CDs. Finally, the impact of the chemical modifications of β-CDs on complexation was investigated, with β-CD and HP-β-CD displaying similar behavior while CM-β-CDs are more sensible to pH due to their ionic charges. These results allowed the validation of SD as a model molecule to characterize the beneficial impact of toCNF/β-CDs for the release of a poorly water-soluble API.

In chapter III.2, toCNF/β-CDs/SD structures were produced in the form of films and cryogels. Release in sink conditions was conducted with two different protocols, namely continuous and intermittent release, and this highlighted the importance of the toCNF network structure that was tightened at acidic pH due to its carboxylic content, which in turn reduced the burst effect phenomena. Disk diffusion tests were implemented to test the antimicrobial properties against two bacterial strains *S. aureus* and *E.coli.* An increase in the antibacterial activity was observed by successive zone of inhibitions, with antibacterial effect lasting for 3 successive applications for toCNF/SD films, 5 for toCNF/β-CD/SD films and up to 7 with toCNF/CM-β-CD/SD films. CM- β-CD, by adsorbing more strongly onto toCNF, held the SD molecules for a longer period of time, resulting in a more durable antibacterial activity.

These results demonstrate that toCNFs/β-CDs, and more specifically toCNF/CM-β-CD materials, are very promising, both for the encapsulation of hydrophobic molecules of interest as well as for their topical delivery for biomedical purposes.

LIST OF FIGURES

REFERENCES

[1] E. Rezvani Ghomi, S. Khalili, S. Nouri Khorasani, R. Esmaeely Neisiany, and S. Ramakrishna, 'Wound dressings: Current advances and future directions', *J Appl Polym Sci*, vol. 136, no. 27, p. 47738, Jul. 2019, doi: 10.1002/app.47738.

[2] H. Du, W. Liu, M. Zhang, C. Si, X. Zhang, and B. Li, 'Cellulose nanocrystals and cellulose nanofibrils based hydrogels for biomedical applications', *Carbohydrate Polymers*, vol. 209, pp. 130–144, Apr. 2019, doi: 10.1016/j.carbpol.2019.01.020.

[3] Y. Liu *et al.*, 'versatile vehicles for drug delivery and wound healing', *Carbohydrate Polymers*, p. 10, 2018.

[4] A. Basu, J. Lindh, E. Ålander, M. Strømme, and N. Ferraz, 'On the use of ion-crosslinked nanocellulose hydrogels for wound healing solutions: Physicochemical properties and application-oriented biocompatibility studies', *Carbohydrate Polymers*, vol. 174, pp. 299–308, Oct. 2017, doi: 10.1016/j.carbpol.2017.06.073.

[5] F. C. Claro, C. Jordão, B. M. de Viveiros, L. J. E. Isaka, J. A. Villanova Junior, and W. L. E. Magalhães, 'Low cost membrane of wood nanocellulose obtained by mechanical defibrillation for potential applications as wound dressing', *Cellulose*, vol. 27, no. 18, pp. 10765–10779, Dec. 2020, doi: 10.1007/s10570-020-03129-2.

[6] A. Isogai, T. Saito, and H. Fukuzumi, 'TEMPO-oxidized cellulose nanofibers', *Nanoscale*, vol. 3, no. 1, pp. 71–85, 2011, doi: 10.1039/C0NR00583E.

[7] J. Li *et al.*, 'Nanocellulose-Based Antibacterial Materials', *Adv. Healthcare Mater.*, vol. 7, no. 20, p. 1800334, Oct. 2018, doi: 10.1002/adhm.201800334.

[8] K. Littunen *et al.*, 'Synthesis of cationized nanofibrillated cellulose and its antimicrobial properties', *European Polymer Journal*, vol. 75, pp. 116–124, Feb. 2016, doi: 10.1016/j.eurpolymj.2015.12.008.

[9] H. Durand *et al.*, 'Pure cellulose nanofibrils membranes loaded with ciprofloxacin for drug release and antibacterial activity', *Cellulose*, May 2020, doi: 10.1007/s10570-020-03231-5.

[10] A. Errokh, A. Magnin, J.-L. Putaux, and S. Boufi, 'Hybrid nanocellulose decorated with silver nanoparticles as reinforcing filler with antibacterial properties', *Materials Science and Engineering: C*, vol. 105, p. 110044, Dec. 2019, doi: 10.1016/j.msec.2019.110044.

[11] D. Dehnad, H. Mirzaei, Z. Emam-Djomeh, S.-M. Jafari, and S. Dadashi, 'Thermal and antimicrobial properties of chitosan–nanocellulose films for extending shelf life of ground meat', *Carbohydrate Polymers*, vol. 109, pp. 148–154, Aug. 2014, doi: 10.1016/j.carbpol.2014.03.063.

[12] S. V. Kurkov and T. Loftsson, 'Cyclodextrins', *International Journal of Pharmaceutics*, vol. 453, no. 1, pp. 167–180, Aug. 2013, doi: 10.1016/j.ijpharm.2012.06.055.

[13] S. Rajapakse, M. Chrishan Shivanthan, N. Samaranayake, C. Rodrigo, and S. Deepika Fernando, 'Antibiotics for human toxoplasmosis: a systematic review of randomized trials',

Pathogens and Global Health, vol. 107, no. 4, pp. 162–169, Jun. 2013, doi: 10.1179/2047773213Y.0000000094.

[14] G. S. El-Feky, S. S. Sharaf, A. El Shafei, and A. A. Hegazy, 'Using chitosan nanoparticles as drug carriers for the development of a silver sulfadiazine wound dressing', *Carbohydrate Polymers*, vol. 158, pp. 11–19, Feb. 2017, doi: 10.1016/j.carbpol.2016.11.054.

[15] M. Q. Khan *et al.*, 'Fabrication of antibacterial electrospun cellulose acetate/ silver-sulfadiazine nanofibers composites for wound dressings applications', *Polymer Testing*, vol. 74, pp. 39–44, Apr. 2019, doi: 10.1016/j.polymertesting.2018.12.015.

[16] M. Venkataraman and M. Nagarsenker, 'Silver Sulfadiazine Nanosystems for Burn Therapy', *AAPS PharmSciTech*, vol. 14, no. 1, pp. 254–264, Mar. 2013, doi: 10.1208/s12249-012-9914-0.

[17] A. Delrivo, A. Zoppi, and M. R. Longhi, 'Interaction of sulfadiazine with cyclodextrins in aqueous solution and solid state', *Carbohydrate Polymers*, vol. 87, no. 3, pp. 1980–1988, Feb. 2012, doi: 10.1016/j.carbpol.2011.10.025.

[18] T. Loftsson and M. E. Brewster, 'Pharmaceutical applications of cyclodextrins: basic science and product development: Pharmaceutical applications of cyclodextrins', *Journal of Pharmacy and Pharmacology*, vol. 62, no. 11, pp. 1607–1621, Nov. 2010, doi: 10.1111/j.2042-7158.2010.01030.x.

[19] S. Fourmentin, N. Morin-Crini, and G. Crini, 'Cyclodextrines et complexes d'inclusion', in *Cyclodextrines, propriétés, chimie et applications*, Presse Universitaire de Franche-Comté, pp. 57–84.

[20] A. Delrivo, A. Zoppi, G. Granero, and M. Longhi, 'Studies of ternary systems of sulfadiazine with β-cyclodextrin and aminoacids', p. 10.

[21] N. Rajendiran, G. Venkatesh, and J. Saravanan, 'Supramolecular aggregates formed by sulfadiazine and sulfisomidine inclusion complexes with α- and β-cyclodextrins', *Spectrochimica Acta Part A: Molecular and Biomolecular Spectroscopy*, vol. 129, pp. 157–162, Aug. 2014, doi: 10.1016/j.saa.2014.03.028.

[22] A. A. Hegazy, S. S. Sharaf, G. S. El-Feky, and A. E. Shafei, 'Preparation and evaluation of the inclusion complex of silver sulfadiazine with cyclodextrin', *International Journal of Pharmacy and Pharmaceutical Sciences*, vol. 5, no. SUPPL.1, pp. 461–468, 2013.

[23] M. V. G. de Araújo *et al.*, 'Sulfadiazine/hydroxypropyl-β-cyclodextrin host–guest system: Characterization, phase-solubility and molecular modeling', *Bioorganic & Medicinal Chemistry*, vol. 16, no. 10, pp. 5788–5794, May 2008, doi: 10.1016/j.bmc.2008.03.057.

[24] J. Szejtli, 'Utilization of cyclodextrins in industrial products and processes', *Journal of Materials Chemistry*, vol. 7, no. 4, pp. 575–587, 1997, doi: 10.1039/a605235e.

[25] J. Szejtli, 'Introduction and General Overview of Cyclodextrin Chemistry', *Chem. Rev.*, vol. 98, no. 5, pp. 1743–1754, Jul. 1998, doi: 10.1021/cr970022c.

[26] M. L. Bender and M. Komiyama, *Cyclodextrin chemistry*. Springer-Verlag, 1978.

[27] M. E. Brewster and T. Loftsson, 'Cyclodextrins as pharmaceutical solubilizers', *Advanced Drug Delivery Reviews*, vol. 59, no. 7, pp. 645–666, Jul. 2007, doi: 10.1016/j.addr.2007.05.012.

[28] G. Crini, S. Fourmentin, M. Fourmentin, and N. Morin-Crini, 'Principales applications des complexes d'inclusion cyclodextrine/substrat', p. 21, 2019.

[29] P. Saokham, C. Muankaew, P. Jansook, and T. Loftsson, 'Solubility of Cyclodextrins and Drug/Cyclodextrin Complexes', *Molecules*, vol. 23, no. 5, p. 1161, May 2018, doi: 10.3390/molecules23051161.

[30] C. Yuan, Z. Jin, and X. Xu, 'Inclusion complex of astaxanthin with hydroxypropyl-β-cyclodextrin: UV, FTIR, 1H NMR and molecular modeling studies', *Carbohydrate Polymers*, vol. 89, no. 2, pp. 492–496, Jun. 2012, doi: 10.1016/j.carbpol.2012.03.033.

[31] M. Wszelaka-Rylik and P. Gierycz, 'Isothermal titration calorimetry (ITC) study of natural cyclodextrins inclusion complexes with drugs', *Journal of Thermal Analysis and Calorimetry*, vol. 111, no. 3, pp. 2029–2035, Mar. 2013, doi: 10.1007/s10973-012-2251-4.

[32] C. S. Mangolim *et al.*, 'Curcumin–β-cyclodextrin inclusion complex: Stability, solubility, characterisation by FT-IR, FT-Raman, X-ray diffraction and photoacoustic spectroscopy, and food application', *Food Chemistry*, vol. 153, pp. 361–370, Jun. 2014, doi: 10.1016/j.foodchem.2013.12.067.

[33] H.-J. Schneider, F. Hacket, V. Rüdiger, and H. Ikeda, 'NMR Studies of Cyclodextrins and Cyclodextrin Complexes', *Chem. Rev.*, vol. 98, no. 5, pp. 1755–1786, Jul. 1998, doi: 10.1021/cr970019t.

[34] K. A. Connors, 'The Stability of Cyclodextrin Complexes in Solution', *Chem. Rev.*, vol. 97, no. 5, pp. 1325–1358, Aug. 1997, doi: 10.1021/cr960371r.

[35] S. S. Jambhekar and P. Breen, 'Cyclodextrins in pharmaceutical formulations II: solubilization, binding constant, and complexation efficiency', *Drug Discovery Today*, vol. 21, no. 2, pp. 363–368, Feb. 2016, doi: 10.1016/j.drudis.2015.11.016.

[36] T. Loftsson, D. Hreinsdóttir, and M. Másson, 'Evaluation of cyclodextrin solubilization of drugs', *International Journal of Pharmaceutics*, vol. 302, no. 1–2, pp. 18–28, Sep. 2005, doi: 10.1016/j.ijpharm.2005.05.042.

[37] P. Mura, 'Analytical techniques for characterization of cyclodextrin complexes in aqueous solution: A review', *Journal of Pharmaceutical and Biomedical Analysis*, vol. 101, pp. 238–250, Dec. 2014, doi: 10.1016/j.jpba.2014.02.022.

[38] R. Zhao, C. Sandström, H. Zhang, and T. Tan, 'NMR Study on the Inclusion Complexes of β-Cyclodextrin with Isoflavones', *Molecules*, vol. 21, no. 4, p. 372, Mar. 2016, doi: 10.3390/molecules21040372.

[39] S. M. Ali, A. Maheshwari, F. Asmat, and M. Koketsu, 'COMPLEXATION OF ENALAPRIL MALEATE WITH β-CYCLODEXTRIN: NMR SPECTROSCOPIC STUDY IN SOLUTION', *Quim. Nova*, p. 4.

[40] D. Greatbanks and R. Pickford, 'Cyclodextrins as chiral complexing agents in water, and their application to optical purity measurements', *Magn. Reson. Chem.*, vol. 25, no. 3, pp. 208–215, Mar. 1987, doi: 10.1002/mrc.1260250306.

[41] M. V. Rekharsky *et al.*, 'Thermodynamic and Nuclear Magnetic Resonance Study of the Interactions of .alpha.- and .beta.-Cyclodextrin with Model Substances: Phenethylamine, Ephedrines, and Related Substances', *J. Am. Chem. Soc.*, vol. 117, no. 34, pp. 8830–8840, Aug. 1995, doi: 10.1021/ja00139a017.

[42] M. Wszelaka-Rylik and P. Gierycz, 'Isothermal titration calorimetry (ITC) study of natural cyclodextrins inclusion complexes with tropane alkaloids', *J Therm Anal Calorim*, vol. 121, no. 3, pp. 1359–1364, Sep. 2015, doi: 10.1007/s10973-015-4658-1.

[43] M. Jorfi and E. J. Foster, 'Recent advances in nanocellulose for biomedical applications', *Journal of Applied Polymer Science*, vol. 132, no. 14, p. n/a-n/a, Apr. 2015, doi: 10.1002/app.41719.

[44] N. Lin and A. Dufresne, 'Nanocellulose in biomedicine: Current status and future prospect', *European Polymer Journal*, vol. 59, pp. 302–325, Oct. 2014, doi: 10.1016/j.eurpolymj.2014.07.025.

[45] N. S. Sharip and H. Ariffin, 'Cellulose nanofibrils for biomaterial applications', *Materials Today: Proceedings*, vol. 16, pp. 1959–1968, 2019, doi: 10.1016/j.matpr.2019.06.074.

[46] K. Syverud, 'Tissue Engineering Using Plant-Derived Cellulose Nanofibrils (CNF) as Scaffold Material', in *ACS Symposium Series*, vol. 1251, U. P. Agarwal, R. H. Atalla, and A. Isogai, Eds. Washington, DC: American Chemical Society, 2017, pp. 171–189. doi: 10.1021/bk-2017-1251.ch009.

[47] N. Hasan *et al.*, 'Recent advances of nanocellulose in drug delivery systems', *J. Pharm. Investig.*, vol. 50, no. 6, pp. 553–572, Nov. 2020, doi: 10.1007/s40005-020-00499-4.

[48] R. Kolakovic, L. Peltonen, A. Laukkanen, J. Hirvonen, and T. Laaksonen, 'Nanofibrillar cellulose films for controlled drug delivery', *European Journal of Pharmaceutics and Biopharmaceutics*, vol. 82, no. 2, pp. 308–315, Oct. 2012, doi: 10.1016/j.ejpb.2012.06.011.

[49] N. Lavoine, I. Desloges, and J. Bras, 'Microfibrillated cellulose coatings as new release systems for active packaging', *Carbohydrate Polymers*, vol. 103, pp. 528–537, Mar. 2014, doi: 10.1016/j.carbpol.2013.12.035.

[50] C. Darpentigny *et al.*, 'Antimicrobial cellulose nanofibril porous materials obtained by supercritical impregnation of thymol', *ACS Applied Bio Materials*, Mar. 2020, doi: 10.1021/acsabm.0c00033.

[51] F. Rol, M. N. Belgacem, A. Gandini, and J. Bras, 'Recent advances in surface-modified cellulose nanofibrils', *Progress in Polymer Science*, Sep. 2018, doi: 10.1016/j.progpolymsci.2018.09.002.

[52] T. Saito, Y. Nishiyama, J.-L. Putaux, M. Vignon, and A. Isogai, 'Homogeneous Suspensions of Individualized Microfibrils from TEMPO-Catalyzed Oxidation of Native Cellulose', *Biomacromolecules*, vol. 7, no. 6, pp. 1687–1691, Jun. 2006, doi: 10.1021/bm060154s.

[53] H. Durand *et al.*, 'Two-step immobilization of metronidazole prodrug on TEMPO cellulose nanofibrils through thiol-yne click chemistry for in situ controlled release', *Carbohydrate Polymers*, vol. 262, p. 117952, Jun. 2021, doi: 10.1016/j.carbpol.2021.117952.

[54] C. Ruiz-Palomero, M. L. Soriano, and M. Valcárcel, 'β-Cyclodextrin decorated nanocellulose: a smart approach towards the selective fluorimetric determination of danofloxacin in milk samples', *The Analyst*, vol. 140, no. 10, pp. 3431–3438, 2015, doi: 10.1039/C4AN01967A.

[55] G. Yuan *et al.*, 'Cyclodextrin functionalized cellulose nanofiber composites for the faster adsorption of toluene from aqueous solution', *Journal of the Taiwan Institute of Chemical Engineers*, vol. 70, pp. 352–358, Jan. 2017, doi: 10.1016/j.jtice.2016.10.028.

[56] D. O. Castro, N. Tabary, B. Martel, A. Gandini, N. Belgacem, and J. Bras, 'Effect of different carboxylic acids in cyclodextrin functionalization of cellulose nanocrystals for prolonged release of carvacrol', *Materials Science and Engineering: C*, vol. 69, pp. 1018–1025, Dec. 2016, doi: 10.1016/j.msec.2016.08.014.

[57] D. Gomez-Maldonado *et al.*, 'Cellulose-Cyclodextrin Co-Polymer for the Removal of Cyanotoxins on Water Sources', *Polymers*, vol. 11, no. 12, p. 2075, Dec. 2019, doi: 10.3390/polym11122075.

[58] S. Saini, 'β-Cyclodextrin-grafted TEMPO-oxidized cellulose nanofibers for sustained release of essential oil', *J Mater Sci*, p. 13, 2017.

[59] N. Lavoine, N. Tabary, I. Desloges, B. Martel, and J. Bras, 'Controlled release of chlorhexidine digluconate using β-cyclodextrin and microfibrillated cellulose', *Colloids and Surfaces B: Biointerfaces*, vol. 121, pp. 196–205, Sep. 2014, doi: 10.1016/j.colsurfb.2014.06.021.

[60] P. Liu *et al.*, 'Dissolution Studies of Poorly Soluble Drug Nanosuspensions in Non-sink Conditions', *AAPS PharmSciTech*, vol. 14, no. 2, pp. 748–756, Jun. 2013, doi: 10.1208/s12249-013-9960-2.

[61] A. Bauer, W. Kirby, J. Sherris, and M. Turck, 'Antibiotic susceptibility testing by a standardized single disk method', *Am J Clin Pathol.*, vol. 45, no. 4, pp. 493–6, Apr. 1966.

[62] Commité de l'antibiogramme de la Société Française de Microbiologie, 'Recommandation 2020 V.1.1 Avril'.

[63] B. Michel, J. Bras, A. Dufresne, E. B. Heggset, and K. Syverud, 'Production and Mechanical Characterisation of TEMPO-Oxidised Cellulose Nanofibrils/β-Cyclodextrin Films and Cryogels', *Molecules*, vol. 25, no. 10, p. 2381, May 2020, doi: 10.3390/molecules25102381.

[64] E. Scholar, 'Sulfadiazine', in *xPharm: The Comprehensive Pharmacology Reference*, S. J. Enna and D. B. Bylund, Eds. New York: Elsevier, 2007, pp. 1–5. doi: 10.1016/B978-008055232-3.62690-X.

[65] C. L. Fox and S. M. Modak, 'Mechanism of Silver Sulfadiazine Action on Burn Wound Infections', *Antimicrob Agents Chemother*, vol. 5, no. 6, pp. 582–588, Jun. 1974, doi: 10.1128/AAC.5.6.582.

[66] E. Schoondermark-van de Ven, T. Vree, W. Melchers, W. Camps, and J. Galama, 'In vitro effects of sulfadiazine and its metabolites alone and in combination with pyrimethamine on Toxoplasma gondii', *Antimicrob Agents Chemother*, vol. 39, no. 3, pp. 763–765, Mar. 1995, doi: 10.1128/AAC.39.3.763.

[67] T. F. Fok, 'PRETERM INFANTS – NUTRITIONAL REQUIREMENTS AND MANAGEMENT', in *Encyclopedia of Food Sciences and Nutrition (Second Edition)*, Second Edition., B. Caballero, Ed. Oxford: Academic Press, 2003, pp. 4784–4792. doi: 10.1016/B0-12-227055-X/00973-1.

[68] D. J. Maggs, 'Chapter 3 - Ocular Pharmacology and Therapeutics', in *Slatter's Fundamentals of Veterinary Ophthalmology (Fourth Edition)*, Fourth Edition., D. J. Maggs, P. E. Miller, and R. Ofri, Eds. Saint Louis: W.B. Saunders, 2008, pp. 33–61. doi: 10.1016/B978-072160561-6.50006-X.

[69] J. T. Poolman and A. S. Anderson, 'Escherichia coli and Staphylococcus aureus: leading bacterial pathogens of healthcare associated infections and bacteremia in older-age populations', *null*, vol. 17, no. 7, pp. 607–618, Jul. 2018, doi: 10.1080/14760584.2018.1488590.

[70] M. Abdul Qadir, M. Ahmed, and M. Iqbal, 'Synthesis, Characterization, and Antibacterial Activities of Novel Sulfonamides Derived through Condensation of Amino Group Containing Drugs, Amino Acids, and Their Analogs', *BioMed Research International*, vol. 2015, pp. 1–7, 2015, doi: 10.1155/2015/938486.

[71] A. L. Koch, 'Diffusion through agar blocks of finite dimensions: a theoretical analysis of three systems of practical significance in microbiology', *Microbiology*, vol. 145, no. 3, pp. 643–654, Mar. 1999, doi: 10.1099/13500872-145-3-643.

GENERAL CONCLUSION AND PERSPECTIVES

This Ph.D. project investigated the functionalization of TEMPO-oxidized cellulose nanofibrils (toCNFs) with β-cyclodextrin (β-CD) and β-CD derivatives to develop innovative biomedical devices. The three main objectives were (i) to prepare CNF/β-CDs structures with controlled architecture as well as to identify the impact of different process parameters to obtain materials with suitable properties for biomedical applications, (ii) to find solutions to characterize the adsorption of various β-CDs onto CNFs, and (iii)to assess the beneficial impact of β-CDs on the release and/or antimicrobial properties of the prepared structure with a low water-soluble active principal ingredient (API).

Therefore, this project was at the interface of several disciplines, including process engineering, materials science, chemistry and microbiology. Many different experiments were conducted with the use of various characterization techniques. Both fundamental (ITC, QCM-d, NMR, etc.) and applied characterization methods (mechanical and water sorption properties, drug release protocols, microbiology protocols, etc.) as well as various imaging techniques (AFM, TEM, SEM) were used to investigate the morphological properties of the produced nanofibers and nanostructures. This variety of experiments enabled to answer several research questions. The progress made on the main objectives as well as the perspectives will be detailed in this section.

As such, the literature review given in **Chapter I** provided the reader with general background information as well as detailed data from recent scientific publications. An overview of biomaterials science was addressed, with descriptions of various applications and their inherent challenges, a description of the fundamentals in microbiology as well as an elaboration on the different classes of materials used nowadays, with a focus on natural biopolymers. General principles on isolation of nanocellulosic materials were given, and the different processing routes were thoroughly described. The potential of such materials for a wide variety of applications was highlighted, with an emphasis on their use for recent biomedical applications. A promising way to improve nanocellulose-based materials for biomedical applications with cyclodextrin-functionalization was presented with a description of this class of molecules, its inclusion complex properties as well as the potential characterization techniques. Finally, the description of previous works involving both cyclodextrins and nanocellulose was given to highlight the remaining challenges.

In **Chapter II**, the **production of toCNF/β-CD nanostructures were reported**. Materials were processed in the form of membranes by solvent casting or in the form of cryogels by freeze-drying. The impact of various process parameters over water sorption and mechanical properties was investigated, namely charge rate, process pH and addition of β-CDs. Two toCNF suspensions with different charge content were produced, viz. 756 ± 4 μmol/g and 1048 ± 32 μmol/g, and materials were processed from these suspensions at neutral and acidic pH, and with/without 10 wt% β-CD. It was shown that the water sorption behavior for films was driven by adsorption, with a clear impact of the chemical properties of the fibers (charge content, pH and adsorption of cyclodextrin). Modified toCNF cryogels (acidic pH and addition of cyclodextrins) displayed slightly lower mechanical properties linked to the modification of the cell wall porosity structure, due to the adsorption of β-CDs onto toCNFs. The interactions between the fibrils increased through hydrogen bonding at acidic pH. The order of magnitude of the compression modulus for both unmodified and modified cryogels was in line with values for soft tissue (between 17 and 150 kPa). Additionally, esterification between β-CDs and toCNFs under acidic conditions was performed by freeze-drying, and such cryogels exhibited a lower decrease in mechanical properties in the swollen state. Optimization of this process is an interesting perspective for further studies, as well as testing the mechanical properties with successive loading protocols, which could be more representative of the stress experienced by the scaffold *in-situ*.

The **characterization and quantification of the adsorption of β-CD and its derivatives onto toCNFs** was further studied. Isothermal Titration calorimetry was used to measure the thermodynamic parameters of interaction between β-CD and toCNFs, which, to the best of our knowledge, has never been reported before. The association constants determined at 25°C and 35°C validate the hypothesis of H-bonding-driven adsorption and enabled an estimation of β-CD binding capacity of around 19 μmol/g_{toCNF}. This order of magnitude was confirmed by QCM-d measurements. Moreover, β-CD derivatives, namely HP-β-CD and CM-β-CD, had binding capacities much higher than natural β-CD, with values of up to 47.6 μmol/g_{toCNF} for CM-β-CD. Indeed, the introduction of hydroxyl and carboxyl groups on β-CD derivatives as well as the presence of a spacer increased the availability of these functional groups and led to an important increase in the number of CD molecules

adsorbed onto toCNFs via H-bonds. The release of β-CD and its derivatives from toCNF structures was then assessed with a phenolphthalein-based titration method. It was observed that the higher the binging capacity, the lower the amount of CD released. As such, structures of toCNF/β-CD released up to 95% of the introduced CD after 24h, compared to only around 20% for toCNF/CM-β-CD structures. The different protocols implemented contribute to a better understanding and quantification of the adsorption of β-CDs onto toCNFs, and will help to design optimized toCNF/β-CD materials with lasting functionalization without the use of any cross-linker or harmful solvent. In perspective, the characterization of the hydroxyl accessibility and availability on toCNF, along with molecular modeling, would help to better represent the grafting density of β-CDs onto toCNFs. Additionally, adsorption phenomena might be investigated via other experimental means, such as surface plasmon resonance (SPR), and cross-inking of CM-β-CD to toCNF could be tried with divalent ions such as Ca^{2+}.

Subsequently, **the final design of toCNF/β-CD structures and the impact of β-CD derivatives on the mechanical properties** were reported. The morphological properties of two toCNF suspensions with similar charge rate, one industrially available (I-toCNFs) and the other lab-made (H-toCNFs), were compared. It turned out that the smaller nanofibrils length for I-toCNF (207 ± 75 nm) compared to H-toCNF (317 ± 102 nm), as well as a more homogeneous length distribution and lower residual fiber content led to better water sorption properties. As such, U-toCNF was selected as the final suspension for the final design of toCNF/β-CDs structures. The adsorption of β-CD derivatives onto toCNFs decreased the water sorption properties for I-toCNF cryogels, with absorption capacity down to around 30 g/g for I-toCNF/CM-β-CD compared to 58 g/g for neat I-toCNF cryogels. As expected, it led to a diminution of the mechanical properties, especially for the elastic behavior with a decrease in compression modulus, but the values (around 90 KPa) are still suitable for further biomedical applications. For such applications, cytotoxicity/cytocompatibily studies will be needed. It was also suggested that such modified materials could be also of high interest for filtration/depollution applications.

The main results and perspectives for Chapter II are presented in Table 1.

Table 1: Summary of the main results and perspectives on Chapter II

Production of β-cyclodextrin functionalized nanocellulose structures

Impact of process over mechanical properties of toCNF/βCD materials

❑ *Process of toCNF/β-CD materials*
- ➢ Two toCNF with various charge rate, neutral or acidic pH, 0%wtβ-CD or 10%wt β-CD
- ➢ Membranes by solvent-casting, oven drying 40°C/24h
- ➢ Cryogels by freeze-drying 0.3 mbar/24h

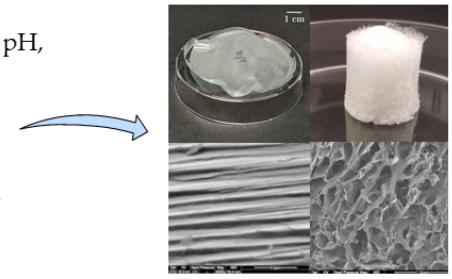

❑ *Impacts on water sorption and mechanical properties*
- ➢ Water sorption in films driven by chemical makeup of the fibers
- ➢ Modification of the cell-wall porous structures with β-CD adsorption and increased interfibrils interactions at acidic pH.
- ➢ Decrease of the mechanical properties of cryogels under modifications, Compression modulus in the range of soft tissue.

❑ *Mechanical properties in wet environment*
- ➢ Potential esterification between β-CD and toCNF by freeze-drying at acidic pH

Perspectives
- ❑ Optimization of the quantity of β-CD introduced without recrystallization
- ❑ Successive loading-test in wet environment
- ❑ Process of mechanically tailored materials

Adsorption characterization of various β-CDs onto toCNF

❑ *Physico-chemical interactions*
- ➢ Various β-CD derivatives to increase interactions with toCNF
- ➢ ITC measurement between β-CD and toCNF
- ➢ QCM-d between β-CDs and toCNF, increased interactions with derivatives
- ➢ Adsorption driven by H-bonding

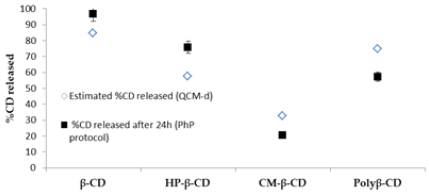

❑ *Quantification of adsorption*
- ➢ Estimation of binding capacity up to 47 µmol/g for CM-β-CD
- ➢ Release of β-CDs from toCNF films and cryogels with phenolphthalein titration method
- ➢ Low release of β-CDs derivatives, down to ≈20% for CM-β-CD

Perspectives
- ❑ Hydroxyls accessibility and availability
- ❑ ITC with β-CDs derivatives
- ❑ Molecular modelling of the interactions

Final design of toCNF/β-CDs derivatives materials

❑ *Selection of the most suited toCNF suspension*
- ➢ Characterization of the morphological properties of toCNF suspensions
- ➢ Selection of an industrially available toCNF suspension

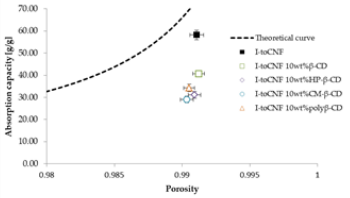

❑ *Impact of β-CDs derivatives*
- ➢ Local deflect in the cell-wall structures causing decrease in absorption capacity
- ➢ Moderate diminution of mechanical properties
- ➢ CD-functionnalized toCNF structures without cross-linker or harmful solvents.

Perspectives
- ❑ Cytotoxicity of produced materials
- ❑ Applications in filtration/depollution

In Chapter III, the **inclusion complex formation between the various β-CDs and a model active principle ingredient (API)** was studied. Sulfadiazine (SD), one of the most used prophylactic agents for burn wound along with its silver derivative, was selected as model molecule because of its intrinsic low water solubility and broad spectrum of antimicrobial activity. Phase solubility diagram (PSD) in water at pH 7 confirmed the formation of inclusion complex between β-CDs and SD in a 1:1 inclusion stoichiometry, and the formation constant ranging from 197 to 245 M^{-1} is enough to consider that the use of β-CDs is beneficial for increasing solubility and bioavailability of SD. The penetration of SD inside the β-CD cavity was investigated by ^{1}H-NMR. The results highlighted the penetration of the pyrimidine moiety of SD inside the lipophilic cavities of β-CD and its derivatives, with a slightly deeper penetration for CM-β-CD, linked to the presence of negative charges. Finally, ITC measurements were conducted at pH 6, and the higher formation constant values compared to those determined with PSD, ranging from around 500 M^{-1} for β-CD and HP- β-CD up to around 1100 M^{-1} for CM-β-CD, suggested a potential adsorption of SD around the CD in addition to the inclusion phenomenon. This suggestion was confirmed by assessing the impact of ionic charges with a lower formation constant of CM-β-CD with the negatively charged silver sulfadiazine (around 680 M^{-1}). This study validated the choice of SD as a model molecule to assess the potential beneficial impact of β-CDs on the release and antimicrobial properties of toCNF-based structures.

Subsequently, **the drug release and antimicrobial properties of toCNFs/β-CDs/SD materials** were reported. First, standard protocols of release in sink conditions, i.e. a volume of release medium at least five times higher than the one of the SD saturated solution, were implemented. Continuous release protocols highlighted the impact of process pH on the release properties, with ≈ 95% SD released after 60 min for films cast at neutral pH and ≈85% SD after 120 min for films processed under acidic pH. Indeed, the toCNF network structure tightened at acidic pH due to its carboxylic content and naturally reduced the burst effect phenomenon. These observations were confirmed by the intermittent release protocols. However, such protocols in sink conditions were not suitable for characterizing the impact of β-CDs. As such, disk diffusion assays were implemented to test the antimicrobial properties against two bacterial strains *S. aureus* and *E.coli.* An increase in the antibacterial activity was assessed by successive inhibition zones, with antibacterial effect lasting for 3 successive

applications for toCNF/SD films, 5 for toCNF/β-CD/SD films and up to 7 with toCNF/CM-β-CD/SD films. The formation of inclusion complexes between SD and the various β-CDs improved the solubility of SD as well as prolonged the release of SD molecules from the inclusion complex. Additionally, CM-β-CD adsorbs more strongly onto toCNFs, and therefore holds the SD molecules for a longer period of time, resulting in a more durable antibacterial activity. This result highlighted the successful improvement of toCNF based structures by β-CD derivatives functionalization for the topical release of a low water-soluble API. Additionally, results obtained for cryogels, which display antibacterial activity up to 18 successive applications are really promising. Improvement of the mechanical properties of such materials will be necessary to assess the maximal number of successive applications with an antibacterial effect.

The main results and perspectives for Chapter III are presented in Table 2.

Table 2: Summary of the main results and perspectives on Chapter III

β-CDs- functionalized nanocellulose for drug release applications

Inclusion complex formation between SD and various β-CDs

❑ *Selection of a model molecule*
- ➢ Sulfadiazine (SD), low-water soluble prophylactic agent

❑ *Inclusion complex formation*
- ➢ Solubility enhancement of SD (Phase solubility diagram)
- ➢ Association constant measurement via ITC, around 500 M^{-1} with β-CD and HP-β-CD and 1100 M^{-1} with CM--β-CD at pH6.
- ➢ Investigation on the importance of ionic charges on potential self-assembly with Silver Sulfadiazine
- ➢ Solid inclusion complex by freeze-drying

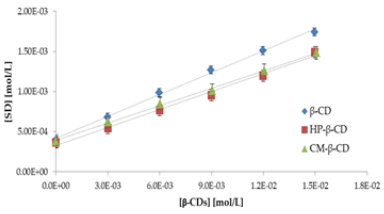

❑ *Conformation*
- ➢ Investigation of the conformation of SD molecules into β-CDs cavity via ^{1}H-NMR
- ➢ Pyrimidine moiety of SD included into the lipophilic cavity, deeper penetration with CM-β-CD

Perspectives
- ❑ Optimization of sample preparation for 2D-NMR
- ❑ Molecular modelling to investigate potential self-assembly
- ❑ Silver Sulfadiazine

Drug release and antimicrobial properties of toCNF/β-CDs/SD material

❑ *Release in sink conditions*
- ➢ Different protocols implemented (continuous and intermittent release)
- ➢ Moderate burst effect due the entanglement properties of toCNF network
- ➢ Less burst effect with samples processed at pH3 due to tighter network in toCNF structures
- ➢ No beneficial impact of β-CDs in sink conditions

❑ *Antimicrobial properties*
- ➢ Diffusion disk methods , with successive zone of inhibitions (ZOI)
- ➢ Antibacterial affect up to 7 successive applications with toCNF/CM-β-CD/SD films
- ➢ Antibacterial effect up to a minimum of 18 successive applications for cryogels

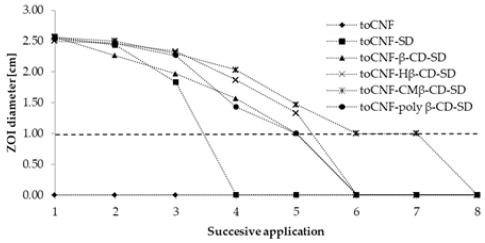

Perspectives
- ❑ Different Active Principal Ingredients
- ❑ Improving cryogels mechanical properties to improve the number of successive applications possible
- ❑ Proof of concept on burn wound model

In this PhD project, the main objectives were achieved; toCNF/β-CD structures were produced in a fast and reliable way in "2D structures" under the form of films and in "3D structure" in the form of cryogels. Characterization and quantification of β-CD adsorption onto toCNFs was given, and the impacts of the adsorption on various properties of the materials were assessed. The use of β-CD derivatives was proven to be beneficial for lasting functionalization of toCNFs and allowed to significantly improve the topical delivery of a low water-soluble API.

This study may be useful for future work dealing with β-cyclodextrin functionalization of cellulose nanofibrils for biomedical applications, but also for other applications, such as depollution or filtration.

EXTENDED FRENCH ABSTRACT
RESUME ETENDU EN FRANÇAIS

Dans le cadre de ce projet de thèse, les **biomatériaux** sont des matériaux biocompatibles adaptés pour être exploités en contact avec des tissus biologiques, et des organismes ou micro-organismes vivants [1]. Le développement des biomatériaux tels que nous les connaissons aujourd'hui trouve son origine à la fin des années 40, initié par le développement des connaissances scientifiques à la fois en médecine et en science des matériaux. Si les premiers biomatériaux ont été développés à l'origine pour d'autres applications et appliqués à la médecine dans une solution "prête à l'emploi", ils ont évolué pour former un domaine multidisciplinaire représenté par une vaste communauté de chercheurs et d'industries développant des solutions pour une grande variété d'applications telles que le relargage contrôlé et ciblé de principe actif, le développement de pansement « actif » ou encore l'ingénierie tissulaire [2]. En fonction de l'application, différentes familles de matériaux sont utilisées, les plus fréquents étant les métaux, les céramiques, les composites ou les polymères. Les biomatériaux métalliques sont utilisés pour les applications de support de charge en raison de leur résistance élevée à la fatigue (i.e. sollicitation mécanique alternée). Les biomatériaux céramiques sont utilisés pour les propriétés de surfaces permettant une bonne interaction avec les surfaces osseuses dans le cadre de la fabrication de prothèses et plus particulièrement pour les zones d'articulation en raison de leur dureté et de leur résistance à l'usure. Enfin, les matériaux polymères sont généralement utilisés dans les applications de pansement ou ingénierie tissulaire pour leur flexibilité et leur stabilité.

Les matériaux polymères, qui présentent une grande variété de propriétés physiques, ainsi qu'une multitude de possibilités, en termes de taille, de propriétés mécaniques, d'hydrophobie et de fonctionnalisation chimique, sont largement utilisés comme biomatériaux. Cependant, les polymères dérivés des ressources pétrolières sont encore les plus utilisés de nos jours, et leur utilisation présente plusieurs problèmes. D'un point de vue médical, la libération potentielle de résidus ou de sous-produits liés à la synthèse de ces matériaux (plastifiants par exemple) peut entraîner une réaction inflammatoire indésirable chez le patient. De plus, les ressources pétrolières n'étant pas renouvelables, il serait préférable, d'un point de vue environnemental, de trouver une alternative plus durable. À ce titre, les polymères biosourcés synthétiques, tels que l'acide polylactique (PLA), ont été considérés comme une alternative intéressante dans le domaine du médical [3]. Cependant,

les alternatives les plus prometteuses sont les biopolymères naturels. Ainsi, les biopolymères tels que la chitine, le collagène ou la cellulose, par exemple, sont de plus en plus exploités comme biomatériaux [4]–[6].

Dans ce contexte, les **nanofibrilles de cellulose (CNFs) sont un matériau prometteur**. Les CNFs sont des nanoparticules flexibles formées par des faisceaux de chaînes de cellulose qui sont une succession de sous-unités de glucose liées par des liaisons glycosidiques β-1-4, comme l'illustre la Figure 1.A. Les CNFs sont produites à partir d'une matière première cellulosique, généralement extraite du bois. Cette cellulose est le polymère le plus abondant et le plus renouvelable sur Terre. Les CNFs sont isolées par une combinaison de prétraitements chimiques/enzymatiques et de traitements mécaniques. La variété des prétraitements existants [7] permet une d'obtenir une grande variété de chimie de surface, permettant d'adapter les CNFs à de nombreuses applications, comme illustré sur la Figure 1.B., et favorisant ainsi la récente industrialisation de la production de CNFs à l'échelle mondiale. Ces dernières années, l'utilisation de CNFs pour l'élaboration de pansement [8], [9], le relargage contrôlé de principes actifs [10] et l'ingénierie tissulaire [11] ont été rapportées. Dans l'ingénierie tissulaire, le scaffold (i.e. le matériau support de la croissance cellulaire) doit stimuler les cellules pour qu'elles se différencient, prolifèrent et forment le tissu biologique souhaité. L'interaction entre la matrice et les cellules doit être stimulée par l'action de signaux, qui peuvent être une stimulation mécanique, des composés chimiques ou des facteurs de croissance (généralement des protéines) [12]. L'utilisation de CNFs pour l'ingénierie tissulaire est encouragée par de récentes études qui confirment leur innocuité [13], [14], l'élaboration de structures poreuses adaptées à la croissance cellulaire [15] et des propriétés mécaniques modulables [16], [17]. Dans les applications de délivrance de principe actif, l'objectif est d'obtenir **un relargage contrôlé et prolongé de la molécule active au site biologique d'intérêt**, mais également d'augmenter la biodisponibilité de cette molécule. Plusieurs études ont montré que l'utilisation de CNF est prometteuse pour prolonger la durée de relargage de différents principes actifs, notamment grâce à la formation d'un réseau intriqué et enchevêtré de nanofibrilles [18]. Cependant, des améliorations doivent être mises en œuvre pour obtenir un meilleur contrôle du chargement et de la libération du principe actif. En outre, la conception de structures de formes

multiples, en "2D" sous la forme de membrane ou en "3D" sous la forme de structure poreuse, doit être analysée en termes d'efficacité et d'adéquation aux applications souhaitées.

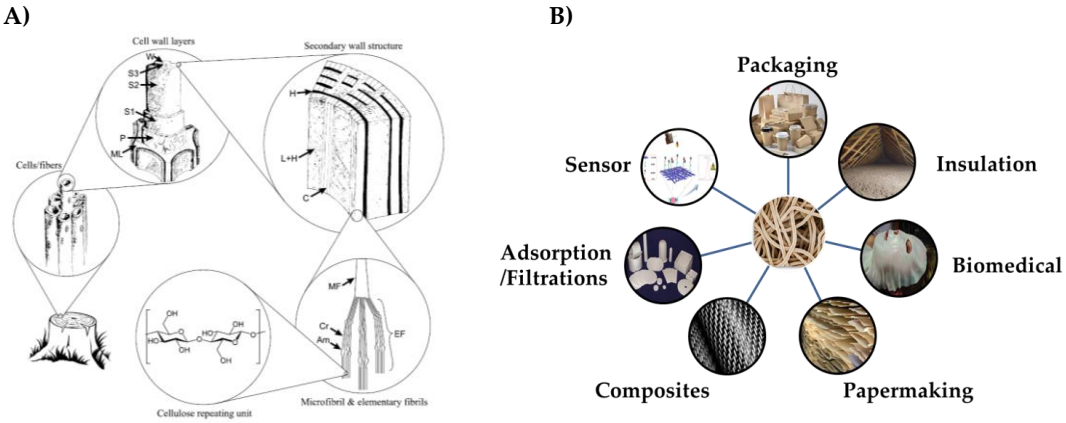

Figure 1: A) Structure hiérarchique du bois, extrait de [19] B) Applications potentielles des CNFs

Une stratégie prometteuse pour résoudre ces différentes problématiques est l'utilisation de **cyclodextrines (CDs).** Les cyclodextrines sont des oligosaccharides cycliques naturels constitués de sous-unités glucose liées par des liaisons glycosidiques α-1-4, comme le montre la figure 2.A. En raison de leur conformation, avec une cavité interne hydrophobe et une surface extérieure hydrophile, ces macromolécules présentent des propriétés d'encapsulation (également appelée « molécule cage ») et peuvent former un complexe d'inclusion avec des composés hydrophobes, comme le montre la Figure 2.B. [20], [21]. Ces propriétés ont conduit à leur utilisation dans divers domaines, tels que les cosmétiques, l'alimentation, l'environnement et la médecine [22]–[24]. Considérées comme non-toxique, certaines cyclodextrines sont largement utilisées dans le domaine pharmaceutique en tant qu'excipient de médicament [25], [26]. Pour ces applications, la β-CD, une cyclodextrine composée de 7 sous-unités de glucose, et ses dérivés sont les plus utilisés [27], [28].

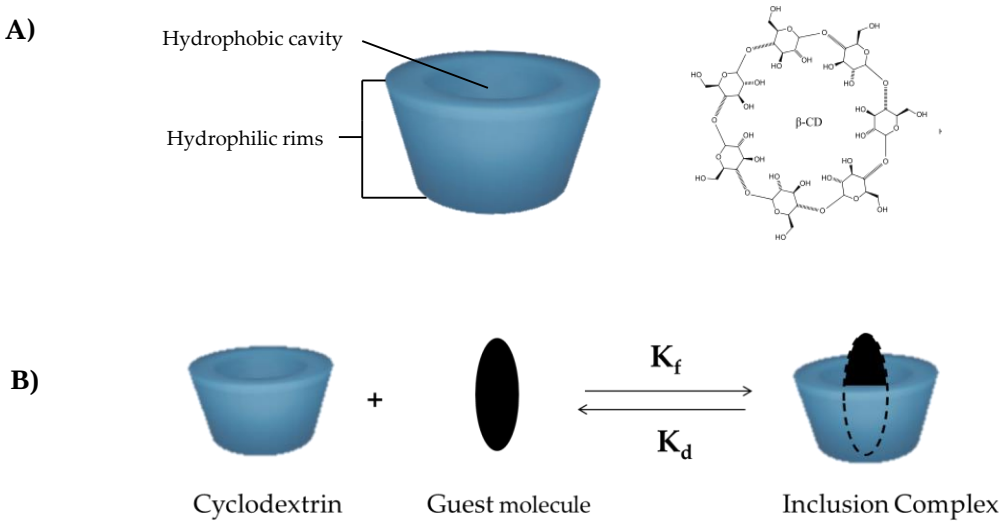

Figure 2: Représentation schématique de A) β-cyclodextrine et B) formation d'un complexe d'inclusion de stoichiometrie 1 :1

Les études s'intéressant à **l'association des CDs et des CNFs** n'étaient pas nombreuses avant ce projet, avec seulement une douzaine de publications sur le sujet, et elles ont toutes souligné la difficulté d'évaluer la fonctionnalisation par adsorption ou greffage des β-CDs sur les CNFs en raison de la grande proximité chimique des deux composants (tous deux à base de glucose), ce qui a été le principal inconvénient à cette association, bien que cela soit prometteur en théorie. De plus, d'autres défis sur ce sujet consistent à trouver des solutions pour améliorer la fonctionnalisation des CNFs par les β-CDs sans utiliser d'agent de liaison ou de solvant nocif. A cet égard, s'appuyer sur une capacité d'adsorption irréversible et l'utilisation de dérivés de β-CD pourrait être intéressante. En effet, les CNFS grâce à leur très grande surface spécifique ont démontré ces dernières années la possibilité d'adsorber des molécules et poly-électrolyte de manière irréversible. En parallèle, certains dérivés de β-CD présentent des groupes carboxyle ou hydroxypropyl, ce qui pourraient augmenter le potentiel d'interaction avec les CNFs. Cependant, au commencement de ce projet, cette stratégie n'avait pas été largement rapportée.

Le présent travail de recherche, intitulé "Nanocellulose fonctionnalisée par des cyclodextrines pour des applications biomédicales" est un projet collaboratif entre le Laboratoire de Génie des Procédés Papetiers (LGP2) à Grenoble (France) et RISE PFI/NTNU à Trondheim (Norvège). Ce travail est soutenu par l'Agence Nationale de la Recherche dans

le cadre du programme "Investissements d'avenir" Glyco@Alps et par NTNU à travers son département de génie chimique.

Les principaux objectifs de ce travail de recherche étaient de fournir des matériaux à base de nanocellulose avec des propriétés améliorées grâce aux caractéristiques spécifiques de la β-CD et de ses dérivés. A ce titre, les principaux objectifs étaient de :

- Préparer des structures CNF/β-CD avec une architecture contrôlée ainsi qu'identifier l'impact des différents paramètres du processus d'élaboration afin obtenir des matériaux avec des propriétés adaptées aux applications biomédicales.

- Trouver des solutions expérimentales pour caractériser l'adsorption de divers β-CDs sur les CNFs.

- Évaluer l'impact bénéfique des β-CDs sur la libération et/ou les propriétés antimicrobiennes de la structure en utilisant un principe actif peu soluble dans l'eau.

Afin d'atteindre ces objectifs, une collaboration active a été développée au cours de ces trois années, avec une mobilité à Trondheim en 2019 pour réaliser des expériences dans les installations de NTNU et de RISE PFI, mais aussi avec des partenaires locaux à Grenoble, qui ont permis d'utiliser certaines techniques de caractérisation (CERMAV).

Ce manuscrit s'attache, en trois chapitres comme présenté sur la Figure 3, à retranscrire de manière précise et détaillée la démarche de recherche menée ainsi que les résultats obtenus pour la production, la caractérisation et l'application de matériaux CNF/β-CD. Ce projet se situe à l'interface de plusieurs disciplines, notamment le génie des procédés, la science des matériaux, la chimie et la microbiologie. De nombreuses expériences ont été menées en utilisant diverses techniques de caractérisation. Des méthodes de caractérisation fondamentale (ITC, QCM-d, NMR, etc.) et appliquée (propriétés mécaniques et de sorption d'eau, protocoles de libération de médicaments, protocoles de microbiologie, etc.) ainsi que diverses techniques d'imagerie (AFM, TEM, SEM) ont été mises en place. Cette variété d'expériences a permis de répondre à plusieurs questions de recherche, qui seront résumées dans la section suivante.

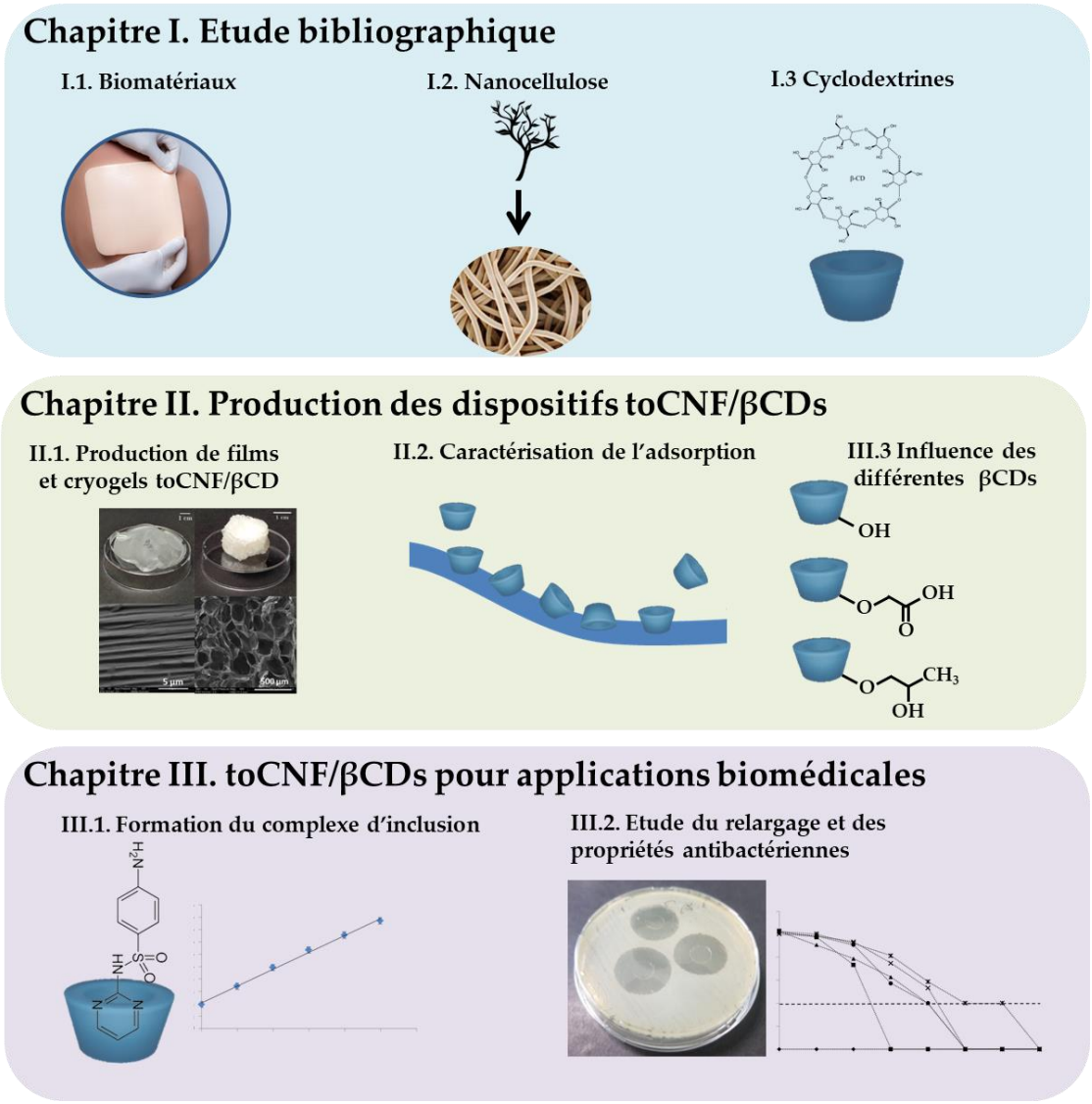

Figure 3: Représentation schématique de la structure du manuscrit

L'étude bibliographique présentée au **Chapitre I** fourni au lecteur des informations générales ainsi que des données détaillées issues de publications scientifiques récentes. Une vue d'ensemble de la science des biomatériaux a d'abord été abordée, avec la description de diverses applications et de leurs défis inhérents, des principes fondamentaux de la microbiologie et des différentes classes de matériaux utilisés de nos jours, en mettant l'accent sur les biopolymères naturels. Les principes généraux de l'isolation et la préparation des matériaux nanocellulosiques ont été donnés, et les différentes voies de traitement ont été décrites en détail. Le potentiel de ces matériaux pour une grande variété d'applications a été souligné, en mettant l'accent sur leur utilisation pour des applications biomédicales récentes.

Une voie prometteuse pour améliorer les matériaux à base de nanocellulose pour des applications biomédicales avec la fonctionnalisation par des cyclodextrines a été présentée avec une description de cette famille de molécules, de ses propriétés de complexation ainsi que des techniques de caractérisation potentielles. Enfin, la description des travaux antérieurs impliquant à la fois les cyclodextrines et la nanocellulose a été donnée pour mettre en évidence les défis à relever.

Dans le **Chapitre II**, la **production de matériaux toCNF/β-CD d'une manière rapide et fiable** a été rapportée. Les matériaux ont été mis en forme sous forme de membranes « 2D » par une méthode d'évaporation de solvant (« solvent casting ») ou sous forme de cryogels « 3D » par lyophilisation (« freeze-drying »). L'impact de divers paramètres du processus sur la sorption d'eau et les propriétés mécaniques a été étudié, à savoir le taux de charge, le pH et surtout l'ajout ou non de β-CD. Ainsi, deux suspensions de toCNF avec différents taux de charge ont été produites, à savoir 756 ± 4 μmol/g et 1048 ± 32 μmol/g, et des matériaux ont été élaborés à partir de ces suspensions à pH neutre et acide, et avec/sans 10%wtβ-CD. Il a été démontré que le comportement de sorption de l'eau pour les films est clairement impacté par la composition chimique des fibres (teneur en charge, pH et adsorption de la cyclodextrine). Les cryogels de toCNF modifiés (pH acide et ajout de cyclodextrines) ont présenté des propriétés mécaniques inférieures liées à la modification de la structure de la paroi des porosités, en raison de l'adsorption de β-CD sur le toCNF et d'une interaction accrue entre les nanofibrilles par liaison hydrogène à pH acide. L'ordre de grandeur du module de compression pour les cryogels non modifiés et modifiés est toutefois conforme aux valeurs des tissus mous (entre 17 et 150 kPa). De plus, l'estérification entre βCD et toCNF dans des conditions acides a été réalisée par lyophilisation, et ces cryogels ont présenté une diminution plus faible des propriétés mécaniques à l'état gonflé. L'optimisation de ce processus est une perspective intéressante pour des études ultérieures, ainsi que le test des propriétés mécaniques avec des protocoles de compression successives, qui pourraient être plus représentatifs de la contrainte subie par le scaffold in-situ.

Ensuite, la caractérisation et la quantification de l'adsorption de β-CDs et de ses dérivés sur les toCNFs ont été étudiées dans le détail. L'ITC a notamment été utilisée pour mesurer les paramètres thermodynamiques de l'interaction entre β-CD et toCNF, ce qui, à

notre connaissance, n'avait jamais été rapporté auparavant. Les constantes d'association déterminées à 25°C et 35°C valident l'hypothèse d'une adsorption par liaisons hydrogène et ont permis d'estimer la capacité de liaison de la β-CD à environ 19 μmol/gtoCNF. Cet ordre de grandeur a été confirmé par des mesures QCM-d. De plus, les dérivés du β-CD, à savoir HP-β-CD et CM-β-CD, présentaient des capacités d'adsorption supérieures à celles de la β-CD naturel, avec des valeurs allant jusqu'à 47,6 μmol/gtoCNF pour la CM-β-CD. En effet, l'introduction de groupes hydroxyle et carboxyle sur les dérivés de β-CD ainsi que la présence d'un espaceur ont augmenté la disponibilité de ces groupes fonctionnels et ont conduit à une augmentation importante du nombre de molécules de CD adsorbées sur les toCNF via liaisons hydrogène. La libération de β-CD et de ses dérivés des structures toCNF a ensuite été évaluée par une méthode de titrage à base de phénolphtaléine. Il s'est avéré que plus la capacité d'adsorption est élevée, plus la quantité de CD libérée est faible. Ainsi, les structures toCNF/β-CD ont libéré jusqu'à 95% des CDs introduites après 24h, contre seulement environ 20% pour les structures de toCNF/CM-β-CD. Les différents protocoles mis en œuvre contribuent à une meilleure compréhension et quantification de l'adsorption des β-CD sur les toCNFs, et permettront de concevoir des matériaux toCNF/β-CD optimisés avec une fonctionnalisation durable sans l'utilisation d'agent de liaison ou de solvant nocif. En perspective, la caractérisation de l'accessibilité et de la disponibilité des hydroxyles sur les toCNFs, ainsi que la modélisation moléculaire des interactions, permettraient de mieux représenter la densité de greffage des β-CDs sur les toCNFs.

Enfin, la **conception finale des structures toCNF/β-CD et l'impact des dérivés β-CD sur les propriétés mécaniques** ont été rapportés. Les propriétés morphologiques de deux suspensions de toCNF avec un taux de charge similaire, l'une disponible industriellement (I-toCNF) et l'autre fabriquée en laboratoire (H-toCNF), ont été comparées. Il s'est avéré que la longueur des nanofibrilles pour I-toCNF (207 ± 75 nm) comparée à H-toCNF (317 ± 102 nm), ainsi qu'une distribution beaucoup plus homogène de la longueur et un contenu plus faible en fibres résiduelles ont conduit à de meilleures propriétés de sorption d'eau avec I-toCNF. En tant que telle, I-toCNF a été sélectionnée comme la suspension finale pour notre étude. L'adsorption des dérivés de β-CD sur les toCNFs a diminué les propriétés d'absorption d'eau des cryogels I-toCNF, avec une capacité d'absorption d'environ 30 g/g pour I-toCNF/CM-β-CD comparé à 58 g/g pour les cryogels I-toCNF purs. Comme prévu, cela a conduit à une

diminution des propriétés mécaniques, en particulier pour le comportement élastique avec une diminution du module de compression, mais les valeurs (environ 90 KPa) sont encore appropriées pour les applications biomédicales. Pour ces applications, des études de cytotoxicité/cytocompatibilité seront nécessaires, mais ces matériaux modifiés pourraient également être d'un grand intérêt pour les applications de filtration et de dépollution.

Les principaux résultats et perspectives du chapitre II sont présentés dans le Tableau 1.

Tableau 1 : Principaux résultats et perspectives du chapitre II

Production de structures nanocellulose/β-cyclodextrine

Impact du procédé sur les propriétés mécaniques

❑ *Production de matériaux toCNF/β-CD*
- 2 toCNF avec ≠ taux de charges , pH neutre ou acide, 0%mβ-CD ou 10%m β-CD
- Membranes par évaporation de solvant, séchage 40°C/24h
- Cryogels par lyophilisation 0.3 mbar/24h

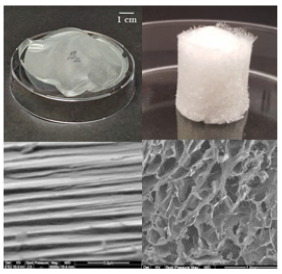

❑ *Impacts sur la sorption d'eau et les propriétés mécaniques*
- Sorption pour les films principalement liée à la chimie de surface des fibres
- Modification des parois des porosités par adsorption de β-CD et augmentation des interactions inter-fibrilles à pH acide.
- Diminution des propriétés mécaniques des cryogels modifiés. Module de compression dans la gamme des tissus mous.

❑ *Propriétés mécaniques en milieu humide*
- Estérification potentielle entre β-CD et toCNF par lyophilisation à pH acide.

Perspectives
- ❑ Optimisation de la quantité de CD introduite
- ❑ Compressions successives en milieu humide
- ❑ Conception de matériaux avec des propriétés mécaniques adaptables

Caractérisation de l'adsorption de β-CDs sur toCNF

❑ *Interactions physico-chimiques*
- Différent dérivés de β-CD pour augmenter les interactions avec les toCNFs
- Mesures ITC entre β-CD et toCNF
- QCM-d entre les β-CDs et toCNF, plus fortes interactions avec les dérivés
- Adsorption par liaison hydrogène

❑ *Quantification de l'adsorption*
- Estimation des capacités d'adsorption jusqu'à 47 µmol/g pour CM-β-CD
- Relargage des β-CDs depuis films et cryogels avec utilisation de phénolphtaléine
- Faible relargage des dérivés de β-CDs , ≈20% pour CM-β-CD contre ≈95% pour β-CD après 24h

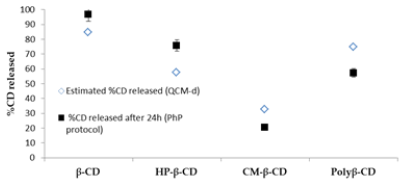

Perspectives
- ❑ Accessibilité et disponibilité des hydroxyles
- ❑ ITC avec les dérivés de β-CDs
- ❑ Modélisation moléculaire des interactions

Conception finales des matériaux toCNF/β-CDs

❑ *Sélection de la suspension de toCNF*
- Caractérisation des propriétés morphologiques des différentes toCNFs
- Sélection d'une suspension disponible industriellement

❑ *Impact des dérivés de β-CDs*
- Déformation locale des structures des paroi des porosités entrainant une diminution de la capacité d'absorption
- Diminution modérée des propriétés mécaniques
- Structures toCNFs fonctionnalisées avec des β-CDs sans agent de liaison ni solvant toxiques

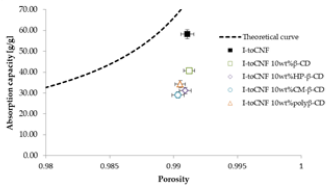

Perspectives
- ❑ Cytotoxicité / cytocompatibilité
- ❑ Applications en filtration / dépollution

Dans le **Chapitre III**, **la formation de complexes d'inclusion entre les différentes β-CDs et un principe actif modèle a été étudiée**. La sulfadiazine (SD), l'un des agents prophylactiques les plus utilisés avec son dérivé argentique pour le traitement des plaies par brûlures, a été choisie comme molécule modèle en raison de sa faible solubilité intrinsèque dans l'eau et de son large spectre d'activité. Le diagramme de solubilité de phase (PSD) dans l'eau à pH7 a confirmé la formation d'un complexe d'inclusion entre les β-CDs et la SD avec une stœchiométrie d'inclusion 1:1, et les constantes de formation allant de 197 à 245 M^{-1} sont suffisantes pour considérer que l'utilisation des β-CDs est bénéfique pour augmenter la solubilité et la biodisponibilité de la SD. La conformation de la SD à l'intérieur de la cavité des β-CDs a été étudiée par ^{1}H-RMN, et a mis en évidence la pénétration de la fraction pyrimidine de la SD à l'intérieur de la cavité lipophile des β-CDs, avec une pénétration légèrement plus profonde pour la CM-β-CD, liée à la présence de charges négatives. Enfin, des mesures ITC ont été réalisées à pH6, et les valeurs de constantes de formation plus élevées que celles déterminées avec PSD, allant d'environ 500 M^{-1} pour la β-CD et la HP-β-CD jusqu'à environ 1100 M^{-1} pour la CM-β-CD, ont suggéré une adsorption potentielle de SD autour des CDs en plus du phénomène d'inclusion. Cette suggestion a été confirmée en évaluant l'impact des charges ioniques avec une constante de formation plus faible de la CM-β-CD avec la sulfadiazine argentique chargée négativement (environ 680 M^{-1}). Cette étude a validé le choix de la SD comme molécule modèle pour évaluer l'impact bénéfique potentiel des β-CDs sur le relargage et les propriétés antimicrobiennes des structures à base de toCNFs.

Par la suite, **le relargage de principe actif et les propriétés antimicrobiennes des matériaux toCNF/β-CDs/SD** ont été rapportées. Tout d'abord, des protocoles standards de libération en conditions sink, c'est-à-dire avec un volume de milieu de libération au moins cinq fois supérieur à celui de la solution saturée de SD, ont été mis en œuvre. Les protocoles de relargage en continu ont mis en évidence l'impact du pH lors de la mise en forme sur les propriétés de relargage, avec ≈ 95%SD libérés après 60 min pour les films préparés à pH neutre et ≈85%SD après 120 min pour les films préparés à pH acide. En effet, la structure du réseau de toCNFs, resserrée à pH acide en raison de la présence de fonctionnalités d'acide carboxylique, a naturellement réduit le phénomène de « burst release » (i.e. le relargage quasi-immédiat du principe actif lors du contact avec le milieu de relargage). Ces

observations ont été confirmées par les protocoles de relargage intermittent. Cependant, ces protocoles en conditions sink n'étaient pas adaptés à la caractérisation de l'impact des β-CDs. Ainsi, des essais de zone d'inhibition ont été mis en œuvre pour tester les propriétés antimicrobiennes contre deux souches bactériennes *S. aureus* (Gram +) et *E. coli* (Gram -). Une augmentation de l'activité antibactérienne a été évaluée par des zones d'inhibition successives, avec un effet antibactérien pour 3 applications successives pour les films toCNF/SD, 5 pour les films toCNF/β-CD/SD et jusqu'à 7 avec les films toCNF/CM-β-CD/SD. La formation de complexes d'inclusion entre la SD et les différentes β-CDs a amélioré la solubilité de la SD ainsi que retardé le relargage des molécules de SD incluses dans les CDs. De plus, la CM-β-CD, en s'adsorbant plus fortement sur les toCNFs, a retenu les molécules de SD pendant une période plus longue, ce qui a entraîné une activité antibactérienne plus durable. Ce résultat a mis en évidence l'amélioration des structures à base de toCNF avec la fonctionnalisation par les β-CDs pour le relargage topique d'un principe actif peu soluble dans l'eau. De plus, les résultats obtenus pour les cryogels, qui présentent une activité antibactérienne jusqu'à 18 applications successives sont vraiment prometteurs. Une amélioration des propriétés mécaniques de ces matériaux est nécessaire pour pouvoir estimer le nombre maximum d'applications successives maintenant un effet antibactérien afin de fournir une preuve de concept à grande échelle.

Les principaux résultats et perspectives du chapitre III sont présentés dans le Tableau 2.

Tableau 2: Principaux résultats et perspectives du Chapitre III

toCNF/β-CDs pour applications biomédicales

Formation du complexe d'inclusion entre la SD et différentes β-CDs

❑ *Sélection d'une molécule modèle*
- ➢ Sulfadiazine (SD), agent prophylactique peu soluble dans l'eau

❑ *Formation du complexe d'inclusion*
- ➢ Augmentation de la solubilité de la SD (Diagramme de phase de solubilité)
- ➢ Mesure des constantes d'association par ITC, environ 500 M^{-1} avec β-CD et HP-β-CD et 1100 M^{-1} avec CM--β-CD à pH6.
- ➢ Étude de l'importance des charges ioniques sur l'auto-assemblage potentiel avec la sulfadiazine argentique.
- ➢ Complexe d'inclusion sous forme solide

❑ *Conformation*
- ➢ Etude de la conformation des molécules de SD dans les cavités de β-CDs par ^{1}H-RMN
- ➢ Partie pyrimidine de la SD incluse dans la cavité lipophile, pénétration plus profonde avec CM-β-CD

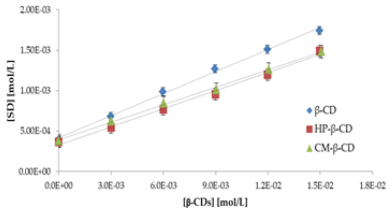

Perspectives

- ❑ Optimisation de la préparation d'échantillons pour RMN-2D
- ❑ Modélisation moléculaire pour étudier un potentiel auto-assemblage
- ❑ Sulfadiazine argentique

Relargage et propriétés antibactériennes des matériaux toCNF/β-CDs/SD

❑ *Relargage en condition sink*
- ➢ Différents protocoles mis en place (relargage continue et intermittent)
- ➢ « Burst effect » modéré lié à l'intrication naturelle du réseau de toCNF
- ➢ Moins de « burst effect » avec les matériaux produits à pH3 lié aux liaisons inter fibrillaires entre les toCNF
- ➢ Pas d'impact des β-CDs observable en conditions sink

❑ *Propriétés antibactériennes*
- ➢ Méthode des disques de diffusion , avec zones d'inhibitions successives
- ➢ Effet antibactérien jusqu'à 7 applications successives avec les films toCNF/CM-β-CD/SD
- ➢ Effet antibactérien jusqu'à un minimum de 18 applications successives pour les cryogels

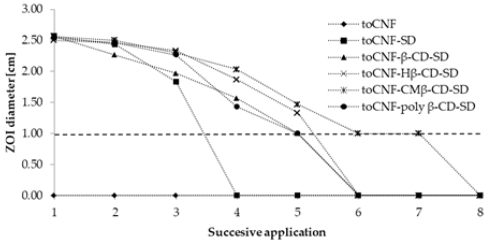

Perspectives

- ❑ Différents principes actifs
- ❑ Améliorer les propriétés mécaniques des cryogels pour augmenter le nombre d'applications successives possibles
- ❑ Preuve de concept sur un modèle de peau brûlée

Pour conclure sur ce projet de thèse, les principaux objectifs ont été atteints. Des structures toCNF/β-CDs ont été produites de manière rapide et fiable en "structure 2D" sous forme de films et en "structure 3D" sous forme de cryogels. La caractérisation et la quantification de l'adsorption des β-CDs sur les toCNFs ont été menées, et l'impact de l'adsorption sur diverses propriétés des matériaux a été évalué. L'utilisation de dérivés de β-CDs s'est avérée très bénéfique pour la fonctionnalisation durable du toCNF et a permis d'améliorer significativement la délivrance topique d'un principe actif faiblement soluble dans l'eau.

Cette étude peut être utile pour de futurs travaux traitant de la fonctionnalisation par la β-cyclodextrine de nanofibrilles de cellulose pour des applications biomédicales, mais également pour d'autres applications, telles que la dépollution ou la filtration.

RÉFÉRENCES

[1] M. Vert *et al.*, 'Terminology for biorelated polymers and applications (IUPAC Recommendations 2012)', *Pure and Applied Chemistry*, vol. 84, no. 2, pp. 377–410, Jan. 2012, doi: 10.1351/PAC-REC-10-12-04.

[2] B. D. Ratner, 'Biomaterials: Been There, Done That, and Evolving into the Future', *Annu. Rev. Biomed. Eng.*, vol. 21, no. 1, pp. 171–191, Jun. 2019, doi: 10.1146/annurev-bioeng-062117-120940.

[3] V. DeStefano, S. Khan, and A. Tabada, 'Applications of PLA in modern medicine', *Engineered Regeneration*, vol. 1, pp. 76–87, 2020, doi: 10.1016/j.engreg.2020.08.002.

[4] F. Copes, N. Pien, S. Van Vlierberghe, F. Boccafoschi, and D. Mantovani, 'Collagen-Based Tissue Engineering Strategies for Vascular Medicine', *Front. Bioeng. Biotechnol.*, vol. 7, p. 166, Jul. 2019, doi: 10.3389/fbioe.2019.00166.

[5] H. Gao *et al.*, 'Construction of cellulose nanofibers/quaternized chitin/organic rectorite composites and their application as wound dressing materials', *Biomater. Sci.*, vol. 7, no. 6, pp. 2571–2581, 2019, doi: 10.1039/C9BM00288J.

[6] R. J. Hickey and A. E. Pelling, 'Cellulose Biomaterials for Tissue Engineering', *Front. Bioeng. Biotechnol.*, vol. 7, p. 45, Mar. 2019, doi: 10.3389/fbioe.2019.00045.

[7] F. Rol, M. N. Belgacem, A. Gandini, and J. Bras, 'Recent advances in surface-modified cellulose nanofibrils', *Progress in Polymer Science*, Sep. 2018, doi: 10.1016/j.progpolymsci.2018.09.002.

[8] A. Rees *et al.*, '3D Bioprinting of Carboxymethylated-Periodate Oxidized Nanocellulose Constructs for Wound Dressing Applications', *BioMed Research International*, vol. 2015, pp. 1–7, 2015, doi: 10.1155/2015/925757.

[9] T. Hakkarainen *et al.*, 'Nanofibrillar cellulose wound dressing in skin graft donor site treatment', *Journal of Controlled Release*, vol. 244, pp. 292–301, Dec. 2016, doi: 10.1016/j.jconrel.2016.07.053.

[10] R. Kolakovic, L. Peltonen, A. Laukkanen, J. Hirvonen, and T. Laaksonen, 'Nanofibrillar cellulose films for controlled drug delivery', *European Journal of Pharmaceutics and Biopharmaceutics*, vol. 82, no. 2, pp. 308–315, Oct. 2012, doi: 10.1016/j.ejpb.2012.06.011.

[11] E. Campodoni *et al.*, 'Polymeric 3D scaffolds for tissue regeneration: Evaluation of biopolymer nanocomposite reinforced with cellulose nanofibrils', *Materials Science and Engineering: C*, vol. 94, pp. 867–878, Jan. 2019, doi: 10.1016/j.msec.2018.10.026.

[12] D. Howard, L. D. Buttery, K. M. Shakesheff, and S. J. Roberts, 'Tissue engineering: strategies, stem cells and scaffolds', *Journal of Anatomy*, vol. 213, no. 1, pp. 66–72, Jul. 2008, doi: 10.1111/j.1469-7580.2008.00878.x.

[13] A. Rashad, K. Mustafa, E. B. Heggset, and K. Syverud, 'Cytocompatibility of Wood-Derived Cellulose Nanofibril Hydrogels with Different Surface Chemistry', *Biomacromolecules*, vol. 18, no. 4, pp. 1238–1248, Apr. 2017, doi: 10.1021/acs.biomac.6b01911.

[14] L. Alexandrescu, K. Syverud, A. Gatti, and G. Chinga-Carrasco, 'Cytotoxicity tests of cellulose nanofibril-based structures', *Cellulose*, vol. 20, no. 4, pp. 1765–1775, Aug. 2013, doi: 10.1007/s10570-013-9948-9.

[15] K. J. De France, T. Hoare, and E. D. Cranston, 'Review of Hydrogels and Aerogels Containing Nanocellulose', *Chemistry of Materials*, vol. 29, no. 11, pp. 4609–4631, Jun. 2017, doi: 10.1021/acs.chemmater.7b00531.

[16] K. Syverud, H. Kirsebom, S. Hajizadeh, and G. Chinga-Carrasco, 'Cross-linking cellulose nanofibrils for potential elastic cryo-structured gels', *Nanoscale Research Letters*, vol. 6, no. 1, p. 626, 2011, doi: 10.1186/1556-276X-6-626.

[17] K. Syverud, S. R. Pettersen, K. Draget, and G. Chinga-Carrasco, 'Controlling the elastic modulus of cellulose nanofibril hydrogels—scaffolds with potential in tissue engineering', *Cellulose*, vol. 22, no. 1, pp. 473–481, Feb. 2015, doi: 10.1007/s10570-014-0470-5.

[18] N. Lin and A. Dufresne, 'Nanocellulose in biomedicine: Current status and future prospect', *European Polymer Journal*, vol. 59, pp. 302–325, Oct. 2014, doi: 10.1016/j.eurpolymj.2014.07.025.

[19] O. Nechyporchuk, M. N. Belgacem, and J. Bras, 'Production of cellulose nanofibrils: A review of recent advances', *Industrial Crops and Products*, vol. 93, pp. 2–25, Dec. 2016, doi: 10.1016/j.indcrop.2016.02.016.

[20] S. V. Kurkov and T. Loftsson, 'Cyclodextrins', *International Journal of Pharmaceutics*, vol. 453, no. 1, pp. 167–180, Aug. 2013, doi: 10.1016/j.ijpharm.2012.06.055.

[21] J. Szejtli, 'Introduction and General Overview of Cyclodextrin Chemistry', *Chem. Rev.*, vol. 98, no. 5, pp. 1743–1754, Jul. 1998, doi: 10.1021/cr970022c.

[22] E. M. M. Del Valle, 'Cyclodextrins and their uses: a review', *Process Biochemistry*, vol. 39, no. 9, pp. 1033–1046, May 2004, doi: 10.1016/S0032-9592(03)00258-9.

[23] G. Crini, S. Fourmentin, M. Fourmentin, and N. Morin-Crini, 'Principales applications des complexes d'inclusion cyclodextrine/substrat', p. 21, 2019.

[24] N. Morin-Crini, P. Winterton, S. Fourmentin, L. D. Wilson, É. Fenyvesi, and G. Crini, 'Water-insoluble β-cyclodextrin–epichlorohydrin polymers for removal of pollutants from aqueous solutions by sorption processes using batch studies: A review of inclusion mechanisms', *Progress in Polymer Science*, vol. 78, pp. 1–23, Mar. 2018, doi: 10.1016/j.progpolymsci.2017.07.004.

[25] F. J. Otero-Espinar, J. J. Torres-Labandeira, C. Alvarez-Lorenzo, and J. Blanco-Méndez, 'Cyclodextrins in drug delivery systems', *Journal of Drug Delivery Science and Technology*, vol. 20, no. 4, pp. 289–301, 2010, doi: 10.1016/S1773-2247(10)50046-7.

[26] S. S. Jambhekar and P. Breen, 'Cyclodextrins in pharmaceutical formulations I: structure and physicochemical properties, formation of complexes, and types of complex', *Drug Discovery Today*, vol. 21, no. 2, pp. 356–362, Feb. 2016, doi: 10.1016/j.drudis.2015.11.017.

[27] O. Cusola, N. Tabary, M. N. Belgacem, and J. Bras, 'Cyclodextrin functionalization of several cellulosic substrates for prolonged release of antibacterial agents', *Journal of Applied Polymer Science*, vol. 129, no. 2, pp. 604–613, Jul. 2013, doi: 10.1002/app.38748.

[28] T. Loftsson and M. E. Brewster, 'Pharmaceutical applications of cyclodextrins: basic science and product development: Pharmaceutical applications of cyclodextrins', *Journal of Pharmacy and Pharmacology*, vol. 62, no. 11, pp. 1607–1621, Nov. 2010, doi: 10.1111/j.2042-7158.2010.01030.x.

ENGLISH ABSTRACT

The purpose of this project is to combine oxidized cellulose nanofibrils (toCNFs) and various β-cyclodextrins (β-CDs) to design improved materials for biomedical applications. The combination of toCNFs and β-CDs, although promising, faces some challenges, notably characterization of this association. Thus, this project aims at developing innovative materials combining toCNF and various β-CD derivatives, with the objective of characterizing the adsorption phenomena and improving drug release of poorly-water soluble active principal ingredient (API) and consequently prolonging antimicrobial properties. First, the production of toCNF/β-CD materials was reported, with an investigation on the impact of various process parameters on water sorption and mechanical properties. The adsorption of β-CDs was characterized via different experimental tools, and it was shown that β-CD derivatives adsorb up to 10 times more onto toCNF than β-CD. The formation of an inclusion complex between a model API and the various β-CDs was thoroughly characterized. Finally, the functionalization of toCNF with β-CDs showed improvement of the antimicrobial properties of films with increased efficiency for carboxymethylated-β-CD. The results of this project contribute to the knowledge on interaction of cyclodextrin and nanocellulosic materials and are a step-towards their efficient application in biomedical field as well as other applications such as depollution.

Keywords: *cellulose nanofibrils, β-cyclodextrins, adsorption characterization*

RESUME EN FRANÇAIS

Le but de ce projet est de combiner des nanofibrilles de cellulose oxydées (toCNFs) et divers dérivés de β-cyclodextrines (β-CDs) afin de concevoir des matériaux performants pour des applications biomédicales. L'association de toCNF et de β-CDs, bien que prometteuse, fait face à certains défis, notamment la caractérisation de cette association. Ainsi, ce projet vise à caractériser les phénomènes d'adsorption entre toCNF et β-CDs afin d'améliorer le relargage de principes actifs (PA) faiblement solubles dans l'eau et ainsi favoriser les propriétés antimicrobiennes de ces matériaux. Tout d'abord, après production de matériaux toCNF/β-CD, une étude sur l'impact de divers paramètres de mise en forme sur la sorption d'eau et les propriétés mécaniques a été réalisée. L'adsorption des β-CDs a été caractérisée par différents moyens expérimentaux, et il a été démontré que les dérivés β-CD s'adsorbent jusqu'à 10 fois plus sur les toCNF que les β-CDs. La formation d'un complexe d'inclusion entre un PA modèle et les différents β-CDs a été caractérisée de manière approfondie. Enfin, l'adsorption sur les toCNF de β-CDs s'est avérée améliorer les propriétés antimicrobiennes des films avec une efficacité prolongée avec le dérivé de β-CD carboxyméthylée. Les résultats de ce projet contribuent à une meilleure connaissance des interactions entre les matériaux nanocellulosiques et diverses cyclodextrines et sont une étape vers leur application dans le domaine biomédical ainsi que d'autres applications telles que la dépollution.

Mots-clés: *nanofibrilles de cellulose, β-cyclodextrines, caractérisation d'adsorption*